USE OF RECOVERY-BY-SIZE DATA FROM BATCH TESTING IN ESTIMATING THE PERFORMANCE OF CONTINUOUS FLOTATION OPERATIONS

by

ROBERT BHEKI KHUMALO

Student number: 34332227

submitted in accordance with the requirements for

the degree of

DOCTOR OF PHILOSOPHY

in the subject

Engineering, Science and Technology

at the

UNIVERSITY OF SOUTH AFRICA

SUPERVISOR: Prof FRANCOIS MULENGA

May 2021

DECLARATION

I declare that **"Use of Recovery-by-Size Data from Batch Testing in Estimating the Performance of Continuous Flotation Operations"** is my own work and that all the sources that I have used or quoted have been indicated and acknowledged by means of complete references.

_____ _____

Robert B. Khumalo Date

Acknowledgements

But thanks [be] to God, which giveth us the victory through our Lord Jesus Christ. 1st Corinthians {15:57} (KJV)

I will like to send my deepest gratitude to my supervisor Prof Francois Mulenga who ignited the spark of giving this research a try. His support and guidance throughout the study has been awesome.

It is a great privilege to have my wife – Zanele and my daughter – Thobeka in my life, as they were able to work with me behind the scenes. Emotional and spiritual upliftment that, they have rendered to me mixed with their unconditional love have seen me gaining strength to continue up to the end.

Lastly, UNISA is praised for its dual role of being a preferred institution to conduct this research and provided funds to execute it. Without UNISA, this will have been a dream that was not going to be realized.

Abstract

The work title 'Use of Recovery-by-Size Data from Batch Testing in Estimating the Performance of Continuous Flotation Operations' seeks to validate available theories against recovery-by-size batch flotation data and to use that available batch data to scale up the flotation process. The output of such objectives will be to bridge a knowledge gap in refined empirical models and also lead to a tool capable of predicting performance of continuous flotation from batch flotation data.

Batch flotation tests were done from a sulphide copper bearing ore at 2, 6, 12 and 20 min flotation times. Continuous flotation tests were also done in two sets:

- Sampling overall flotation circuit samples for feed, concentrate and tails.
- Sampling of each cell in a bank (roughers, cleaners and re-cleaners) for feed, concentrate and tails which is referred to as cell-by-cell sampling.

A number of scale-up methods were useful in scale-up from batch flotation to continuous operation with the ModSim software used do the simulation work and this proved to be effective and dependable.

A size fraction of around 102 µm (intermediate size fraction) gave the highest recoveries compared to fine size fraction (19 µm) and coarse size fraction (up to 638 µm). The Scale-up validation techniques (kinetics, concentrate grade, recovery, sizing and overall) lead to different results of batch and continuous data.

Statement of Novelty

The work conducted attributes itself with the contribution to the existing scientific body of knowledge. Summary of such original contribution is but not limited to:

- Designing of laboratory experimental work under certain conditions, which was later taken to the plant environment with different conditions but produced results that were comparable.
- Capability of using dimensional similitude scale-up approach, which resulted in a scale-up factor of 1.25. This scale-up factor may be used by the engineer(s) to scale-up flotation cells of the same ore type and type of cell machine.
- The application of scale-up validation technique using sizing method of batch flotation elemental Cu versus continuous flotation elemental Cu produced a correlation constant (R^2) = 0.9921. A high correlation of this nature gives more credibility on the results produced and improves confidence in their application.
- With the use of King's flotation model, a simulator in the form of a complete ModSim mass balance flowsheet was developed for a continuous flotation plant. Key areas where such a simulator will find its use is in continuous improvement projects or plant modifications that may be implemented.

TABLE OF CONTENTS

LIST OF FIGURES

LIST OF TABLES

LIST OF SYMBOLS

A	Cell cross sectional area (m^2)
A_{air}	Air flowrate (m^3/s)
A_b	Total bubble surface area per unit of pulp volume
Ae	Aeration (air flow) number
A_s	Impeller aspect ratio
a,b,c,d_d&e	Bubble surface area flux model parameters
c	Concentrate grade ((% or g/t)
C_A	Carrying capacity using P_{80} or R_F ($kg/s/m^2$ or $t/h/m^2$)
C_i	Mass flow rate of component i in the concentrate from a cell with units of ($kg.min^{-1}$)
$C_{i,j}(O)$	Feed grade of particle i,j (% or g/t)
$C_{i,j}(t)$	Tailings grade of particle i,j (% or g/t)
C_R	Carrying rate ($kg/s/m^2$ or $t/h/m^2$)
CTOT	Total concentrate solids flow rate assuming no suppression of flotation rates ($kg\ min^{-1}$)
d	particle size (µm)
D	Impeller diameter (m)
d_b	Mean diameter of distribution of bubbles with different sizes (m)
d_i	Equivalent spherical diameter of particle size *i* (m)
d_p	Sauter mean particle diameter (m)
d_{pi}	Size of particles in size class *i* (µm)

$d_{p\ max}$	Size of the largest particle that can be floated without detachment from the bubble (µm)
D_{ps}	Particle size in microns
E(t)	Residence time distribution function
ENT_i	Degree of entrainment for a particle size *i*
f	Feed / head grade ((% or g/t)
F_i	Mass flow rate of component *i* fed to the cell (kg min^{-1})
FMAX	Maximum solids concentrate flow rate (kg min^{-1})
F(k)	Rectangular distribution function
Fr	Froude number
F(S, 1.0)	Fraction of slow floating component in the liberated class
F(S, C)	Fraction of the slow floating component for particles of chalcopyrite fraction C
f_τ	Function that calculates the average value of area covered by bubble (S) throughout the cell can be calculated from the spread of bubble residence times
g	Gravitational acceleration constant (9.81m/s^2)
h_{froth}	Froth height (m)
J_g	Superficial gas velocity (m/s)
k	Flotation rate constant (s^{-1} or min^{-1})
K	Constant that is characteristics for a given type of flotation cell
k_{ac}	Continuous flotation rate constant (s^{-1} or min^{-1})
k_{app}	Apparent flotation rate constant (s^{-1} or min^{-1})

k_{app}/k_b	Ratio between apparent flotation rate constant and batch flotation rate constant as a function of dimensionless parameters
k_b	Batch flotation rate constant (s^{-1} or min^{-1})
k_c	Collection zone rate constant (s^{-1} or min^{-1})
k_i	Flotation rate constant for this component (s^{-1} or min^{-1}).
k_j	Residual constant that is specific to the particle type and is independent of particle size
k_{max}	Maximum flotation rate constant (s^{-1} or min^{-1})
K(s)	Flotation rate of the slow component (s^{-1} or min^{-1})
L	Distance between impeller and launder (m)
m	Mass of the mineral class (i.e. the grade)
m_i	Mass of the mineral - m in size class i.
n	Sample size
n_r	Number of ideal tanks in series
N_c or N	Number of cells in series or can be impeller rotational speed (1/s)
N_f	Constant that is characteristics for a given type of flotation cell
Ni	Impeller rotational speed (1/s)
N_s	Impeller peripheral speed
P	Floatabilty constant and is dimensionless or proportionality constant that is a function of ore type and pulp chemistry
PDw	Power draw ($kg.m^2/s^3$)
Po	Power number
P_{80}	80% passing screen size (µm)

Q or Q_{air}	Air flowrate (m^3/s)
Q_c^w	Water flux into the froth zone from the collection zone (ml/s)
Q_{conc}^w	Water flux to the concentrate (ml/s)
Q_g	Air flowrate into the cell (m^3/min)
Q_{pulp}	Pulp flowrate (m^3/s)
R_c	Recovery of particles in the collection zone (%)
R_c^w	Collection recovery of water (%)
R_e	Reynolds number at impeller zone
$R_{ent,i}$	Recovery of particles by entrainment of i^{th} size class (%)
R_f	Froth recovery - k/k_c (%)
R_f^w	Froth recovery of water (%)
$R_{i,j}$	Flotation recovery in size class i and grade class j (%)
R(t) or %Rec	Recovery according to flotation (%)
$R(\tau)$	Recovery according to residence time (%)
R_∞	Maximum recovery (%)
R_w	Water recovery (%)
S	Fraction of the surface area of a single bubble that is not covered by adhering solid particles (m^2)
S_{av}	Available bubble surface area averaged over the entire bubble population in the flotation cell (m^2)
S_b	Bubble surface area flux (1/s)
t	Flotation time (s)
t1	Tails grade ((% or g/t)

T	Cell diameter (m)
T_t	Total solids tailings flow rate (kg min-1)
t_r	Time taken for residence time distribution (RTD) testing
t_{avg}	Average or mean residence time (s)
V	Cell effective volume (m^3)
W	Mass of solids in the cell (kg)
W_i	Mass component *i* in the cell (kg),
W/T_t	Mean residence time for solids in the cell (min)
Z	Constant usually at zero (0) or maybe less than zero (<0)

GREEK SYMBOLS

α	Constant from relationship between τ_{fs} and k
α_{fe}	Froth effect
αs	Is the variance
β_{cf}	Constant from curve-fitting or can be cell mixing effect
ξ	Rate of k_{ac} to k_b or scale-up factor
ε_g	Gas holdup m^3 air per m^3 pulp
γ	Particle segregation effect or can be surface tension of the air – liquid interface (kg/s^2)
ρ_p	Particle (solids) density or can be pulp density
ρ_L	Liquid density (kg/m^3)
μm	Microns meter i.e. unit of particle size
μ_p	Pulp viscosity (kg/m/s)
η	Dimensionless recovery(ratio of rec to max. rec)
$\eta(D)$	Factor that represents the surface area covered by 1kg of solid
τ_S	Effective solids residence time
τ_L	Effective liquid residence time
τ_{fs}	Specific froth residence time (s)
τ_{fg}	Froth residence time (s)
τ_{LT}	Bubble lifetime (s)
τ_p	Residence time (s)
τs	Expected residence time or space time

$\bar{\tau}$	Average residence time of the bubbles
δ	Average thickness of the lamellar films in the froth (m)
$\Phi_j(d_{pi})$	Factor allowing for the effects of size and type of particles or function describing the effect of particle size *i* on flotation rate that is also dependent on particle type *j*
ϕ(D)	Function that accounts for all the influence of the particle size or function to describe the variation of flotation rate constant with particle size
φ	Ratio of mixing condition
φ_s	Bubble surface coverage
$\varphi_{s,max}$	Maximal bubble surface coverage
ζ	Entrainment parameter of the particle size for which the degree of entrainment is 20 %
ʊ	Drainage parameter related to the preferential drainage of coarse particles
Γ(Nc)	Gamma function

DESCRIPTIONS OF TERMS

Batch flotation	Flotation process that is done in the laboratory under controlled environment and it is given start and end time.
Cleaners	Stage which initially receives the concentrates either from roughers or scavengers to upgrade it.
Continuous flotation	Flotation process that is happening in the plant environment which is a dynamic environment and this is mainly running 24 hours a day except if there are breakdowns (unplanned equipment stoppages) or planned maintenance.
Flotation	Process that separates valuable and invaluable minerals on the basis of differences in surface properties enhanced by reagents added and it also happens by injection of air bubbles into a moving stream of aqueous slurry (solids and water) containing a mixture of particles mainly coming from milling circuit (Mesa and Brito-Parada, 2019).
Grade	Percentage purity of the material of interest which can be in the feed, concentrate and tailings (Wills and Napier-Munn, 2006).
Particle size distribution (PSD)	Means of reporting by displaying the distribution of a material that has been segregated between the different particle size fractions of which it is composed or is the measurement of the size of the granulates contained in a certain batch of material and their distribution in relation to different sizes contained there (Parry, 2006).
Re-cleaners	Stage that follows the cleaners and is for the final upgrading of concentrate before it leaves flotation circuit.

Recovery	Percentage expression of the required product in the original feed that is recovered or end up reporting in the concentrates (Opperman *et al*., 2002).
Roughers	First stage of flotation cells after the milling circuit.
Run of mine (ROM)	Ore in its natural, unprocessed state just as it is when blasted and this can have top size of approximately 300 mm which will be heterogeneous or mixed with waste (Minnitt,2014).
Scavengers	Second stage after the roughers which improves / upgrade the rougher tails.

Chapter 1 Introduction

1.1 Introduction

The mining industry constantly strives to improve their mineral recovery especially in the flotation circuits. During this time, high flotation recovery is used as a proxy for high plant efficiency, which in turn positively affects the revenue of the mining business.

Flotation has been reported to treat more than 10 billion tons of various mineral ores annually (Xian-ping *et al.,* 2011). It is also used in the treatment of products such as wastewater, bacteria, coal, clays, corn, resins, proteins, fats, rubber, dyes, glass, plastics, fruit juices, and cane sugar (Bu *et al*., 2017).

It was envisaged in this study to measure flotation recoveries of mono-sized copper-bearing ore feed samples in batch flotation cells. Mono-sized feeds were to be batch-floated to collect information relevant to the scale-up scheme as originally proposed by King (2012). The idea is to capture the effects of particle size as the latter plays an important role in the flotation of liberated ore particles (Xian-ping *et al*., 2011). The collected recovery-by-size data is expected to enable a better understanding of the response of the ore to industrial flotation operations in terms of grade and recovery.

The experimentation entailed batch laboratory flotation work in a controlled environment. After that, a sampling campaign was carried out in an existing plant where conditions are less controlled. The two datasets were processed using scale-up models and theories available in the literature. Scale-up models included gas dispersion, flotation kinetics, and carrying capacity (Harris *et al*., 2013). Finally, an improved scale-up model was proposed based on the recovery-by-size batch flotation data and the findings from existing scale-up models.

1.2 Problem statement

Although extensive research has been published on flotation, it is still not easy to design and control industrial operations (Sutherland, 1981; Reuter and Van Deventer, 1990; Perry *et al*., 1997; Yianatos *et al*., 2005; Steyn, 2012). One reason for this is that robust tools for scale-up from batch to industrial flotation are yet to be developed. Recovery-by-size data could be regarded as a viable option for further enquiry on flotation scale-up. It is anticipated that the envisaged solution would address one key problem, that is, to determine whether industrial flotation performance can be predicted from recovery-by-size batch flotation data.

1.3 Hypotheses

Batch and industrial flotation data have been qualitatively compared in the past as epitomised in Figure 1.1. It can be seen that "n" shapes shift upwards while flattening with batch flotation time on the one hand and the number of cells in a row of flotation bank on the other.

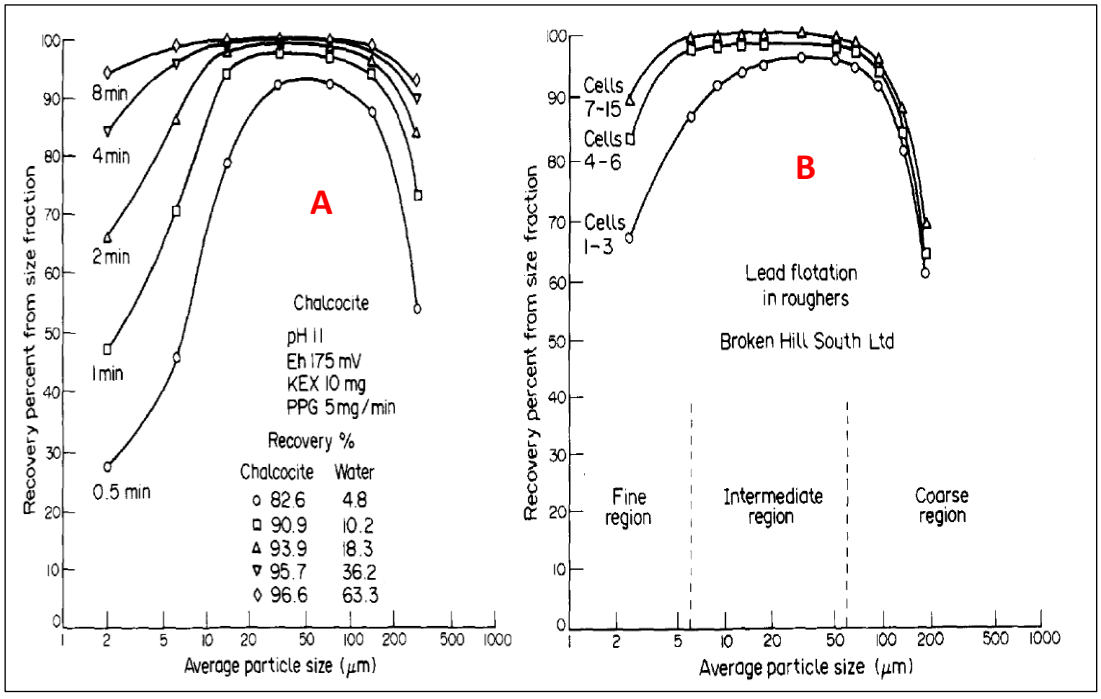

Figure 1.1 Laboratory (**A**) and plant (**B**) recovery-by-size data (McIvor and Finch, 1990; Trahar, 1981)

The other observation is that the intermediate size range somewhat similar between batch and continuous flotation. It is therefore posited that for each batch test setup, there exists a batch flotation time for which the recovery-by-size curve is similar to that of a bank made up of a fixed number of flotation cells.

1.4 Research objectives

From the problem statement in the previous section, it was undertaken to relate recovery-by-size batch flotation data with routinely collected continuous flotation data. Once the batch data has been obtained, various theories (e.g. King, 2012; Wills and Napier-Munn, 2006; McIvor and Finch, 1990; Trahar, 1981; Jowett, 1969; Multani and Waters, 2019) were tested to establish the typical effects of particle size shown in Figure 1.2.

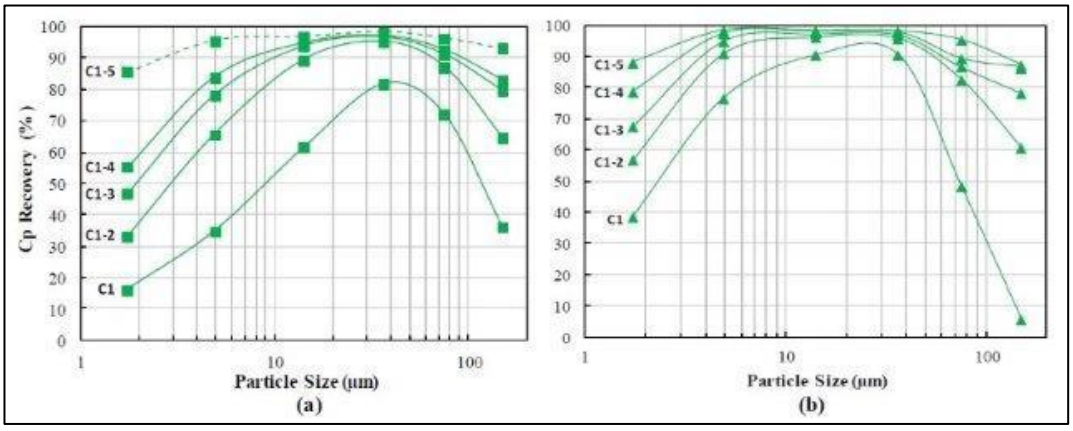

Figure 1.2: Example of Chalcopyrite recovery-by-size curve showing (a) Baseline test and (b) Acid/aeration test (Multani and Waters, 2019)

The primary objective therefore was to validate existing theories against collected recovery-by-size batch flotation data and in the process identify gaps for refined empirical models. The use of different flotation residence times was applied and that needed to be checked of what effects it brought about. The secondary objective was to use the laboratory findings for scale-up to a production environment. Potentially, the research findings would lead to a tool capable of estimating the performance of continuous flotation operations from batch flotation recovery-by-size data.

1.5 Research questions

Flotation is a complex multi-component process that is enjoying extensive scientific enquiry. And even though flotation has been in use for over a century, a lot is yet to be studied.

In terms of this doctoral study, the two research questions below underpin the scope of the work done. They can be summarised as follows:

- How the recovery-by-size data from batch flotation tests can be scaled up to model the response of the ore in an industrial plant environment while covering identified gaps that may exist?
- How does flotation residence time affect recovery-by-size data from batch flotation tests?

1.6 Scope and delimitation of the research study

The research focused on determining the relationship between batch flotation recovery-by-size data and performance of continuous flotation plants. However, flotation is known to be complex while the preparation of mono-sized feed samples in sufficient quantity is logistically challenging (Lotter *et al*., 2014; Holmes, 2002). For these reasons, only three particle size classes were considered: fine particles, intermediate particles and coarse particles. So, the upscaling approaches used were also limited to the three size classes.

It is equally important to note that the effect of ultra-fine particles was excluded from the scope of this work. This is because these particles do not respond well to conventional flotation cells. Their study is still important but including such ultra-fines would have widened the scope of the testwork beyond what was initially intended. Furthermore, the acquisition of associated laboratory equipment to analyse these sizes would have been costly and outside the budget of this research.

Finally, although the research is primarily of academic interest, recommendations for industrial operation have been highlighted.

1.7 Outline of the thesis

The doctoral thesis is organised in eight chapters. Chapter one deals with the background to the research, the research problem, the objectives and questions of the study as well as the scope and delimitation of the work done.

In Chapter two, the existing literature on froth flotation and its characterisation is reviewed. The theoretical and empirical modelling of the flotation process from the point of view of laboratory batch tests and industrial surveying are then covered. The paradigm of recovery-by-size data in batch flotation is also discussed. Finally, the gap existing in the available body of knowledge is identified. This becomes the foundation of the experimental work ahead hinging on the idea of recovery-by-size data proposed by King (2012).

Chapter three presents the experimental programme for batch and continuous flotation data gathering. The collection and preparation of representative feed samples for laboratory batch flotation tests is also discussed. The samples were collected on key streams around the plant under usual operating conditions and following accepted industrial protocols. Challenges faced during the sampling campaign are finally identified as they impact the quality of data collected.

The recovery-by-size data collected by laboratory batch flotation tests is analysed in Chapter four. The experimental laboratory results are characterised and discussed in line with their anticipated scale-up.

Chapter five analyses the continuous flotation plant data presented in Chapter three collected by means of conducting plant surveys. This is followed by Chapter six which then subsequently tests against the selected scale-up models. At the end, specific techniques like kinetics, concentrate grade, recovery, sizing and overall are used in validating these scale-up models. Production of a proposed performance model for the industrial plant is achieved in the Chapter six.

Chapter seven focuses on using the theories existing around recovery-by-size data as a basis for scale-up modelling. The Modular Simulator or ModSim is used to this end. ModSim is a computer-based simulation package specialising in mineral processing operations and built upon the population balance model (King, 2012). Opportunities for improvements on the ModSim models are presented and discussed in the light of the new data published in this thesis.

Chapter eight gives a summary of the main conclusions while answers to the research questions are provided. Finally, recommendations for future work or improvement opportunities are made with the view to expand the applicability of the proposed scale-up model.

Chapter 2 Literature review

In this chapter, past scientific works on froth flotation are critically reviewed. The body of knowledge covered is mainly linked to the research objectives set out for this doctoral study.

The need of this study is highlighted after considering the merits and shortcomings of existing flotation scale-up models. Emphasis is put on recent work, i.e. less than-ten years old, in order to capture the fast-paced theoretical developments made in flotation modelling. Finally, work older than ten years is scanned to ensure for completeness of the literature review.

2.1 Introduction

Flotation is the process that is used to separate valuable from valueless minerals on the basis of their difference in surface properties enhanced by the addition of reagents. Air bubbles are injected into the slurry consisting of a mixture of finely milled ore particles and water (Taggart, 1921; Gaudin *et al*., 1931; Zuniga, 1935, Zaidenberg, *et al.,* 1964; Wills and Napier-Munn, 2006; Radmehr *et al*., 2018). Having been rendered hydrophobic (i.e. water hating), valuable ore particles attach against air bubbles by true flotation. The particle-laden bubbles then rise up to the surface to form a layer of froth. On the other hand, valueless particles are made hydrophilic (i.e. easily attracted to water) and remain at the bottom of the flotation vessel.

Before flotation happens, the material is extracted from a mine after blasting. Heterogeneous rock fragments, known as run-of-mine (ROM), are produced with top size of approximately 300 mm (Minnitt, 2014). The ROM undergoes liberation by crushing and milling before it is sent to flotation. However, particles coarser than approximately 425 μm are known to be difficult to float (Kohmuench *et al*., 2018). This leads to their low recovery due to the excessive turbulence in

conventional mechanical flotation machines (Xian-ping *et al*., 2011; Hay and Rule, 2003; Hay, 2005; Sutherland, 1977). Flotation reagents plays a crucial role in making sure that recovery of valuable mineral is achieved. Most important reagents used are collectors which are the organic compounds that do a selective function on the surfaces of certain mineral particles (Egya-Mensah, 1999). The other reagent types are frother and these are the type of reagents that operate on surface by interacting with the water content of the slurry, and in so doing they reduce its surface tension which in turn allows for the formation of thin liquid films that make up the stable froth layer (Bhondayi, 2014). The regulatory reagents comprise activators and depressants that will encourage or supress mineral attachment to air bubbles, while controlling or regulating the pH of the flotation process (Wills and Napier-Munn, 2006).

Flotation takes place effectively within a certain size range generally referred to as the optimum or final grind. When the grind is finer than the optimum, then more reagents are utilised to get the required recovery (Pease *et al*., 2005). Conversely, a coarser grind necessitates longer flotation residence times and in the worst case, a regrinding section (Wills and Napier-Munn, 2006).

Pease *et al*. (2005) showed that flotation recovery varies as a function of particle size following the “n” shape illustrated in Figure 2.1. This “n” shape can be divided into three regions: the fine tail where liberated fines experience poor flotation, the coarse tail where unliberated particles are not recovered, and the plateau representing the optimum grind. Flotation recovery, mineral liberation and reagent dosage generally dictate the relative location of the three regions. Each should be monitored in a flotation plant with the view to widen the plateau region as much as possible.

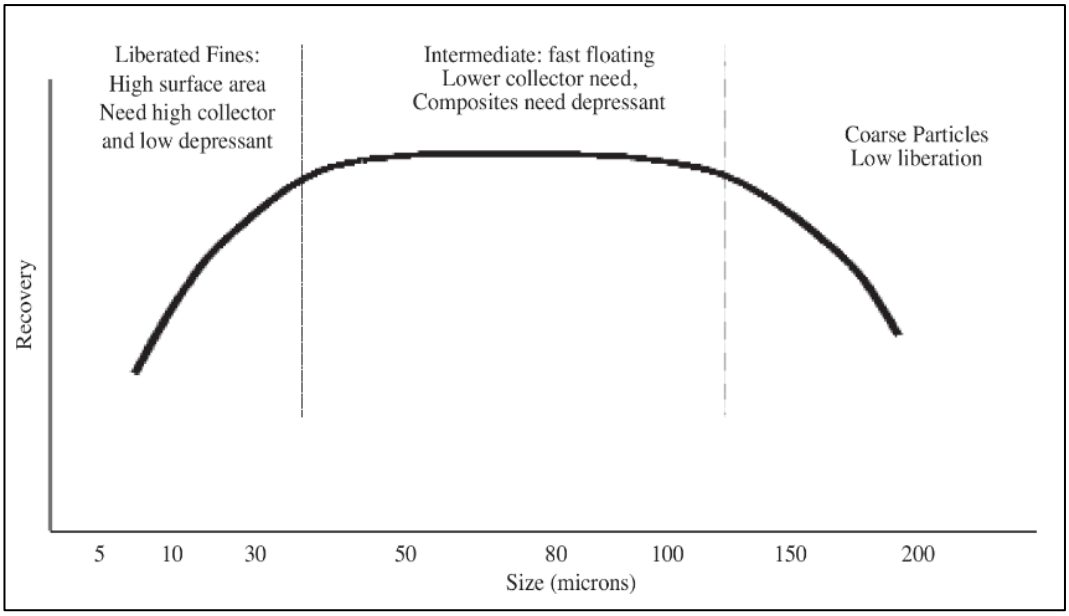

Figure 2.1: Typical recovery-by-size curve (Pease *et al*., 2005)

The flotation process is commonly employed for the selective separation of a mineral species from a liquid-solid suspension of both valuable and unwanted gangue mineral particles (Gorain *et al*., 2000). There are factors that need to be considered in order for the flotation process to achieve its goal. In case such factors are not observed properly; then, the process may be unsuccessful and result in loss of revenue for the business.

The next section looks at the most important factors and gives insight into each for a better understanding of their individual contribution to the whole process.

2.2 Factors determining flotation performance

There exist two types of flotation processes: dispersed and dissolved (Peleka and Matis, 2016). In dispersed-air flotation, air is put in the system by propellers or pumped by diffusers with bubble size achieved in the range of 100 – 1000 µm. In contrast, dissolved-air flotation deals with clarifying wastewaters by removal of suspended oil or solids. Air is dissolved in the wastewater by applying pressure and releasing it in a flotation tank. This produces tiny bubbles that adhere to the suspended matter and float to the surface where they are removed by skimming.

The factors that affect dispersed flotation can be categorised into four groups: ore properties, hydrodynamic properties, design variables, and operational variables (Smar *et al*., 1994). They are discussed for dispersed flotation in line with the scope of this thesis.

2.2.1 Ore properties

Ore properties refer to particle size, floatability, particle shape, mineralogy, slurry feed density, and feed grade to name just the most important ones in flotation.

2.2.1.1 Particle size

The primary function of particle analysis is to obtain quantitative data about the size distribution of particles in the material (Wills and Napier-Munn, 2006). In flotation operations, particles of size between 5 µm and 10 µm are generally considered to be fine; they are coarse when larger than 70 µm while anything in between is intermediate (Trahar, 1981; Bhondayi, 2014).

Trahar and Warren (1976) were able to demonstrate that flotation performance degrades with particle fineness. They also found that the effects of particle size on recovery, grade, and flotation rate are more complex than normal. This and the work of others e.g. Sutherland (1981 & 1989); Multani and Walters (2019) and Kohmuench *et al*. (2018) show that particle size does play a great role in flotation.

It must be noted that the exact size of irregular particles cannot be accurately measured. Terms like length, breadth, thickness or diameter have little meaning because so many different values of these quantities can be determined (Allen, 1997). Despite this, particle analysis by for example sieving, are conventionally represented in the form of a particle size distribution (PSD) as shown in Figure 2.2.

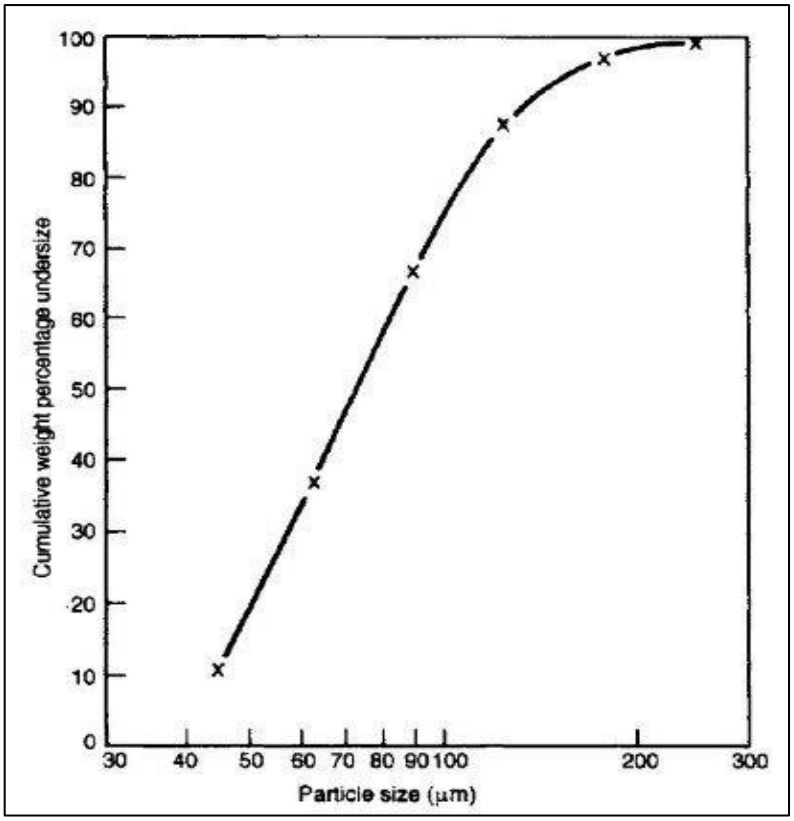

Figure 2.2: Particle size distribution (PSD) from screen analysis (Wills and Napier-Munn, 2006)

2.2.1.2 Floatability

Floatability can be regarded as a kinetic characteristic that incorporates other particle properties affecting their amenability to flotation (Woods, 1994). It refers to the fact that particles in a flotation cell are either hydrophobic (move away from water) or hydrophilic (move towards water). Indeed, when air bubbles shed their load of particles, hydrophobic particles are most likely to re-attach to the air bubbles rising up from below. On the other hand, hydrophilic particles generally making up the valueless material or gangue get lost (Bennie, 2013).

Gorain *et al*. (1998) were able to express flotation kinetics as a function of floatability as shown below:

$$k = P.S_b.R_f \qquad (2.1)$$

where k is first order rate constant; P is a dimensionless floatability constant; S_b is bubble surface area flux; and R_f is fractional froth recovery.

Equation (2.1) shows a strong dependency of flotation rate or the rate at which particles are floated out of slurry with their floatability, i.e., propensity to float.

2.2.1.3 Particle shape

In the flotation separation process, particle shape plays a significant role in the attachment and detachment of particles against bubbles (Ma *et al*., 2018). This is because the shape of a particle defines sites on its surface against which the particle can attach to a bubble. Descriptions like granular or acicular are usually adequate to convey the approximate shape of the particle in question (Wills and Napier-Munn, 2006). But in practice, quantifying shape has been challenging.

2.2.1.4 Mineralogy

Mineralogy refers to the information pertaining to the relative abundance of minerals, the liberation characteristics of valuable minerals, as well as mineral grain and mineral association (Evans *et al*., 2011). Instruments for mineralogical analysis include scanning electron microscope (SEM), backscattered-electron (BSE) microscope, and energy dispersive spectrometry (EDS) (Bushell, 2012). Figure 2.3 shows an example of the output of mineralogical analysis where a quantitative evaluation of minerals by scanning electron microscopy (QEMSCAN) was used. Free refers to particles with > 95% of their surface identified as the given mineral and Liberated refers to particles with > 80% of their surface as the given mineral (Jordens *et al*., 2016). Binary is the situation when particles are mixtures of different minerals which may also consist of gangue and this is usually a great deal more complicated (Jordens *et al*., 2016). The breakdown of mineral flotation recovery by mineral association aids in determining the effectiveness of reagents on different minerals.

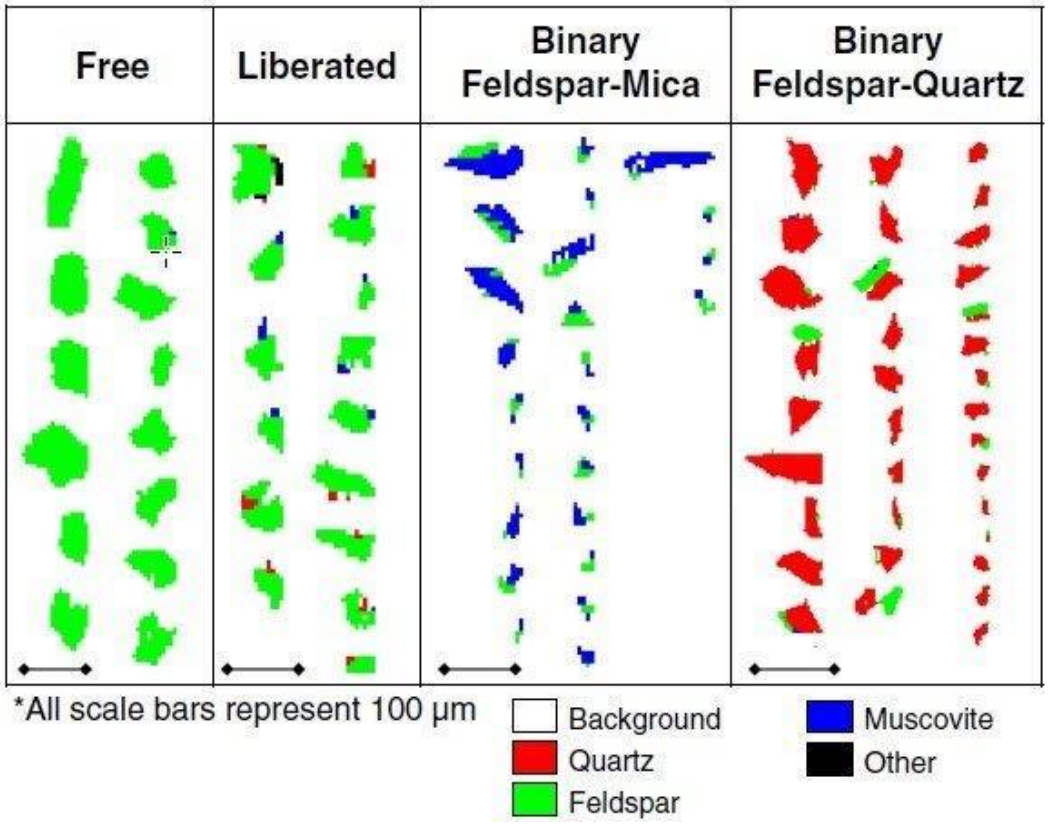

Figure 2.3: Classification according to mineral association for particles in the flotation concentrate containing feldspar (Jordens *et al*., 2016)

Mineralogical data provide a direct output that highlights the metallurgical properties and recoverability of the desired particles in samples gathered from strategic locations in the flotation recovery plant (Bushel, 2012). It can then be said that, the flotation performance of an ore is determined by its mineralogy.

2.2.1.5 Slurry feed density

This is measured in terms of mass per volume (t/m^3 or kg/m^3) or fraction of solids by weight. Flotation cells require a certain amount of solid particles in the slurry feed to operate optimally. This has been reported to be between 55 % and 70 % solids by weight (Wills and Napier-Munn, 2006).

2.2.1.6 Feed grade

Grade is defined as percentage purity of the material of interest which can be in the feed, concentrate and tailings (Wills and Napier-Munn, 2006). Figure 2.4 shows the relation between apatite (P_2O_5) feed grade (content) and recovery including bubble size. In order to meet the requirements of the phosphate industry then the P_2O_5 feed grade must be > 30 % and P_2O_5 recovery should be > 60 % (Reis *et al*., 2020). In this case, 30 % of P_2O_5 is its cut-off feed grade meaning below this feed grade then it will not be economical to process phosphate as recoveries will be lower than the minimum required by the plant. Different minerals have different cut-off feed grades and these are characterised by different plant recovery requirements.

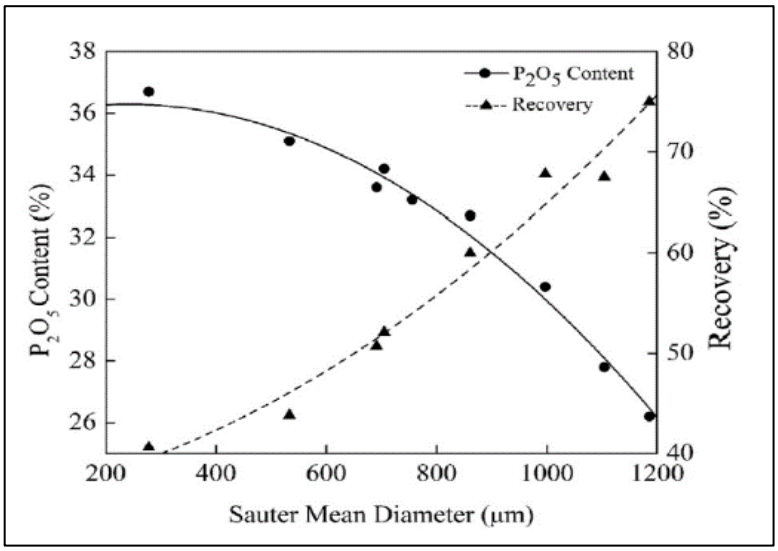

Figure 2.4: Relationship of P_2O_5 feed grade and recovery (%) using Sauter mean diameter (microns) (Reis *et al*., 2020)

2.2.2 Hydrodynamic properties

Hydrodynamics properties that can be said to largely influence flotation performance include bubble size, bubble surface area flux, entrainment, entrapment, and superficial gas velocity. Their effects on flotation have received significant attention in the last two decades (Rodrigues *et al*., 2001; Yianatos and Contreras, 2010; Steyn, 2012; Ding and Gustafsson, 2000; Ferreira and Loveday,

2000). Of particular interest has been the development of theoretical models describing the micro-processes of collision, attachment, detachment and bubble stability during flotation (Newell, 2006). The theoretical models are discussed in the subsequent sections.

2.2.2.1 Bubble size

It has been generally accepted that bubbles created in mechanical flotation cells of all designs are of size between 0.1 and 1 mm (Wills and Napier, 2006; Gorain *et al*., 1998; Gorain *et al*., 1999; Hernandez-Aguilar *et al*., 2004).

The mean diameter of a distribution of bubbles of different sizes can be expressed as an arithmetic mean:

$$d_b = \frac{\sum_{i=1}^{i=n} d_i}{n} \tag{2.2}$$

where d_i is equivalent spherical diameter and n is the number of bubbles.

Equation (2.2) is appropriate for describing physical processes where the mean value of the population is needed. But, in the flotation processes the main function of bubbles is to collide with particles and carry the values into the concentrate (Egya-Mensah, 1998). The bubble surface area therefore is the main size factor and thus the probability of a collision between bubble and particle is directly proportional to the area presented by the bubble (Jameson and Allum, 1984).

2.2.2.2 Bubble surface area flux

Bubble surface area flux can be defined as the rate of production of bubble surface area in the cell per unit of surface area of the cell (Jameson and Allum, 1984). It is mathematically defined as follows:

$$S_b = \frac{6\,J_g}{\varepsilon_g} \tag{2.3}$$

where: S_b is the bubble surface area per unit volume of pulp (m^2/m^2s)

J_g is the volumetric air flowrate (m^3/s) per m^2 of cell cross-sectional area

ε_g is the gas holdup m^3 air per m^3 pulp

6 is the constant assumed for spherical and uniform bubbles.

Gorain *et al*. (1996) compared different studies as shown in Figure 2.5; they were subsequently able to show that a linear relationship exists between bubble surface area flux and flotation rate constant. In mathematical terms, this can be expressed as follows:

$$k = P * S_b + Z \quad (2.4)$$

where: k is the flotation rate constant

P is the proportionality constant that is a function of ore type and pulp chemistry

Z is a constant usually at zero (0) or maybe less than zero (< 0)

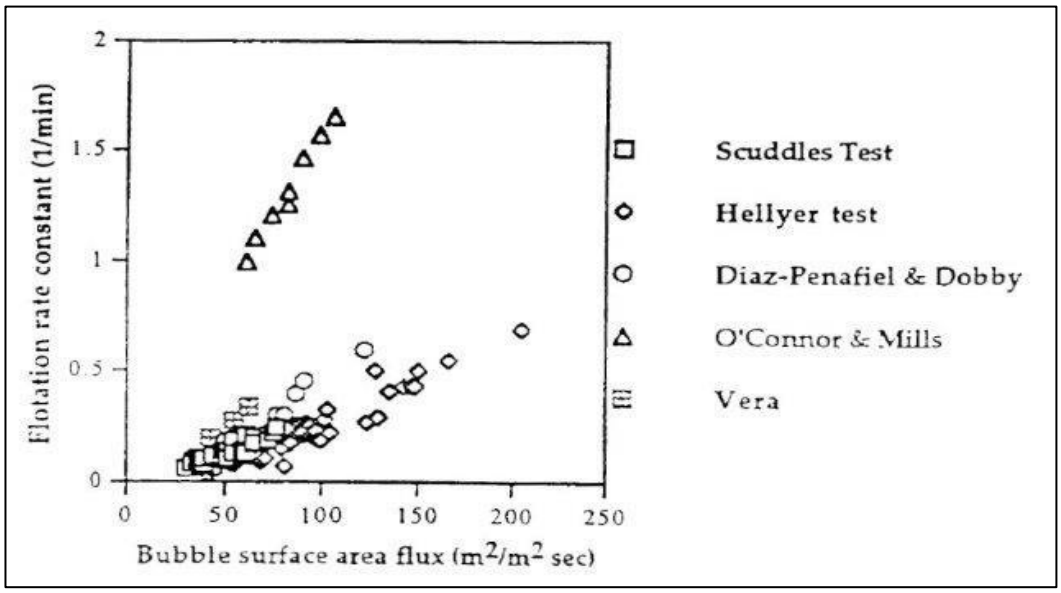

Figure 2.5: Comparison of S_b and K done from work by different researchers (Gorain, *et al*., 1996)

Alexander *et al*. (2000) compared the flotation rate constant of a pilot cell to that of an industrial cell over a range of surface area flux values. They observed that

not only does Equation (2.4) hold but also that the equation may be independent of operating parameters and dimensions of the cell as shown in Figure 2.6.

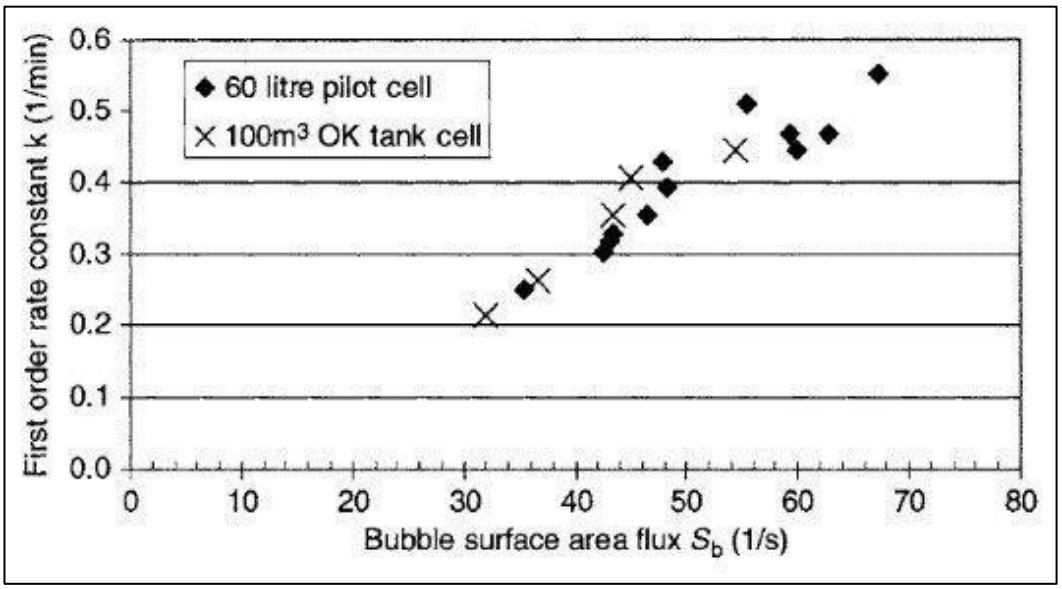

Figure 2.6: First order rate constant and bubble surface area flux relationship in a 60 litre pilot cell and a 100 cubic meters OK cell (Alexander *et al*., 2000)

2.2.2.3 Entrainment

Smith and Warren (1989) described entrainment as the process by which particles enter the base of flotation froth and are transferred up and out of the flotation cell suspended in the water between bubbles. There is usually two mechanisms that explain entrainment: the first is for unattached particles to be carried upwards in bubble lamellae (Moys, 1978) and the second where particles are carried in the wake of ascending air bubbles (Yianatos *et al*., 1986).

Entrainment should be avoided in flotation as it lowers the concentrate grade owing to low selectivity between gangue and valuable materials. Zheng *et al*. (2005) have developed a relationship to that end:

$$R_{ent,i} = ENT_i * R_w \quad (2.5)$$

where: $R_{ent,i}$ is the recovery of particles by entrainment of i^{th} size class

R_w is the water recovery

ENT_i is the degree of entrainment defined as follows:

$$ENT_i = \frac{mass\ of\ free\ gangue\ particles\ of\ the\ i^{th}\ size\ class\ /\ unit\ of\ water\ in\ concentrate}{mass\ of\ free\ gangue\ of\ the\ i^{th}\ size\ class\ /\ unit\ of\ water\ in\ the\ pulp} \quad (2.6)$$

2.2.2.4 Entrapment

This is the process whereby particles are physically entrapped in between the froth attached to air bubbles. It may also be referred to as aggregation (Wills and Napier-Munn, 2006).

Entrapment is non-selective as both gangue and valuable minerals are indiscriminately likely to be recovered by this process. Zheng *et al*. (2006) have shown that entrapment is closely related to the froth structure.

2.2.2.5 Superficial gas velocity

The superficial gas velocity can be described as the volumetric flowrate of bubbles through the flotation cell per unit cross-sectional area of the cell (Egya-Mensah, 1998). The difference in superficial gas velocity at different locations gives an indication of the air dispersion characteristics in the cell (Schubert *et al*., 1982).

Figure 2.7 shows the dependency of the superficial gas velocity with the air flowrate in flotation cells from various manufacturers (Gorain *et al*., 1996; Egya-Mensah, 1998).

The observation captured in Figure 2.7 subsequently led to the mathematical definition of superficial gas velocity:

$$J_g = \frac{Q_g}{A} \quad (2.7)$$

where: J_g is the superficial gas velocity (m/min)

Q_g is the air flowrate into the cell (m^3/min)

A is the cross-sectional area of the cell (m^2).

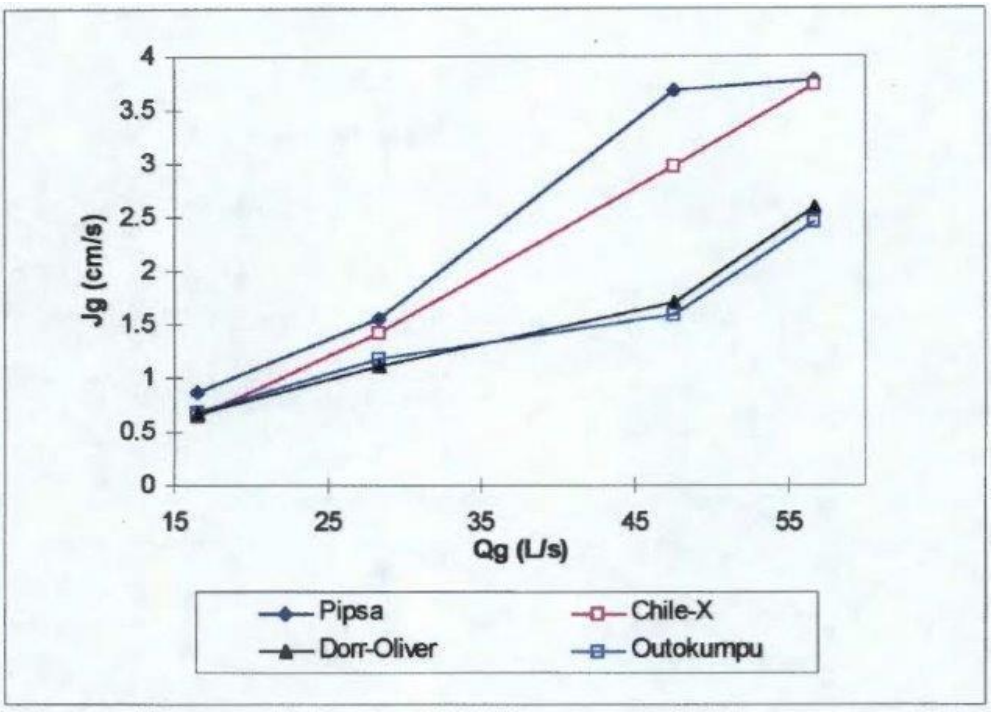

Figure 2.7: Effect of air flowrate (Qg) on superficial gas velocity (Jg) produced by different impellers at constant impeller speed (Gorain *et al*., 1996; Egya-Mensah, 1998)

2.2.3 Design variables

This section looks into some key design variables or parameters that need to be considered during the design stage of the continuous flotation plant. Such variables need to be carefully thought of as they are permanent for the lifespan of the plant. A brief description are given to the following: plant capacity, number of stages, plant configuration and cell volume.

2.2.3.1 Plant capacity

This relates to the throughput given in tons per hour (t/h or tph) that the flotation plant is designed to handle under normal conditions.

Factors that influence plant capacity relate to residence time in flotation banks, circuit stream destination and cell operating parameters such as froth depth, air flowrate, and mass pull (Harris *et al*., 2013).

Operating the flotation plant over its design plant capacity may lead to the overflowing of launders, mechanical equipment failures, lower recoveries and poor concentrate grades.

2.2.3.2 Number of stages

The number of stages in a flotation circuit to utilise is usually determined as part of the scale-up design criteria. Yianatos (2003) pointed out that the design of flotation cells is often a matter of experience combined with judgement. He further argued that this is also the result of a certain level of prejudice rather than design from a detailed analysis based on first principles like scale-up methods.

In determining the number of stages using scale-up design criteria, the main dimensionless groups considered are the Froude number, the power number and the air flow number (Fallenius, 1979). These dimensionless numbers are further explored in Section 2.8.

2.2.3.3 Plant configuration

Flotation cells in the plant can be arranged either in series or in parallel. Egya-Mensah (2006) reported that the configuration in series has cells usually shaped and partitioned into two or more cells. This enables easy interconnection and easy pulp flow along the bank.

A simple flotation plant configuration is exemplified in Figure 2.8; however, actual configurations can get more complicated. The main reason for this is the quest for a stable operation that meets the specifications of the final concentrate needed.

And in this quest, Wills and Napier-Munn (2006) for example have proposed a way of smoothing out grade fluctuations and providing a smooth flow to the plant.

They recommended that a large storage agitator be interposed between the grinding section and the flotation plant. In doing so, variations in grade and tonnage are smoothed by the storage agitator from which material is pumped at a controlled rate to the flotation plant.

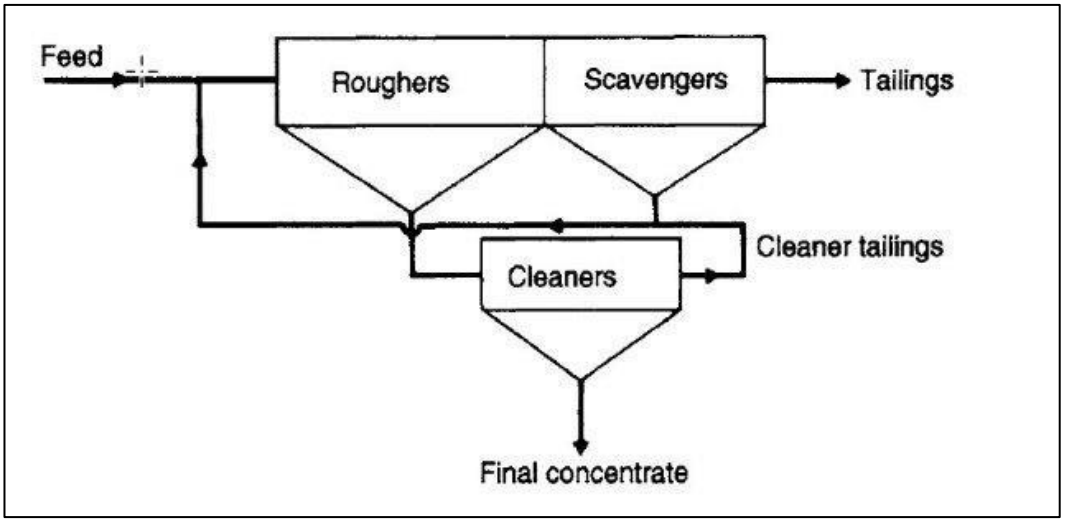

Figure 2.8: Simple rougher-scavenger-cleaner flotation plant configuration (Wills and Napier-Munn, 2006)

Hu (2014) regards a continuous flotation circuit as a plant configuration consisting of a bank of cells connected in series with recycles to improve final recovery and grade. From that point of view, the circuit can be made up of four main stages: roughing, scavenging, cleaning, and re-cleaning.

The rougher section refers to the first bank of cells that treats the fresh flotation feed, where the majority of the valuable material will be recovered. The scavenging section or scavenger is the bank of cells that treats the barren (less valuable minerals for recovery) tails from the roughers. The aim of a scavenger is to maximise recovery, and the tailings are discarded. Some flotation plants may do without a scavenging section. A cleaner is the term used for the bank of cells that cleans the concentrates from the roughers to reduce the amount of gangue (unwanted material) in the product. The tailings of the cleaners contain a significant amount of valuable material and are often recycled back to the roughers. Last is the re-cleaner or the bank that follows the cleaners. It is the final

upgrading of the concentrate before it leaves the flotation circuit. The tailings from the re-cleaners are generally recycled back to the cleaners feed.

2.2.3.4 Cell volume

Flotation cell volumes can go as high as 300 m^3 or above. Gorain *et al*. (2000) have noted several advantages of installing larger cell volumes including a reduction in capital costs, plant size, power consumption, maintenance, reagent consumption and easy process control.

Harris and Lepetic (1966) have developed a correlation of the cell effective volume (V) and cell diameter (T) described as:

$$V = KT^{N_f} \tag{2.8}$$

Parameters K and N_f are constants characteristic of the type of flotation cell and its manufacturer. Their respective values have mostly been found to be $2 < N_f < 3$ and $0.6 < K < 1.3$ with typical values of N_f = 2.6 and K = 0.9 (Egya-Mensah, 2006).

2.2.4 Operational variables

Operational variables include mass pull, froth depth, air rate, and reagent dosage. These variables have an impact on the final flotation product and therefore need to be controlled within acceptable limits.

2.2.4.1 Mass pull

The mass recovery (also known as mass pull or pulling rate) is defined as the percentage ratio of the recovered material in the concentrate to the amount of feed material in the flotation circuit:

$$\%Mass\ pull = \frac{Mass\ of\ concentrate}{Mass\ of\ feed} * 100 \tag{2.9}$$

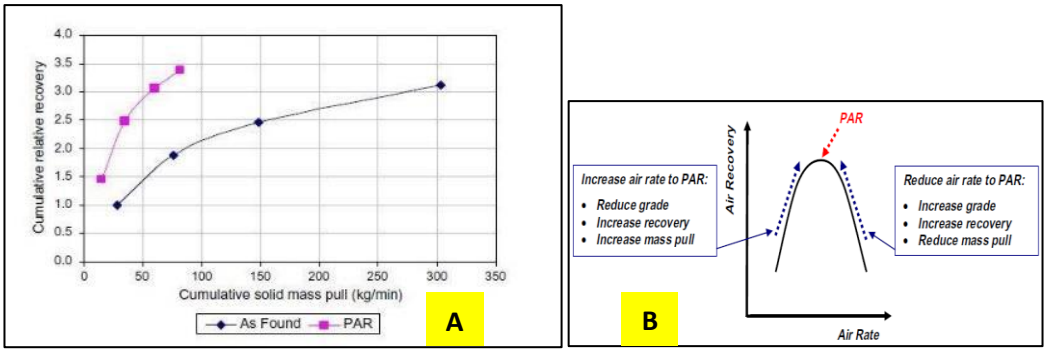

Figure 2.9: Relationship between cumulative mass pull and cumulative Pt recovery for the two air profiles at Western Limb Tailings Re-treatment Plant –WLTRP [A] and general effect of air recovery optimisation on flotation performance [B] (Hadler *et al*., 2010)

Hadler *et al*. (2010) studied the effect of mass pull on flotation recovery. They noted an increase in cumulative recovery for a marked drop in mass pull as shown in Figure 2.9[A]. This was obtained as the air rate was reduced from As Found to Peak Air Recovery (PAR) values as also supported in Figure 2.9[B].

In another separate study, Hay (2010) reported a strong dependency of mass pull with chromite (Cr_2O_3) grade for all flotation streams that were surveyed as shown in Figure 2.10.

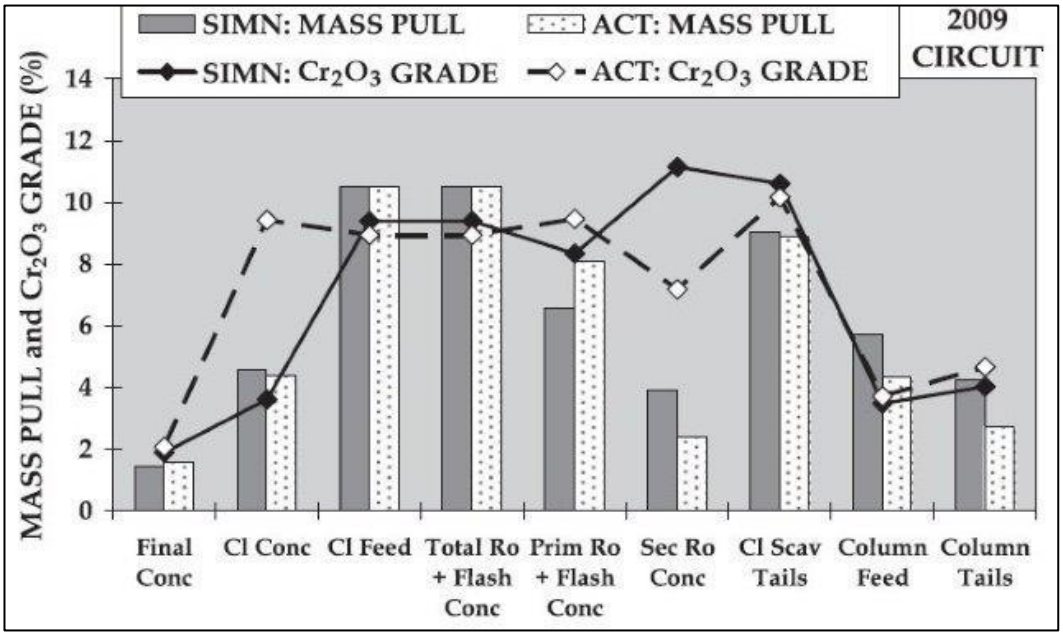

Figure 2.10: Simulated vs. actual: Northam circuit – 2009 (Hay, 2010)

In recent times, it has become possible to automate the mass pull control such that an algorithm is set to calculate optimum level set-points or aeration rates (Singh *et al*., 2003; Muller *et al*., 2010).

2.2.4.2 Froth depth

Operationally, froth depth can be measured with a manual froth depth measuring equipment or an automated on-line sensing device.

Perez-Garibay *et al*. (2010) have shown that there is a relationship between froth depth and air recovery. They used data collected on a laboratory scale flotation column where air recovery was observed to decrease as froth depth increased. Another study, Farrokhpay (2011) showed that an optimum froth depth exists at which higher mineral recovery can be obtained.

It can finally be seen in Figure 2.11 that concentrate grade increases with froth depth in both runs. Similar trends are observed in the dropback grade. This implies that a large number of valuable particles detach from the froth zone in deeper froths (Rahman *et al*., 2015). Note that the dropback reported in Figure 2.11 is achieved by having froth directly collecting detached particles from froth zone without allowing them to recirculate in between pulp and froth zone. In this case then, changes in froth depth are not expected to significantly impact on the collection zone.

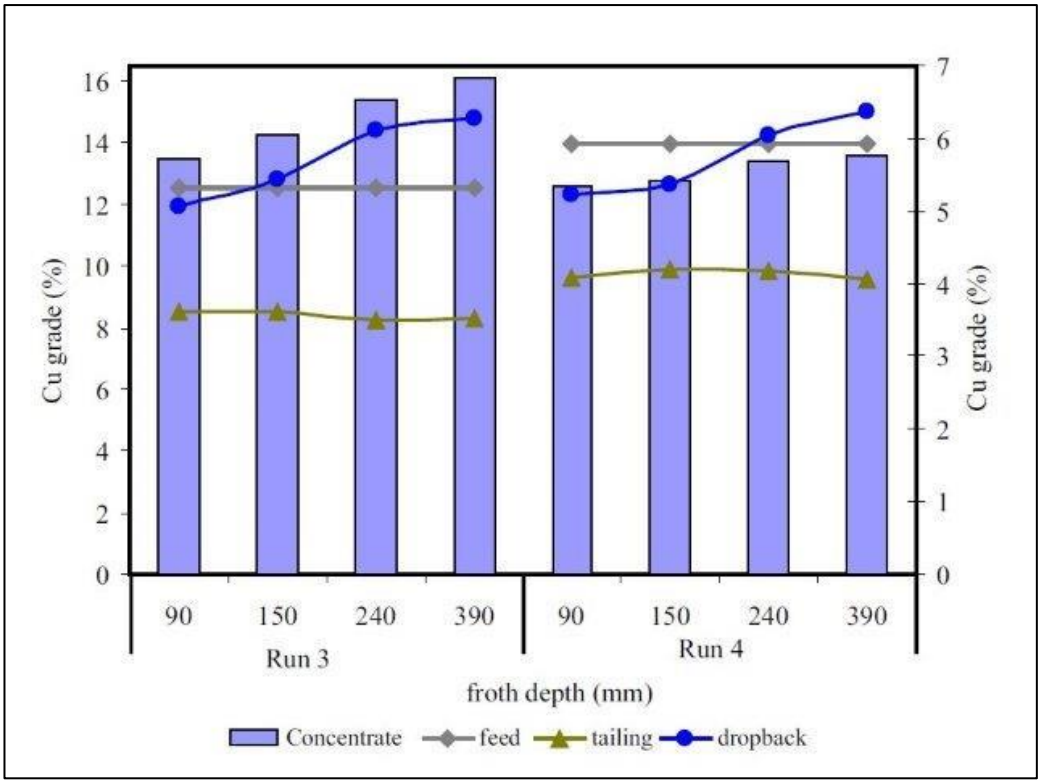

Figure 2.11: Overall Cu grade as a function of froth depth where left axis – concentrate grade & right axis – feed, tailings plus dropback particles grade (Rahman *et al*., 2015)

2.2.4.3 Air rate (air flowrate)

Successful flotation requires the addition of air at a certain rate generally termed as air rate or air flowrate. The air entering flotation cell forms different cavities behind the blades of the impellers where it gets dispersed to the pulp as shown in Figure 2.12.

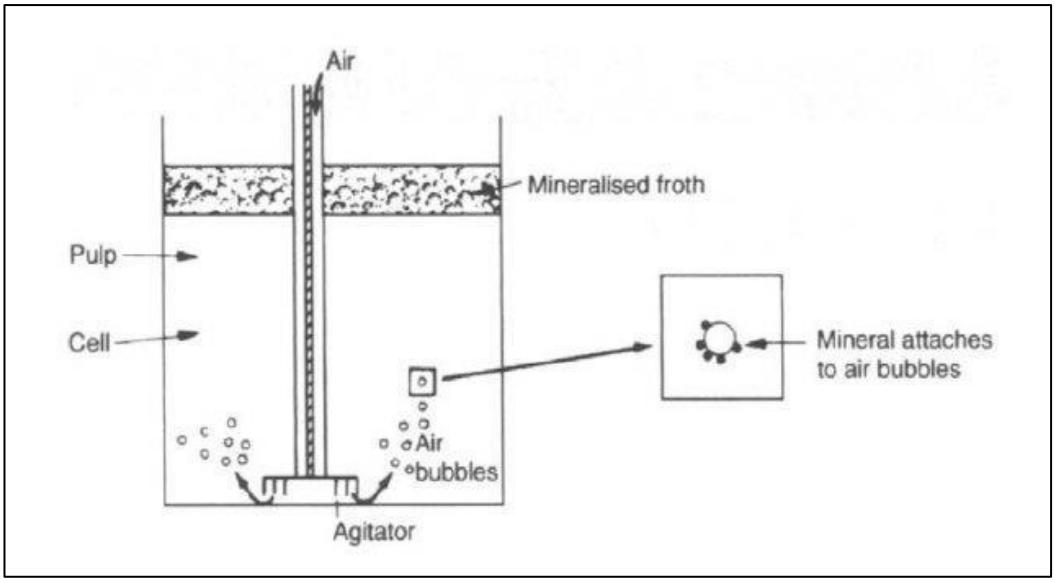

Figure 2.12: Principles of flotation – air addition in a cell

(Wills and Napier-Munn, 2006)

According to Van't Riet and Smith (1974), there are four different types of air cavities that form behind the impeller; namely, vortex, clinging, large, and 3-3 cavities. It is important to study these various air cavities in gas dispersion because of their effects on the power draw, the liquid pumping capacity of the impeller, the liquid hydrodynamics around the impeller, the gas dispersion and the mass transport. Research showed that at low air flow number < 0.01, gas is captured by the vortex system to form vortex air cavities while with high air flow number > 0.03, large cavities are formed behind the impeller blades (Nienow and Wisdom, 1974; Bruijn *et al*., 1974; Egya-Mensah, 1998).

In addition to the above, there is compelling evidence to suggest that the type of impeller also has a bearing on the formation of cavities. Figure 2.13 for example shows that bubble size is sensitive to the type of impeller. Indeed, impellers manufactured by Outokumpu produced the smallest bubble size at all air flowrates tested while Pipsa had the largest bubble size in the same range of air flowrates.

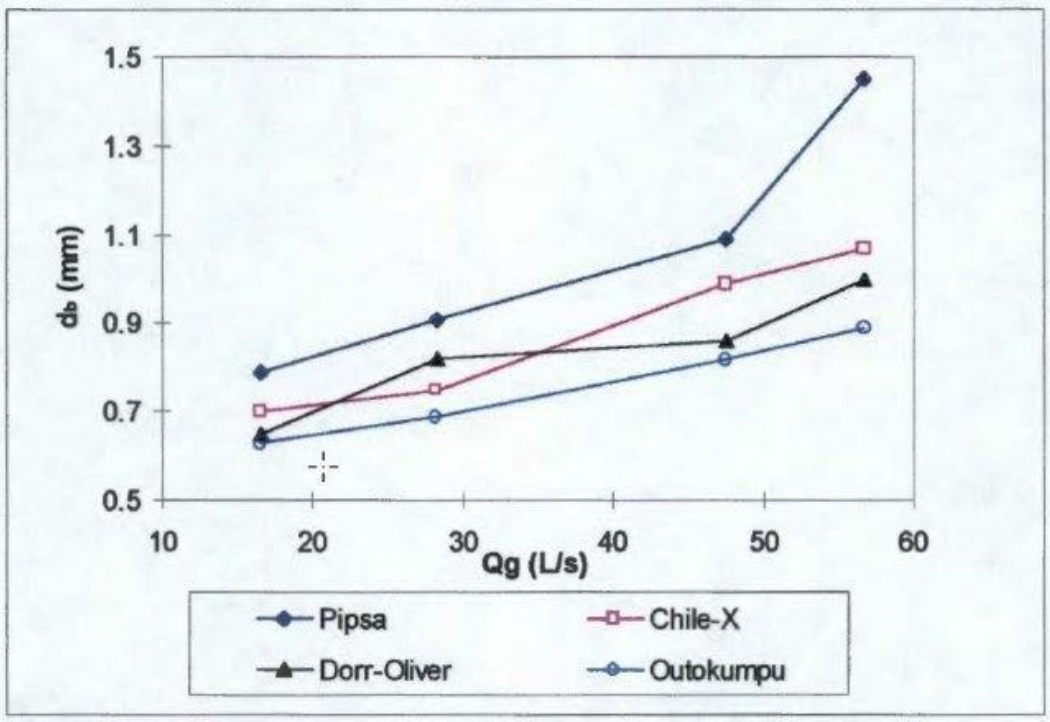

Figure 2.13: Effect of air flowrate (Qg) on mean bubble size (d_b) produced by different impeller systems at constant impeller speed (Gorain *et al*., 1995; Egya-Mensah 1998)

2.2.4.4 Reagent dosage

The role of flotation reagents is to assist with the recovery of valuable minerals. This is done by causing mineral particles to rise with bubbles to the surface while inhibiting the gangue from rising.

The chemical condition of the pulp in the flotation tank is key to ensuring that optimal performance is obtained. Indeed, there is a certain degree of hydrophobicity that a desired mineral should have to effectively attach to a bubble and separate from the gangue minerals (Bhondayi, 2014). Three classes of reagents are primarily used in flotation: collectors, frothers, and regulators.

Collectors are organic compounds that perform a selective function on the surfaces of certain mineral particles. They attach to the water-mineral interface and render the particle hydrophobic. Molecules or ions of the collector in turn

adsorb and ensures the attachment of particles to air bubbles (Egya-Mensah, 1998).

Frothers are the type of reagents that operate on surface by interacting with the water content of slurry. In so doing, they reduce its surface tension which then allows the formation of thin liquid films. This makes up the stable froth layer and consequently strong and long-lasting bubbles that can carry particles without breaking easily (Bhondayi, 2014).

Nazari *et al*. (2018) studied the effect of frother at various impeller speeds, air flowrates and particle sizes. They found that nanometre-sized bubbles increased the recovery of particles of size -212 +106 µm more than that of sizes -300 +212 µm and -425 +300 µm.

Regulators, also known as regulatory reagents, comprise of activators and depressants. They encourage or supress mineral attachment to air bubbles while controlling or regulating the pH of the flotation process (Wills and Napier-Munn, 2006).

In practice, a series of laboratory batch flotation tests needs to be conducted before the flotation circuit designer is able to determine the reagent best suited to a plant for the ore being processed. As part of continuous improvement, reagent testing is something that needs to be done frequently. This is because of the new reagents constantly flooding the market as well as the characteristics of the ore changing with time.

From the discussion covered so far, it is evident that all the factors mentioned have a unique role to play in the recovery and final grade of a flotation circuit. One thing is also clear: froth flotation whether batch or continuous has a multi-component, multi-variable, and complex nature. The next sections review amongst others the relationship between batch and continuous flotation.

2.3 Mineral liberation

Liberation is described as the release of the valuable minerals from the associated gangue minerals at the coarsest possible particle size (Wills and Napier-Munn, 2006). Mineral liberation is mostly achieved by comminution or rock breaking as a pre-requisite for the downstream operations like flotation. A brief description of how liberation can be characterised is given in this section.

2.3.1 Fragmentation

Barbery (1991) came up with the term of random uniform isotropic fragmentation which describes pure trans-granular breakage, random breakage and interfacial area conservation. His seminal work has since steered to the development of measurement techniques of quantifying phase boundary fracture.

Little *et al*. (2016) are arguably the latest who have explored the interrelation between mineral liberation, particle fracture, and flotation response. They noted wide variations in the deportment of certain minerals to different size fractions after fragmentation. They therefore argued that flotation response can provide a good indication of whether non-random breakage occurred or not. Although the findings have scientific value, the researchers cautioned that flotation response could not discriminate between preferential breakage and phase boundary fracture.

2.3.2 Shape characterisation

The shape of a mineral particle affects the basic interactions of that particle with water, air and other particles or equipment (Little *et al*., 2015). There exist numerous techniques for the characterisation of particle shape. In the context of mineral processing applications, parametrical and harmonical analyses are the most prominent (Pirard, 1989).

Parametrical analysis involves descriptors based on basic dimensions of a particle or two-dimensional projections of the particle. The descriptors such as Ferret

diameter, aspect ratio, angularity and roundness can be produced. Harmonical analysis, on the other hand, resorts to advanced concepts like Fourier analysis and fractal analysis. It basically uses a function or a set of coefficients to describe an object which in this case would be the shape of the mineral particle (Little *et al*., 2015). Table 2.1 summarises the three key descriptors of particle shape that are finding wide use and acceptance in mineral processing operations.

Table 2.1: Particle shape descriptors (Little *et al*., 2015)

Descriptor	**Formula**	**Inverse**
Aspect ratio	$\frac{Long\ axis}{Short\ axis}$	$\frac{Long\ axis}{Short\ axis}$
Cicularity	$\frac{4\pi\ .Area}{Perimeter^2}$	Angularity - $\frac{4\pi\ .Area}{Perimeter^2}$
Roundness	$\frac{4\ .\ Area}{\pi\ .Long\ axis^2}$	$\frac{\pi\ .Long\ axis^2}{4\ .Area}$

2.3.3 Quantifying mineral liberation

Mineral liberation can be measured as the fraction of the mineral specie within the particle containing it. That is why it is usually presented as a composition distribution showing the proportions of particles with a range of compositions.

Figure 2.14 shows an example of enclosed mineral species with a platinum bearing rock matrix. Such mineral textures can be described using categorical variables including liberated platinum group minerals (PGM), PGM associated with base metal sulphides (BMS), PGM enclosed within silicate or oxide gangue, and PGM attached to silicate or oxide gangue particles.

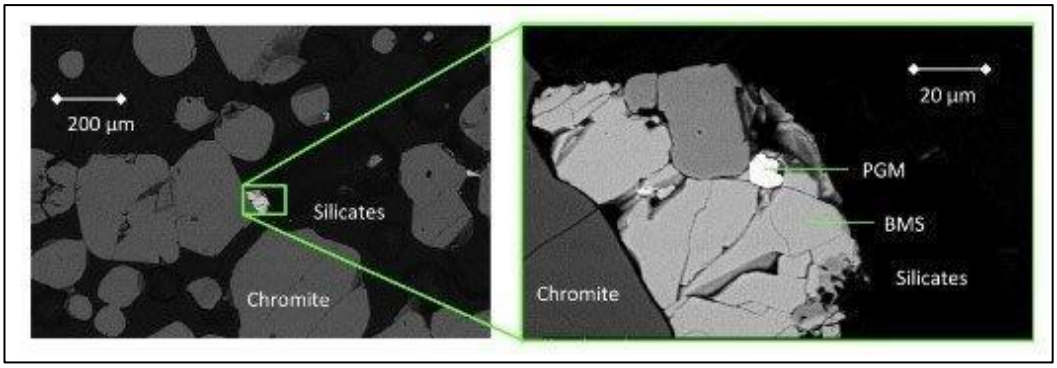

Figure 2.14: PGM categorical variables from backscattered electron images of the platinum bearing reef known as UG2 (Little *et al*., 2016)

Nowadays, the quantification of liberation is routinely done using the dedicated scanning electron microscope known as mineral liberation analyser (MLA). Techniques such as the quantitative evaluation of minerals by scanning electron microscopy (QEMSCAN) and the automated scanning electron microscopy with energy dispersive X-ray spectrometry (auto-SEM-EDS) system are also utilised.

Concentrators are increasingly using automated systems to monitor the degree of mineral liberation in their processes. Thousands of two-dimensional cross-sectional images of particles are obtained and the associated EDS information and accompanying software allow for detailed mineralogical analysis of the particles within the sample. Equivalent sphere diameters are estimated from the intercept length of cross-sectional boundaries of grains. Stereological corrections are finally done to account for the transformation from three to two dimensions (King and Schneider, 1998; Wills and Napier-Munn, 2006; Little *et al*., 2016).

It is widely accepted that the knowledge of mineral liberation is key to a successful flotation. This means that in comminution, liberation should be recognised as a performance indicator more important than particle size. This is because the degree of liberation of valuable minerals almost solely dictates the theoretically achievable grade-recovery curve of a downstream separation process (Little *et al*., 2016). A lot of development is still needed around mineral liberation but proxies such as flotation response will continue to be used. This is likely to remain until

such time when liberation information can be obtained accurately at a shorter turnaround time.

2.4 Experimental measurement of flotation performance

This section will look into the types of flotation testing that can be done mainly in the laboratory to determine flotation performance. Since flotation plays a crucial role in the mineral value chain then it is required to accurately quantify its impact in determining flotation performance. The coverage of this section takes into account the types of batch flotation tests like simple batch flotation test, lock-cycle flotation testing, recovery-by-size flotation testing including its model and lastly continuous flotation testing.

2.4.1 Types of batch flotation tests

Batch flotation test is an acceptable metallurgical method to evaluate the flotation behaviour of the ore on a small scale. A wide volume of research done in academia and research institutes makes use of batch flotation testing. Operating mines also have internal departments that embark on routine batch flotation testing programmes to improve plant performance. Some mines may occasionally outsource such a service.

Runge (2010) argued that batch flotation tests were traditionally performed for four main reasons: first, to determine the ultimate flotation design; second, to screen potential reagents; third, to determine the optimum feed grind size; and last, to predict the change in performance of different ore types. In addition to this, batch flotation tests can be used in combination with plant data. Done that way, the approach enables one to explore potential improvements in plant performance through simulation (Ramlall and Loveday, 2015).

Batch flotation tests may be classified into three categories: rougher/scavenger batch flotation tests, cleaner batch flotation tests, and lock-cycle batch flotation tests.

The primary objective of rougher/scavenger batch flotation test is to determine the optimum primary grind to a rougher flotation, reagent scheme and reagent dosages (Sousa *et al.*, 2017). The test is mainly done on the run of mine (ROM) that is collected, properly prepared, and floated in the laboratory. In some instances, the feed reporting to the roughers or scavengers may be collected and floated in the laboratory as is. This is usually referred to as hot batch flotation test.

The cleaner batch flotation test usually follows rougher/scavenger batch flotation test. In this test, concentrates from rougher/scavenger batch flotation test are taken and further floated. As such, the results from cleaner batch flotation is indicative of the cleaner circuit performance. The latter is estimated in terms of mineral recovery, reagent selectivity and ability to achieve required mineral concentrate grades.

The lock-cycle batch flotation test is centred on testing middlings in the form of cleaner tails as well as scavenger concentrates and tails, as seen in Figure 2.15. The middlings are recycled to the appropriate flotation stage in the subsequent testing cycle. This is to simulate the continuous process operation using bench scale batch flotation equipment (Wills and Napier-Munn, 2006). According to Agar (2000), lock-cycle tests are frequently used in mineral processing laboratories during the flowsheet development exercise in order to confirm batch results and to get an approximation of a continuous circuit material balance. It can be argued that lock-cycle batch flotation testing may show the performance of the recleaner circuit which is usually the final stage of the flotation circuit. The downside of the lock-cycle flotation tests includes but is not limited to: difficult to conduct it properly, expensive to execute it and lock-cycle tests are prone to failure in reaching steady state (Agar, 2000).

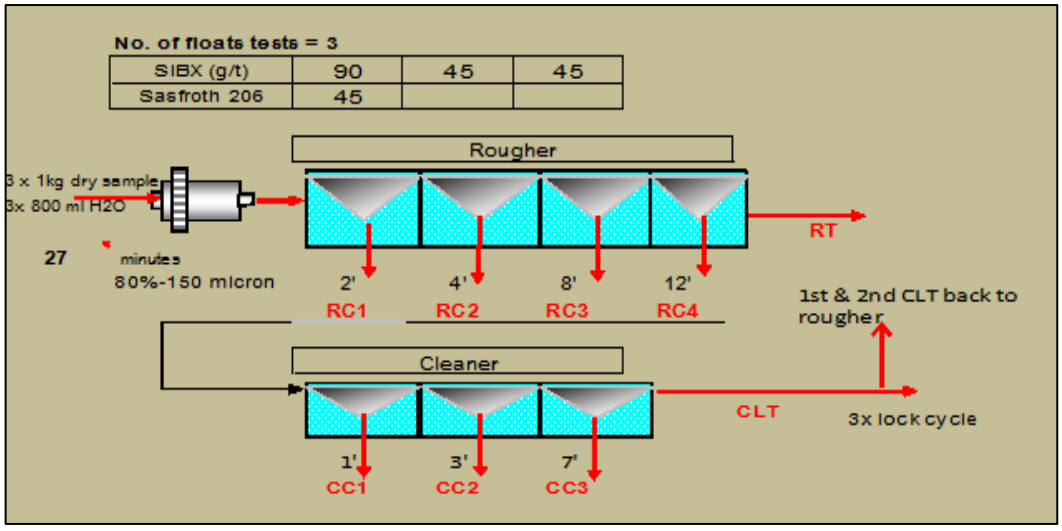

Figure 2.15: Lock-cycle flotation testing workflow

Wills and Napier-Munn (2006) have given guidelines as to when the lock-cycle batch flotation test can be said to have reached equilibrium. Indeed, after a certain number of cycles have been performed, the test is deemed complete when at least one of the following happens:

- The weights of recycle streams stabilise.
- The combined weights of the final concentrate plus the final tails stabilise and approximate the weight of fresh ore charged to each new cycle.
- The assays of the final concentrate and the final tails stabilise and the calculated head assay approximates the actual head assay.
- The metallurgical distribution between the final concentrate and the final tails stabilise.

2.4.2 Simple batch flotation testing

Batch flotation tests other than lock-cycle batch flotation tests are referred to in this thesis as simple batch flotation tests. They include rougher/scavenger batch flotation test, hot batch flotation test, and cleaner batch flotation tests presented in the previous sub-section.

Samples resulting from simple or lock-cycle batch flotation tests have to undergo preparation before they are sent for grade analysis. It is at this preparation stage

that different techniques may be applied to the samples generated. Particle size analysis for example is required for the purpose of producing recovery-by-size data.

Matis and Mavros (1991) noted that variations in flotation recovery with particle size in industrial concentrators were first studied in 1931 by Gaudin and co-workers. They collected flotation data on copper, lead and zinc ores in a series of cells and correlated cumulative recoveries with particle size as exemplified in Figure 2.15.

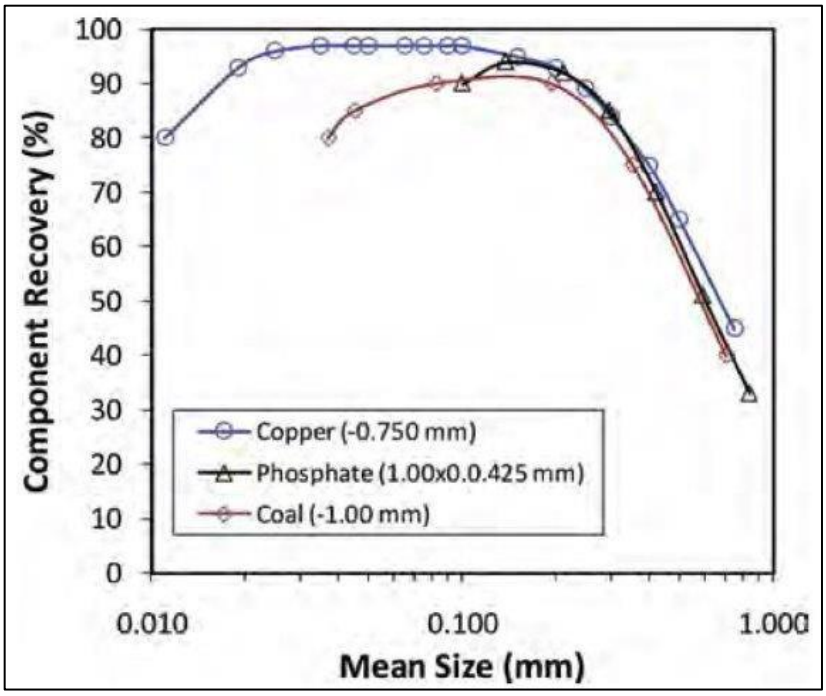

Figure 2.16: Example of recovery-by-size flotation results (Gaudin *et al.*, 1931)

From the work by Gaudin *et al*. (1931), Wasmund (2014) made the observation that the recovery-by-size "n" shape in Figure 2.16 is ubiquitous in the mining industry. He also noted low recoveries at the fine and coarse particles and posited that the problem cannot be addressed by adjusting the grind size.

By the same token, Dworzanowski (2014) noted that the physical recovery of an iron ore with a wide particle size distribution is problematic. This was observed regardless of the process applied whether it is gravity concentration, magnetic

separation, or flotation. The same pattern was reported in numerous scientific articles that looked into the recovery-by-size phenomenon over the years. See for example Fuerstenau (1980), Trahar (1981), Panoupolos *et al*. (1986), King and Schneider (1998), Gorain *et al*. (1999), Yianatos *et al*. (2003), Vianna (2004), Newcombe *et al*. (2012) as well as Multani and Waters (2019).

Another notable observation on recovery-by-size data is in relation to flotation entrainment. This term means flotation recovery due to water as opposed to flotation due to attachment to air bubbles or true flotation. Here, Wang (2016) was able to demonstrate that the "n" shape is in fact the result of true flotation while entrainment was exempted from the phenomenon as shown in Figure 2.17.

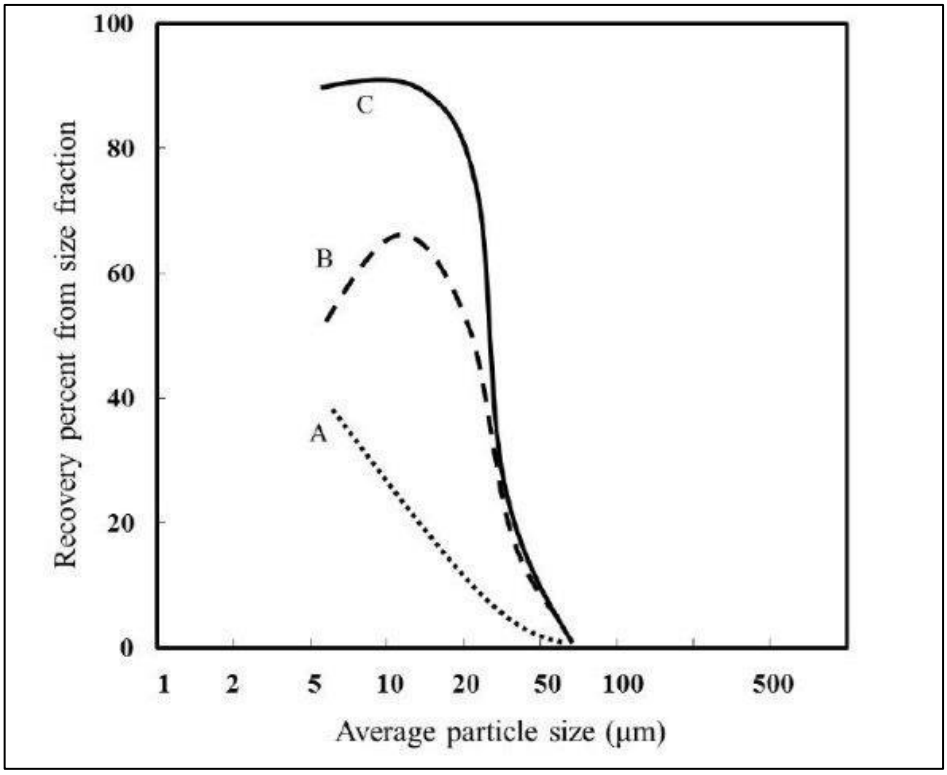

Figure 2.17: Recovery of siderite as a function of the average particle size. A is the recovery by entrainment; B is the recovery by true flotation; and C is the recovery by entrainment and true flotation (Wang, 2016)

It is clear that the recovery-by-size curve has important information to show regarding the performance of the flotation plant. An example of such information

is the plateau range of particles expected to experience high grade and recovery in a flotation circuit (Radmehr *et al.*, 2018). Outside this range, recovery falls gradually below 10 µm. In contrast, a sharp decline is noted above approximately 100 µm to form what Kohmuench *et al*. (2018) call the trunk of the elephant.

In summary, recovery-by-size analysis is used to determine accurately the range of particles neither fine nor coarse enough that will incur high flotation performance (Chimwani, 2014; Rule and Anyimadu, 2007; Gaudin *et al*., 1931).

2.4.3 Recovery-by-size flotation model

Concordant studies have shown that the degree of mineral liberation increases with particle fineness (Banisi and Farzaneh, 2004; King, 1972). However, particles in the intermediate size range (i.e. approximately between 10 µm and 70 µm) are most readily floated.

The relative position of the highly floatable size range for two minerals with different degrees of hydrophobicity is another important factor. Low recovery in the coarse size region may be related to poor flotation rate kinetics due to the particle size itself. But, it is specifically in this region that the locking of mineral gangue particles is most apparent (McIvor and Finch, 1990).

King (2012) derived a model allowing for the complex contribution of bubble size, mineral liberation, hydrophobicity, and particle size to flotation recovery:

$$R_{i,j} = \frac{C_{i,j}(0) - C_{i,j}(t)}{C_{i,j}(0)} = 1 - exp\left[-k_j \, S_{av} \, \Phi_j\left(d_{pi}\right) t\right] \qquad (2.10)$$

where $R_{i,j}$ is the flotation recovery in size class i and grade class j

$C_{i,j}(0)$ is the feed grade of particle i,j

$C_{i,j}(t)$ is the tailings grade of particle i,j

d_{pi} is the size of particles in size class i

k_j is the residual constant that is specific to the particle type; it is independent of particle size

$\Phi_j(d_{pi})$ is the factor allowing for the effects of size and type of particles and is related to flotation rate constant (k_j) or this is said to be the function describing the effect of particle size *i* on flotation rate that is also dependent on particle type *j*

S_{av} is the available bubble surface area averaged over the entire bubble population in the flotation cell

t is the flotation time.

The function $\Phi_j(d_{pi})$ is deemed to be responsible for the effects of particle size on the probabilities of collision, attachment and detachment. King (2012) proposed the following empirical model to account for all the aforementioned micro-processes contribution to froth flotation:

$$\Phi_j(d_{pi}) = 2.33\left(\frac{\varepsilon}{d_{pi}^2}\right)^{\frac{1}{2}} exp\left(-\frac{\varepsilon}{d_{pi}^2}\right)\left(1-\left(\frac{d_{pi}}{d_{p\,max}}\right)^{\frac{1}{5}}\right) \quad (2.11)$$

where: ε is the constant related to the level of turbulence in the flotation pulp

$d_{p\,max}$ is the size of the largest particle that can be floated without detachment from the bubble

Figure 2.18 illustrates the application of the recovery-by-size model encapsulated (i.e. Equation 2.10) to galena tested under different flotation times. One can see that batch flotation residence time does affect flotation recovery. King (2012) tested his phenomenological model to flotation times between 0.5 and 16 min. Although the model is shown to display good prediction ability, he argued that it is yet to be proved to work at longer flotation times.

The production of Figure 2.18 takes into consideration the different flotation times (t) which in this case were 0.5, 1.0, 4.0 and 16.0 min. The average bubble surface area S_{av} can be obtained from plant or laboratory measurements. On the other hand, the respective values of d_{pi} and $d_{p\,max}$ are estimated from particle size analysis. Parameter k_j is determined by calibrating simulation outputs against

experimental data. The value of k_j may also be extracted from historical data of the flotation plant especially if the parameter has been noted to slightly vary over a longer period of time.

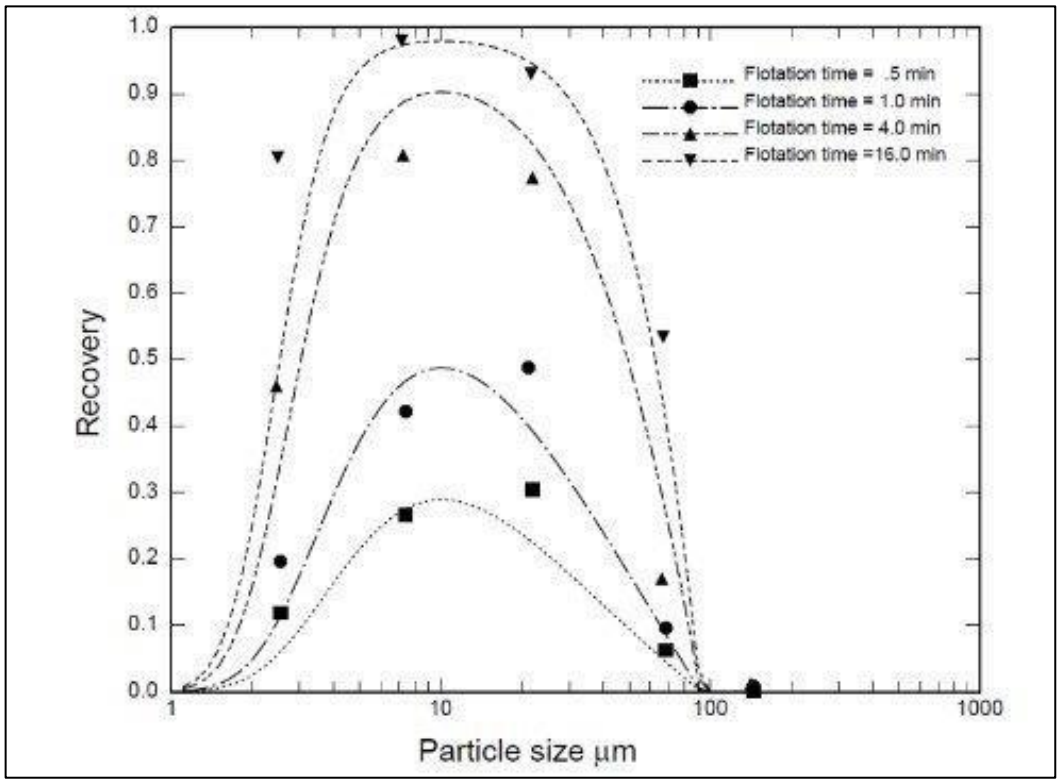

Figure 2.18: Recovery-by-size of galena in a batch flotation cell (King, 2012)

The final comment on Figure 2.18 is that flotation residence time does have an impact on flotation recovery with higher recoveries noted at longer times. In addition to this, intermediate particle size range consistently gives higher flotation recoveries. Wills and Napier-Munn (2006) have determined that flotation activity falls off very rapidly above the optimum particle size due to the low degree of liberation of the minerals. The decreasing ability of bubbles to lift coarse particles is also a major contributor to the drop in recovery. This suggests that floated material consists of a fast-floating fraction in the intermediate size range and a reluctant fraction comprising unliberated coarse particles as well as fines. There is therefore a need for research into the unliberated coarse particles and the fine particles in order to improve recovery. The above limitation became the basis for

the formulation of this doctoral research. It is conjectured that the modelling of batch flotation data collected on narrowly sized feeds may pave a way forward for efficient scale-up. Subsequent sections present a review of existing scale-up techniques before the hypothesis is formulated.

2.4.4 Pilot plant flotation testing

Flotation is regarded as the preferred method of mineral recovery for many of the most important minerals that are recovered and large tonnages of ore are processed by flotation annually (King, 2012). Laboratory batch flotation is mostly used to assess the flotation behaviour at a small scale. This method is suitable for research work done in academia and even for continuous plants in order for them to better control their flotation circuit.

Between laboratory testing and continuous flotation plant, tests can also be done using what is known as a pilot plant. This is a facility of intermediate size that enjoys the versatility in changing operating variables like recirculating loads, aeration rates, froth flow-rates, and launder wash-water rates (King, 1978). The amount of sample needed for pilot testing is also small relative to a production plant and, it can be used independently while the continuous operation is maintained. This therefore enables one to mimic full-scale operation in the control environment inherent to a pilot plant. Even though pilot plant work bridges the gap between laboratory batch flotation and continuous plant flotation but, this is not so popular due to its cost implications and lack of skilled people to effectively utilise it and take care of it.

A simplified pilot plant flotation circuit can be seen in Figure 2.19 where the flotation behaviour of phoscorite was measured (King, 1978). Dobby and Savassi (2005) as well as Yianatos *et al*. (2012) have reported a change of flotation rate in the collection zone along a bank of cells based on the results of batch flotation tests. Work done on continuous flotation plant showed decrease in the froth recovery along a rougher bank in two industrial rougher circuits (Tsatouhas *et al*.,

2005). The above examples prove that batch flotation, pilot plant flotation and continuous flotation can be used interchangeably to discover different flotation findings for research work or plant control purposes.

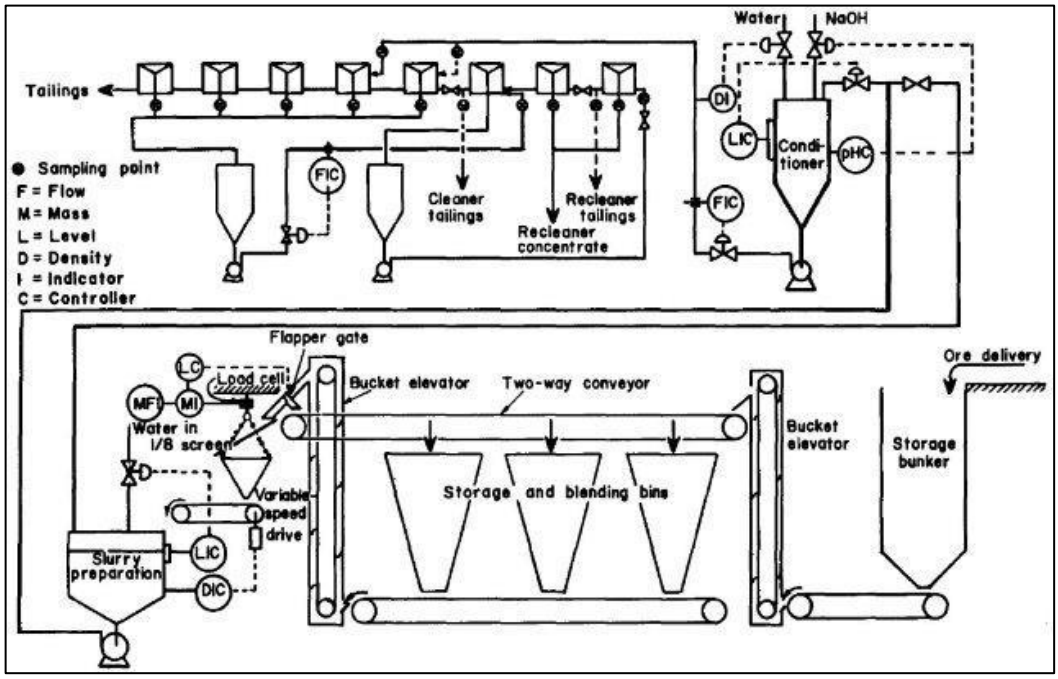

Figure 2.19: Example of a pilot plant flotation circuit (King, 1978)

2.4.5 Continuous flotation testing

Laboratory testwork is central to the advancement of scientific knowledge, to the development of new flotation technologies, and to the improvement of existing ones. It is also used to gain valuable insights in the anticipated performance of a production plant referred to in this study as continuous flotation circuit.

Tools that are widely resorted to in the analysis of continuous flotation circuits include data reconciliation, mass balancing, empirical modelling and computer-based simulation of the steady state operation (Napier-Munn, 1995). These techniques are preferred as costs associated with design, commissioning and troubleshooting are reduced (Reyes Bahena *et al*., 2006).

Engineers generally provide technical expertise for the smooth running of the plant. They also explore improvement initiatives to maintain efficiency. However,

the industrial data accumulated is hardly shared thereby slowing down scientific enquiry. This study is set to contribute towards closing that gap.

2.5 Scale-up of batch flotation

Most studies of flotation start in the laboratory; they are then carried out in a pilot plant before reaching a continuous operation. This progression is termed flotation scale-up or flotation up-scaling. There exists a wide variety of scale-up methods with the most prominent being gas dispersion scale-up, flotation kinetics scale-up, dimensional similitude scale-up, and carrying capacity scale-up.

In the subsequent sections, a review is done on the abovementioned scale-up procedures. The scope is motivated by the fact that these scale-up techniques lend themselves to empirical analysis and hence offer a degree of flexibility.

2.5.1 Gas dispersion scale-up

Scale-up based on gas dispersion in flotation cells has been described in the literature. The method makes use of the relationship between the flotation rate of valuable minerals and the gas dispersion within the flotation cell. Such a relationship was found to be valid as long as the ratio between froth height (h_{froth}) and superficial gas velocity (J_g) remained constant. This ratio is known as the froth residence time (τ_{fg}). Assuming this to be the case, the gas dispersion based scale-up model can be expressed as follows (Gorain *et al.*, 1998):

$$\tau_{fs} = \frac{\tau_{fg}}{L} = \frac{h_{froth}}{J_g\, L} \tag{2.12}$$

Equation (2.12) helps to cater for the condition where the flotation rate constant and froth residence time may change for different cell sizes. The term τ_{fs} represents the specific froth residence time calculated using the distance L between impeller and launder.

Another methodology for up-scaling proposed by Gorain *et al*. (1998) makes use of values obtained from the specific froth residence time τ_{fs} and the corresponding flotation rate constant k:

$$k = \alpha\, exp\left(-\beta_{cf}\tau_{fs}\right) \quad (2.13)$$

Values of k are obtained by performing tests at different froth depths, impeller speeds and air flow rates. The value of constant α is obtained by establishing the relationship between τ_{fs} and k. Constant β_{cf}, on the other hand, is estimated by curve-fitting Equation (2.13) to batch data collected at different froth depths. The value of k is determined at various values of τ_{fs} under specified bubble surface area flux. It must also be noted that α and β_{cf} are mainly curve fitting parameters with no physical meaning associated with them.

Nelson *et al.* (2002) observed that during scale-up of flotation cells, dissimilar results can be expected for larger cells. This is ascribed to the fact that when the volume of a cell is tripled in a proportional scale-up, the surface area only doubles. Gorain *et al*. (1998) also found that the relationship between k and τ_{fg} is dependent on cell size and therefore not directly useful for scale-up. It is only when τ_{fg} is replaced by specific froth residence time τ_{fs} that meaningful results are obtained. Indeed, τ_{fs} takes into account the effect of froth transportation distance in cells of different sizes. As such the relationship between k and τ_{fs} is more likely to be independent of cell size.

2.5.2 Flotation kinetics scale-up

Scale-up based on flotation kinetics was developed by Yianatos *et al*. (2005) on work done at the Minera Escondida concentrator. A plant survey was performed over a 7-hour period to evaluate the performance of the flotation circuit made of six banks of 160 m^3 Wemco cells. Batch tests were also conducted while data collected was fitted to the equation below:

$$R(t) = R_{\infty}.\int_0^{\infty}\int_0^{\infty}(1 - e^{-kt}).F(k).E(t)dk.dt \quad (2.14)$$

The rectangular distribution of kinetic distribution function $F(k)$ in Equation (2.14) is defined as follows:

$$\begin{cases} F(k) = \frac{1}{k_{max}} \quad for\ 0 < k < k_{max} \\ F(k) = 0 \quad for\ k_{max} < k < \infty \end{cases} \tag{2.15}$$

The rectangular distribution function accounts simultaneously for different kinetic properties of the complex minerals found in the particulate material (Yianatos and Henriquez, 2006; Yianatos *et al*., 2012) while parameter k_{max} represents the maximal value of the first-order flotation rate constant.

Yianatos *et al*. (2005) have also defined the residence time distribution function $E(t)$ for a continuous operation with N_c cell in series:

$$E(t) = \frac{t^{N_c-1}.e^{-\left(\frac{t.N_c}{\tau}\right)}}{(\tau/N_c)^{N_c}.\Gamma(N_c)} \tag{2.16}$$

where $\Gamma(N_c)$ is the Gamma function described by $\Gamma(N_c) = (N_c - 1)!$ to account for the non-integer values of N_c.

By substituting Equations (2.15) and (2.16) into Equation (2.14) and by considering that $E(t) = \delta(t)$ where $\delta(t)$ refers to the undistributed residence time; then, the following can be obtained:

$$R(\tau) = R_\infty.\left(1 - \frac{1 - (1+k_{max}\,\tau_p)^{1-N_c}}{(N_c-1)\,k_{max}\,\tau_p}\right) \tag{2.17}$$

$$R(t) = R_\infty.\left(1 - \frac{1 - e^{-k_{max}\,t}}{k_{max}\,t}\right) \tag{2.18}$$

Equations (2.15) and (2.16) represent the flotation kinetics based scale-up model proposed by Yianatos *et al*. (2005). It must be noted that Equation (2.17) is designed to be used for plant data while Equation (2.18) is mainly for laboratory scale usage.

Typical results from Equations (2.17) and (2.18) can be seen in Table 2.2 where plant results scored a 4 percentage units drop in maximum recovery compared to the laboratory-based predictions.

Table 2.2: Scale-up model parameters from literature (Yianatos *et al*., 2005)

	Batch	Plant
R_∞	95.4%	91.0%
k_{max}	3.5(1/min)	1.4(1/min)

By applying Equation (2.17) to the Minera Escondida concentrator, Yianatos *et al*. (2013) were able to produce the results illustrated in Figure 2.20. Good agreement can be seen between experimental results and simulation. Of note is the asymptote depicted by the simulation curve reflecting the value R_∞ reported as 91.0 % in Table 2.2.

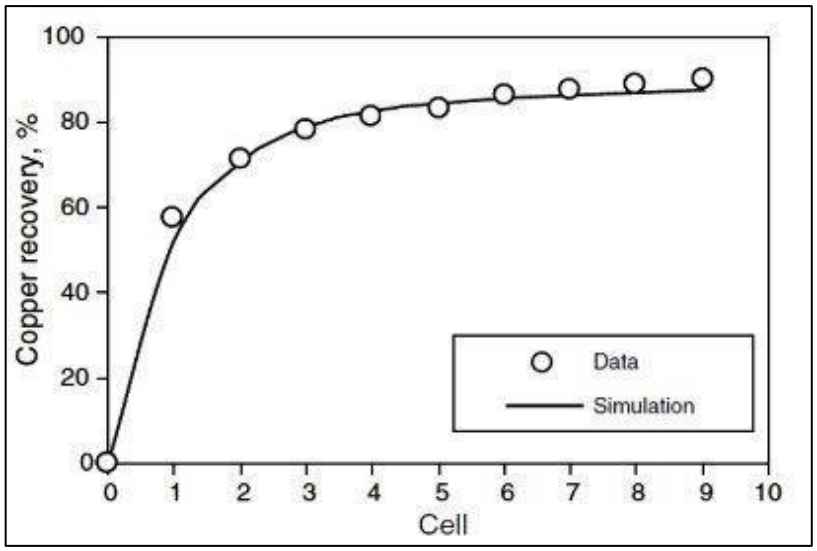

Figure 2.20: Plant survey recovery and model prediction (Yianatos *et al*., 2005)

The drawback of this scale-up procedure is that other factors were found to have a strong influence on the plant results. However, the model does not take them into consideration. The secondary reagents addition in the middle of the cell bank is one such factor not captured by Equations (2.17) and (2.18).

Another drawback is that direct comparison of batch tests with a bank of flotation cells is complicated. This is because the recovery in the last cells of the bank is relatively small (Boeree, 2014). Equally, the verification of the scale-up procedure

using pilot plant results proved difficult in comparison to laboratory batch tests. Yianatos *et al*. (2005) attributes this to the fact that laboratory tests require smaller representative samples that are easier to handle. This argument however is still yet to be ascertained with follow-up research.

2.5.3 Dimensional similitude scale-up

The dimensionless numbers method is used to create similar conditions within flotation cells of different scales (Boeree, 2014). Dimensionless numbers allow comparisons of systems that are different. Table 2.3 provides a list of dimensionless numbers that can be used in flotation research.

Table 2.3: Dimensionless numbers used for flotation scale-up (Harris and Mensah-Biney, 1977; Nelson *et al*., 2002; Truter, 2010; Boeree, 2014)

Dimensionless number	Equation	Variables
Reynolds number (impeller zone)	$Re = \frac{NiD^2\rho_p}{\mu_p}$	Ni = impeller rotational speed (1/s) D = impeller diameter (m) ρ_p = pulp density (kg/m^3) μ_p = pulp viscosity (kg/m/s) g = gravitational acceleration constant (9.81m/s^2) Q_{air} = air flowrate (m^3/s) PDw = power draw (kg.m^2/s^3) ρ_L = liquid density (kg/m^3) γ = surface tension of the air-liquid interface (kg/s^2) Q_{pulp} = pulp flowrate (m^3/s)
Froude number	$Fr = \frac{Ni^2D}{g}$	
Aeration (air flow) number	$Ae = \frac{A_{air}}{NiD^3}$	
Power number	$Po = \frac{PD}{\rho_p Ni^3 D^5}$	
Weber number	$We = \frac{Ni^2D^3\rho_L}{\gamma}$	
Volumetric flow number	$Vo = \frac{Q_{pulp}}{NiD^3}$	

By making use of Equation (2.20), it is possible to estimate the mixing condition parameter (φ) with the use of dimensional similitude scale-up method as shown in Figure 2.21. In this case, the two-dimensional recovery (η) was used and calculated as written below:

$$\eta = \frac{R(t)}{R_\infty} \tag{2.19}$$

The idea is to maintain the dimensionless numbers in Table 2.2 constant for successful scale-up.

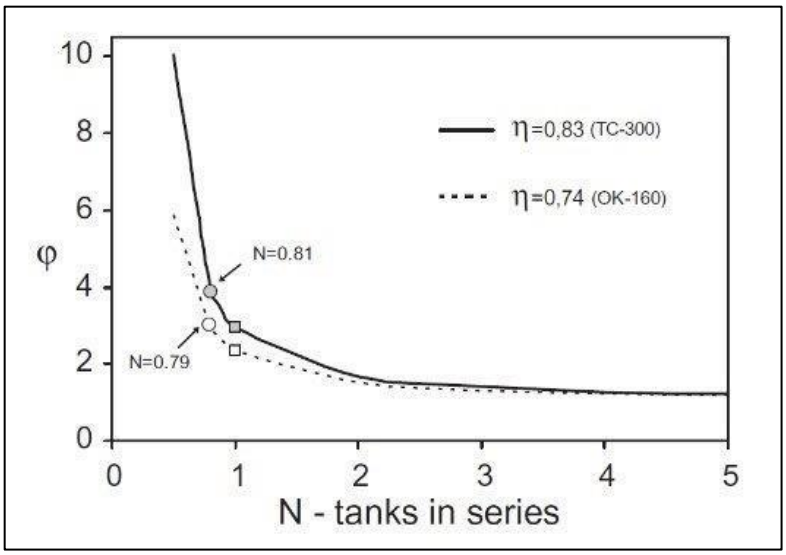

Figure 2.21: Estimation of parameter φ in Equation (2.20) using the dimensional similitude method (Yianatos *et al*., 2010)

Boeree (2014) showed that the diameter and the rotational speed of the impeller are known to directly influence turbulence and energy dissipation which then affects recovery. By ensuring a constant ratio of diameter and rotational speed of the impeller between cells of different dimensions, it became possible to express the scale-up procedure as follows:

$$\frac{k_{app}}{k_b} = \xi.\alpha_{fe}.\beta.\gamma = \xi.\frac{k_{app}}{k_c}.\left(\frac{\varphi(N=1)}{\varphi(N\neq 1)}\mathrm{I}_\eta\right).\frac{\tau_s}{\tau_L} \qquad (2.20)$$

where k_{app} is the apparent flotation rate

k_b is the flotation rate in a laboratory batch cell

k_c is the collection zone rate constant

ξ is the ratio between actual flotation rate in the collection zone of single perfectly mixed industrial cell (k_c) and flotation rate in a laboratory batch cell (k_b)

α_{fe} is the froth effect

β is the cell mixing effect

γ is the particle segregation effect

φ is the mixing condition parameter

N is the impeller rotational speed (1/s)

η is the dimensionless recovery; it is reported in the expression to be a function (I) of N defined at N = 1 over function (I) of N with N having any other value than 1 across domain η

τ_s is the effective solid residence time

τ_L is the effective liquid residence time.

Table 2.4 shows how the dimensionless numbers did not change between two flotation cells of different design and geometry. This was achieved initially by taking samples from the plant and immediately conducting batch flotation tests and keeping the same pulp conditioning and the same particle size distribution of the plant feed.

Table 2.4: Dimensionless parameters and scale-up factors (Yianatos *et al*., 2010)

Cell type	Volume (m^3)	K_{app} / K_b	α (froth)	β (mixing)	γ (segregation)	ξ (scale-up factor)	S_b (1/s)
Tankcell	300	0.24	0.48	0.76	0.89	0.75	44.5
Outotec	160	0.21	0.44	0.79	0.89	0.68	41.7

For the plant flotation tests, the short-cut method was applied (Yianatos and Henriquez, 2006). This method consists of sampling five points in the rougher flotation circuit in order to determine the recovery of the first cell as well as the total flotation line recovery. The first cell of the line was characterized to compare the collection rate with that of the batch flotation tests. Applying the above techniques assured the researchers that their dimensionless numbers were kept constant.

The use of dimensionless numbers based scale-up requires extensive research especially for Greenfield flotation circuits. This is mainly because there would be neither performance information available for optimal particle size distribution, nor physical and chemical conditions of the anticipated plant.

The second problem is that care should be taken to make sure that the dimensionless numbers lie within realistic ranges. For flotation bank design, Yianatos *et al*. (2010) recommend the use of a methodology consisting of the sequential calculation of each individual cell. For this purpose, the dimensionless factors α, β and γ (accounting respectively for the froth, mixing and segregation effects) must be estimated for each cell downstream from the flotation bank (Yianatos *et al*., 2010; Gorain *et al*., 2010). This ensures that the dimensionless numbers are complied with, but the algorithmic exercise is quite laborious.

2.5.4 Carrying capacity scale-up

Yianatos and Contreras (2010) define the carrying rate in a flotation cell as the mass transport of solids by bubbles per unit of time per unit of cell cross-sectional area. The carrying capacity is the maximum carrying rate that may represent a limitation when a large fraction of solids needs to be recovered from the pulp (Boeree, 2014). It is expressed in kg/s/m^2 or t/h/m^2.

Espinoza-Gomez *et al*. (1988) proposed an empirical model for the carrying capacity of mechanical cells:

$$C_A = 0.068 \,.\, P_{80} \,.\, \rho_p \tag{2.21}$$

where P_{80} is the sieve mesh at which 80 % of the feed material pass through and ρ_p is the density of the particles making up the feed.

Alternative models of carrying rate and carrying capacity have also been proposed (Yianatos and Contreras, 2010):

$$C_R = \varphi_S \,.\, \frac{\pi}{6} \,.\, S_B \,.\, d_p \,.\, \rho_p \tag{2.22}$$

$$C_A = \varphi_{S.max} \,.\, \frac{\pi}{6} \,.\, S_B \,.\, d_p \,.\, \rho_p \,.\, R_f \tag{2.23}$$

where φ_S is the superficial gas velocity; S_B is the Sauter mean bubble diameter; d_p is the Sauter mean particle size; ρ_p is the solids density; and R_f is the froth recovery.

Espinoza-Gomez *et al*. (1988) conducted some work on Equation (2.21) and reported the following: C_A = 2.28 t/h/m^2 for Kidd Greek Copper Mine and C_A = 9.66 t/h/m^2 for Inco Copper Mine.

The differing values of the carrying capacity noted above are not uncommon as noted by Boeree (2014) when Equations (2.22) and (2.23) are applied. This is also true with the estimation of bubble loads in flotation cells. Indeed, the work done by Seaman *et al*. (2004) yielded bubble loads of 135.8 – 141.9 kg/m^3 in a 50 m^3 Zn cell at Teck Cominco's Red Dog Mine. Yianatos *et al*. (2008) found bubble loads of 26 – 51 kg/m^3 in a 130 m^3 Cu rougher circuit at Codelco's El Teniente mine.

Boeree (2014) explained that Equations (2.22) and (2.23) are difficult to use at the pulp-froth interface due to large amount of entrained material in mechanical cells. Such can be a limiting factor for proper scale-up since bubble load is related to volume while carrying rate and capacity are related to the cross-sectional area.

Seaman *et al*. (2004), on the other hand, noted that carrying rate scale-up method assumes that air in the cell is well dispersed. This is only true for small cells but no large mechanical flotation cells. It is therefore recommended to take several measurements over the cross sectional area in larger cells in order to determine the average bubble load.

All in all, one needs to keep the limitations discussed above and associated solutions in mind when using carrying capacity scale-up methodology.

2.5.5 Empirical scale-up

The Australian Mineral Industries Research Association (AMIRA) P9 Project has been involved in conducting different laboratory and plant tests mainly related to flotation and comminution. Two of the empirical models for flotation that have

come out from the AMIRA initiative are briefly discussed in this section. These are the entrainment and the bubble surface area flux empirical models.

2.5.5.1 Entrainment empirical model

The entrainment and drainage of particles in a flotation froth have long been recognised as important factors affecting both concentrate grade and recovery. This is expressed in the set of equations below representing the entrainment empirical model (Savassi *et al*., 1998):

$$ENT_i = \frac{2}{exp\left(2.292\left(\frac{d}{\zeta}\right)^{adj}\right)+exp\left(-2.292\left(\frac{d}{\zeta}\right)^{adj}\right)} \quad (2.24)$$

$$adj = 1 - \frac{ln\left(\frac{1}{\upsilon}\right)}{exp\left(\frac{d}{\zeta}\right)} \quad (2.25)$$

In the model above, two empirical parameters are apparent: the entrainment parameter (ζ) or the particle size for which the degree of entrainment is 20 % and the drainage parameter (ʊ) related to the preferential drainage of coarse particles.

The form of the empirical partition curve for typical parameters can be seen in Figure 2.22, which experimental values for the degree of entrainment correspond to the work by White (1974). The entrainment parameter (ζ) is a cutting size for the entrainment partition curve similar to the cut size parameter used in hydrocyclone modelling but, a cut size at 20 % is chosen when modelling entrainment to improve the fit at the tail end of the curve. The drainage parameter (ʊ) improves the flexibility of the entrainment partition curve while increasing drainage parameter values indicate increasing preferential drainage of coarse particles (Savassi *et al*., 1998).

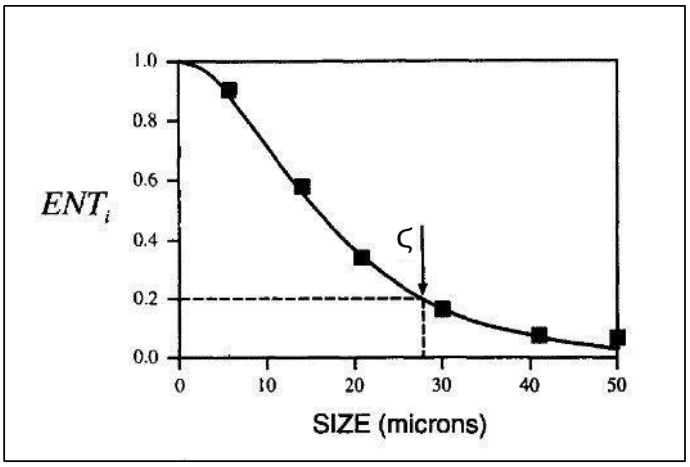

Figure 2.22: The empirical partition curve for ς = 28 µm and ʊ = 1.00 (Savassi *et al*., 1998)

It must be noted that this scale-up model only applies with the use of particle size as a factor affecting entrainment. However, in continuous flotation systems where there is true flotation and entrainment happening simultaneously, contribution of each factor must be individually measured.

2.5.5.2 Bubble surface area flux model

Bubble surface area flux (S_b) has been seen as a good measure of the gas dispersion in a flotation cell (Gorain *et al*., 1999). It is summarised in Equation (2.3).

Gorain *et al*. (1999) cited two main reasons for the development of the scale-up model based on bubble surface area flux:

- To have a model the parameters of which can be measured easily in the plant and if necessary the parameters should be estimated accurately by design engineers, plant metallurgists and cell manufacturers.
- To have a model that integrates independent variables studied extensively by the Julius Kruttschnitt Mineral Research Centre (JKMRC) in previous tests programs at different concentrators as part of the AMIRA P9 project.

The final format of the model representing the relationship between S_b and the independent variables is summarised below:

$$S_b = a\, N_s^b \left(\frac{Q}{A}\right)^c A_s{}^{d_d} P_{80}{}^e \qquad (2.26)$$

where: N_s is the impeller peripheral speed

Q/A is the air flow rate per unit cell cross-sectional area

A_s is the impeller aspect ratio

P_{80} is the 80 % passing feed size

$a,\ b,\ c,\ d_d, e$ are the parameters of the model.

The scale-up model in Equation (2.26) was tested on the Hellyer and Scuddles concentrators respectively. Parameters a, b, c, d_d and e were estimated by curve fitting. The final results of the validation of bubble surface area flux model yielded a coefficient of determination R^2 = 0.81 and is shown in Figure 2.23.

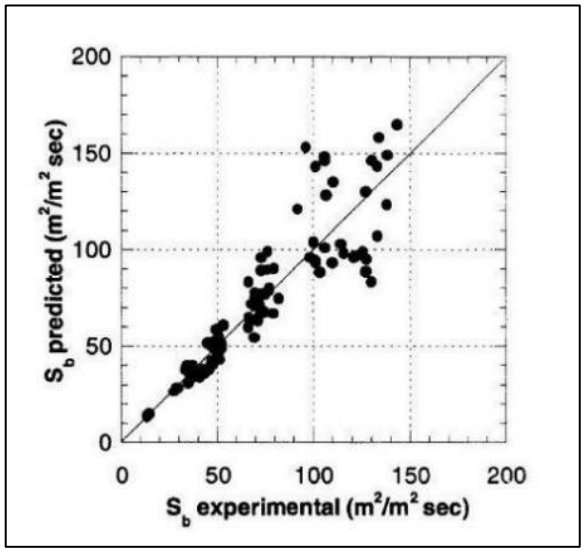

Figure 2.23: Predicted versus experimental bubble surface area flux using Equation (2.26) over the 100 data sets obtained from the Hellyer and Scuddles concentrators (Gorain *et al.*, 1999)

The bubble surface area flux scale-up model tends to over-estimate the values of S_b at higher Q/A or N_s values. This occurs when the cell is operating at or close to flooding conditions or turbulence. In its current form, the model is still unable to predict S_b effectively for both forced and self-induced flotation air cells.

2.5.6 Phenomenological scale-up

The most widely accepted phenomenological model of flotation scale-up is the compartmental model. This model basically discretizes the flotation system in two compartments and applies relevant mass transfer sub-models to each compartment (Amelunxen *et al*., 2014).

The sub-models consist of the following components schematically rendered in Figure 2.24:

- Mineral recovery, R_c, in the collection zone that corresponds to the hydrophobic minerals and follows a pseudo first order plug-flow kinetics model.
- Mineral recovery, R_f in the froth zone that corresponds to the hydrophobic particles recovered in the collection zone.
- Mineral recovery by entrainment that corresponds to uncollected hydrophilic and hydrophobic particles in the collection zone.

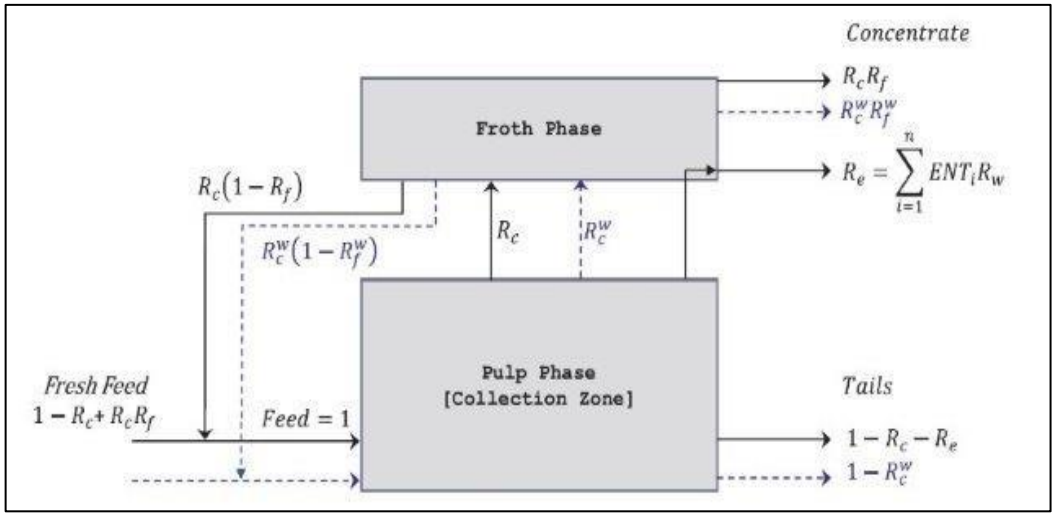

Figure 2.24: Representation of the two-compartment model, including water vectors (Amelunxen *et al*., 2018)

The two-compartment scale-up model is developed by combining the equations describing the mass transfer of water around the two compartments. It can be symbolically represented as follows (Amelunxen *et al*., 2014; Amelunxen *et al*., 2018; Newcombe, 2014):

$$R(t) = \frac{R_c(t)R_f}{1-R_c(t)+R_c(t)R_f} + m\sum_{i=1}^{n}\frac{ENT_i}{m_i}R_w(t) \quad (2.27)$$

$$R_w(t) = \frac{R_c^w(t)R_f^w}{1-R_c^w+R_c^wR_f^w} \quad (2.28)$$

$$R_f^w(t) = \frac{Q_{conc}^w(t)}{Q_c^w} \quad (2.29)$$

Water is treated in a similar fashion to solids with a collection recovery component (R_c^w) and a froth recovery component (R_f^w).

Finally, note that this model assumes spherical particles for the entrainment which may become a source of significant error for some minerals. The model also works best when the scraping frequency of the froth is fast at the beginning of the test because slow scraping rates make it difficult to extrapolate Q_{conc}^w.

2.5.7 Brazilian approach to scale-up

Flotation research in Brazil dates back to the 1950's (De Araudjo and Peres, 1995). The Brazilian government has been sponsoring flotation research under the name Coordenação de Aperfeiçoamento de Pessoal de Nível Superior (CAPES). Some of the institutions involved in flotation research may include Conselho Nacional de Desenvolvimento Científico e Tecnológico (CNPq), The Federal University of Minas Gerais (UFMG) and Federal University of Rio Grande do Sul - Post-Graduation Program in Mining, Metallurgical, and Materials Engineering (UFRGS-PPGE3M). There has also been collaborations between Brazilian universities and the University of Cape Town (UCT) for example.

Two scale-up methods brought about by the CAPES programme are succinctly discussed: the particle surface area and the residence time distribution (RTD) methods.

2.5.7.1 Particle surface area method

The model is best suited to be tested in a pilot plant where each test has a specific froth height in the first rougher cell to allow an evaluation of froth recovery (Dos Santos *et al*., 2014; Dos Santos 2018).

Basically, samples collected from pilot testing are screened at different sizes; then, the size fractions undergo chemical and mineralogical analysis. Data mass balance can then be done following a hierarchical procedure of reconciliation. In this procedure the first level restricts and conditions the reconciliation in the following sub-level (Dos Santos and Galery, 2018; Savassi, 2006).

Figure 2.25 exemplifies how the surface area of chalcopyrite determines the flotation effectiveness in the first rougher stage. The underlying method suggests that, under a set of chemical and hydrodynamic conditions, the flotation of an ore with a simple texture and ground to an appropriate size is predominantly determined by the mineral surface area available for collection.

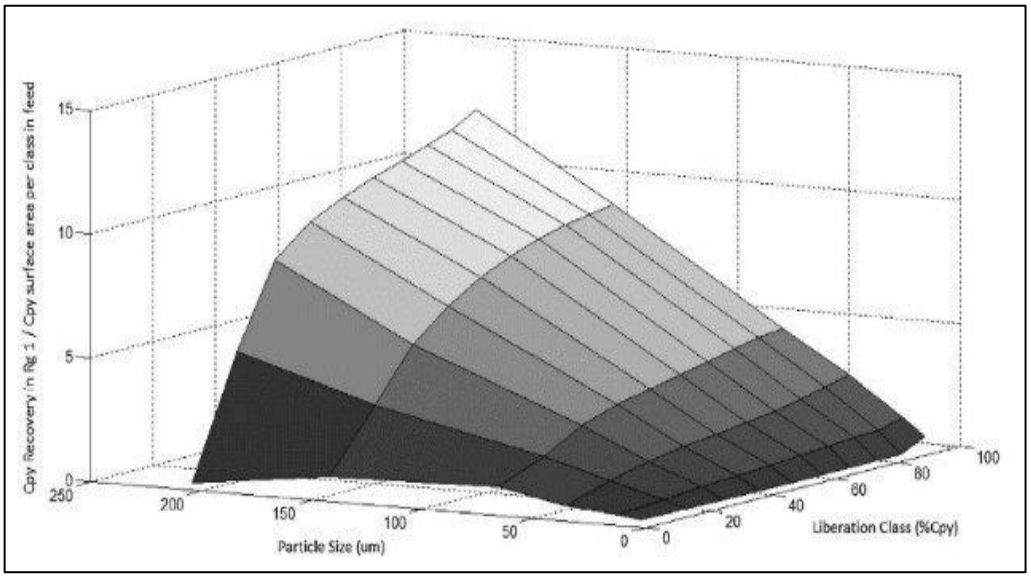

Figure 2.25: Surface area vs. Particle size vs. Liberation class (Dos Santos, 2018)

The particle surface area concept described above may be used as the basis for scale-up from pilot to continuous flotation plant. The concept may also assist with

the analysis and comparison of flotation conditions, process control tactics, new equipment and different flotation circuit configurations (Dos Santos, 2018).

The weakness to this method is that it cannot rely on laboratory data but mainly pilot plant testing. This simply means that more resources are required beyond the costly operation of pilot plants needed for testwork.

2.5.7.2 Residence time distribution method

The performance of mechanical flotation cells has been reported to be strongly influenced by hydrodynamics, i.e., the bulk or macroscopic flow of fluid in a vessel (Souza Pinto *et al*., 2018). There is also a level of similarity between mechanical flotation cells and continuous stirred tank reactors (CSTR) in terms of material flow. However, their dissimilarity is purported due to the phenomena of short-circuiting and stagnant zones occurring through mechanical flotation cells (Lelinsk *et al*., 2002; Yianatos *et al*., 2008).

The above has been summarised in the form of the residence time distribution (RTD) function, $E(t)$, for mechanical flotation cells using CSTR descriptions as follows:

$$E(t) = \frac{{t_r}^{n_r-1} e^{\frac{-t_r n_r}{\tau_S}}}{\left(\frac{\tau_S}{n_r}\right)^{n_r}(n_r-1)} \quad (2.30)$$

$$n_r = \frac{t_{avg}^2}{\alpha_S^2} \quad (2.31)$$

where: $E(t)$ is RTD function

t_r is the time for RTD testing

t_{avg} is the average/mean residence time

n_r is the number of ideal tanks in series

τ_s is the expected residence time or space time

α_S is the variance.

RTD studies conducted by tracer methods have been used to evaluate the quality of mixing as well as the deviations from ideal CSTR behaviour (Fogler, 1999; Patwardhan *et al*., 2003; Yianatos *et al*., 2008). Figure 2.26 exemplifies the RTD response of mechanical flotation cells or the mass fraction of tracer that exits the cell before the circulation time (Souza Pinto *et al*., 2018).

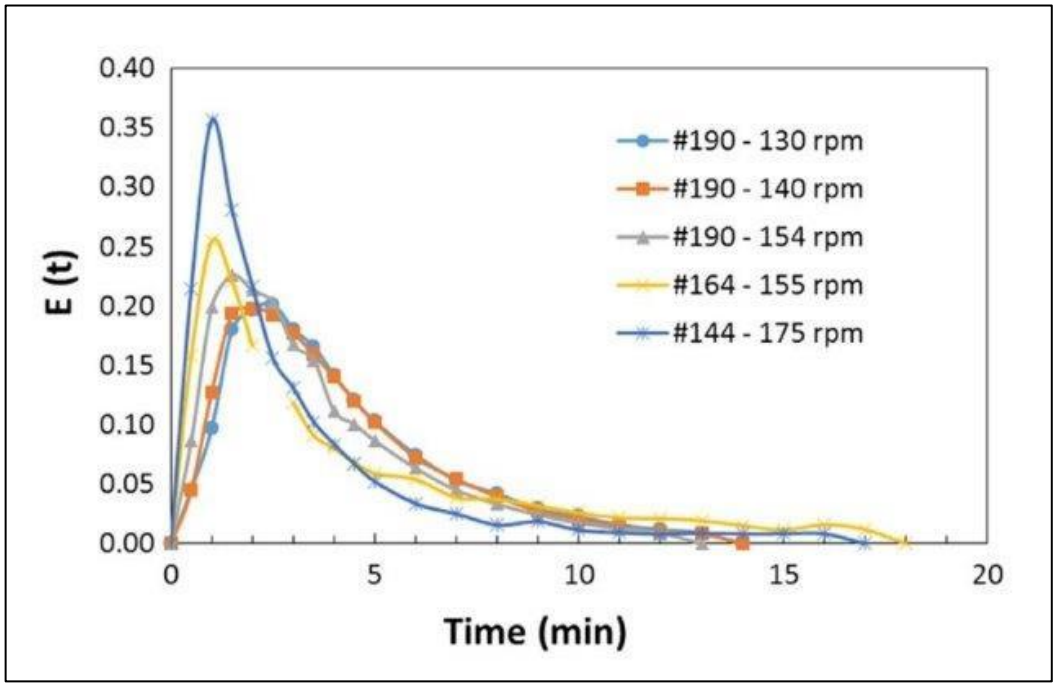

Figure 2.26: RTD function for the three flotation cells (Souza Pinto *et al*., 2018)

The peak of the RTD curve in Figure 2.26 can be assumed to be an approximate indicator of the circulation time. Further analysis of RTD results may lead to inferring scale-up estimates based on the circulation time. And even though RTD studies are simple to conduct and analyse, they can be very labour intensive.

2.6 ModSim modelling overview

The three flotation models within ModSim software (King, 2012) are briefly explained below.

2.6.1 Klimpel (KLIM) model

The kinetic model for the flotation cell that assumes that each type of particle has a floatable and a non-floatable component. This model is popular as a simple but useful and consistent model for the comparison of collectors and other conditions in industrial flotation systems. The floatable component of each particle type is recovered at a rate that is proportional to the amount of that species in the flotation cell. The influence of the bubble surface area and the characteristics of the froth phase are neglected entirely. The effect of particle size on the flotation kinetics is also neglected. The water balance over the cell is established by specifying the percent solids in the concentrate. Water can be added directly to the froth launders in which case the final percent solids in the froth must be specified as well.

Table 2.5: KLIM model parameters within ModSim

#	**Parameters description**
1	Number of cells in the bank
2	Volume of each cell
3	Volume fraction of air in the pulp
4	Percent solids in concentrate
5	Number of banks in parallel
6	Ultimate recovery for G-class 1
7	Kinetic constant for G-class 1

Equation linked to the KLIM model (Klimpel, 1980):

$$R = R_{\infty}\left[1 - \left(\frac{1-e^{-kt}}{kt}\right)\right] \quad (2.32)$$

where: R is the flotation recovery

R_{∞} is the ultimate or maximum recovery

k is the flotation rate constant or kinetic constant

t is the flotation time

2.6.2 King (FLTK) model

This model is the discrete distributed flotation kinetic constant model. The true cell residence time is calculated from the tailings flowrate. The percentage solids in the froth is assumed or known and this fixes the water balance. The Pogorely model for bubble loading is incorporated so that heavy bubble loads will reduce the flotation capacity in the cell. The froth phase is modelled using the froth transmission coefficient which is defined as the fraction of solid crossing the pulp-froth interface that is actually recovered in the concentrate stream. The remainder of the solid is returned to the pulp phase. It must be noted that, the specific flotation rate constants are mass transfer coefficients because they model the rate of transfer of particulate matter across the phase boundary from pulp to bubble surface. The units of the specific flotation rate constants are therefore in meters per seconds (ms^{-1}).

This model allows water to be added to the concentrate launder so that the solid content of the concentrate that finally leaves the bank is less than the solid content of the concentrate that leaves each cell. The water can be added at a pre-specified rate or ModSim will calculate the addition rate to meet a required final solid content in the concentrate.

Table 2.6: FLTK model parameters within ModSim

#	**Parameters description**
1	Number of cells in series for this bank
2	Cell volume
3	Aeration rate in m^3 of air per m^3 of cell volume
4	Froth transmission coefficient
5	Bubble size
6	Bubble residence time
7	Estimate of cell holding time
8	Percent solids in the concentrate
9	Number of banks in parallel
10	Particle size at maximum recovery
11	Largest floatable particle
12	Specific flotation rate constants - one for each S-classs

The following section below gives an overview of the equation(s) linked to the FLTK model (King, 1972):

The rate of flotation particles is characterised by property given in Equation (2.33). In this expression, k is a rate constant which allows for all small-scale effects that influence the rate of flotation. Function ϕ(D) accounts for all the influence of the particle size, A_b is the total bubble surface area per unit of pulp volume, S is the fraction of the surface area of a single bubble that is not covered by adhering solid particles and W is the mass of solids in the cell. The units of Equation (2.33) are in kg/s.

$$k, g, D = k\phi(D)A_bSWf(k, g, D) \tag{2.33}$$

Pogorely (1962) and Zaidenberg (1964) have managed to model S by assuming that the bubbles rise without coalescence through a perfectly mixed pulp. This is achieved by having τ_{LT} representing the bubble lifetime and V the cell volume as shown in Equation (2.34). The factor that represents the surface area covered by 1 kg of solid is given by η(D) and this varies approximately as 1/D.

$$VA\frac{dS}{d\tau_{LT}} = -WAS\int_0^\infty\int_0^1\int_0^\infty \eta(D)k\phi(D)f(k, g, D)dk\ dg\ dD \tag{2.34}$$

Integration of Equation (2.34) yields Equation (2.35)

$$S = exp\left(-\frac{WK\tau_{LT}}{V}\right) \tag{2.35}$$

where K is represented by Equation (2.36)

$$K = \int_0^\infty\int_0^1\int_0^\infty k\eta(D)\phi(D)f(k, g, D)dk\ dg\ dD \tag{2.36}$$

The average value of S throughout the cell can be calculated from the spread of bubble residence times. This can be denoted by f_τ then the average will be given by Equation (2.37).

$$S_{av} = \int_0^\infty \frac{f_\tau(\tau b)}{\tau b}\int_0^{\tau b} exp\left(-\frac{WK\tau}{V}\right)d\tau\ d\tau b \tag{2.37}$$

Under normal operating conditions, only a small spread in bubble residence time is expected so that Equation (2.38) becomes

$$f_\tau(\tau b) = \delta(\tau - \tau b) \quad (2.38)$$

where $\bar{\tau}$ is the average residence time of the bubbles then Equation (2.37) becomes

$$S_{av} = \frac{V}{WK\bar{\tau}}\left[1 - exp\left(-\frac{WK\bar{\tau}}{V}\right)\right] \quad (2.39)$$

2.6.3 Sutherland (FLTN) model

This model is based on the discrete distributed flotation kinetic constant model. The volume of pulp in the cells in the bank must be specified and the pulp residence time is calculated to be consistent with this volume and the tailings flow from the cell. The water balance is fixed by assuming that the solids holdup per unit volume of pulp is fixed. The kinetic constant decreases at larger sizes according to $k = \left(\frac{34.9}{dpi}\right)^{0.9}$ for dpi > 34.9. This model allows water to be added to the concentrate launder so that the solid content of the concentrate that finally leaves the bank is less than the solid content of the concentrate that leaves each cell. The water can be added at a pre-specified rate or ModSim will calculate the addition rate to meet a required final solid content in the concentrate.

Table 2.7: FLTN model parameters within ModSim

#	**Parameters description**
1	Number of cells in the bank
2	Number of banks in parallel
3	Volume of pulp in each cell m^3
4	Solid holdup in kg per cub meter of pulp
5	Air holdup as a percentage of the cell volume
6	Specific flotation rate constants in this bank

Equation(s) linked to the FLTN model (Sutherland, 1977 & 1989) can be summarised briefly as shown below:

For any component *i* the flotation behaviour in any selected cell is represented by the relationship given by Equation (2.40). Where C_i is the mass flow rate of component *i* in the concentrate from a cell (kg min^{-1}), W_i is the mass component *i* in the cell (kg), and k_i is the flotation rate constant for this component (min^{-1}).

$$C_i = k_i W_i \tag{2.40}$$

As the flotation cell is taken to be perfectly mixed then, the air-free concentration of component *i* in the cell is equal to its concentration in the tailings and, a steady mass balance over the cell gives Equation (2.41). Where F_i is the mass flow rate of component *i* fed to the cell (kg min^{-1}), T_t is the total solids tailings flow rate (kg min^{-1}), W/T_t is the mean residence time for solids in the cell (min).

$$W_i = \frac{F_i}{k_i + \frac{T_t}{W}} \tag{2.41}$$

Empirical relationship is used to calculate the total concentrate solids flow rate (CTOT) assuming no suppression of flotation rates. If CTOT exceeds a specified limit (A) for the size of cell operated in this manner then, the maximum solids concentrate flow rate is fixed (FMAX) and the flotation rates suppressed making Equation (2.10) to become Equation (2.42).

$$C_i = SK_i W_i \tag{2.42}$$

Where $0 < S < 1$ and is determined by Equation (2.43)

$$\sum C_i = FMAX \tag{2.43}$$

If FMAX is set constant and equal to A; then, a discontinuity exists in the system and it is more realistic to set FMAX by some arbitrary function of A which though continuous is rather insensitive to A and this can be represented by Equation (2.44).

$$FMAX = 2A\left(1 - \frac{A}{2\,CTOT}\right) \tag{2.44}$$

The fraction of the slow floating component for the liberated material can be plotted against size. Such relationship does show that slow floating component

increases for both large and small sizes and this can be represented empirically by Equation (2.45) where D_{ps} is the particle size in microns and F(S, 1.0) is the fraction of slow floating component in the liberated class given by

$$F(S, 1.0) = 0.02 + 0.45\left(log\frac{D_{ps}}{26}\right)^2 \quad (2.45)$$

The way in which F(S, C) varies with particle composition can be assumed to be independent of size and given by Equation (2.46). Where F(S, C) is the fraction of the slow floating component for particles of chalcopyrite fraction C.

$$F(S, C) = F(S, 1.0) + 0.54(1 - C) \quad (2.46)$$

It is sometimes necessary to vary the rate of flotation for the slow component with particle size. An empirical relation that gave satisfactory results is in Equation (2.47). Where K(s) is the flotation rate of the slow component.

$$K(s) = 0.032\left(\frac{D_{ps}}{34.9}\right)^{-0.9} \quad (2.47)$$

All the above three models are within ModSim software and the user is able to choose any of the models to use for the work being done using this software. Each model is working independently of one another as they have different assumptions that they were built on. In this research work, the methodology followed was that of taking a milling and flotation circuit then conduct sampling campaign to produce data to be used in ModSim. Continuous plant samples of feed, discharge, undersize, oversize, recycle streams, concentrate and tails (milling and flotation circuits) were taken for particle size distribution (PSD) analysis which was the input to the model. Plant parameters were measured as per the requirement of the models within ModSim. Other parameters were taken from the plant design specifications as given by the Original Equipment Manufacturers (OEM) in their manuals. Klimpel's and King's models have been used interchangeably and results obtained can be seen in the next section while other results have been detailed in the Appendix E – H sections.

2.7 Brief history and future of mining in relation to batch and continuous flotation

2.7.1 Introduction

In South Africa, the mining sector contributed about 6.8 % of the gross domestic product (GDP) which translated to R335 billion in 2017 (Minerals Council SA, 2018). It is clear that the mines in South Africa are playing a crucial role in providing employment to job seekers whether skilled, semi-skilled and unskilled. There is also a strong link of the mining sector and the institutions of higher learning and even this research project is proof of such a link. It was then deemed necessary as part of this work to look briefly at the status of this mining sector by going back to its past followed by the present times and project what the future holds. In the next topics, some discussions will be done to cover different aspects of the mining sector and try to relate this to the batch flotation tests and continuous flotation operations.

2.7.2 The mining sector and its past

The use of flotation in mining goes back to the year 1905 where the first commercial plant was built at Broken Hill, Australia and the process was patented in 1906 (Bunyak, 2000; Wills and Napier-Munn, 2006; Lynch *et al*., 1973; De Araudjo and Peres, 1995). The first flotation plants were initially developed to treat the sulphides of copper, lead, and zinc but later other materials like platinum, nickel, gold, etc. were also extracted by the flotation process (Wills and Napier-Munn, 2006). Flotation helped to process materials which were previously regarded as waste due to their low grade and which its predecessor processes like gravity concentration or cyanidation could not beneficiate profitably (Bunyak, 2000).

The laboratory flotation cells used in the early years for tests like batch flotation were looking like those in Figure 2.27 and these are still being used even these days. One of the oldest flotation plants shown in Figure 2.27 and Figure 2.28 is that of Shenandoa-Dives (Mayflower) Mill. Bunyak (2000) described Mayflower Mill process as follows: “The ore arrived from the mine uphill from the mill via tramway

buckets at the arrival terminal located on the right. From the terminal the ore moved by conveyor to the top of the mill building where it was crushed and ground for the flotation process. At the completion of the flotation process, the concentrate arrived at the ore bins in the lowest building level. The mill office building was to the left of the arrival terminal." This process description can be followed in Figure 2.28 which showed the side view of the plant while Figure 2.29 has the detailed process flowsheet.

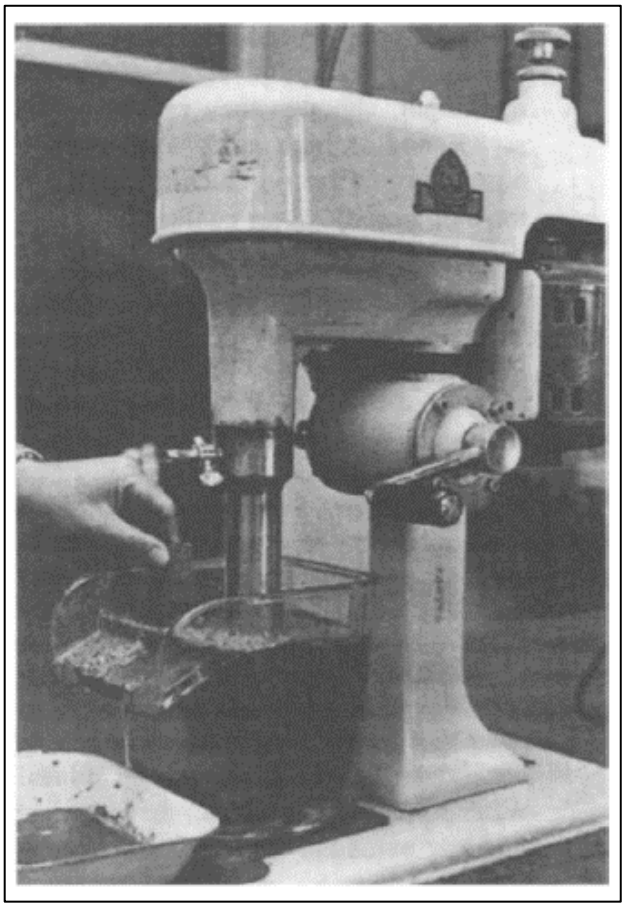

Figure 2.27: Laboratory flotation cell (Wills and Napier-Munn, 2006)

Figure 2.28: Overview of Shenandoa-Dives (Mayflower) Mill (Bunyak, 2000)

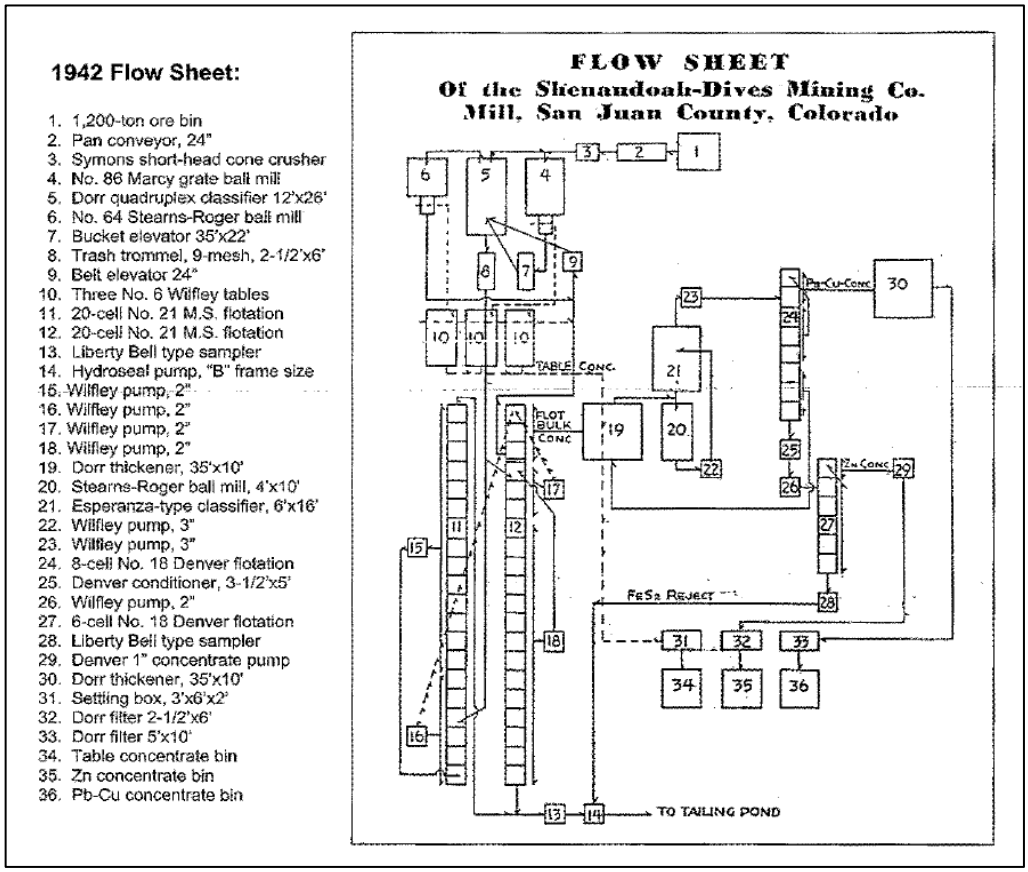

Figure 2.29: Flowsheet of Shenandoah-Dives (Mayflower) Mill (Bunyak, 2000)

Looking at what flotation could achieve in its early years both at laboratory (bench-scale) and in continuous production this was indeed a breakthrough in the mining

sector. Nagaraj and Farinato (2016) referred to the history of flotation as a record of impressive innovations since it was able to sustain efficiencies and productivities even as the quality and grades of ores declined.

2.7.3 The present times of mining sector

There are still lots of laboratory flotation cells used these days as shown in Figure 2.30 and Figure 2.31. These are found in mining companies, research institutions like universities, private laboratories and government laboratories. Some few newer designs of these laboratory flotation cells can be seen but the basics of how flotation tests like recovery-by-size batch flotation still remain the same as it was done in the past.

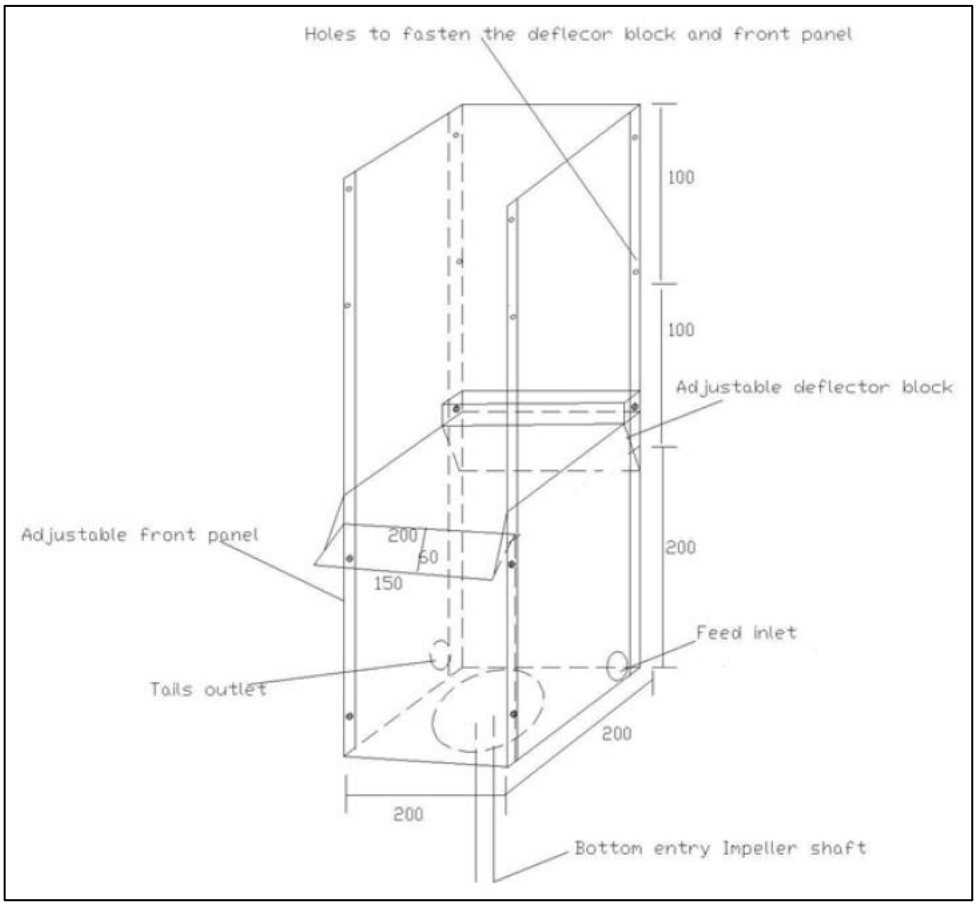

Figure 2.30: Laboratory flotation cell for batch and continuous tests with variable depth and rotor (Bhondayi, 2014)

Figure 2.31: Laboratory flotation cell for batch and continuous tests (Mackay *et al*., 2020)

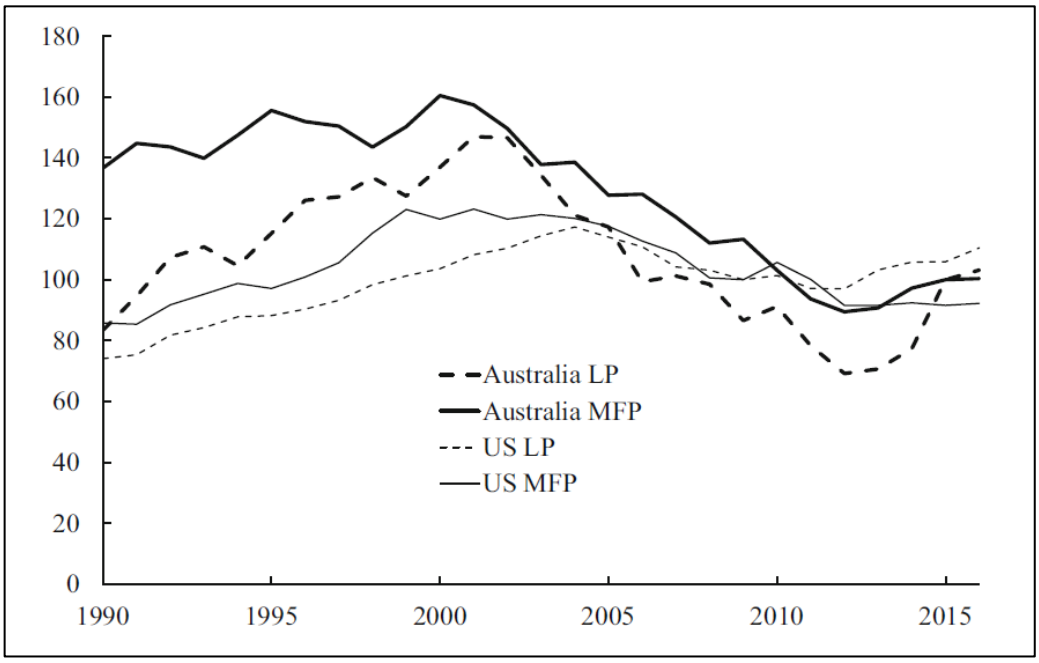

Figure 2.32: Productivity in the Australian and US mining industries (Humphreys, 2019)

The production in the mining sector has not been improving in terms of tonnages achieved as can be seen in Figure 2.32. Even though the information given in Figure 2.32 referred to Australia and United States, in other countries including South

Africa there has not been an increase in productivity recently. On the other hand, Mesa and Brito-Pada (2019) have noticed that size of flotation tanks (cells) have been increasing since the 1900's as can be seen in Figure 2.33. Most of the plants in operation these days have flotation cells way above 100 m^3.

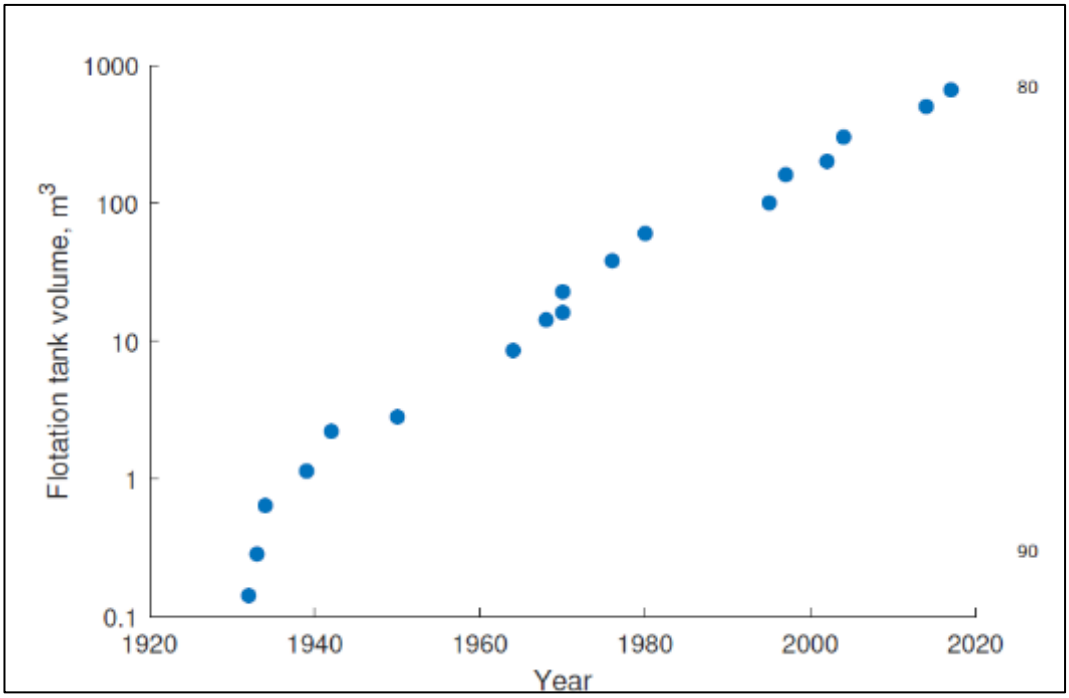

Figure 2.33: Trend in flotation tank size over the last century

(Mesa and Brito-Pada, 2019)

As things have been changing in the mining industry this has also affected flotation processes. The type of the current innovation being experienced is said to be sustainability system complexity adoption (Turk *et al*., 2019) as in Figure 2.34. Such innovation requires more research and education to be done and it must be noted that there has been a lot of changes that have taken place since flotation was introduced in the mining industry in the early 1900's. Nagaraj and Farinato (2016) regarded the innovations of the flotation technology like flotation chemistry research and development as having reached a plateau due to mounting industry challenges related to water consumption, energy consumption, declining in the ore quality, economic uncertainty, etc.

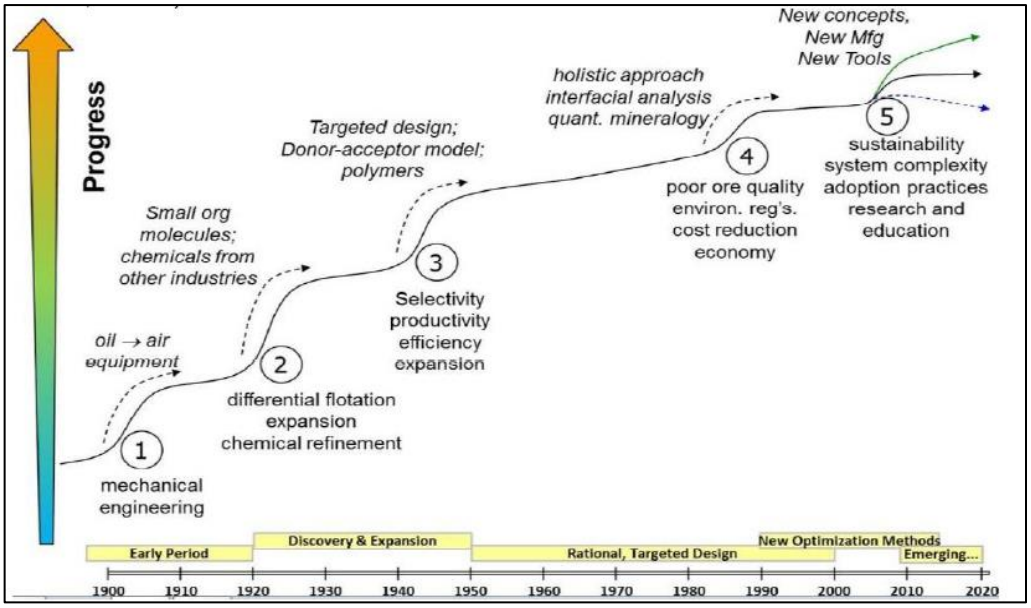

Figure 2.34: Historical progress of innovations (Turk *et al*., 2019)

Based on what flotation has to offer there seems to be a great need to focus on this field so that it will help us in the challenges we are facing at this time. In order to improve things in this current time using flotation, Nagaraj and Farinato (2016) suggested the following: detailed and holistic understanding of practical systems, better integration of chemical effects into flotation models, a more robust education system to produce adequate numbers of qualified engineers, development of novel technologies and chemical schemes that address the challenges identified and a stronger commitment by mining companies to actually adopt proposed innovations.

2.7.4 How is the future of mining sector?

In this ever changing world of technology, the flotation process either applied in the laboratory (batch flotation) or in the plant (continuous flotation operation) will also be affected in one way or the other. One question to consider will be to determine if this flotation process will cope or adapt with what the future holds? With the next 4th industrial revolution (4IR) shown in Figure 2.35 already knocking on our door step then, some form of transformation to flotation is likely to take place. Marcfarlane (2001) has listed the necessary steps as shown in Figure 2.36

of what the mine process has to undergo in order to reach intelligent mine status. It is no doubt that flotation as being part of the mine process will also be expected to partake in this suggested steps towards intelligent mine.

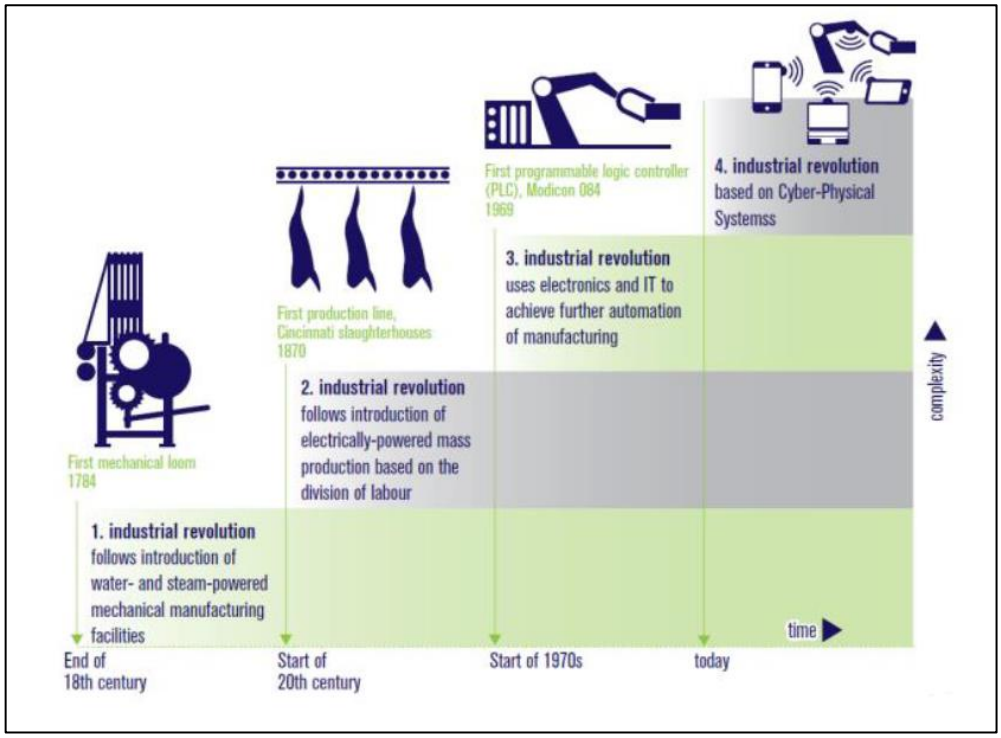

Figure 2.35: The four stages of the Industrial Revolutions – IR (Sishi and Telukdarie, 2018)

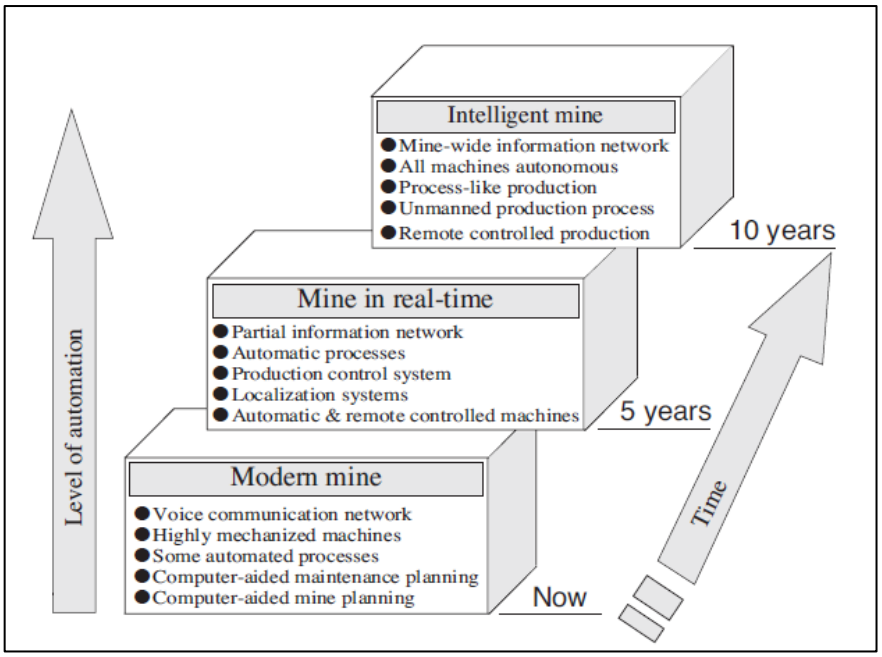

Figure 2.36: Development steps towards the Intelligent Mine (Macfarlane, 2001)

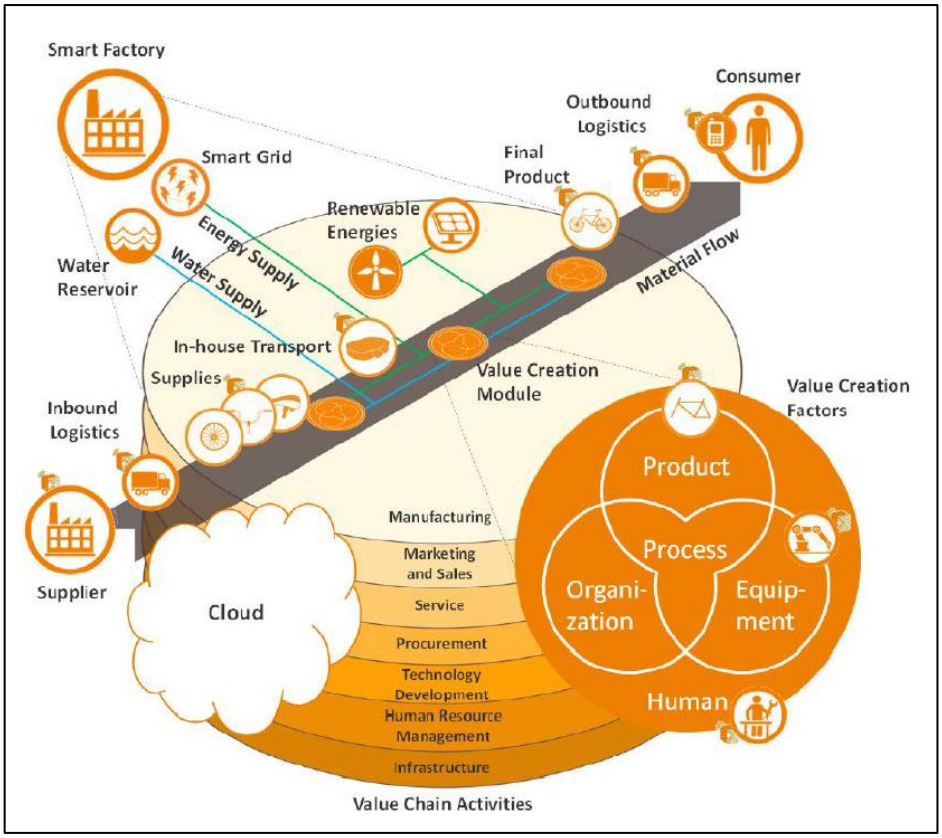

Figure 2.37: Paradigm shift with 4th Industrial Revolution - 4IR

(Sishi and Telukdarie, 2018)

The 4IR is described as the mechanisms for integrating business systems and processes and such paradigm shift is shown in Figure 2.37 (Sishi and Telukdarie, 2018). In batch flotation and continuous flotation operation, the 4IR will improve the following: reporting of assay results, instantaneous visibility on production status against plan, quality, cycle times, machine status, communication with plant operators, quick response to safety and health matters, other operational variables, etc. (Musingwini, 2016; Sishi and Telukdarie, 2018; Humphreys, 2019; Behera and Mulaba-Bafubiandi, 2016). In Figure 2.37, it is clear that not only the mining sector will experience this paradigm shift brought about by the 4IR but, almost all the different industries and their supporting structures will feel the impact. Humphreys (2019) has concluded that with the absence of 4th industrial revolution, the mining industry faces the prospect of rising costs as grades fall and waste volumes growth.

2.7.5 SWOT analysis of the mining sector

The history of flotation in the mining sector has seen the ups and downs since it came into being. The Strength, Weaknesses, Opportunities and Threats (SWOT) analysis in Table 2.8 seeks to sum up what has been highlights and lowlights in this mining sector but also embracing the future with opportunities and threats that may exist.

Table 2.8: SWOT analysis of the mining sector in general

STRENGTHS:	**WEAKNESSES:**
Contributor to gross domestic product (GDP). Provision of employment to most job seekers. Supporting students with bursaries and experiential training. Has been around for more than a century and is likely to progress for many years to come. Is known to partake in community related projects e.g. supporting schools, building or renovating clinics, building community halls, improving road constructions, supporting sporting events, etc.	Favoured by weaker rand-dollar (R/$) exchange. Mostly affected by industrial strikes / protests. Not all are fully equipped to beneficiate minerals to final saleable product hence; there is a need to export unfinished product. May disturb or affect nearby communities by its dust or gas emissions. Is easily susceptible to illegal mining practices. Exposed to failures to comply with Mine Health and Safety Act (MHSA) shown by number of fatalities in the mining sector.
OPPORTUNITIES:	**THREATS:**
Application of 4th industrial revolution set to bring new avenues of how things are done in mining. New innovations to improve current practices.	Lowering of head grades. Depletion of ore reserves. High operational costs (OPEX) and capital costs (CAPEX).

Research and development to better understand new applications. Competing at global scale. Opened up and accommodating women and youth to practice their career at all levels.	Less appetite for investors in mining related projects. Unconducive government fiscal policies. Uncertainty brought about by political interference. Strict rules to obtain mining rights.

2.7.6 Summary on mining sector times

The mining sector has been and continues to form part of the integral contributor to the economy of South Africa and the rest of the world. It has been shown that flotation brought a memorable contribution in how things are done. Bunyak (2000) explained the development of flotation as having been able to solve an industry dilemma and allowed increased minerals production to meet twentieth-century industrial and manufacturing demands. The SWOT analysis done has shown that the mining sector still has something to offer now and going forward, even though there are mounting threats and weaknesses that it possesses. Based on the role that the mining sector has then, it will be necessary to always support batch flotation and continuous flotation operations.

2.8 Conclusions

The review focused on factors affecting dispersed flotation and these have shown that froth flotation has a multi-component, multi-variable and complex nature. Previous work mostly conducted in laboratory flotation has been making use of simple bench-scale (batch) flotation tests, lock-cycle flotation tests and recovery-by-size flotation methods. The scale-up techniques were found to be following empirical analysis in their formation which lead to a certain degree of flexibility achieved in their use. Looking ahead, it was also revealed that flotation still has a major role to play in our society up to the fourth industrial revolution (4IR).

This research work was then put together to properly determine if recovery-by-size data from batch tests were affected by flotation residence time. It can be said that flotation was effective up to a certain time but not the same for fines, medium and coarse size ranges. As the flotation is not only taking place under laboratory environment then, this work had to make use of recovery-by-size data from batch flotation tests and scale-up to model the response of the ore in an industrial environment. A need to develop a simulation tool for scale-up was realised.

Chapter 3 Experimental set-up of batch flotation tests and plant surveying programme

3.1 Introduction

Management principles were applied in the set-up and execution of the experiments that enabled the collection of data relevant to the aim of this doctoral study. These principles entailed the following steps: planning, organising, leading and control (Carpenter *et al*., 2012).

The planning phase was done by taking into consideration the number of samples to be taken as well as, the experimental protocol that meets the standard of a doctoral research. The organisation phase had to do with sourcing the required sampling equipment and personnel to be involved in the sampling activity. This also included the formation of a technical team that would assist with various tasks during the execution of the experiments. The leading part was ensured by the researcher's involvement in all stages of the activities undertaken. Control had to do with making sure that experiments were done according to set procedures such that the quality was not compromised.

The critical phase in the design of the experimental programme followed the five steps advocated by Napier-Munn (1995). These steps are summarised below:

- Definition of the objectives of the experiments.
- Formulation of the objectives mathematically guided by the objectives of the research work.
- Selection of key factors or parameters to be included in the experimental investigation.
- Selection of the testing ranges for the individual factors selected in the previous step.
- Selection of the appropriate experimental design built upon statistical principles.

In line with statistical principles, it was decided that the laboratory testwork and the plant sampling campaign would fall into the type of experiments known as replicated randomised block design. This means that the treatment within each block should be replicated to give a better estimate of the experimental error. This leads to improved efficiency in data collection and possibility of comparison between treatments.

The subsequent sections describe in detail the experimental design of the batch flotation tests. The sampling campaign carried out around the flotation plant is also discussed. Finally, logistical challenges and limitations of the testwork are identified.

3.2 Experimental protocols adopted

3.2.1 Introduction

Laboratory batch flotation tests were done using ROM ore that was carefully prepared for the purpose. These were carried out for the following total flotation times: 2, 6, 12 and 20 min. In each of these flotation times, triplicates were run for consistency and error analysis. Consistency can be measured by estimating the relative standard deviation of replicates which is to be kept below the maximum limit of 5 % (Lotter *et al*., 2014; Gao *et al*., 2013).

Equipment used for batch flotation testing included but not limited to the Denver laboratory flotation machine, sieves, shaker, ovens, weighing balance, splitter, sampling buckets, sample cutters, and scoops. Plant reagent suite was used for conditioning and batch testing at the same concentrations as those that are generally prepared in the continuous flotation circuit. Head grade samples, final concentrates and tailings were sent to the chemical laboratory and analysed for %Cu either by the Atomic Absorption (AA) machine or the X-Ray Fluorescence (XRF) machine.

In terms of continuous flotation testing, two types of sampling campaigns were made. The first one was for the overall flotation recovery which included feed to

flotation circuit and final concentrate followed by final tailings samplings. The second type of sampling involved the taking of each rougher plus cleaner / re-cleaner cells samples (feed, concentrate and tails) in a row. This was to look at the performance of each cell in terms of recovery similar to what was done by McIvor and Finch (1990), Trahar (1981), and King (2012).

3.2.2 Batch flotation methodology

Run-of mine (ROM) material was collected on five different days over two months to form a composite sample. This was done to make sure that samples used for batch float experiments were fairly representative of what the continuous flotation operation is treating.

A sample is said to be representative if it contains the same distribution of particle properties. These include shape, size, and mineral liberation to name a few. In the case of laboratory flotation tests, each sample should have the same distribution of flotation rate constants k defined in Equation (2.1). The distribution of mass fractions for each mineral is also an important property that should be considered in sample preparation (Varadi *et al*., 2010). Runge (2010) also indicated that it is important that all batch flotation tests are performed at the same air rate, impeller speed, froth depth and froth scraping rate. This is to ensure that any change in a batch test results is the consequence of a change in the ore characteristics rather than experimental conditions.

In the experiment done as part of this doctoral study, air rate and impeller speed were kept constant. Efforts were also made to maintain the same scraping rate; however, this depended heavily on the skills of the technician who assisted with the actual flotation tests. The laboratory flotation machine used did not allow for froth depth measurements. This implies that froth depth could only be observed visually and not physically measured but, at least kept within the same level through plant control.

Talking about the collection of recovery-by-size data, it should be noted that two approaches were pursued to that end:

- Sample the ROM ore and conduct batch flotation tests; then, conduct sieving of concentrates, tails and head samples produced after batch testing. Last, send each size fraction to the laboratory for grade analysis.
- Sample feed, concentrates and tails from the flotation plant; then, dry these samples before sieving them. Mass fractions sent for grade analysis thereafter.

In both the two protocols outlined above, recovery was calculated from first principles using the classical two-product equations below (Wills and Napier-Munn, 2006):

$$\%Rec = \left(\frac{f-t}{f}\right) * 100 \quad (3.1)$$

$$\%Rec = \frac{c}{f} * \left(\frac{f-t}{c-t}\right) * 100 \quad (3.2)$$

where: $\%Rec$ is the flotation recovery

f is the feed/head grade

t is the tails grade

c is the concentrate grade.

Upon estimating the recovery for each screen size, the array of recoveries produced over the entire particle size spectrum made up what has been referred to in this thesis as recovery-by-size data. Note that Equation (3.1) takes the form of the first part of Equation (2.10).

The standard procedure for batch flotation testing adopted as part of the experimental work is displayed in Figure 3.1. The symbols used in this figure are: RC1 – first rougher concentrate collected, RC4 – fourth rougher concentrate collected, RT – rougher tailings, neat soln. – pure or undiluted (used as is) solution and g/t – grams per ton which is the reagent dosage measurement.

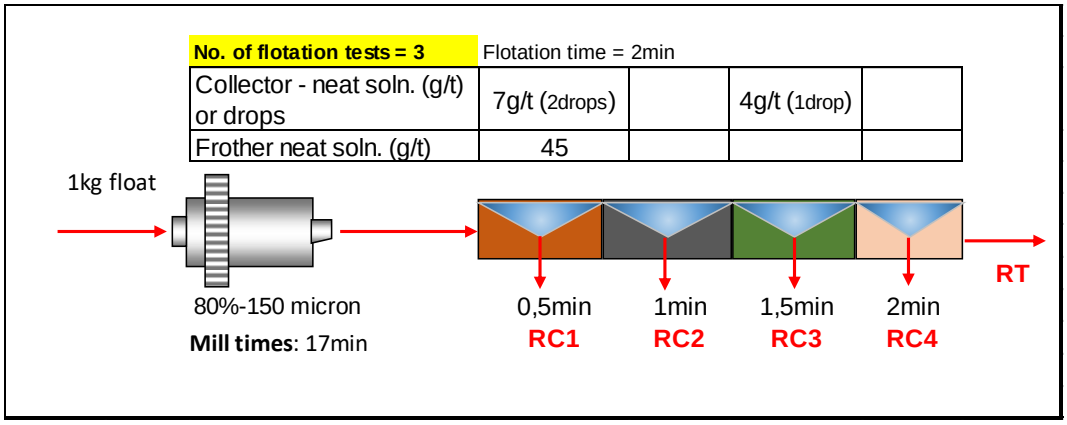

Figure 3.1: Layout of the protocol for batch flotation testing procedure

To elaborate on the procedure, a 2-3 m belt cut of the ROM material was taken in the plant. The belt-cut sample was air-dried for 4 – 5 days until all moisture was removed. The dried sample was then crushed in the laboratory jaw crusher followed by cone crushing to below 2 mm in size. Rhologan screens were used to prepare the -2 mm material which was subsequently portioned in 1 kg samples with a rotary splitter. The use of Rhologan screen of the same size, i.e., 2 mm ensured that the feed samples were the same in all the tests conducted. Afterwards, a laboratory rod/ball mill was used to grind the 1 kg samples and prepare samples for batch flotation testing. For this work, a rod mill of 225 mm length and 200 mm diameter consisting of 187 mm length of 13 – 19 mm diameter rods were added and not balls. Mass of these rods was maintained at 12 – 12.5 kg by continuously weighing them at the end of each test and there would be about a total of 20 – 25 rods used at a time. Design of the rod mill is rubber lined inside and has 6 x liners along the inside perimeter and these liners were angular in shape, 50 mm of length while their highest middle thickness / height was 4.5 mm. The samples were milled down to 80% -150 µm fineness for 17 min and at a constant rotational speed of 10 rpm. Keeping the same milling time then, it was necessary to make sure that mono-sized samples were used for batch testing purpose and this could be achieved as only -2 mm material was subjected to further processing.

In terms of the laboratory batch flotation tests, the same suite of flotation reagents used in the plant served to condition the samples and carry out all the tests. Different total flotation times were considered while each test was triplicated. This was aimed not only at determining the effects of flotation residence time on concentrate grade and recovery, but also at estimating the experimental errors incurred. The flotation machine used was a 2.5 litre Denver flotation cell set at a rotor speed of 1500 rpm. There were four flotation times considered in this testwork, i.e., 2 min, 6 min, 12 min and 20 min. These flotation times were measured by making use of the stopwatch. In all the flotation times used, there would be four concentrates collected at certain intervals as shown in Table 3.1 below. In Figure 3.3, there is an example of 2 min flotation with its cumulative time intervals of collecting concentrates. The concentration of reagents i.e. Collector (Sodium Iso-Butyl Xanthate – SIBX) was diluted to 1 % strength and Frother (Sasfroth 2004) was also neat (undiluted or pure), i.e., 100 %. Since the batch flotation had to resemble the continuous plant operation then no conditioning was done in the laboratory as the plant also does not have conditioning tanks installed. The only conditioning that occurred in the laboratory was that waiting period before each concentrate was collected on the stipulated times. A separate study may need to be done to look into the effect of conditioning time where, different durations of conditioning times will have to be compared with no conditioning.

Table 3.1: Intervals for different flotation times

Intervals	Concentrate collected	TOTAL FLOTATION TIMES			
		2 min	6 min	12 min	20 min
1st	RC1	0.5	1.0	2.0	5.0
2nd	RC2	1.0	2.0	6.0	10.0
3rd	RC3	1.5	4.0	8.0	15.0
4th	RC4	2.0	6.0	12.0	20.0

The concentrate pulling rate to the pans was maintained at no more than 10 seconds when conducting flotation tests. A stopwatch was used to achieve the desired cumulative times between fractions of concentrates collected; for example, for total flotation time of 2 min shown in Figure 3.1, desired cumulative times were 0.5 min, 1 min, 1.5 min and 2 min. The complete set of different flotation times used for the whole experimental conditions can be clearly seen in Table 3.1. The more detailed tables for each flotation time used can be seen in Appendix I. At the end of each test; heads, concentrates and tails were filtered using vacuum filter pump. The filtered samples were then oven-dried at 110°C. These head, concentrate and tail samples were sieved separately from 850 µm down to 38 µm. The mass fractions were obtained in five size classes: -850+425 µm, -425+150 µm, -150+53 µm, -53+38 µm, and -38 µm. Finally, individual materials retained in each size class were sent to the chemical and mineralogical laboratory for grade analysis. The X-Ray Fluorescence (XRF) machine used was from Malvern Panalytical and was the Axios-Max Type (2013). On the other hand, the Atomic Absorbtion (AA) machine type was the 240 FS Series (2016) and was manufactured by Agilent Technologies.

3.2.4 Continuous flotation plant sampling methodology

The same management techniques presented in Section 3.1 were resorted to when planning for plant sampling. The only difference with batch testing is that continuous flotation plant sampling was done on a plant running at full production capacity. In this case then, a great reliance is placed on a very small sample that is supposed to be truly representative of the bulk (Holmes, 2002). For the continuous operation under investigation, composite samples of the streams identified in Figure 3.2 could be taken for only one hour so as not to disturb production. Several samples were also collected at points not shown in Figure 3.2 during the three planned sampling campaigns. However, they were not sampled consistently throughout the three days; hence, triplicates could not be collected. Other researchers like Trahar (1981), McIvor and Finch (1990), and Smar *et al*. (1994)

have done similar plant testwork even though there may have approached it differently in other parts of their studies.

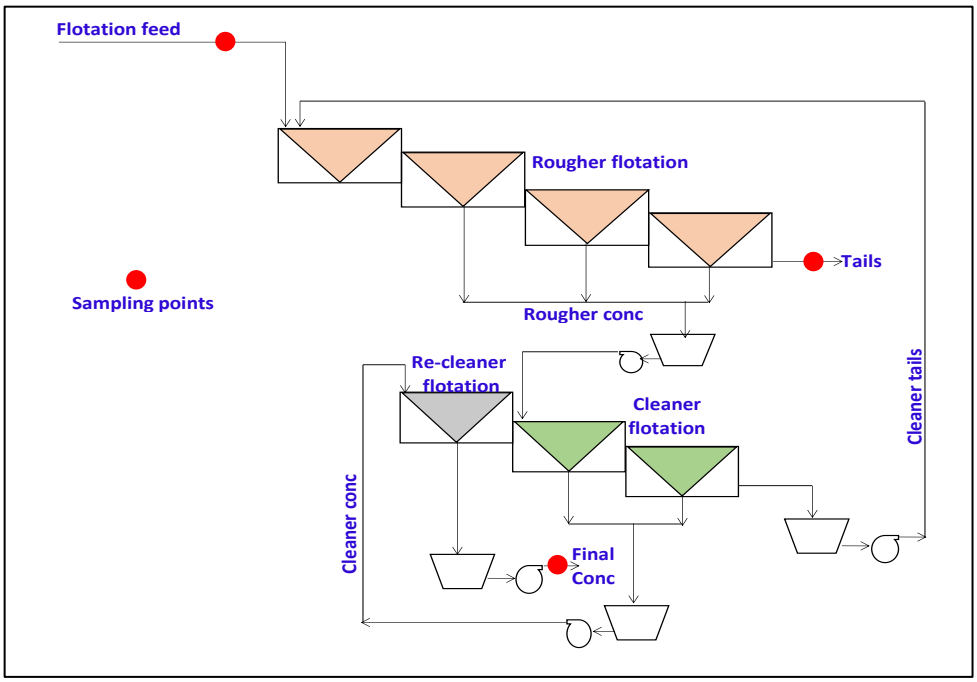

Figure 3.2: Flotation plant circuit showing sampling points

During the allocated sampling time, the plant was closely monitored for steady-state operation. Most parameters like throughput, densities, and reagent dosages were noted to remain fairly constant without any sudden variation from their baseline. Upon ensuring this was the case, samples were collected along selected streams by the sampling team and later sent to the laboratory for analysis. Three such sampling campaigns were arranged on different days for an hour each.

Coming back to Figure 3.2, one needs to point out that samples were collected at the sampling points indicated and analysed to establish the recovery of the plant by particle size. Unlike batch flotation tests, the plant survey did not require sampling at different times as the operation is run and sensibly maintained at a specific throughput (t/h).

The first set of sampling campaign looked at the three main sampling points, i.e., feed to flotation, final concentrate and final tailings. The metallurgical performance in this test was the overall recovery and overall concentrate grade

for the flotation circuit. The second test focused on sampling each cells in the row, i.e., feed to each cell, concentrate of each cell as well as final tailings of each cell. Since the cells in the row were divided into banks then it was easier to composite samples of each bank and reported them per bank instead of per cell as shown in Figure 3.3. The type of cells in the continuous flotation plant were Wemco Fagergren with capacity of 8.5 m^3 each cell. Reagent conditions in the continuous flotation plant were left unchanged to the normal operation.

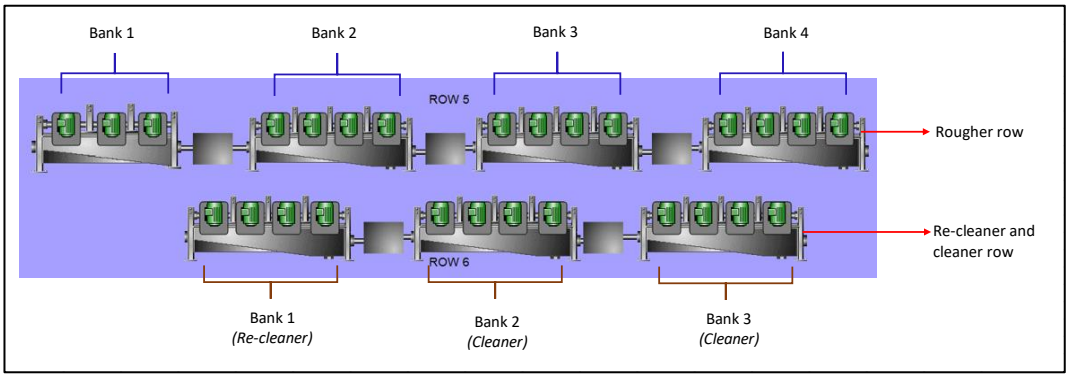

Figure 3.3: Approach used in metallurgical characterisation

In summary, as part of the sampling campaign, stability of the plant was first monitored from the control room over a 2-hour run of plant. Stable operating conditions had to be established before sampling could commence. Three dedicated sample-taking personnel were placed at each sampling point shown in Figure 3.2 with the right sample cutters, buckets and protective clothing. A team leader would oversee the sampling by ensuring synchronised communication between the plant and the control room. At the signal, composite samples were collected at 15-min intervals for the 1-hour duration at each sampling point. The collected samples were then sent to the laboratory for weighing, filtering and oven-drying. Once the samples were retrieved out of the oven, they were prepared following the same procedure used after batch flotation testing and readied for the grade analysis to follow. Last note, three sampling campaigns were done on different days for error analysis.

3.3 Simulation programme used for computer modelling

The key objective of this study is to explore the use of the recovery-by-size flotation recovery model (Equations 2.30 and 2.31) presented in Section 2.4.3. In line with this, it was seen as necessary to simulate the performance of the continuous flotation operation. The idea was to eventually attempt scale-up between collected batch and plant flotation data.

The choice of the simulation tool was primarily based on the availability, accessibility, and relevance of such software. ModSim became the suitable choice for this work as is explained in the sections below. All simulations were undertaken from the academic version of the aforementioned software package.

3.3.1 Overview of ModSim

The name ModSim stands for Modular Simulator, that is, a computer-based steady-state simulator comprised of various modules capable of mimicking the behaviour of most mineral processing operations.

The inception of ModSim goes back to 1972 when the late Prof R.P. King and his PhD student M.A. Ford wrote the first version in FORTRAN. The simulation engine of ModSim was written to handle loop finding, circuit decomposition, and sequential calculation algorithms (King, 2012). The modular structure of ModSim also allows for the addition and modification of models of existing and new unit operations. This has the advantage of being tuned to the needs of any plant operated even under unusual conditions (King, 2012; Hahn and Valentine, 2007).

Currently, ModSim is distributed by Mineral Technologies International Inc. Two versions are available: academic and professional. There are additional features on the professional version not available in the academic version. The notable difference between the two versions is that the option of adding models is not active in the academic version while other functionalities are almost similar. Different equipment are available in ModSim where simulations can be done and some of those equipment are shown in Figure 3.4.

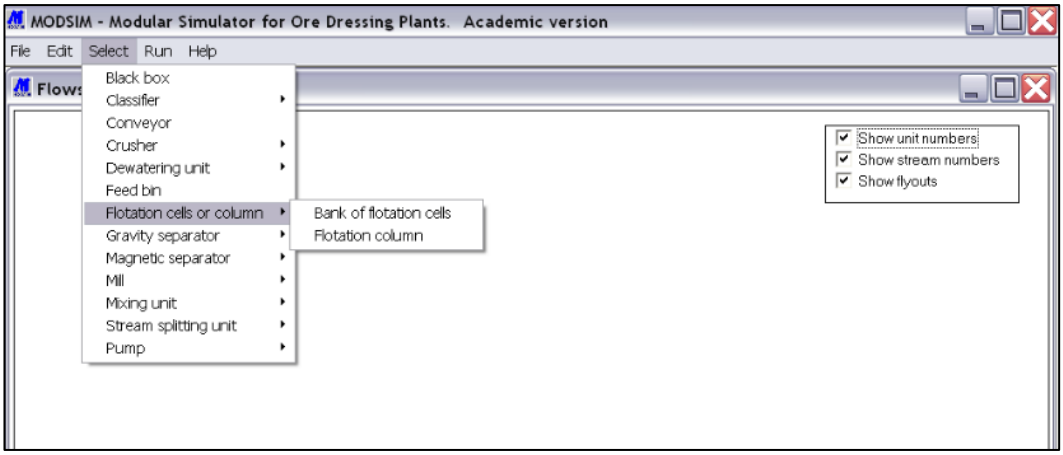

Figure 3.4: List of equipment that can be simulated in ModSim

The detailed mass balance of any ore processing/dressing plant can be done in ModSim. The exercise generally produces the total flow rates of water and solids, the particle size distributions of the solid phase, the distributions of particle compositions and the average assays of the solid phase (Hunt *et al*., 2001; King, 2012). From this perspective, the information outputted may find value in troubleshooting and in the design of plants and equipment. Plant operators can also be given optimal operating conditions obtained from ModSim that would meet the production targets. It must be highlighted that ModSim is not suited for the simulation and design of dynamic operations as well as process control systems.

3.3.2 Characteristics and features of ModSim

ModSim as a steady-state computer-based simulator is known to be affordable, fully interactive and user-friendly (King, 2012; Hahn and Valentine, 2007). The software package is grounded in sustained research and development validated against numerous industrial operations. That is why for each unit operation, ModSim offers several options of models including the most recent found in the scientific literature. Each model behind the unit operation also comes with a set of default parameters.

Perhaps one of the most important features available in ModSim is the ability to simulate mineral liberation across unit operations. This feature alone makes ModSim a good software candidate for the study on flotation operations from the perspective of recovery-by-size data. Indeed, mineral liberation simulation allows one to characterise jointly grade and size distributions and, ultimately, study how liberated minerals will be floated.

The other interesting feature is the availability of a comprehensive user manual that includes a complete description of the mathematical models behind each unit operations. The next section is devoted to presenting the models used for froth flotation as well as their respective input parameters.

3.3.3 Flotation models available in ModSim

In ModSim, all models behind a unit operation are identified by four capital letters. As far as the flotation process is concerned, three models are offered as part of the ModSim academic version 3.6 used in this doctoral thesis. The three flotation models are listed here with their corresponding identifying abbreviations: Klimpel model (KLIM), King model (FLTK) and Sutherland model (FLTN). Each model reacts differently to the data input as they were developed under different conditions and use different sets of input parameters as shown in Figures 3.5 – 3.7.

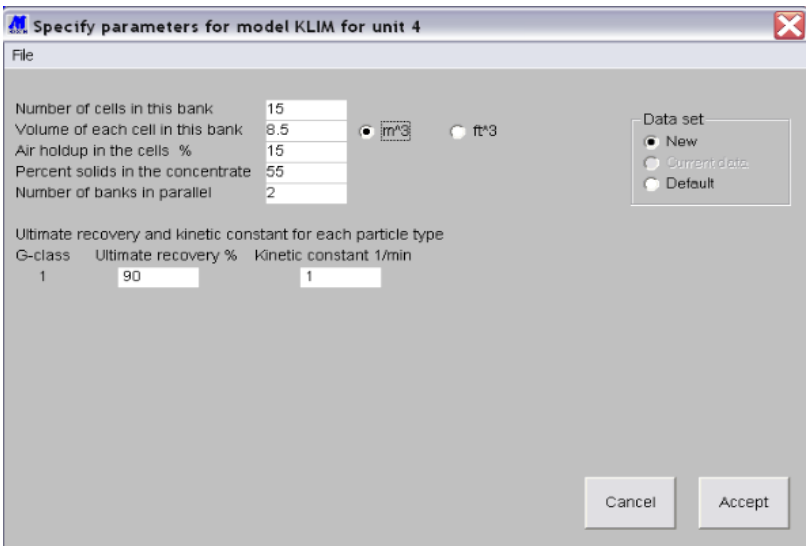

Figure 3.5: ModSim – KLIM model used

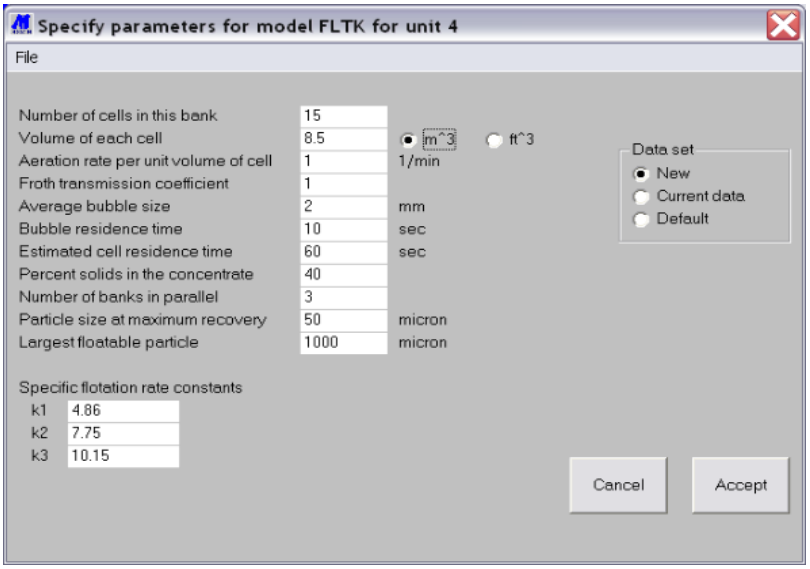

Figure 3.6: ModSim – FLTK model used

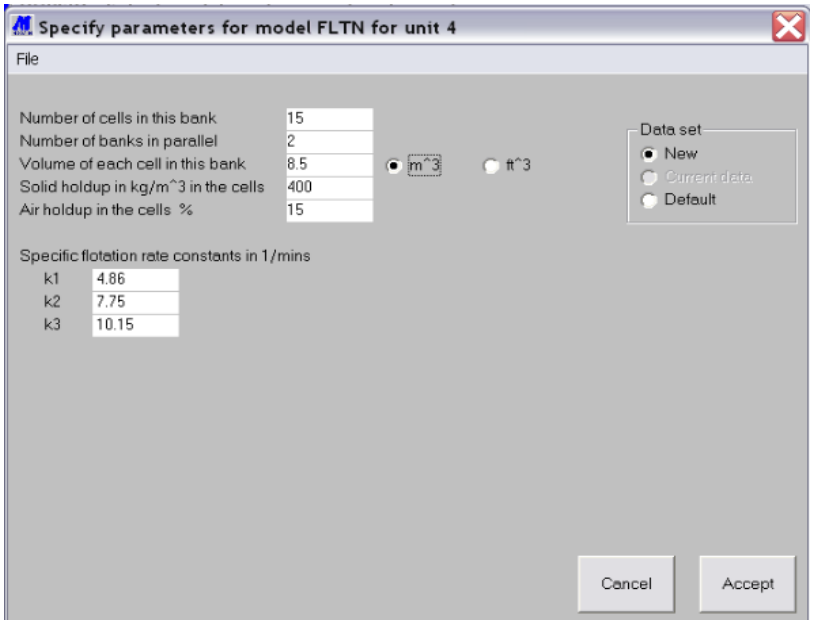

Figure 3.7: ModSim – FLTN model used

The data used in the ModSim models was taken from laboratory testwork conducted, measurements done in the plant, plant design data and historical data that has been collected. Depending on the testwork conducted and data collected then such data to be used in ModSim will differ for each time.

3.4 ModSim approach to scale-up

The first step involved the setting up of the flowsheet to resemble the plant where samples would be taken. Particle size distribution (PSD's) for all the streams were then put into ModSim. Flowrates and densities measured in the continuous flotation plant had to be put in the ModSim. Water addition rates either in sumps or flotation cells also needed to be catered for. Each unit operation had its associated model parameters that needed to be included as explained in the previous section. Once all the above information was inserted then running of simulation was possible.

ModSim simulated results could be presented in different formats depending on what is required at that time. In order to get results of different flotation models tested then re-running of simulations was necessary. Different flotation models were applied for each and every simulation conducted e.g. KLIM and FLTN had different simulation runs respectively. Summary mass balance table was obtained that showed experimental and simulated results. PSD trends were also available for experimental and simulated results. Some calibration of the simulation results were done where the results appeared to be over or under estimated by simulations done. The combination of all results generated then allowed scale-up and model validation processes to be done which will be covered in the later chapters to follow.

3.5 Challenges encountered and solutions

The execution of the planned batch and continuous experiments came with its own challenges. Limitations were also identified in terms of material sampling, surveying campaign and computer simulations. For the successful completion of this research project, several solutions were implemented to mitigate against the challenges as and when they were being experienced. Some of the identified challenges could not be completely overcome; in such cases, notes were made for consideration in the sense-making of results reported in subsequent chapters.

The hydrodynamic characterisation consists of four main distribution mechanisms e.g. flowrate distribution, residence time distribution (RTD), effective cell volume estimation and solid segregation (Yianatos *et al*., 2010). Liquid and solid tracers plus on-line data acquisition measuring unit are needed for flowrate distribution and residence time distribution (RTD) measurements. Data to calculate the effective cell volume estimation and solid segregation can be read from RTD curves thereafter; perform then necessary calculations. In this research, measurements for hydrodynamic characterisation could not be performed as the requirements for such were not readily available. Published data on Wemco cells were then used for this work as reported by Yianatos *et al*. (2005) and Yianatos *et al*. (2010).

The next section Tables 3.1 – 3.2 gives the summary of these challenges and limitations together with mitigating solutions.

Table 3.1: Solutions to selected challenges associated with batch flotation testing

#	Challenge / Limitation	Solution
1	Obtain representative sample of the ROM ore.	Composite samples were taken for 5 days in a two months' time.
2	Preparing of all material collected from the feed conveyor.	Only material of less than 100 mm could be taken and what was above that had to be rejected. This was due to the open side setting of laboratory crusher used.
3	Sampling of belt-cut of more than 3 m size.	Due to the size of the material in the belt then more than 3 m would have been more labour intensive and also would have taken more of production time to have the belt standing for taking samples.
4	Maintaining constant mass pull during flotation testing.	One person was used for the batch flotation testing throughout the testing done.
5	Consistency in sample preparation for chemical analysis.	Approved metallurgical sample preparation procedure was utilised.

Table 3.2: Solutions to the challenges of surveying the continuous flotation circuit

#	Challenge / Limitation	Solution
1	Obtaining stable plant before taking samples and during sampling.	Waiting period of 2 hours was observed while checking SCADA trends for stability. A person was kept in the control room during the 1 hour sampling time to make sure stability of the plant was maintained.
2	Taking samples at the same time in different sampling points.	Watches for sampling personnel had to be synchronised in relation to the Supervisory Control and Data Acquisition (SCADA) computer housed in the control room. A two-way radio communication system was also utilised during sampling.
3	Doing samples on different days under the same operating conditions.	This could not be completely achieved since the operations used are for production other parameters could not be changed just to suit the project work. Records and trends of all conditions on different days for sampling were kept for reference purpose especially when analysing data from sampling.
4	Ease of taking samples from identified sampling points.	Feed and concentrate samples were easy to access and sampling them. Tailings sample proved to be challenging and two people had to be used to get it.
5	Obtaining hydrodynamics parameters from sampling campaign to be used for scale-up	No equipment available to use for hydrodynamics and design data from the Original Equipment Manufacturer (OEM) had to be relied upon. Where design data was not sufficient then published data had to be used.
6	Consistency in sample preparation for chemical analysis.	Approved metallurgical sample preparation procedure was utilised.

3.6 Concluding remarks

The experimental programme conducted as part of both the batch and continuous flotation testing was thoroughly planned and executed. This was to ensure that

good quality data was collected considering all the internal and external factors at play. The shortcomings experienced were noted and mitigating solutions were implemented where possible. ModSim has proved to be capable of doing simulations involving simple and complex circuits. It was also noted that ModSim provided different models for single unit operation which then made simulations not to be limited to only one or few options.

Equipping the flotation plant with the SCADA control system proved very handy in collecting reliable operational data and making sure that stability was observed constantly during the sampling campaign. Proper communication amongst personnel also played a major role as this ensured that all involved in laboratory or plant work were having the same information timely.

The next chapter will look into the data analysis and interpretation of the laboratory batch flotation tests conducted in this research.

Chapter 4 Batch flotation testwork used to characterise ore for scale-up purposes

4.1 Introduction

Batch flotation tests will be mostly used for scaling-up to large flotation cells to be utilised in continuous flotation operation. The surface chemistry conditions experienced in the laboratory may not produce similar results when up-scaled to the production environment that consists of more severe instabilities. This chapter will then look into the batch flotation tests conducted in the laboratory. Analysis of results from batch flotation tests will be explored using different methods from first principles to statistical approach. Discussion of results by making use of error analysis will be carried out followed by conclusions. It is important to note that this chapter will try to show how batch flotation results can be used to eventually characterise ore for scale-up purposes.

4.2 Raw data for batch flotation tests

The samples for batch flotation testwork were taken and prepared in the metallurgical laboratory. Assays results for feed, concentrate and tails from the chemical laboratory based on the testwork conducted can be seen in Table 4.1 – 4.4.

Table 4.1: Raw data for 2-minutes for batch flotation

Mean particle screen size	*Particle screen size range*	2-min Test 1			2-min Test 2			2-min Test 3		
		Head grade	Tails grade	Conc grade	Head grade	Tails grade	Conc grade	Head grade	Tails grade	Conc grade
(µm)	(µm)	(%Cu)	(%Cu)	(%Cu)	(%Cu)	(%Cu)	(%Cu)	(%Cu)	(%Cu)	(%Cu)
638	*-850+425*	0.514	0.169	8.621	0.514	0.110	10.334	0.514	0.064	9.535
288	*-425+150*	0.560	0.225	7.716	0.560	0.074	11.388	0.560	0.037	14.279
102	*-150+53*	0.653	0.056	16.761	0.653	0.073	18.378	0.653	0.033	15.265
46	*-53+38*	0.856	0.169	8.729	0.856	0.135	8.690	0.856	0.042	6.326
19	*-38*	0.753	0.225	3.276	0.753	0.159	2.878	0.856	0.142	2.269

Table 4.2: Raw data for 6-minutes for batch flotation

Mean particle screen size	*Particle screen size range*	6-min Test 1			6-min Test 2			6-min Test 3		
		Head grade	Tails grade	Conc grade	Head grade	Tails grade	Conc grade	Head grade	Tails grade	Conc grade
(µm)	(µm)	(%Cu)	(%Cu)	(%Cu)	(%Cu)	(%Cu)	(%Cu)	(%Cu)	(%Cu)	(%Cu)
638	*-850+425*	0.556	0.061	7.384	0.556	0.118	13.956	0.556	0.173	9.445
288	*-425+150*	0.581	0.058	6.590	0.581	0.074	7.337	0.581	0.109	6.270
102	*-150+53*	0.608	0.033	14.979	0.608	0.033	27.224	0.608	0.033	19.486
46	*-53+38*	0.633	0.048	6.321	0.633	0.062	18.397	0.633	0.061	10.183
19	*-38*	0.674	0.088	1.647	0.674	0.083	2.865	0.674	0.170	1.840

Table 4.3: Raw data for 12-minutes for batch flotation

Mean particle screen size	*Particle screen size range*	12-min Test 1			12-min Test 2			12-min Test 3		
		Head grade	Tails grade	Conc grade	Head grade	Tails grade	Conc grade	Head grade	Tails grade	Conc grade
(µm)	(µm)	(%Cu)	(%Cu)	(%Cu)	(%Cu)	(%Cu)	(%Cu)	(%Cu)	(%Cu)	(%Cu)
638	*-850+425*	0.488	0.051	11.433	0.488	0.057	11.596	0.488	0.060	10.311
288	*-425+150*	0.560	0.033	10.985	0.560	0.032	14.919	0.560	0.032	9.259
102	*-150+53*	0.653	0.032	21.511	0.653	0.033	20.169	0.653	0.035	19.529
46	*-53+38*	0.753	0.040	10.590	0.753	0.048	8.991	0.753	0.055	9.978
19	*-38*	0.856	0.100	2.646	0.856	0.114	2.303	0.856	0.116	2.476

Table 4.4: Raw data for 20-minutes for batch flotation

Mean particle screen size	*Particle screen size range*	20-min Test 1			20-min Test 2			20-min Test 3		
		Head grade	Tails grade	Conc grade	Head grade	Tails grade	Conc grade	Head grade	Tails grade	Conc grade
(µm)	(µm)	(%Cu)	(%Cu)	(%Cu)	(%Cu)	(%Cu)	(%Cu)	(%Cu)	(%Cu)	(%Cu)
638	*-850+425*	0.489	0.049	6.409	0.489	0.049	5.244	0.489	0.049	5.000
288	*-425+150*	0.584	0.038	14.474	0.584	0.038	10.782	0.584	0.038	4.518
102	*-150+53*	0.616	0.035	5.620	0.616	0.035	3.982	0.616	0.035	9.330
46	*-53+38*	0.633	0.051	1.488	0.633	0.051	4.741	0.633	0.051	4.787
19	*-38*	0.715	0.072	4.043	0.715	0.072	1.469	0.715	0.072	1.366

The raw data obtained was subjected to statistical analysis in order to test significance differences. Table 4.5 showed the analysis done for the 2 min raw data. It was found that the p-value of 0.9998 obtained was showing that there was no significant differences. The analysis done were conducted at 95 % confidence level. This outcome allowed the acceptance of the null hypothesis, i.e., there is no difference and this was supported by p-value > 0.05. The same statistical analysis

were also done for 6 min, 12 min and 20 min. The p-values obtained for other batch flotation times were 0.9999, 0.9996 and 0.9977 respectively.

Table 4.5: Chi-square statistics analysis for 2-min raw data batch flotation

Observed Counts									
Mean particle size (µm)	Head grade	Tails grade	Conc grade	Head grade	Tails grade	Conc grade	Head grade	Tails grade	Conc grade
638	0.514	0.169	8.621	0.514	0.110	10.334	0.514	0.064	9.535
288	0.560	0.225	7.716	0.560	0.074	11.388	0.560	0.037	14.279
102	0.653	0.056	16.761	0.653	0.073	18.378	0.653	0.033	15.265
46	0.856	0.169	8.729	0.856	0.135	8.690	0.856	0.042	6.326
19	0.753	0.225	3.276	0.753	0.159	2.878	0.856	0.142	2.269
Expected Counts									
Mean particle size (µm)	Head grade	Tails grade	Conc grade	Head grade	Tails grade	Conc grade	Head grade	Tails grade	Conc grade
638	0.648	0.164	8.767	0.648	0.107	10.043	0.668	0.062	9.267
288	0.756	0.191	10.217	0.756	0.125	11.704	0.779	0.072	10.799
102	1.121	0.284	15.160	1.121	0.185	17.367	1.156	0.107	16.024
46	0.569	0.144	7.694	0.569	0.094	8.814	0.587	0.054	8.133
19	0.241	0.061	3.265	0.241	0.040	3.740	0.249	0.023	3.451
Std. Residuals									
Mean particle size (µm)	Head grade	Tails grade	Conc grade	Head grade	Tails grade	Conc grade	Head grade	Tails grade	Conc grade
637.50	-0.167	0.012	-0.049	-0.167	0.009	0.092	-0.189	0.009	0.088
287.50	-0.225	0.077	-0.782	-0.225	-0.144	-0.092	-0.248	-0.131	1.059
101.50	-0.442	-0.427	0.411	-0.442	-0.261	0.243	-0.468	-0.226	-0.190
45.500	0.380	0.066	0.373	0.380	0.134	-0.042	0.352	-0.053	-0.634
19	1.041	0.663	0.006	1.041	0.596	-0.446	1.217	0.784	-0.636
Chi-Square					9.877				
DF					32				
p-value					0.9999				

The key consideration for comparison purposes using recovery are generally used to estimate scale-up factors from batch flotation to continuous flotation (Boeree, 2014; Yianatos *et al*., 2005). One way to achieve this is to take overall recovery and compare this with a standard batch test under the same condition. Yianatos (2003) pointed out that individual abnormal cell operations can significantly affect the overall residence time in the bank and has proposed the use of separability curves. In this work, flotation bank operation has been modelled in order to get smooth behaviour for the recovery versus time relationship for both plant and batch scale

as shown later in Figures 5.13 and 5.14. In order to separate the effect that mixing and kinetic changes have on the time scale-up factor, a dimensionless ϕ parameter was used which gave a figure of 2.88 as shown in Appendix D.1. The differences in maximum recovery observed in batch and plant operations were accounted for by the use of dimensionless η parameter. This parameter is defined as the ratio between the recovery reached during the operation and the expected maximum recovery. Results obtained in this work were 0.961 for batch and 0.963 for continuous as in Appendix D.1.

4.3 Results of batch flotation tests

The section below tries to explain the results obtained following the methods mentioned above. The three tests (triplicates) done for the batch flotation were averaged and are shown in Table 4.6. Experimental recoveries were calculated with the use of Equation (3.2). The model developed by King (2012) was used to generate the model recoveries to see how they will fit the experimental data. Possible guesses of unknowns in the model were put in by taking what is in the published data then allowing software (MS Excel Solver) used to recalculate these unknowns to estimate values relevant to this work.

In using Equation (3.2) for example in 2 min flotation time: feed grade, tails grade and concentrate grade results obtained at 2 min were used to calculate the recovery. Since the flotation tests were done in triplicate then all three results in 2 min had to be calculated in the same manner. All the experimental recoveries were obtained following the same procedure. Model recoveries were then calculated by making use of Equation (2.10) but this had to be done in conjunction with Equation (2.11). The unknowns of Equation (2.10) that had to be recalculated by MS Excel Solver were k_j and S_{av} but, for Equation (2.11) the unknowns were ε and $d_{p\,max}$. Statistical Chi-squared test has been used to make sense of the data in Table 4.6 and results for such analysis are depicted in Table 4.7.

Table 4.6: Summary of batch flotation results

Size (µm)	Experimental recoveries				Model recoveries			
	Exp 2 min	Exp 6 min	Exp 12 min	Exp 20 min	Mod 2 min	Mod 6 min	Mod 12 min	Mod 20 min
638	78.68	79.80	88.97	90.79	71.22	76.70	88.33	89.21
288	80.87	87.22	94.50	93.95	91.05	95.03	99.64	99.68
102	92.02	94.73	95.05	94.91	99.38	99.91	100.00	100.00
46	87.71	91.51	94.13	93.69	99.92	99.99	100.00	100.00
19	82.59	88.18	91.23	93.69	82.49	88.16	91.14	95.18

Table 4.7: Chi-square statistics analysis for batch flotation results

Observed Counts								
Mean particle size (µm)	Exp 2 min	Exp 6 min	Exp 12 min	Exp 20 min	Mod 2 min	Mod 6 min	Mod 12 min	Mod 20 min
638	78.683	79.796	88.975	90.790	71.223	76.700	88.333	89.211
288	80.869	87.215	94.497	93.950	91.054	95.034	99.643	99.677
102	92.019	94.734	95.051	94.912	99.382	99.907	100.000	100.000
46	87.710	91.514	94.128	93.694	99.919	99.995	100.000	100.000
19	82.589	88.181	91.227	93.687	82.488	88.159	91.140	95.178
Expected Counts								
Mean particle size (µm)	Exp 2 min	Exp 6 min	Exp 12 min	Exp 20 min	Mod 2 min	Mod 6 min	Mod 12 min	Mod 20 min
638	76.476	80.024	84.092	84.663	80.500	83.351	86.854	87.751
288	85.490	89.456	94.003	94.642	89.988	93.176	97.091	98.094
102	89.415	93.563	98.319	98.988	94.120	97.454	101.549	102.598
46	88.373	92.473	97.173	97.834	93.023	96.318	100.365	101.402
19	82.115	85.924	90.292	90.906	86.435	89.497	93.258	94.221
Std. Residuals								
Mean particle size (µm)	Exp 2 min	Exp 6 min	Exp 12 min	Exp 20 min	Mod 2 min	Mod 6 min	Mod 12 min	Mod 20 min
638	0.252	-0.025	0.533	0.666	-1.034	-0.729	0.159	0.156
288	-0.500	-0.237	0.051	-0.071	0.112	0.193	0.259	0.160
102	0.275	0.121	-0.330	-0.410	0.542	0.249	-0.154	-0.256
46	-0.071	-0.100	-0.309	-0.419	0.715	0.375	-0.036	-0.139
19	0.052	0.243	0.098	0.292	-0.425	-0.141	-0.219	0.099
Chi-Square					5.081			
DF					28			
p-value					0.9999			

The batch flotation results are shown in Figure 4.1 where all the different flotation times (2 min, 6 min, 12 min and 20 min) have been put together. The trends of Figure 4.1 have been drawn using data in Table 4.6 shown above.

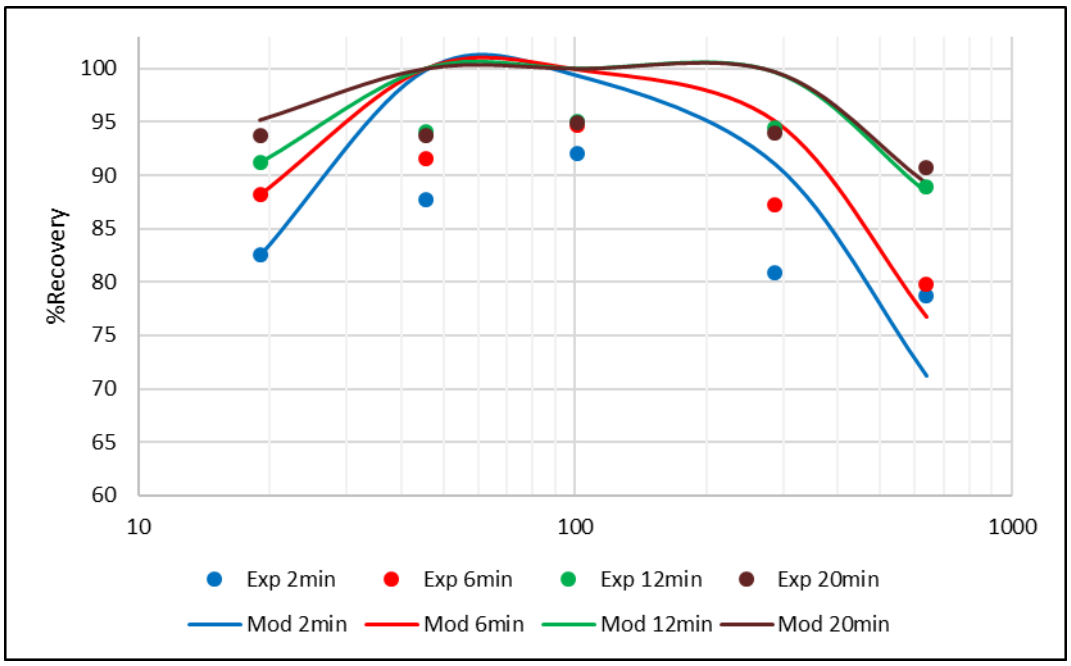

Figure 4.1: Recovery-by-size from batch flotation tests data

The Recovery vs. Time trend was further used to look at the results obtained for batch flotation tests as shown in Figure 4.2. Recoveries used for Figure 4.2 trends were based on the averages taken from results of fine size fractions up to coarse size fractions in each test undertaken. The higher recoveries from the model may be attributed to the higher flotation rate constants obtained which, in turn pushed recoveries to approach the ultimate recoveries calculated. The differences of approximately 4 % shown in Figure 4.2 is quite significant in the production environment. That is the reason why this require one to be cautious when using this approach for industrial application. Another comparison done on the results was that of flotation rate constant and particle size (µm) as shown in Figure 4.3. This is based on Equation (2.11) where $\Phi_j(d_{pi})$ is related to flotation rate constant (k) by definition.

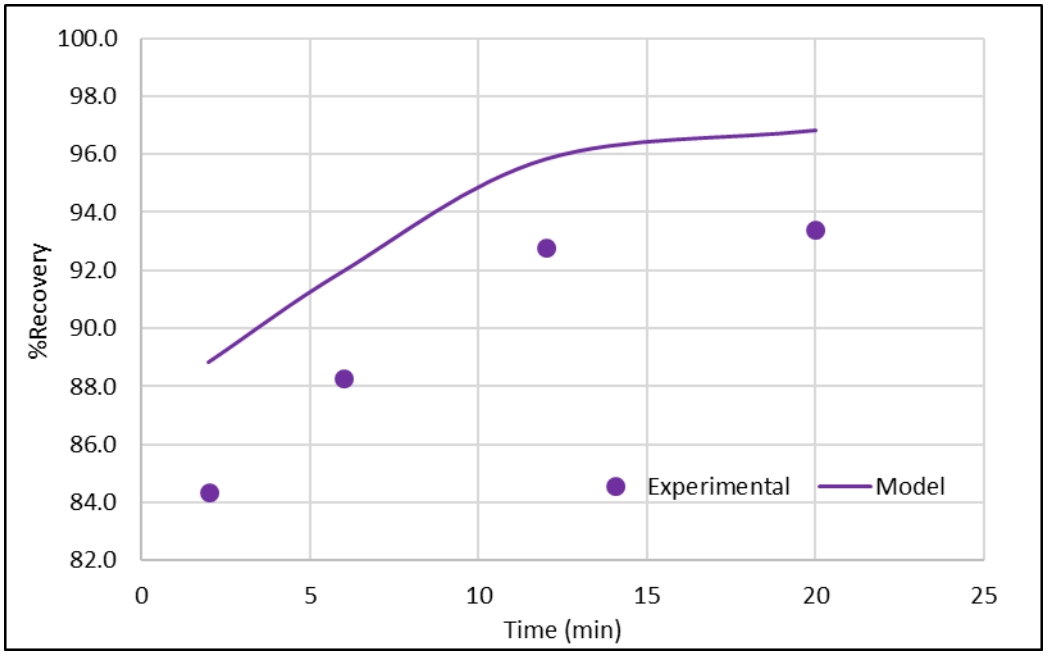

Figure 4.2: Recovery vs. Time - minutes trend from batch flotation tests data

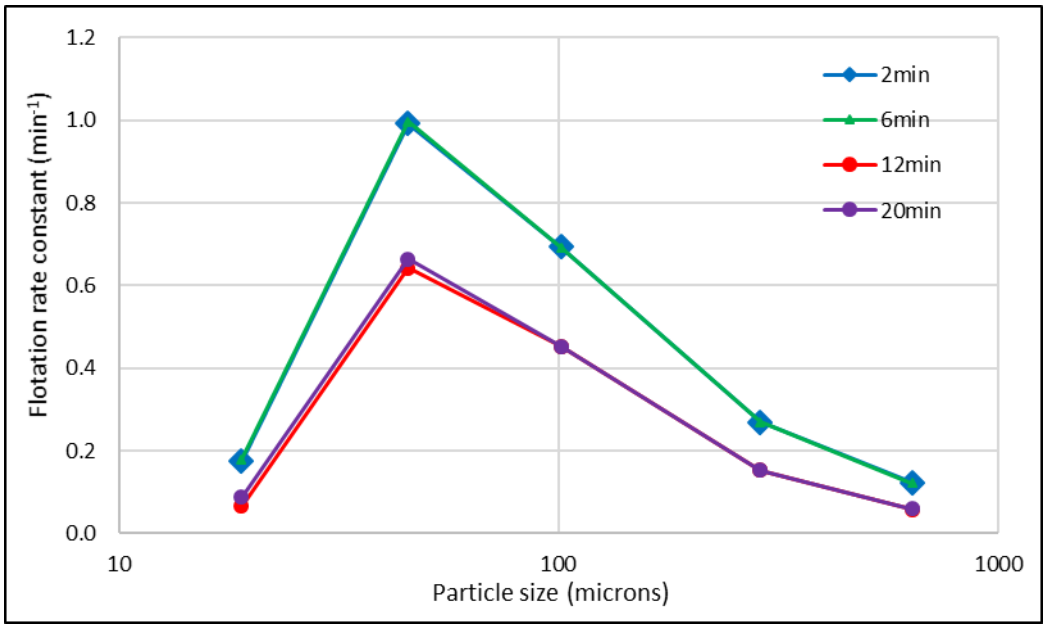

Figure 4.3: Flotation rate constant (k) vs. particle size trends from batch flotation tests data

4.4 Discussion of batch flotation tests

The short flotation time for the batch testing as in Figure 4.1 gave lower recoveries in comparison with longer flotation time. This trend continued in all different size

classes i.e. from fine, medium and coarse. A behaviour like this is in agreement with literature and other researchers like King (2012); McIvor and Finch (1990); Trahar and Warren (1976); and Sutherland (1989). It must be noted that at certain size classes the results of recoveries were almost the same irrespective of flotation time used e.g. model results at 12 min for 102 µm and 20 min for 102 µm both gave 100 % recovery. The error analysis both positive and negative across the particle size ranges for different flotation times appeared to be consistent as shown in Figure 4.4.

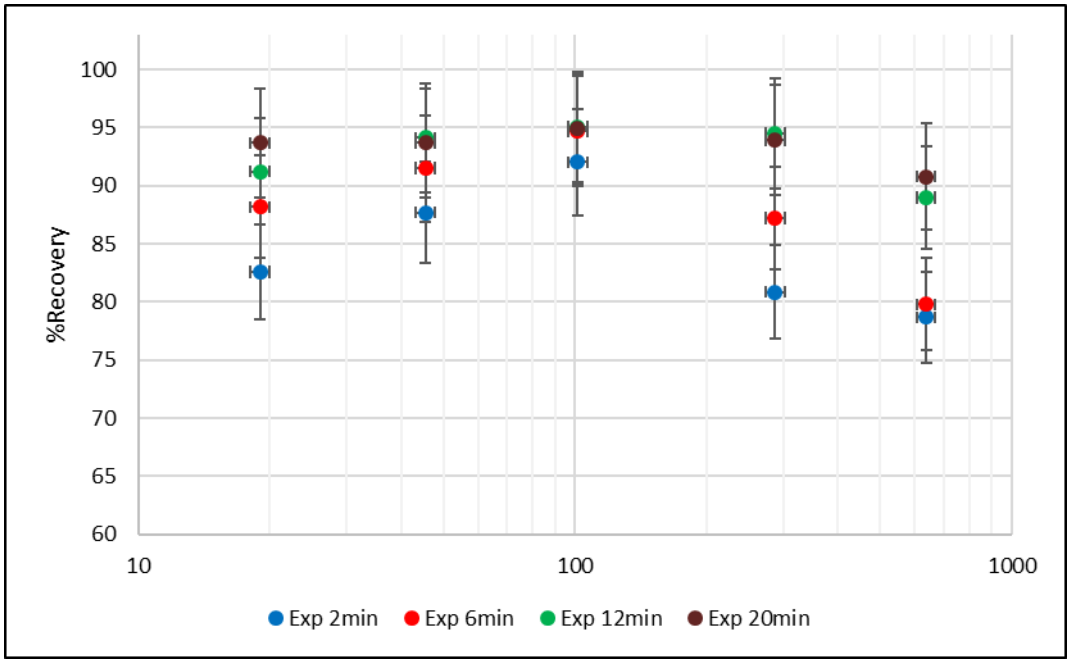

Figure 4.4: Error analysis of recovery-by-size from batch flotation tests data

The use of statistics done on both experimental data and model data can be seen in Table 4.2. The Chi-square was chosen since the comparisons involved more than two sets of data. The combined experimental and model data did not show significant difference as its p-value was more than 0.05. The null hypothesis can be accepted in this situation.

At fine sizes of around 19 µm the recoveries ranged from 83 % to 94 % for the batch flotation tests. The model results also fitted within the same ranges with the exception of 20 min flotation results that were slightly above 95 %. The peak where the recoveries were highest was seen to be around 50 µm and 250 µm for

the batch flotation tests. It can be said that batch results were high within intermediate to coarse size fraction ranges and that yielded highest recoveries of 87 % and 94 % around 50 µm and, at 250 µm recoveries were ranging at 83 % to 94 %. The shorter flotation time in the batch test did give lower recoveries as compared to longer flotation times which is in line with work by Rule and Anyimadu (2007), Pease *et al*. (2005), and Wang (2016).

The coarsest size fraction measured at 638 µm average, where for the batch flotation tests gave recoveries within the range of 78 % for the shorter flotation time to 90 % for the longer flotation time. These show that the coarse size fraction can also be recovered by mainly flotation process which agrees with Valery Jnr. and Jankovic (2002). It must be noted that the model predicted much lower recoveries at the coarsest size fraction e.g. for 2 min (Exp = 78.68% and Mod = 71.22 %). This may be linked to the limited flotation time that was used in this case. It is at 12 min results where this model behaviour was at minimum e.g. (Exp = 88.97 % and Mod = 88.33 %). A separate study may need to be done to better understand the cause of model to behave like this at the coarse size fractions.

A gradual increase in recovery with respect to the time can be seen in the batch flotation test results of Figure 4.2, i.e., Recovery vs. Time curves. Modelling the batch flotation experimental results did work out as simulation followed pattern of experimental results but predicted higher recoveries. Results for Figure 4.2 were based on the averages of Table 4.6 for both experimental and modelling sections then taking into account the flotation time for each average result. In all the trends of Figure 4.3, it was noticed that the highest peak was between 0.6 – 1.0 min^{-1} in terms of flotation rate. This was achieved at the particle size of just below 50 µm. Some differences were seen in the flotation times of 12 min and 20 min where the highest peak of flotation rate came to just above 0.6 min^{-1}. This was still in the particle size range similar to other results obtained. The lower flotation rate did not affect the final recoveries obtained as can be seen with the flotation results reported in Table 4.1.

4.5 Conclusions

The testwork has shown that size fraction does affect recovery of valuable material. The flotation time proved to increase the amount of recovery achieved at any size fraction. The intermediate size fraction was found to produce the highest recoveries compared to fine size fraction and coarse size fraction. This was in agreement with the work by other researchers like Gaudin *et al.* (1931); King (2012); Rule and Anyimadu (2007); and Wang (2016).

The short flotation time and long flotation time had significant differences in recoveries obtained. The batch flotation tests had maximum recovery of 95 %. A deviation observed was mainly on the coarse size fraction where the model predicted lower recoveries as compared to the experimental recoveries. Since there was no clear cause resulting in such deviation then, this suggests a need for a separate study or investigation to better understand the reasons behind this phenomenon. Statistically there was no significant difference observed in the raw data plus the experimental data compared to model data.

Chapter 5 Continuous flotation operation data analysis from plant surveys

5.1 Introduction

In scale-up, batch flotation tests data is used to predict continuous flotation plant performance by, designing flotation plant equipment which would give equivalent batch flotation test results. It is also possible to start from batch flotation tests followed by pilot plant testwork then finally continuous flotation plant while doing scale-up (Boeree, 2014). According to Yianatos (2003), the complexity of the flotation scale-up is due to the mineral characteristics (grade, size, mineralogy), cell characteristics (geometry, power consumption, energy dissipation, bubble and particle size distribution), reagent conditioning and operating conditions (air flowrate, pulp level, froth transport and discharge facilities) which are different and variable in batch and plant operation. In his work, he suggested the use of corresponding separability curves in comparing rougher bank (continuous flotation plant) operation and batch flotation.

This chapter looked into the continuous flotation plant tests conducted by sampling surveys of the overall plant and cell-by-cell. Analysis of results from continuous flotation plant tests were explored using different methods from first principle to statistical approach, similar to what has been done with batch flotation tests. Discussion of results by making use of error analysis were carried out followed by conclusions.

5.2 Raw data for continuous plant flotation surveys

The samples for continuous plant flotation testwork were taken and prepared in the metallurgical laboratory after plant surveys. Assays results for feed, concentrate and tails from the chemical laboratory based on the plant surveys test work conducted can be seen in Table 5.1 – 5.3. There were notable differences in

head grades for coarse fractions where the lowest was 0.292 and highest was 0.646 in Table 5.1. This can be linked poor liberation in those different samples taken in different days. Lack of regrinding in the flotation plant for trials may have also contributed to such high differences.

Table 5.1: Raw data for continuous plant flotation results

Particle screen size range	Mean particle screen size	1st trial - sample 1			1st trial - sample 2			2nd trial - sample 1		
		Head grade	Tails grade	Conc grade	Head grade	Tails grade	Conc grade	Head grade	Tails grade	Conc grade
(µm)	(µm)	(%Cu)	(%Cu)	(%Cu)	(%Cu)	(%Cu)	(%Cu)	(%Cu)	(%Cu)	(%Cu)
-850+425	*638*	0.292	0.132	28.138	0.260	0.131	28.538	0.646	0.510	39.173
-425+150	*288*	0.449	0.117	34.910	0.432	0.114	36.980	0.583	0.410	39.880
-150+53	*102*	0.584	0.069	40.286	0.575	0.066	41.498	0.652	0.268	43.040
-53+38	*46*	0.618	0.064	38.096	0.608	0.063	40.518	0.687	0.152	41.580
-38	*19*	0.618	0.140	28.724	0.604	0.151	29.846	0.660	0.292	32.190

Particle screen size range	Mean particle screen size	2nd trial - sample 2			3rd trial - sample 1			3rd trial - sample 2		
		Head grade	Tails grade	Conc grade	Head grade	Tails grade	Conc grade	Head grade	Tails grade	Conc grade
(µm)	(µm)	(%Cu)	(%Cu)	(%Cu)	(%Cu)	(%Cu)	(%Cu)	(%Cu)	(%Cu)	(%Cu)
-850+425	*638*	0.294	0.149	28.912	0.322	0.176	42.075	0.598	0.388	42.225
-425+150	*288*	0.417	0.124	36.862	0.490	0.183	43.320	0.476	0.168	44.000
-150+53	*102*	0.562	0.074	41.346	0.641	0.109	46.020	0.621	0.093	47.130
-53+38	*46*	0.565	0.070	39.602	0.666	0.143	45.430	0.612	0.116	44.400
-38	*19*	0.578	0.144	28.852	0.651	0.178	33.530	0.682	0.178	33.370

Table 5.2: Raw data for cell-by-cell flotation plant results (roughers)

Particle screen size range	Mean particle screen size	Bank 1			Bank 2			Bank 3			Bank 4		
		Head grade	Tails grade	Conc grade	Head grade	Tails grade	Conc grade	Head grade	Tails grade	Conc grade	Head grade	Tails grade	Conc grade
(µm)	(µm)	(%Cu)	(%Cu)	(%Cu)	(%Cu)	(%Cu)	(%Cu)	(%Cu)	(%Cu)	(%Cu)	(%Cu)	(%Cu)	(%Cu)
-850+425	*638*	0.757	0.491	31.830	0.557	0.358	38.853	0.557	0.325	38.350	0.557	0.296	7.406
-425+150	*288*	0.963	0.491	31.830	0.963	0.446	41.360	0.963	0.406	31.830	0.963	0.369	28.660
-150+53	*102*	0.659	0.295	42.130	0.659	0.269	35.230	0.659	0.244	42.130	0.659	0.222	34.420
-53+38	*46*	0.819	0.438	42.160	0.819	0.398	43.610	0.819	0.362	42.160	0.819	0.329	30.030
-38	*19*	0.585	0.350	37.280	0.585	0.318	35.210	0.585	0.289	37.280	0.585	0.263	19.890

Table 5.3: Raw data for cell-by-cell flotation plant results (cleaners/re-cleaners)

Particle screen size range	Mean particle screen size	Bank 1			Bank 2			Bank 3		
		Head grade	Tails grade	Conc grade	Head grade	Tails grade	Conc grade	Head grade	Tails grade	Conc grade
(µm)	(µm)	(%Cu)	(%Cu)	(%Cu)	(%Cu)	(%Cu)	(%Cu)	(%Cu)	(%Cu)	(%Cu)
-850+425	*638*	0.292	0.189	33.760	0.292	0.189	36.582	0.292	0.222	33.760
-425+150	*288*	0.463	0.261	31.830	0.463	0.249	41.360	0.463	0.306	31.830
-150+53	*102*	0.643	0.295	38.880	0.643	0.269	40.310	0.643	0.244	38.880
-53+38	*46*	0.919	0.438	37.120	0.919	0.398	37.959	0.919	0.362	37.120
-38	*19*	0.690	0.450	27.210	0.690	0.450	26.700	0.690	0.489	27.210

Table 5.4: Chi-square statistics analysis of continuous plant flotation raw data

Observed Counts																			
Mean particle size (µm)	Head grade	Tails grade	Conc grade	Head grade	Tails grade	Conc grade	Head grade	Tails grade	Conc grade	Head grade	Tails grade	Conc grade	Head grade	Tails grade	Conc grade	Head grade	Tails grade	Conc grade	
638	0.292	0.132	28.138	0.260	0.131	28.538	0.646	0.510	39.173	0.294	0.149	28.912	0.322	0.176	42.075	0.598	0.388	42.225	
288	0.449	0.117	34.910	0.432	0.114	36.980	0.583	0.410	39.880	0.417	0.124	36.862	0.490	0.183	43.320	0.476	0.168	44.000	
102	0.584	0.069	40.286	0.575	0.066	41.498	0.652	0.268	43.040	0.562	0.074	41.346	0.641	0.109	46.020	0.621	0.093	47.130	
46	0.618	0.064	38.096	0.608	0.063	40.518	0.687	0.152	41.580	0.565	0.070	39.602	0.666	0.143	45.430	0.612	0.116	44.400	
19	0.618	0.140	28.724	0.604	0.151	29.846	0.660	0.292	32.190	0.578	0.144	28.852	0.651	0.178	33.530	0.682	0.178	33.370	
Expected Counts																			
Mean particle size (µm)	Head grade	Tails grade	Conc grade	Head grade	Tails grade	Conc grade	Head grade	Tails grade	Conc grade	Head grade	Tails grade	Conc grade	Head grade	Tails grade	Conc grade	Head grade	Tails grade	Conc grade	
638	0.469	0.096	31.187	0.454	0.096	32.511	0.592	0.299	35.899	0.443	0.103	32.180	0.508	0.145	38.559	0.548	0.173	38.696	
288	0.529	0.108	35.135	0.512	0.108	36.627	0.666	0.337	40.443	0.499	0.116	36.254	0.572	0.163	43.440	0.617	0.195	43.595	
102	0.581	0.118	38.608	0.562	0.119	40.248	0.732	0.370	44.442	0.548	0.127	39.838	0.629	0.179	47.735	0.678	0.214	47.905	
46	0.560	0.114	37.196	0.542	0.115	38.776	0.706	0.357	42.816	0.528	0.123	38.381	0.606	0.172	45.988	0.653	0.206	46.152	
19	0.422	0.086	28.028	0.408	0.086	29.218	0.532	0.269	32.263	0.398	0.092	28.921	0.456	0.130	34.653	0.492	0.155	34.777	
Std. Residuals																			
Mean particle size (µm)	Head grade	Tails grade	Conc grade	Head grade	Tails grade	Conc grade	Head grade	Tails grade	Conc grade	Head grade	Tails grade	Conc grade	Head grade	Tails grade	Conc grade	Head grade	Tails grade	Conc grade	
638	-0.259	0.117	-0.546	-0.288	0.112	-0.697	0.070	0.386	0.546	-0.224	0.144	-0.576	-0.261	0.083	0.566	0.067	0.518	0.567	
288	-0.110	0.028	-0.038	-0.112	0.017	0.058	-0.102	0.126	-0.089	-0.116	0.024	0.101	-0.108	0.050	-0.018	-0.180	-0.061	0.061	
102	0.004	-0.144	0.270	0.017	-0.154	0.197	-0.094	-0.168	-0.210	0.019	-0.149	0.239	0.016	-0.166	-0.248	-0.069	-0.262	-0.112	
46	0.078	-0.148	0.148	0.090	-0.153	0.280	-0.022	-0.343	-0.189	0.051	-0.150	0.197	0.078	-0.071	-0.082	-0.051	-0.199	-0.258	
19	0.302	0.184	0.131	0.306	0.219	0.116	0.176	0.045	-0.013	0.285	0.170	-0.013	0.288	0.133	-0.191	0.270	0.058	-0.239	
Chi-Square										4.655									
DF										68									
p-value										1.0000									

Chi-square statistical analysis was used on the raw data for the continuous flotation plant in order to test significance differences, as shown in Table 5.4. It was found that the p-value of 1.0000 was obtained which means that there was no significant differences. The analyses done were conducted at 95 % confidence level. This outcome allowed the acceptance of the null hypothesis, i.e., there is no difference (p-value > 0.05) observed in the continuous flotation plant data carried out in the three separate trials. The same statistical analysis were also done for the continuous flotation surveys of cell-by-cell roughers sampling and cell-by-cell

cleaners / re-cleaners which resulted in p-values of 0.9997 and 1.0000 respectively.

5.3 Results of continuous flotation plant surveys

Below is the summary of the results obtained from continuous flotation plant data and its use for the scale-up. Where applicable, comparisons were also made with the published data from other researchers in the same field of study. As explained previously the continuous flotation tests or surveys were divided into two categories, i.e., sampling flotation bank samples for feed, concentrate and tails as the first category. This was then followed by the sampling of each cell in a bank for feed, concentrate and tails; for this work is referred to as cell-by-cell sampling.

Tables 5.5 – 5.7 indicate the results from the three surveys conducted in the continuous flotation plant. Experimental recoveries were worked out from the raw data presented above that consisted of heads, concentrates and tails. The recovery formula used is the one in Equation 3.2 while results of Equation 3.1 (an approximation) can be seen in the Appendix A. Model recoveries were obtained by using Equations 2.10 and 2.11.

Table 5.5: Summary of continuous plant flotation results

Size (µm)	Experimental recoveries				Model recoveries			
	Exp - 1st trial	Exp- 2nd trial	Exp- 3rd trial	Exp- AVG	Mod- 1st trial	Mod- 2nd trial	Mod- 3rd trial	Mod- AVG
638	52.45	35.42	40.38	42.75	43.50	18.26	21.11	27.62
288	74.01	50.24	63.80	62.69	95.36	54.34	73.50	74.40
102	88.50	73.13	84.09	81.91	100.00	80.72	99.62	93.45
46	89.8	83.0	79.9	84.21	100.00	92.74	99.99	97.58
19	76.55	65.87	73.48	71.97	76.52	65.32	73.60	71.81

There were notable differences seen in the experimental versus model recoveries in Table 5.5 and 5.6. This was mostly on the coarse fractions where the model predicted much lower recoveries. Such a condition can be associated with the

model itself no being able to better fit experimental data in coarse fractions. Fine tuning the model by changing the unknowns or guesses may assist in this situation.

Table 5.6: Summary of cell-by-cell flotation plant results (roughers)

Size (µm)	Experimental recoveries				Model recoveries			
	Bank1	Bank2	Bank3	Bank4	Mod Bank1	Mod Bank2	Mod Bank3	Mod Bank4
638	35.57	35.76	33.07	40.94	13.47	15.75	17.22	21.85
288	46.88	50.36	46.42	52.38	27.24	31.38	33.92	41.56
102	55.01	59.15	62.86	66.32	56.57	62.69	65.76	74.79
46	50.00	54.57	58.76	62.68	73.04	78.47	80.40	88.57
19	37.95	40.70	40.30	55.13	32.60	35.79	36.43	52.07

Table 5.7: Summary of cell-by-cell flotation plant results (cleaners/re-cleaners)

Size (µm)	Experimental recoveries			Model recoveries		
	Bank1	Bank2	Bank3	Mod Bank1	Mod Bank2	Mod Bank3
638	49.67	53.52	63.66	29.63	46.87	62.77
288	68.16	75.40	84.89	85.96	97.07	99.60
102	76.10	75.90	84.13	99.97	100.00	100.00
46	63.35	69.61	78.28	100.00	100.00	100.00
19	45.40	55.64	59.89	45.34	55.62	59.88

The data from continuous flotation plant surveys were also tested statistically to see if there was any significant differences in it. Table 5.8 – 5.10 give the statistics results that were obtained. The nature of the data and plant conditions that it was obtained under necessitated the use of the Chi-square statistics method.

Table 5.8: Chi-square statistics analysis of continuous plant flotation survey data

Observed Counts								
Mean particle size (µm)	1st trial	2nd trial	3rd trial	AVG - trial	Mod 1st trial	Mod 2nd trial	Mod 3rd trial	Mod-AVG
638	52.448	35.422	40.378	42.750	43.502	18.263	21.107	27.624
288	74.015	50.242	63.803	62.687	95.364	54.343	73.503	74.403
102	88.499	73.127	84.094	81.907	99.999	80.718	99.618	93.445
46	89.786	82.963	79.893	84.214	100.000	92.744	99.992	97.578
19	76.553	65.866	73.477	71.965	76.525	65.318	73.599	71.814
Expected Counts								
Mean particle size (µm)	1st trial	2nd trial	3rd trial	AVG - trial	Mod 1st trial	Mod 2nd trial	Mod 3rd trial	Mod-AVG
638	37.880	30.560	33.940	34.127	41.266	30.934	36.540	36.247
288	73.791	59.532	66.117	66.480	80.388	60.260	71.182	70.610
102	94.386	76.147	84.570	85.034	102.824	77.08	91.05	90.32
46	97.853	78.944	87.676	88.158	106.601	79.911	94.393	93.635
19	77.392	62.436	69.343	69.724	84.310	63.201	74.655	74.055
Std. Residuals								
Mean particle size (µm)	1st trial	2nd trial	3rd trial	AVG - trial	Mod 1st trial	Mod 2nd trial	Mod 3rd trial	Mod-AVG
638	2.367	0.879	1.105	1.476	0.348	-2.278	-2.553	-1.432
288	0.026	-1.204	-0.284	-0.465	1.670	-0.762	0.275	0.451
102	-0.606	-0.346	-0.052	-0.339	-0.279	0.414	0.898	0.329
46	-0.815	0.452	-0.831	-0.420	-0.639	1.436	0.576	0.408
19	-0.095	0.434	0.496	0.268	-0.848	0.266	-0.122	-0.260
Chi-Square					36.918			
DF					28			
p-value					0.1207			

Table 5.9: Chi-square statistics analysis of cell-by-cell roughers

Observed Counts								
Mean particle size (µm)	Bank1	Bank2	Bank3	Bank4	Mod Bank1	Mod Bank2	Mod Bank3	Mod Bank4
638	35.572	35.758	33.069	40.943	13.470	15.745	17.219	21.846
288	46.878	50.361	46.418	52.380	27.243	31.382	33.918	41.561
102	55.006	59.154	62.862	66.322	56.572	62.693	65.756	74.790
46	49.998	54.575	58.756	62.680	73.037	78.473	80.399	88.572
19	37.951	40.698	40.303	55.128	32.595	35.786	36.425	52.073
Expected Counts								
Mean particle size (µm)	Bank1	Bank2	Bank3	Bank4	Mod Bank1	Mod Bank2	Mod Bank3	Mod Bank4
638	25.022	26.703	26.799	30.800	22.526	24.875	25.945	30.954
288	38.670	41.268	41.416	47.599	34.812	38.443	40.096	47.837
102	58.935	62.894	63.120	72.544	53.056	58.589	61.109	72.907
46	64.012	68.311	68.557	78.792	57.625	63.635	66.373	79.187
19	38.766	41.370	41.518	47.717	34.898	38.538	40.196	47.956

Std. Residuals								
Mean particle size (µm)	Bank1	Bank2	Bank3	Bank4	Mod Bank1	Mod Bank2	Mod Bank3	Mod Bank4
638	2.109	1.752	1.211	1.828	-1.908	-1.830	-1.713	-1.637
288	1.320	1.415	0.777	0.693	-1.283	-1.139	-0.976	-0.907
102	-0.512	-0.472	-0.032	-0.731	0.483	0.536	0.594	0.220
46	-1.752	-1.662	-1.184	-1.815	2.030	1.860	1.722	1.055
19	-0.131	-0.104	-0.189	1.073	-0.390	-0.443	-0.595	0.594
Chi-Square					60.877			
DF					28			
p-value					0.0003			

Table 5.10: Chi-square statistics analysis of cell-by-cell cleaners and re-cleaners

Observed Counts						
Mean particle size (µm)	Bank1	Bank2	Bank3	Mod Bank1	Mod Bank2	Mod Bank3
638	49.672	53.517	63.659	29.628	46.868	62.770
288	68.160	75.398	84.890	85.962	97.070	99.595
102	76.098	75.899	84.128	99.966	100.000	100.000
46	63.351	69.605	78.284	99.999	100.000	100.000
19	45.404	55.643	59.887	45.343	55.622	59.884
Expected Counts						
Mean particle size (µm)	Bank1	Bank2	Bank3	Mod Bank1	Mod Bank2	Mod Bank3
638	42.380	46.214	51.924	50.531	55.944	59.121
288	70.756	77.156	86.691	84.364	93.402	98.706
102	74.220	80.933	90.934	88.494	97.974	103.54
46	70.779	77.181	86.718	84.391	93.432	98.738
19	44.550	48.579	54.582	53.118	58.808	62.147
Std. Residuals						
Mean particle size (µm)	Bank1	Bank2	Bank3	Mod Bank1	Mod Bank2	Mod Bank3
638	1.120	1.074	1.629	-2.941	-1.213	0.475
288	-0.309	-0.200	-0.193	0.174	0.380	0.089
102	0.218	-0.560	-0.714	1.220	0.205	-0.348
46	-0.883	-0.862	-0.906	1.699	0.680	0.127
19	0.128	1.014	0.718	-1.067	-0.415	-0.287
Chi-Square				26.941		
DF				20		
p-value				0.1369		

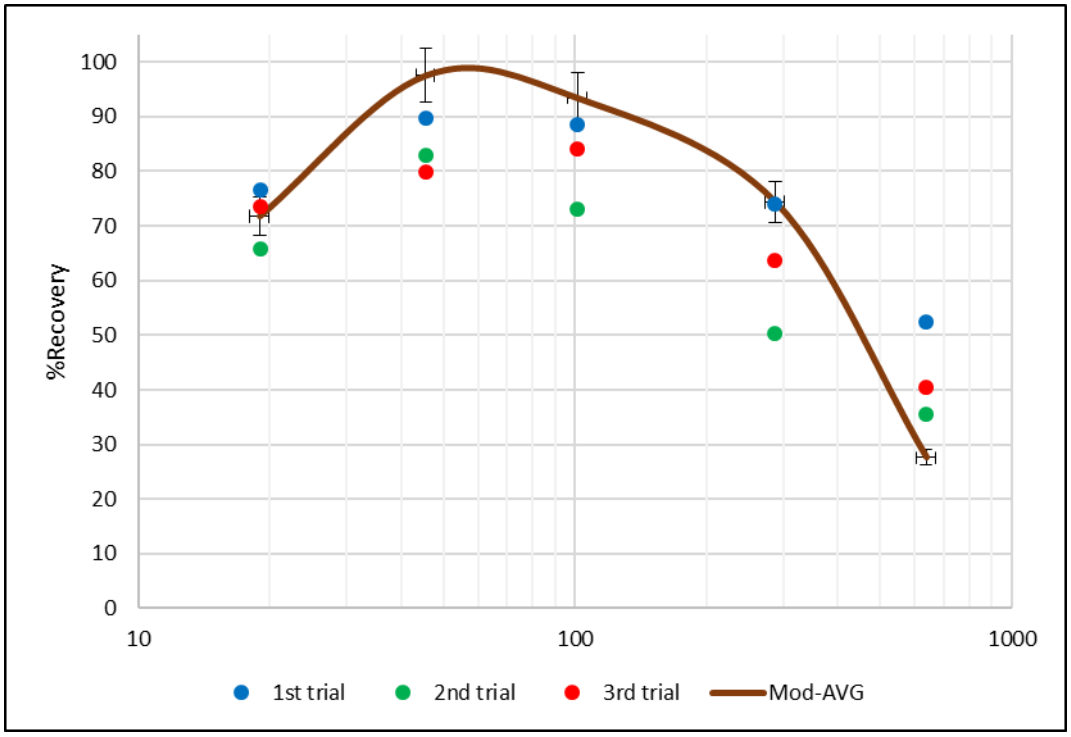

Figure 5.1: Recovery-by-size from continuous plant flotation tests data

The trends from Figures 5.1 – 5.3 were plotted by using data from Tables 5.5 – 5.7. Experimental data has been indicated by the use of dots while smooth lines represent model data. Banks 1 – 4 or Banks 1 – 3 were formed by a certain number of cells e.g. 3 – 4 cells in each row. Samples taken in each cell were composited for individual bank. The trials were done on different days of the plant surveys under similar conditions.

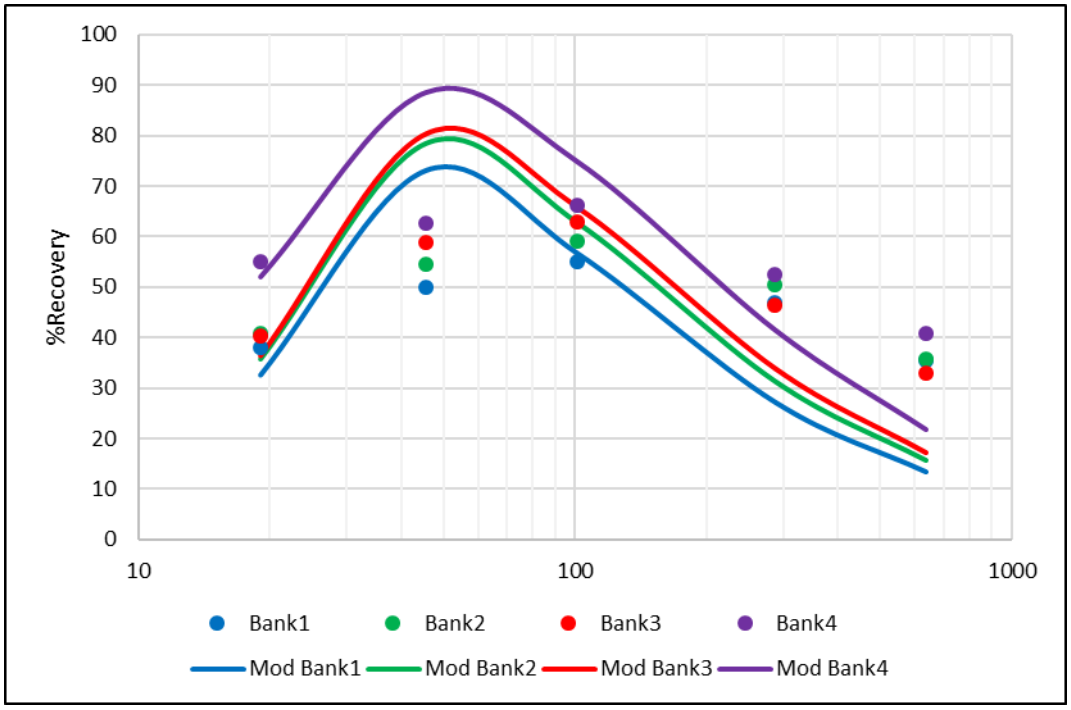

Figure 5.2: Recovery-by-size from cell-by-cell flotation plant tests data (roughers)

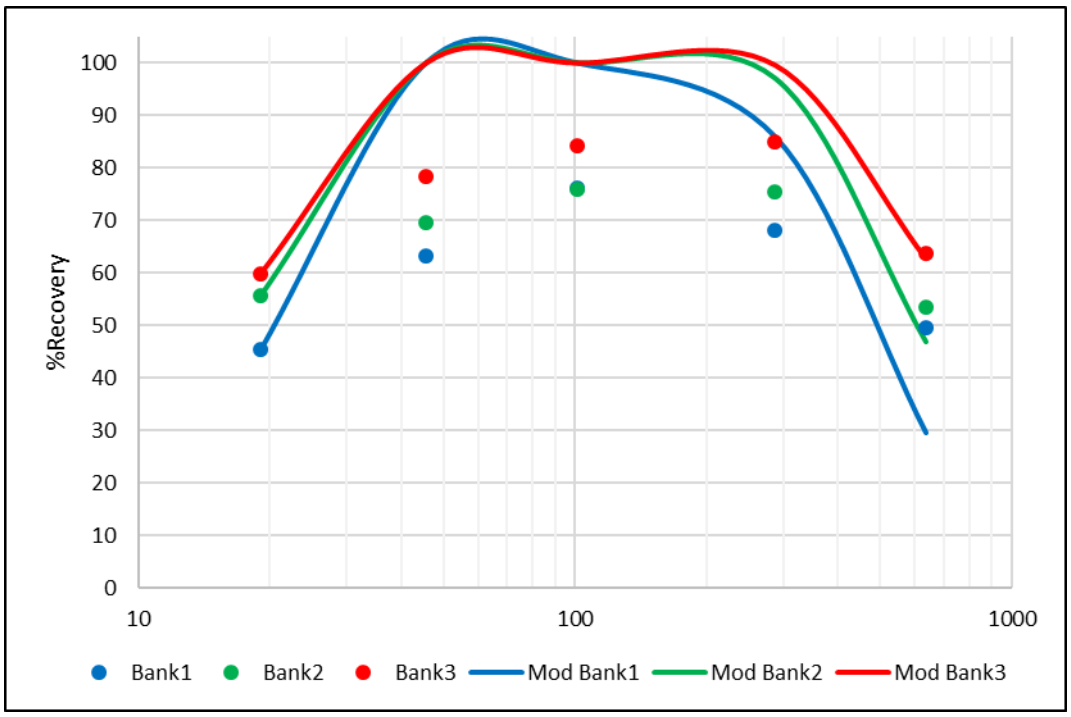

Figure 5.3: Recovery-by-size from cell-by-cell flotation plant tests data (cleaners / re-cleaners)

Results based on each of the cells for continuous flotation can be seen from Figures 5.2 – 5.3. Samples were collected from each cell and composited according to the banks formed by that certain number of cells which varied from 3 to 4 cells. Rougher cells were taken in two rows and results were averaged and are shown in Figure 5.2.

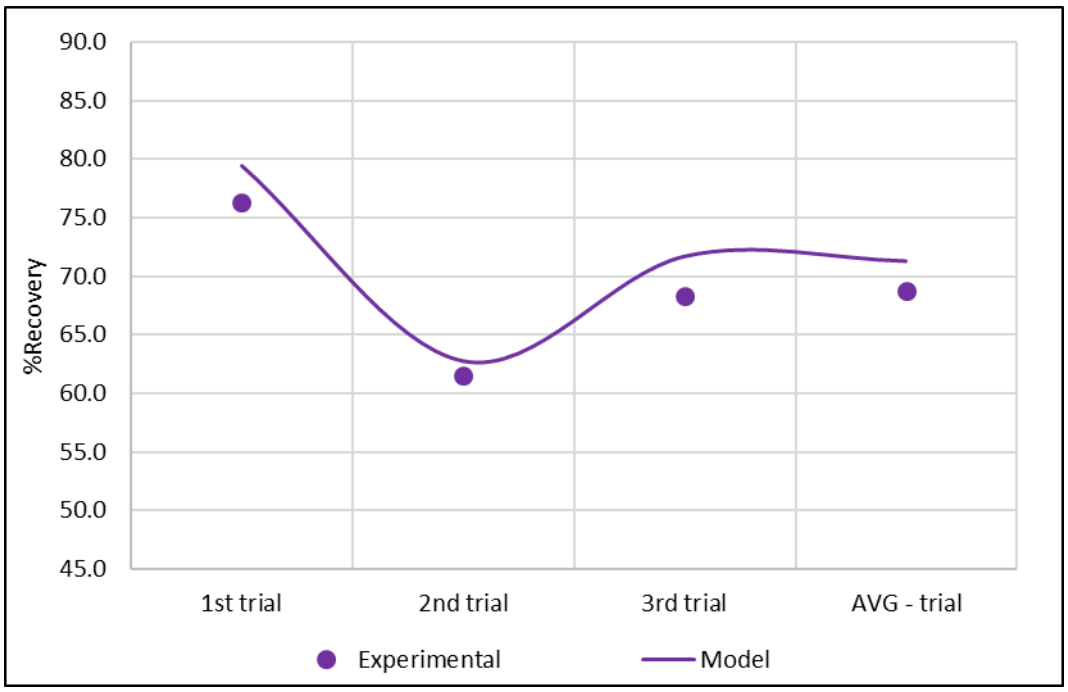

Figure 5.4: Recovery per trial trends from continuous plant flotation tests data

The recovery per trials and banks trends were further used to look at the results obtained in continuous plant flotation surveys as shown in Figures 5.4 – 5.6. The experimental and model averages as shown in Tables 5.5 – 5.7 were used in plotting these three Figures of 5.4 – 5.6.

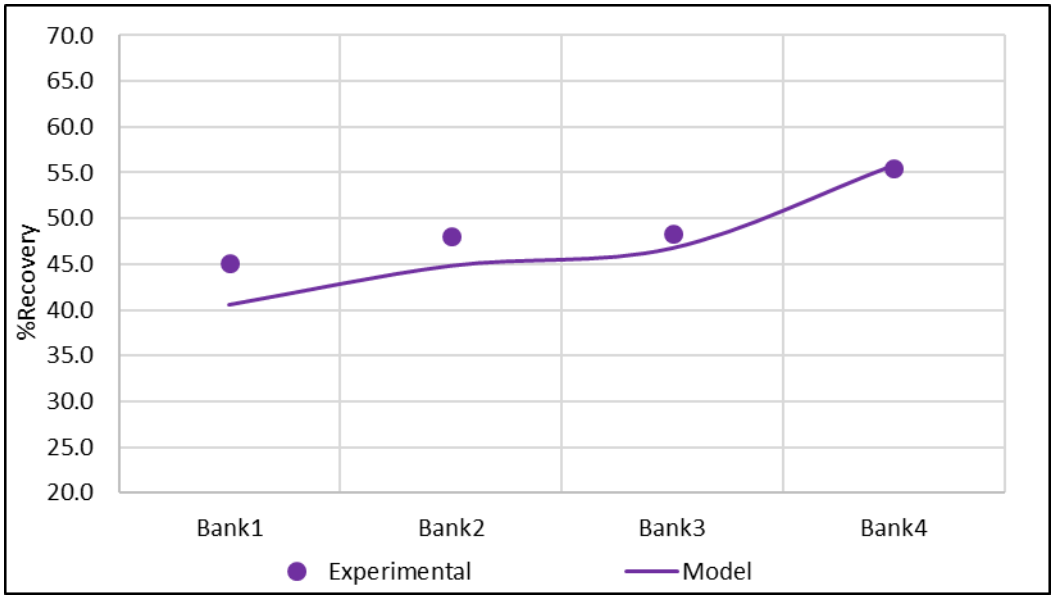

Figure 5.5: Recovery per banks trends from cell-by-cell flotation plant (roughers)

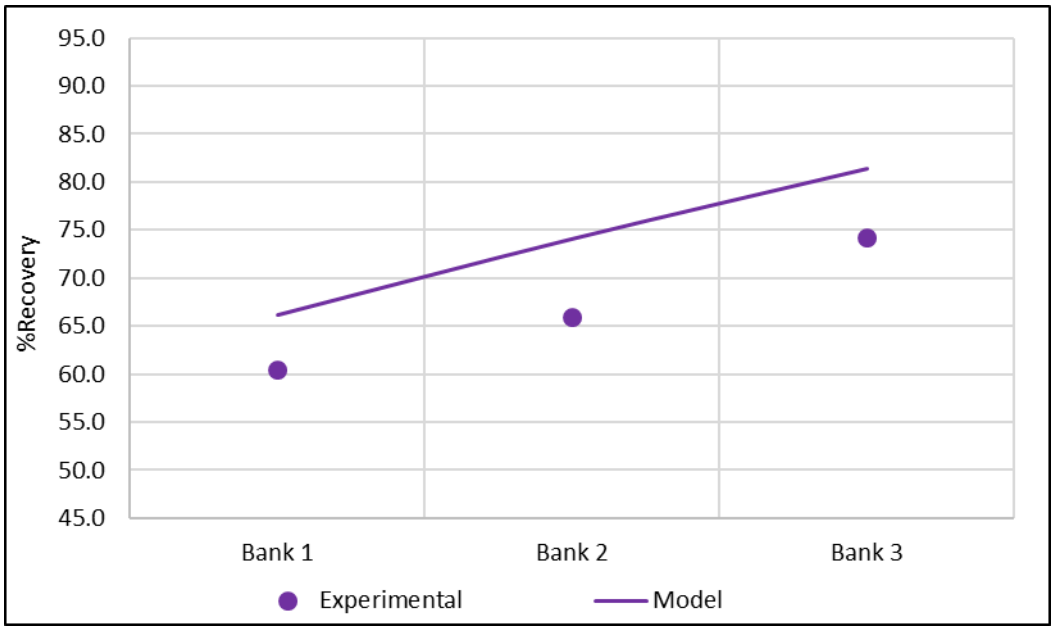

Figure 5.6: Recovery per banks trends from cell-by-cell flotation plant (cleaners / re-cleaners)

Another comparison done on the results was that of flotation rate constant and particle size (µm) as shown in Figures 5.7 – 5.9. Equation (2.11) was used in estimating the flotation rate constant.

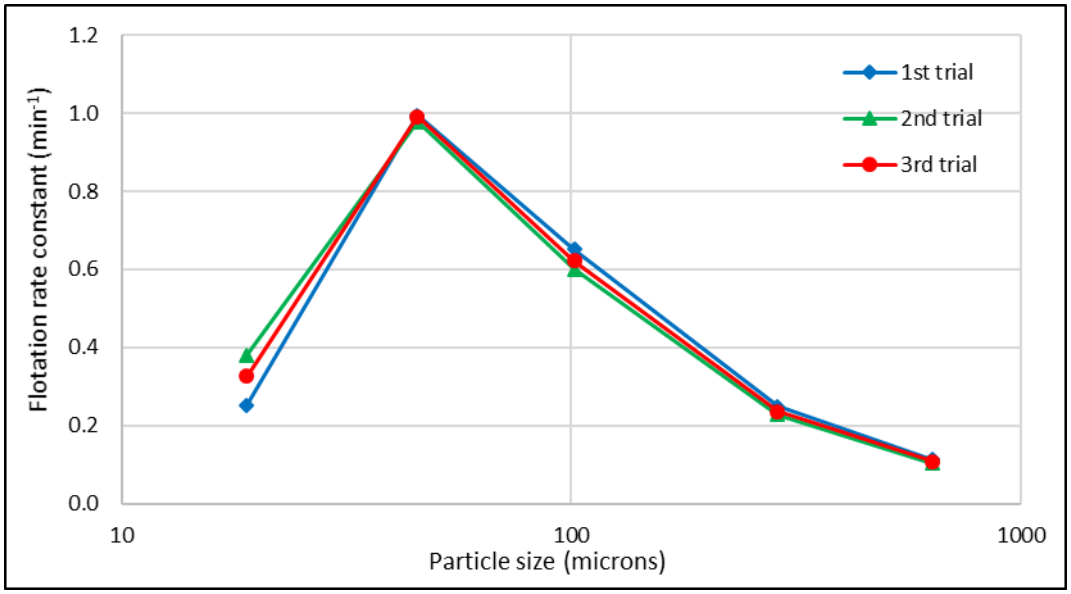

Figure 5.7: Flotation rate constant (k) vs. particle size trends from continuous plant flotation survey data

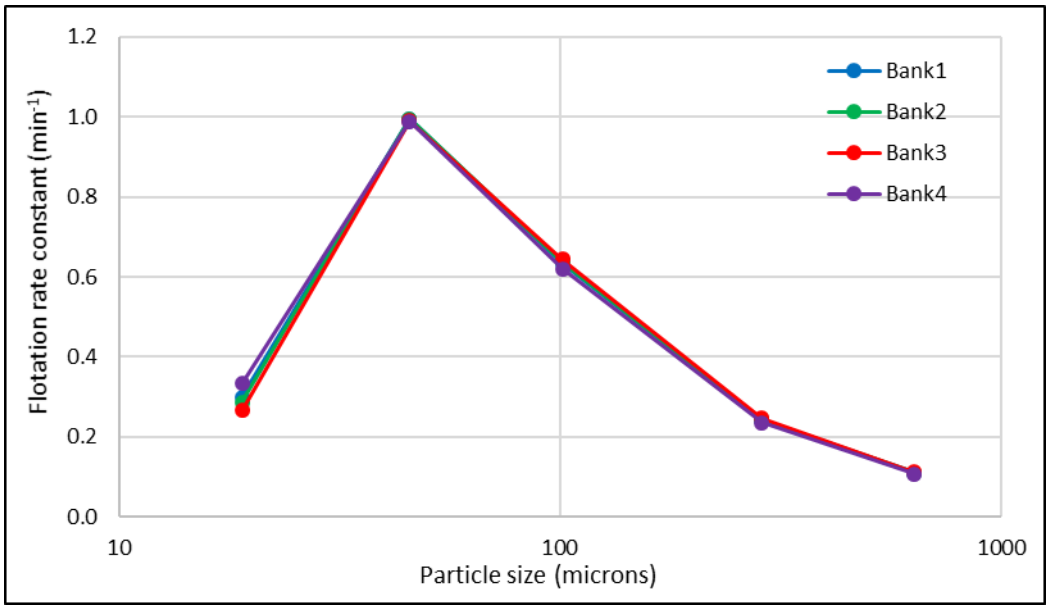

Figure 5.8: Flotation rate constant (k) vs. particle size trends from cell-by-cell flotation plant survey data (roughers)

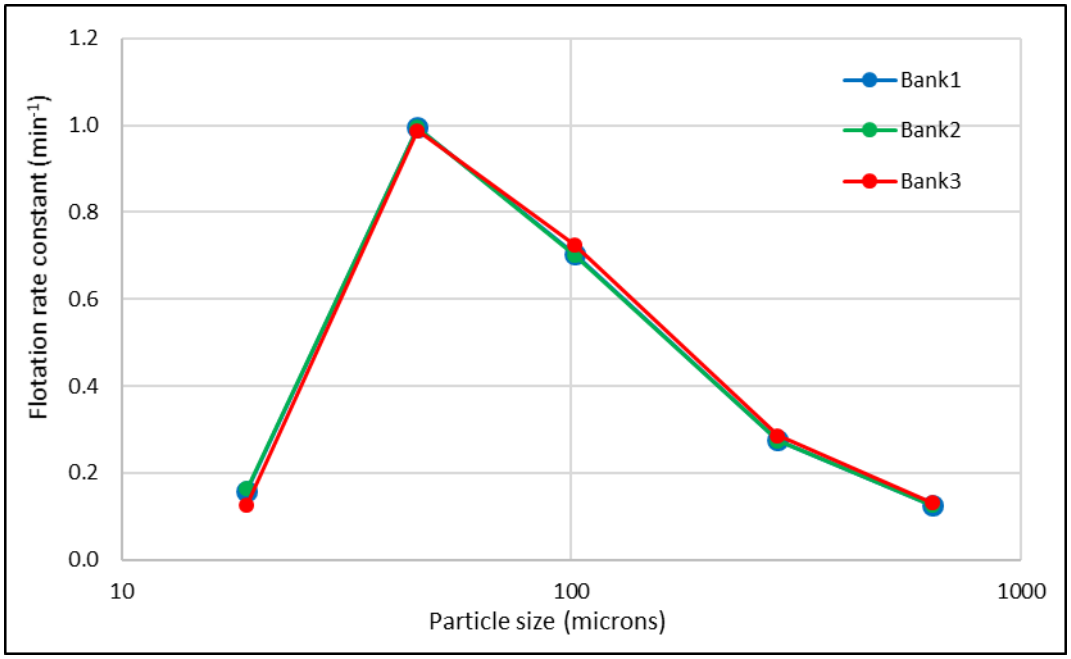

Figure 5.9: Flotation rate constant (k) vs. particle size trends from cell-by-cell flotation plant survey data (cleaners / re-cleaners)

5.5 Discussion of continuous flotation plant surveys

The continuous plant flotation recovery figures at fine sizes were found to be at the range of 66 % to 77 % as shown in Figure 5.1. Modelling of the plant results did fit experimental results but in other points some deviations were observed. These deviations may be due to the high sensitivity of the model to plant instabilities. The peak where the recoveries were highest for the continuous plant tests was found to lie between 40 µm and 100 µm and this is in line with Figure 2.1, i.e., recovery-by- size. It can be shown that, continuous plant recoveries were highest with figures of 80 % to 90 % at 40 µm and at 100 µm recoveries were 72 % and 88 %. The continuous plant recovery results at the coarsest size fraction produced minimum recovery of 35 % and maximum recovery of 52 %. The varying continuous plant performances can be linked to plant conditions on those specific days when sampling survey was done. The first trial showed higher errors compared to other days as shown in Figure 5.10. It can also be seen that the average results absorbed all the errors of the three trials and reduced them to be very low to such an extent that they were negligible in the plots of Figure 5.10.

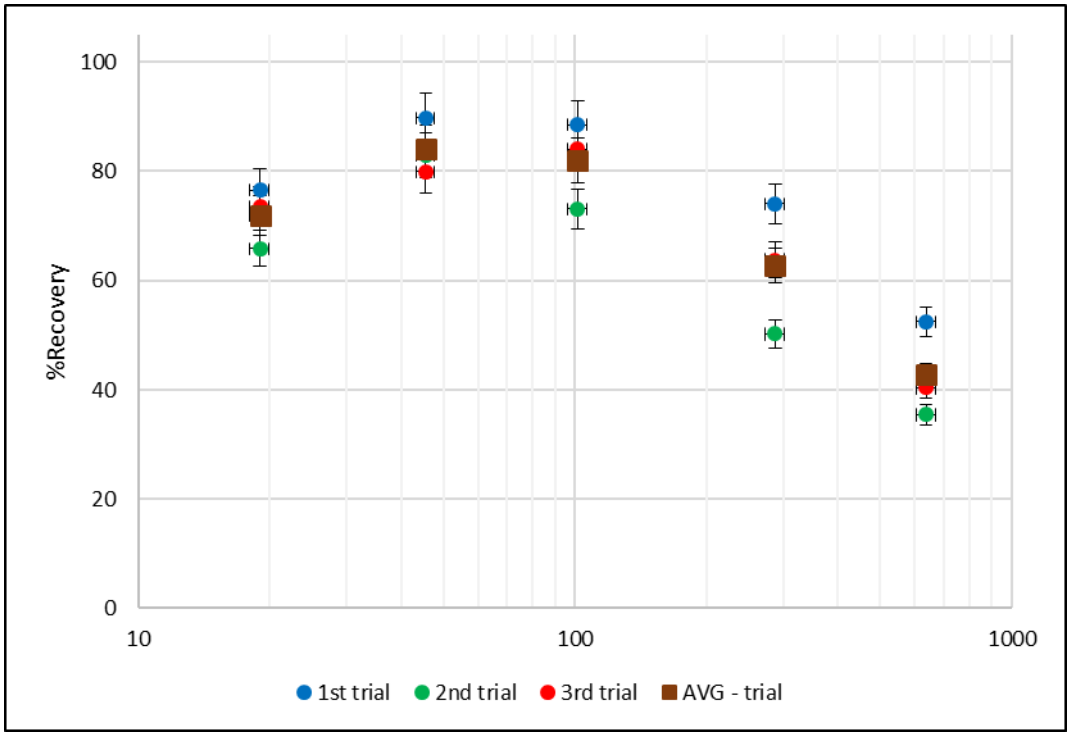

Figure 5.10: Error analysis of recovery-by-size from continuous flotation plant surveys data

The highest peak of rougher recoveries was within particle size ranges of 45 µm to 100 µm and this was seen in all the banks found in the rows as seen in Figure 5.2; following recovery-by-size curve of Pease *et al.* (2005). Based on experimental results highest recovery of roughers came to 66.3 % but this could go up to recovery of 88.6 % as predicted by the model. The flotation row that consisted of cells for re-cleaners and cleaners was also sampled and those results are in Figure 5.3. The re-cleaners (bank 1) showed lower recoveries in all its particle sizes as compared to the cleaners (bank 2 and 3). This would have been expected since re-cleaners are supposed to have the highest concentrate grade in the flotation circuit. It must be noted that in this particular circuit bank 2 can also form part of recleaner or cleaner depending on the circumstances of recovery and grade requirements. In terms of best performance re-cleaners bank had its highest recovery of 76.1 % while cleaners could go as high as above 84 % in Bank 3.

Error analysis for both roughers and cleaners / re-cleaners can be seen in Figures 5.11 – 5.12. From fine to medium size ranges, Bank 4 of roughers showed a slightly

higher error compared to others as in Figure 5.11. Bank 3 of the cleaners in Figure 5.12 had higher errors in the medium size ranges. The last banks of both roughers and cleaners appeared to be the ones with higher errors compared to the others. Practically in the continuous plant, the last banks tend to experience slow frothing shown by smaller bubbles (Lotter *et al*., 2014). The last banks may also be prone to sliming conditions and these noted problems of these banks are thought to have contributed to the higher errors seen in the data analysis.

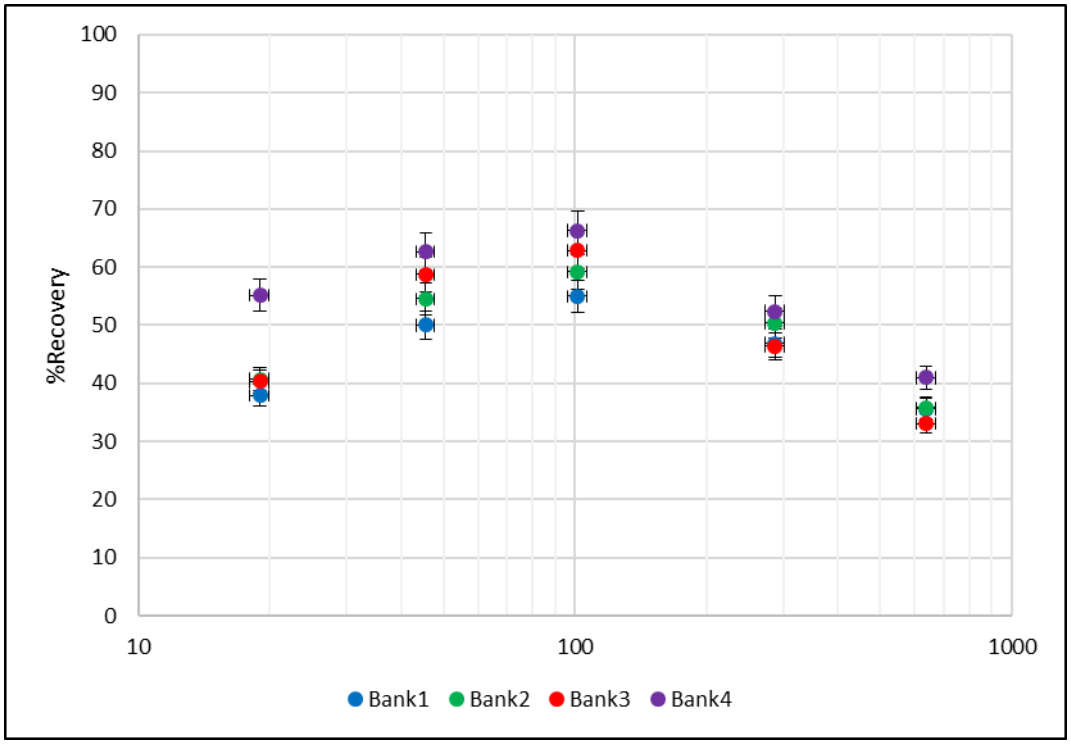

Figure 5.11: Error analysis of recovery-by-size from cell-by-cell flotation plant survey data (roughers)

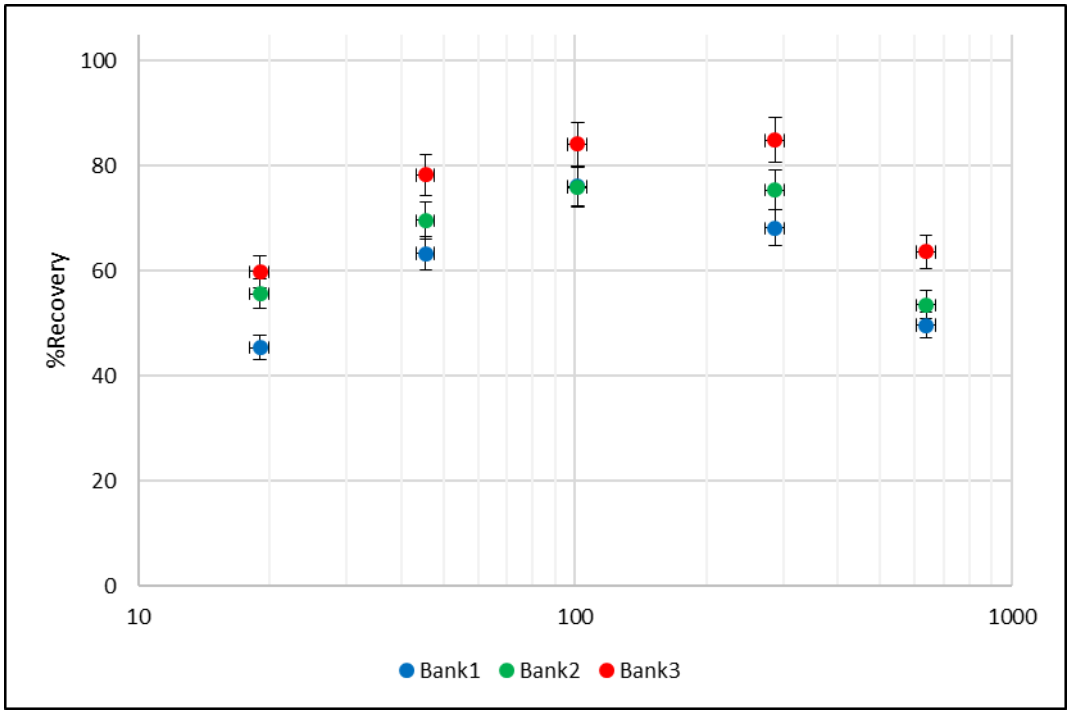

Figure 5.12: Error analysis of recovery-by-size from cell-by-cell flotation plant survey data (cleaners and re-cleaners)

The continuous plant flotation results in Figure 5.4 were not showing any form of pattern followed as the results varied a lot. Considering that plant conditions can be harsh and depend on many factors mainly equipment related, process related and human related, unstable behaviour is likely to occur. The modelling of the continuous plant flotation data followed experimental results but predicted an increase in recoveries of around 4 % difference. This difference is high but one may relate it to the fact that where dynamic conditions took place as in flotation then more noise on the results would appear. The cell-by-cell flotation results had a steady recovery increase from the first cell up to the last cell as shown in Figures 5.5 – 5.6. It can be expected that in these banks of cells, the concentrate grade would be the opposite of what is seen in the recoveries.

Statistics done for the continuous flotation plant, cell-by-cell of roughers and cleaners / re-cleaners followed the Chi-square method as seen in Tables 5.8 – 5.10. Different p-values were obtained, i.e., continuous flotation plant p-value = 0.1207, cell-by-cell roughers p-value = 0.0003 and cell-by-cell cleaners / re-cleaners p-value = 0.1369. Based on the p-values obtained, it can be seen that the roughers

were the ones that had significant difference since its p-value was lower than 0.05. The higher number of cells or banks in the roughers resulting in more process interruptions or instabilities may be contributing factor to the significant difference observed statistically. Since there was no significant difference in the continuous flotation plant and cleaners / re-cleaners results the null hypothesis can be accepted in both cases.

In all the trends of Figures 5.7 – 5.9, it was noticed that the highest peak was at the 1.0 min^{-1} in terms of flotation rate. This was achieved at the particle size of just below 50 µm. The results of flotation rate constant [k or $\Phi_j(d_{pi})$] agreed with King (2012) statement that constant 2.33 in Equation 2.11 normalises function such that $\Phi_j(d_{pi})$ becomes 1.0. The roughers showed a slightly sharper curve from beginning to the highest point as compared to cleaners and re-cleaners behaviour. Towards the end the roughers were flatter as compared to the cleaners and this can be seen at the particle size of 288 µm which was related to Y-axis figure of 0.233 while that of cleaners / re-cleaners was at 0.285. The overall results (i.e. feed – concentrate – tails) in Figure 5.7 were less sharp at the beginning and more flat at the end. In spite of the instabilities that continuous flotation experiences, the flotation rate constant along different particle sizes did not show major differences to each other.

5.6 Conclusions

The data from the three plant surveys has been successfully analysed in this chapter. The key findings can be summarised as: overall recovery figures at fine sizes were found to be at the range of 66 % to 77 %, the highest peak of rougher bank recoveries was within particle size ranges of 45 µm to 100 µm and re-cleaners bank had its highest recovery of 76.1 % while cleaners bank could go as high as 80.0 % on average. These results are much lower compared to the batch flotation testwork results in the previous chapter (Chapter 4). It is clear that plant performance will tend to be lower than the laboratory performance for the same

ore analysed as has been found by researchers such as Alexander *et al*. (2000); Lotter *et al*. (2014), and Boeree (2014).

In the application of statistics it was found that continuous flotation plant p-value was 0.1207, cell-by-cell roughers p-value was 0.0003 and cell-by-cell cleaners / re-cleaners p-value was 0.1369. Based on the p-values obtained, it can be seen that the roughers were the ones that had significant difference since its p-value was lower than 0.05. In terms of flotation rate constant for all three sets of continuous flotation results, it was noticed that the highest peak was at the 1.0 min^{-1} at particle size of below 50 µm. It must be noted that the continuous operation where the plant surveys were conducted had no scavengers and that is why nothing is said about this part of the flotation circuit. The available parts of the flotation circuit that could be surveyed can be seen in Figure 3.2.

Chapter 6 The use of scale-up approaches and the applying of validation methods

6.1 Introduction

Scale-up methods are generally based on specific assumptions on the continuous operation. For example, assumptions can be made on the gas dispersion in the flotation cells (Gorain *et al*., 1997; Wills and Napier-Munn, 2006; Mesa and Brito-Parada, 2019). The kinetics of flotation is another aspect that can be considered (Yianatos *et al*., 2005). There have also been reports of scale-up procedures based on dimensional similitude and cell condition (Xia *et al*., 2009; Rodrigues *et al*., 2001; Heiskanen, 2013). The carrying capacity of air bubbles is another parameter that can underpin a scale-up technique (Yianatos and Contreras, 2010).

The use of scale-up factors is still necessary because the knowledge and measurement technologies are insufficient for a reliable prediction of the flotation plant performance from laboratory tests using physical variables alone (Yianatos *et al*., 2010). Figure 6.1 shows the scale-up factors that can be used from batch flotation tests (laboratory) to continuous flotation operation (industrial).

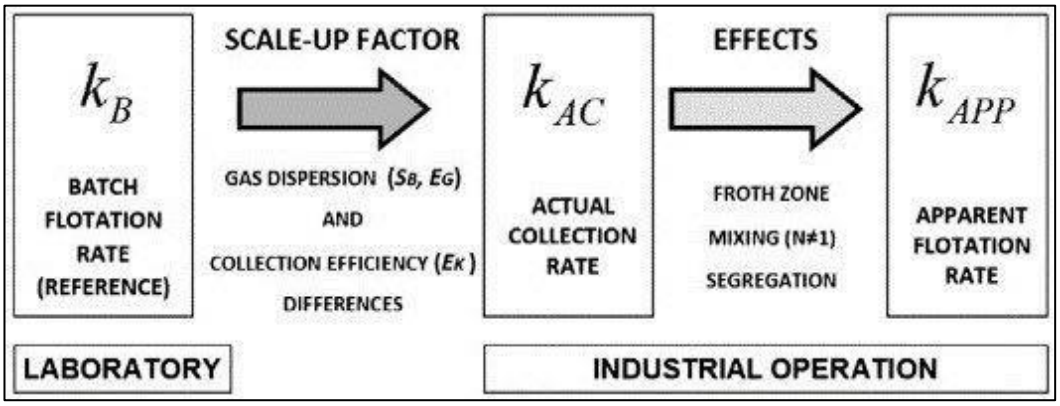

Figure 6.1: The scale-up approach (Yianatos *et al*., 2010)

In the literature review (i.e. Chapter 2), different scale-up approaches were presented. Data collected, conditions of batch testing as well as continuous flotation plant necessitated the choice of scale-up approaches to be selected as

these were the determining factors. Gas dispersion, flotation kinetics, dimensional similitude and carrying capacity were the scale-up approaches that suited this research work. Equations associated with these chosen scale-up approaches were in the following order i.e. gas dispersion scale-up (Equations 2.10 and 2.11), flotation kinetics scale-up (Equations 2.12 – 2.16), dimensional similitude scale-up (Equation 2.17 – 2.18), and carrying capacity scale-up (Equations 2.19 – 2.21). Results from the use of these four scale-up approaches are discussed in this chapter. Different methodologies that can be applied to validate results from the scale-up approaches are also discussed.

6.2 Gas dispersion scale-up approach

In gas dispersion approach to scale-up a relation between the rate at which valuable minerals float and the gas dispersion effects within a flotation cell is considered.

In this research conducted, Equations (2.12) and (2.13) have been used and results in Table 6.1 and Table 6.2 were produced. It was possible to make comparisons of batch flotation results versus continuous flotation results. The specific froth residence time was seen to increase more than three times from batch flotation to continuous flotation but, the froth residence time under the same conditions was close to ten times increase from batch to continuous flotation. There was almost close to double of the constant from relation between τ_{fs} and k when looking at batch flotation to continuous flotation. The curve-fitting constant showed a decrease from batch to continuous flotation. It can be seen that some predictions can be made from batch flotation to estimate continuous flotation with the use of Equations (2.12) and (2.13). Caution will have to be exercised, as continuous dynamic flotation conditions may not always follow predictions of stable batch flotation conditions.

Table 6.1: Summary of gas dispersion scale-up results from Equation (2.12)

Description	Symbol	Flotation results	
		Batch	Continuous
Specific froth residence time (s)	τ_{fs}	93.8	300.9
Froth residence time (s)	τ_{fg}	5.6	54.2
Froth height (m)	h_{froth}	0.045	0.13
Superficial gas velocity (m/s)	J_g	0.008	0.0024
Distance between impeller and launder (m)	L	0.06	0.18

Table 6.2: Summary of gas dispersion scale-up results from Equation (2.13)

Description	Symbol	Flotation results	
		Batch	Continuous
Flotation rate constant	k	0.37	0.46
Constant from relationship between τ_{fs} and k	α	0.57	1.02
Constant from curve-fitting	β	0.0048	0.0027
Specific froth residence time (s)	τ_{fs}	93.8	300.9

6.3 Flotation kinetics scale-up approach

Equations (2.17) and (2.18) were used as part of flotation kinetics scale-up with results shown in Table 6.3, Figures 6.4, and Figure 6.5. It was noticed that the batch flotation recovery results differed by more than 25 % when compared to the plant recovery flotation results. At the laboratory, maximum recovery increased by almost the same figure i.e. 25 % of the batch flotation recovery while continuous flotation could only see a 6 % increase before reaching maximum recovery. This could mean that the plant was running close to its optimum as the difference between recovery achieved and maximum predicted recovery was this minimal.

The generation of Figure 6.2 using Equation (2.17) involved using all flotation times (t) of 2, 6, 12 and 20 min. Experimental recovery was taken as average recoveries obtained in each flotation as shown in Table 4.6, for example, 2 min flotation time gave a recovery of 84.37 %. Maximum recovery R_∞ and maximum flotation rate constant K_{max} were calculated by running Excel Solver. The same procedure was followed even for the generation of Figure 6.3. The difference in continuous flotation came in having to determine residence time (τ_p) and experimental recovery which had to be done for each flotation bank of cells in a row.

Table 6.3: Summary of flotation kinetics scale-up results

Description	Symbol	Flotation results	
		Batch	Continuous
Recovery according to flotation / residence time	R(t) / R(τ)	89.71	60.84
Maximum recovery	R_{∞}	93.59	66.84
Maximum flotation rate constant	K_{max}	4.8	0.1
Flotation / residence time	t / τ_p	20	27
Number of cells in series	N_c	1	15

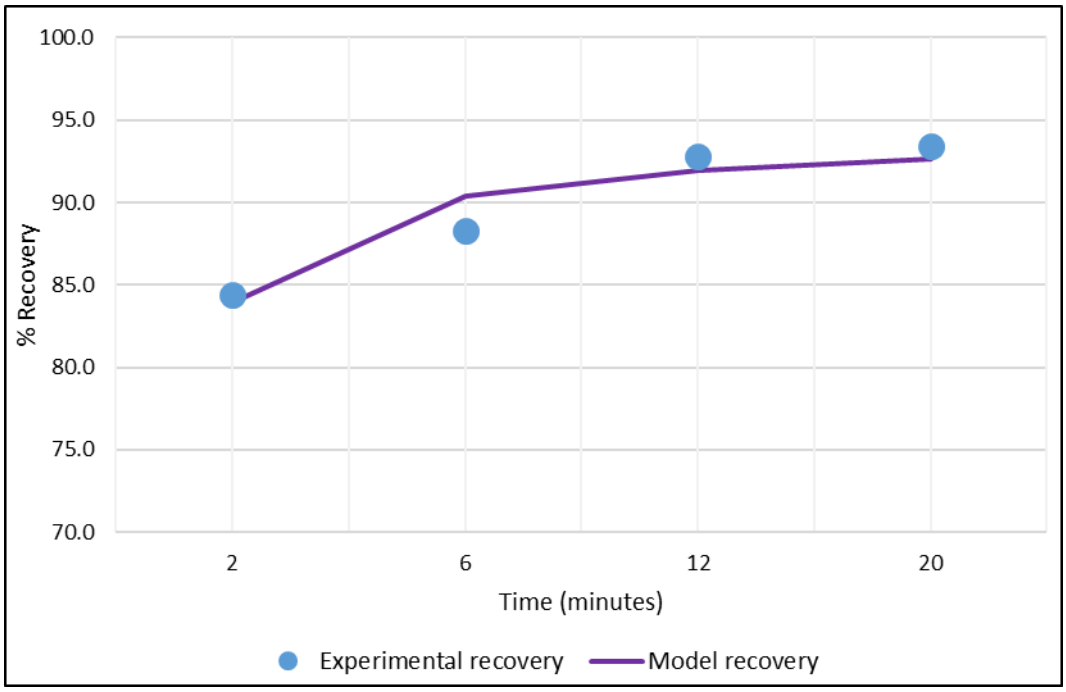

Figure 6.2: Batch flotation vs. model prediction results

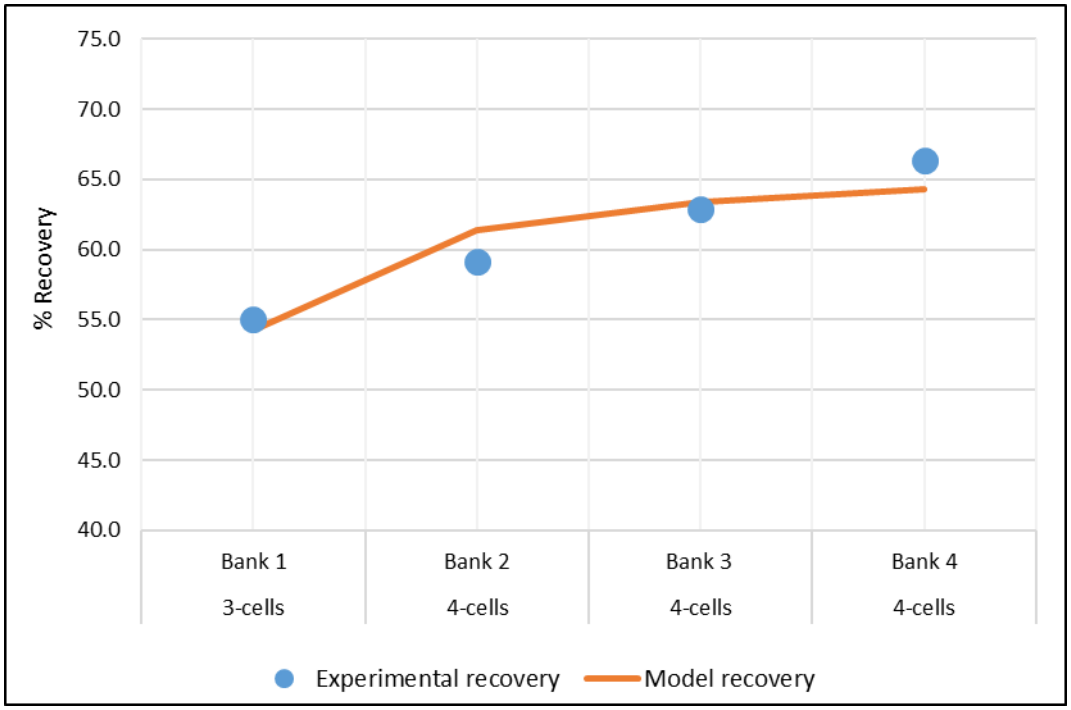

Figure 6.3: Continuous flotation survey vs. model prediction results

The comparison from Figures 6.2 and Figure 6.3 showed that model recoveries were able to fit the experimental recoveries with minimal difference between the two. It must be noted that these two figures resemble Figure 2.20 explained earlier. The laboratory results operated with recovery ranges of 84 % – 93 % but, continuous flotation dropped to recovery ranges of 55 % – 66 %. The lower flotation rate from the continuous flotation was seen as the contributing factor of these lower recoveries. This may also mean that some more thought will be required when applying the kinetics approach to scale-up of flotation. The sensitivity of the flotation rate may require more tests to be conducted at different conditions to determine the repeatability of this parameter in those conditions being tested.

6.4 Dimensional similitude scale-up approach

The use of dimensionless similitude can be applied in processes like flotation because they allow comparison of systems that are vastly different and taking into consideration that these numbers do not have any true physical dimensions

(Boeree, 2014). The different phases in flotation i.e. liquid, gas and solid may use dimensionless number with the application of computational fluid dynamics (CFD).

Yianatos *et al*. (2010) and Yianatos (2012) have made use of the dimensionless similitude scale-up approach in comparing two different cells as shown in Table 6.4. A similar approach was then followed in this research by making use of the Wemco cells (available in continuous flotation plant used) and results were compared with already published data. It can be seen that the scale-up factor came to 1.25 which is what the designer may then use in sizing the flotation cells for the same ore type and cell type. The flotation rate constant needs to be first determined in the laboratory flotation batch tests and thereafter the estimated scale-up factor (1.25 in this research) can be used to determine the actual flotation rate constant of the tested cell type. The more detailed table of results in applying dimensional similitude scale-up can be seen in Appendix C. In the brownfield environment, it has been recommended that a sequential calculation be used for the dimensionless parameters by estimating each individual cell in a bank (Yianatos *et al*., 2010).

Table 6.4: Comparing dimensional similitude scale-up results with published data

Cell type	Volume (m^3)	K_{app} / K_b	α (froth)	β (mixing)	γ (segregation)	ξ (scale-up factor)	S_b (1/s)	Reference
Tankcell	300	0.24	0.48	0.76	0.89	0.75	44.5	Yianatos *et al*. (2010)
Outotec	160	0.21	0.44	0.79	0.89	0.68	41.7	Yianatos *et al*. (2010)
Wemco	128	0.01	0.59	0.02	0.56	1.25	38.4	This research

6.5 Carrying capacity scale-up approach

In the past, carrying capacity has been mostly associated with column flotation cells (Boeree, 2014). It was decided for this project to also use this approach even though flotation cells where this was applied were Wemco cells which are

rectangular in shape. Table 6.5 gives a summary of the results obtained from applying Equations (2.21 – 2.23) under Literature Review section. There were notable differences in the final results of the carrying capacities when size (P_{80}) and froth recovery (R_f) were used. Considering the conditions that size (P_{80}) and froth recovery (R_f) were measured and calculated at, such differences will be expected. It would be recommended that the design engineer looks at both methods then; determine the final flotation cell size given by both methods of carrying capacities before deciding on final design to adopt. In comparing published data with this research results as shown in Table 5.16, the C_R values showed -77.9 % difference while R_f differed by +27.1 %. The different cell types, conditions of testing and ore types used may justify these differences observed.

Table 6.5: Summary of carrying capacity scale-up results

Description	Symbol	Value	Comment
80% passing size (µm)	P_{80}	150	Plant data – internal report
Particle (solids) density	ρ_p	3.2	Plant data – internal report
Bubble surface coverage	φ_s	7%	Published data by Yianatos and Contreras (2010)
Bubble surface area flux	S_B	38.42	Plant data – internal report
Sauter mean particle diameter	d_p	0.06	Plant data – internal report
Maximal bubble surface coverage	$\varphi_{s,max}$	22%	Published data by Yianatos and Contreras (2010)
Froth recovery (k/k_c)	R_f	59%	
Carrying rate	C_R	0.27	
Carrying capacity (using P_{80})	C_A	32.64	
Carrying capacity (using R_F)	C_A	0.50	

Table 6.6 Comparison of carrying capacity scale-up results with published data

Tests done	**C_R**	**R_f**	**Reference**
4 tests AVG	1.22	46%	Yianatos and Contreras (2010)
4 tests AVG	0.27	59%	This research
% Difference	-77.9	+27.1	-

6.6 Scale-up validation

Data used for scale-up needed to be validated in order to see how reliable and trustworthy would its use be for practical purposes. Validation would also be a tool to test repeatability of this work with previous work done by other researchers in the same field of study. Techniques or mechanisms used in this work for validation included kinetics, concentrate grade, recovery and upgrade ratios.

6.6.1 Kinetics validation

In the kinetics technique for validation, flotation rate constant (k in min^{-1}) was the parameter used for comparing batch flotation and continuous flotation. Both continuous flotation sampling methods done were effected in this comparison i.e. overall circuit sampling which consisted of feed, concentrate and tailing for the flotation plant. The second continuous flotation sampling done was based on individual cells of the row and is then termed as cell-by-cell. Flotation rate constant (k) results can be seen in Table 6.7 as well as Figure 6.4. Results compared fairly well in most of the screen fractions with only 19 microns size fraction that gave notable differences. The differences in the averages of the batch and continuous flotation data sets were very minimal as they were around 0.1 which translated to less than 20 % difference.

Table 6.7: Summary of kinetics validation data

Size	Batch flotation	Continuous flotation (overall circuit)	Continuous flotation (cell by cell)
(μm)	(min^{-1})	(min^{-1})	(min^{-1})
638	0.091	0.108	0.117
288	0.211	0.238	0.257
102	0.573	0.624	0.666
46	0.824	0.988	0.992
19	0.127	0.319	0.233

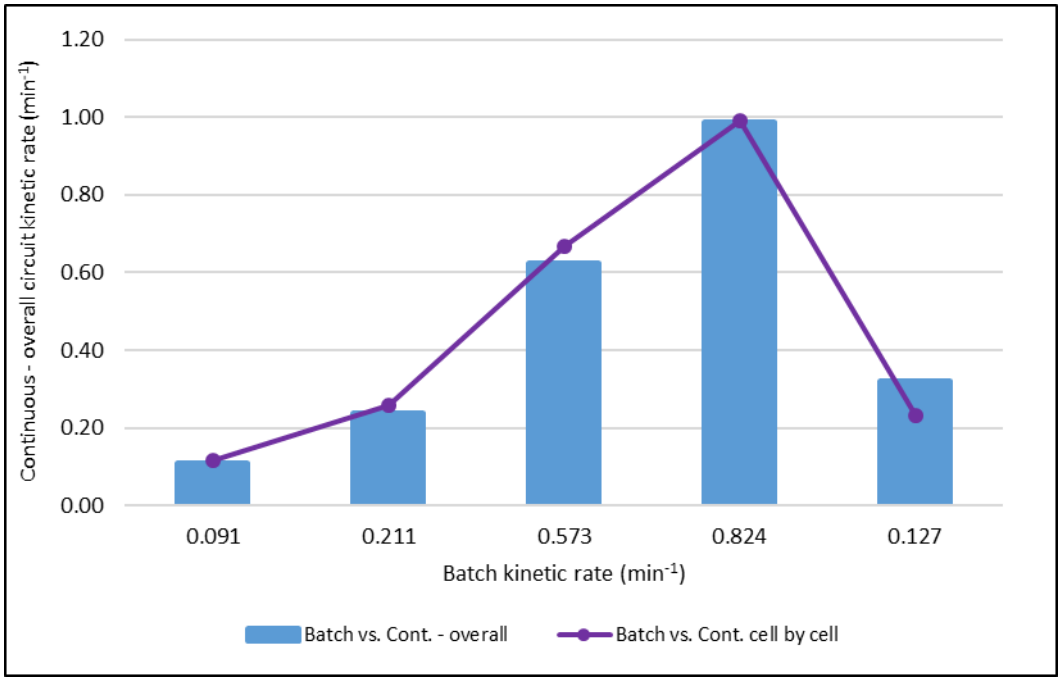

Figure 6.4: Batch flotation vs. Continuous flotation kinetics scale-up validation

6.6.2 Concentrate grade validation

Validation by making use of concentrate grade values from batch flotation and continuous flotation can be seen in Table 6.8 and Figure 6.5. The batch flotation had significantly lower concentrate grade compared to continuous flotation. The laboratory concentrate grade is estimated to be around four times (3.85 to be precise) lower than the plant concentrate grade. Since the batch flotation test conducted was mainly the rougher-rate like (single concentrate scraping) then concentrate grade is expected to be compromised to what the plant will actually see. The lock-cycle test batch flotation would be the ideal test to better explain or relate the concentrate grade of laboratory testwork versus continuous flotation results.

Newcombe (2014) used a method of cumulating concentrate grades for the comparison of batch flotation and continuous flotation (flash flotation cell). In this method a factor of 1.03 was seen, i.e., laboratory concentrate grade results were 1.03 times in relation to continuous flotation concentrate grade results. It is believed that a similar application of cumulative concentrate grades or conducting

lock-cycle tests would see the current 3.85 factor being reduced maybe by half or even more. Such work can be for future improvement initiative.

Table 6.8: Summary of concentrate grade validation data

Size	Batch flotation	Continuous flotation (overall circuit)	Continuous flotation (cell by cell)
(µm)	(%Cu)	(%Cu)	(%Cu)
638	9.11	34.84	29.45
288	9.88	39.33	31.20
102	16.02	43.22	37.33
46	8.27	41.60	36.50
19	2.42	31.09	27.67

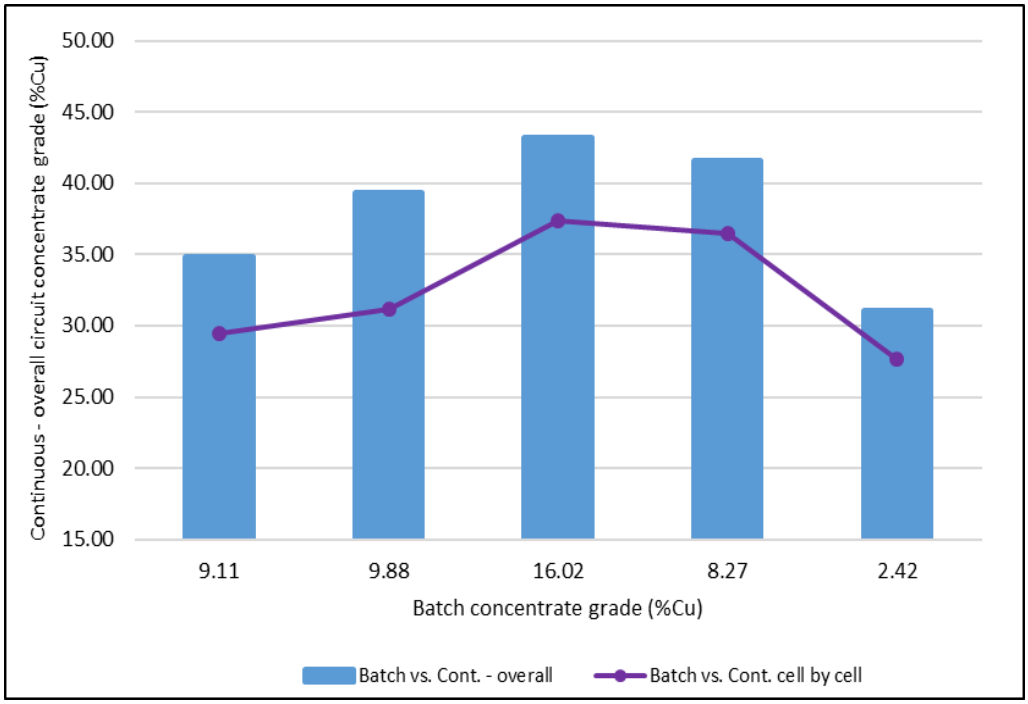

Figure 6.5: Batch flotation vs. Continuous flotation concentrate grade scale-up validation

6.6.3 Recovery validation

The scale-up validation by the use of recovery results can be seen in Table 6.9 and Figure 6.6. The data for the continuous flotation plant of the overall circuit had

better results as compared to the cell by cell performance. It must be noted that both the continuous flotation results were far lower than the batch flotation test results. This can be linked to the more stable and controlled environment that the batch flotation tests were conducted at it. It must be noted that the highest peak of recovery in the continuous overall circuit recovery was seen at finer screen size, i.e., 46 µm while continuous flotation cell by cell agreed with batch flotation results at 102 µm. This may be related to the fineness or coarseness of grind during the experiment in each conditions.

Table 6.9: Summary of recovery validation data

Size	Batch flotation	Continuous flotation (overall circuit)	Continuous flotation (cell by cell)
(µm)	(%)	(%)	(%)
638	84.56	42.75	44.60
288	89.13	62.69	60.64
102	94.18	81.91	68.50
46	91.76	84.21	62.46
19	88.92	71.97	47.86

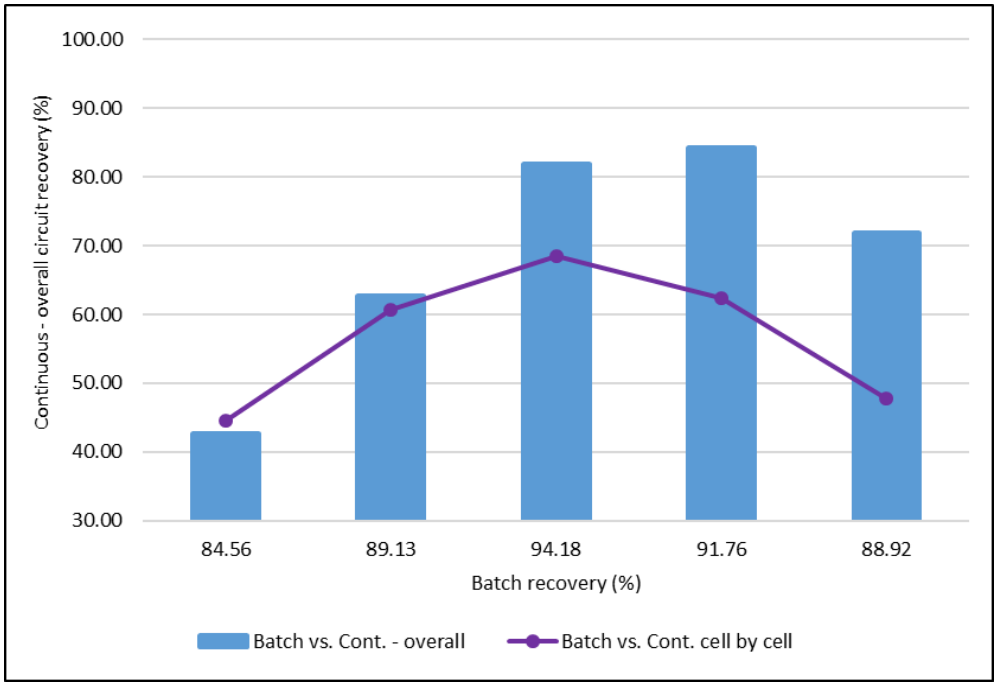

Figure 6.6: Batch flotation vs. Continuous flotation recovery scale-up validation

6.6.4 Sizing (size)

Newcombe (2014) used a method of sizing by taking flotation product samples then wet screening at 38 µm; drying the screen products; dry screening the +38 µm material from 38 µm upwards following the square-root-two series to a top screen size of 850 µm. Results of elemental sizing can be seen in Figure 6.7. Almost the same procedure for sizing was followed in this work resulting in Figure 6.8 but, in this case, polynomial trendline better fitted the experimental data with R^2 = 0.9921. Sizing similar to what has been done in Figure 6.8 can also be performed on feed and tailings flotation samples. Decision can then be taken by the researcher to send each screen fraction of the sizing samples or combine certain screen fractions to form one sample to be analysed. The feed, concentrate and tailings assays with the use of a two-product formula will then yield recovery. This calculated recovery will be based on the selected screen fraction of the sizing samples hence the term recovery-by-size or size-by-size recovery.

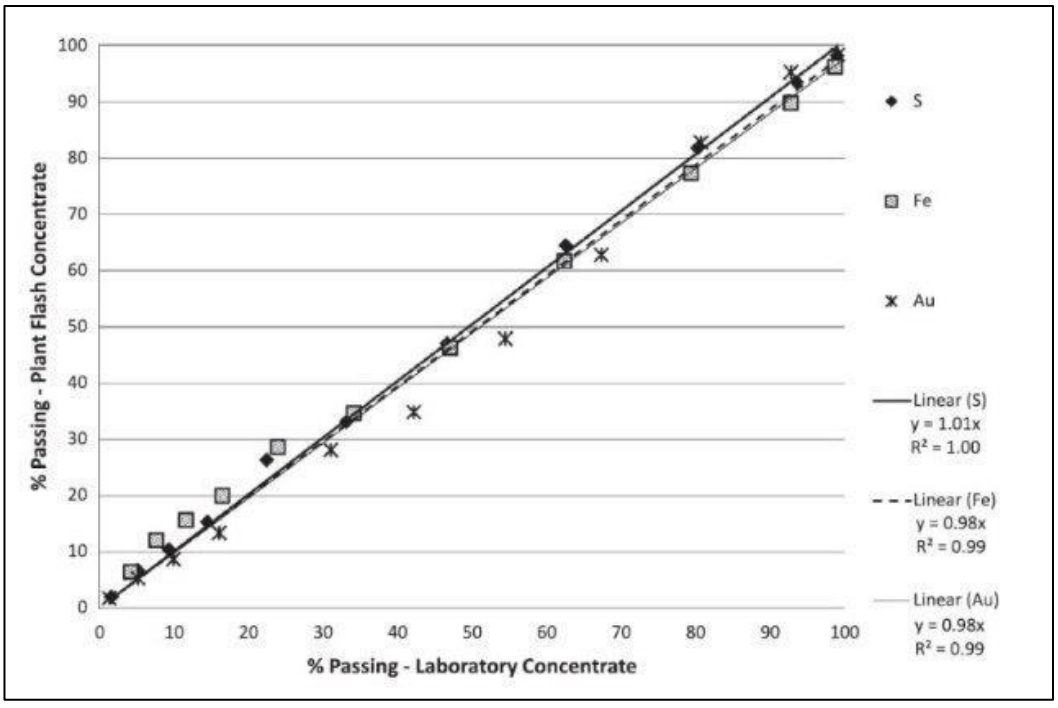

Figure 6.7: Elemental (S, Fe & Au) sizing distribution of batch flotation vs. continuous flotation (Newcombe, 2014)

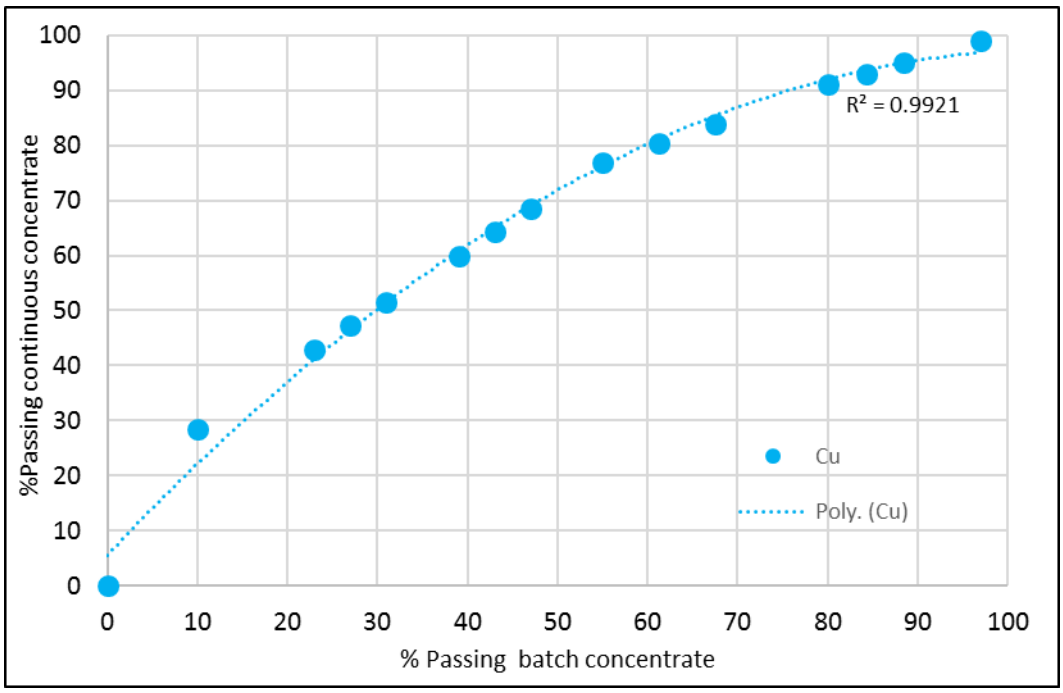

Figure 6.8: Elemental (Cu) sizing distribution of batch flotation vs. continuous flotation

6.6.5 Overall validation

Another comparison done for the scale-up validation looked at the use of upgrade (enrichment) ratios. This is mainly the ratio of the concentrate grade to the feed (head) grade. Wills and Napier-Munn (2006) explained the upgrade ratio as the ratio of the grade of the concentrate to the grade of the feed and is related to the efficiency of the process. In a case where one is not able to get enrichment ratio for the batch flotation plant, Newcombe (2014) has suggested the use of the first concentrate of the batch flotation test as shown in Table 6.10 and Figure 6.9.

The results for batch flotation and continuous flotation cell by cell are closely related to each other as in Table 6.10. The continuous flotation overall circuit is much higher than the other numbers for comparison. This may be linked to assays errors since upgrade ratios look at two parameters i.e. concentrate and feed grade and both of these will be dependent on assays results for their accuracy. Some of

the feed grade assays results were noticed to be much lower than most of the other results received. This may have also contributed in increasing upgrade ratio in the overall circuit results.

Work conducted by Newcombe (2014) in Table 6.11 had highest plant upgrade ratio of 9.5 while this work in Table 6.10 showed highest value being 21.65 in cell by cell but overall circuit was at 86.70. Averages of 9.63 and 15.02 were seen when using first concentrate grade and upgrade ratio calculated for batch flotation respectively. It is then proved that one can use the first concentrate grade for the batch flotation instead of having to calculate the upgrade ratios.

Table 6.10: The use of upgrade ratios for validation

Size	Batch flotation	Batch flotation	Continuous flotation (overall circuit)	Continuous flotation (cell by cell)
(µm)	1st conc. (%Cu)	(c/f) ratio	(c/f) ratio	(c/f) ratio
638	9.50	17.79	86.70	17.37
288	11.13	17.29	82.88	17.64
102	16.80	25.33	71.34	21.65
46	7.92	11.50	66.46	19.15
19	2.81	3.20	49.17	15.94

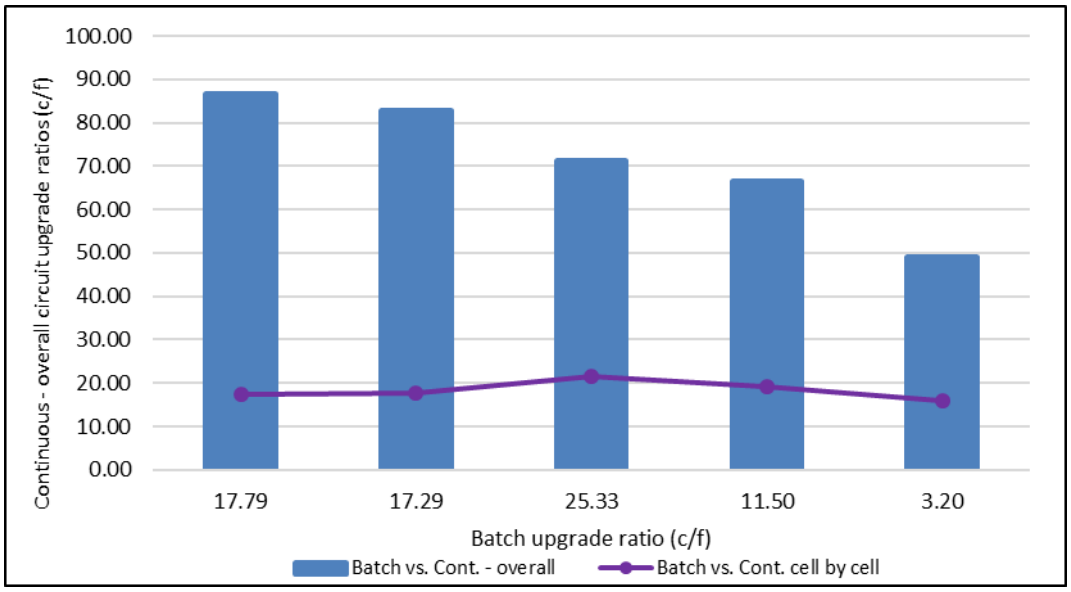

Figure 6.9: Batch flotation vs. Continuous flotation upgrade ratios scale-up validation

Table 6.11: Comparison of pyrite plant upgrade ratios and batch flotation first concentrate (Newcombe, 2014)

Size class	Sulphur		Gold	
(µm)	Plant	Lab	Plant	Lab
+300	2.3	18.9	2.7	17.4
-300/+212	4.3	28.6	3.2	28.7
-212/+150	5.1	30.1	6.9	16.5
-150/+106	5.4	27.1	6.8	16.2
-106/+75	5.0	23.4	5.5	20.1
-75/+53	5.1	24.4	6.0	26.5
-53/+38	5.5	20.9	7.0	28.5
-38	8.8	29.7	9.5	4.5

Results in Table 6.11 and Table 6.12 showed how other validation work appeared from the work by Newcombe (2014). These results can be used in conjunction with what was presented in this work in Table 6.10 and Table 6.7. According to Newcombe (2014) the batch flotation had highest flotation rate constant of 0.727 min^{-1} while this work showed a figure of 0.824 min^{-1}. This work gave a higher flotation rate for plant results that averaged at 0.990 min^{-1} while work from Newcombe (2014) had results of 0.207 min^{-1}.

At longer flotation time (90 sec) recoveries in Table 6.13 were 67.9 % for batch flotation and in Table 6.9 batch highest recovery was 94.18 %. Continuous flotation from plant flash cell managed to reach 62.5 % recovery at -38 µm while flotation cells in this research (Wemco) were able to average at recovery of 76.35 % with screen size of 74 µm. The type of material being floated, the type of flotation cell used and residence time applied maybe playing major role in such differences observed.

Table 6.12: Comparison of k (min^{-1}) values of pyrite (Newcombe, 2014)

Size class (µm)	Plant flash k (min^{-1})	Laboratory k (min^{-1})
+212	0.003	0.357
-212/+150	0.042	0.543
-150/-75	0.071	0.659
-75/+38	0.207	0.727
-38	0.163	0.423

Table 6.13: Comparison of pyrite plant recovery values for the plant flash flotation and batch flotation (Newcombe, 2014)

Size class (µm)	Plant flash (%)	40s Batch (%)	90s Batch (%)
+300	1.1	19.3	29.3
-300/+212	7.3	32.6	51.2
-212/+150	14.0	34.8	55.6
-150/+106	23.3	40.5	64.6
-106/+75	28.9	40.6	59.9
-75/+53	35.4	47.8	67.9
-53/+38	42.5	37.8	55.7
-38	62.5	24.2	44.7

The different scale-up validation techniques were seen to be key in identifying weaknesses and strengths of the whole scale-up work conducted. When comparing this work with what has been done by other researchers, there were similar things or trends that could be drawn but also differences existed in other areas. Some of the other opportunities for further improvement have been noted during the validation techniques. It would be strongly recommended for such improvement actions to be deliberated or conducted when such an opportunity arises.

6.7 Conclusions

The scale-up from batch flotation to continuous flotation was found to be possible with the approaches applied. The different methods used gave results that will

require the design engineers to make that responsible choice based on the information at their disposal. In this research, the sizing validation technique has proved to best fit the scale-up from batch testing to industrial application. The high correlation constant (R^2) obtained of 0.9921 singles out the sizing technique in this instance as the best validation method used in this research. The beauty of applying different approaches was that one was not confined to one solution even if, it did not look feasible for the application to be used in it.

The use of published data is recommended in comparing results obtained but it must be taken into consideration the parameters like: cell types, ore types, experimental or plant conditions that such published data was generated with. For practical application, it is highly recommended to try first the pilot flotation application of the scale-up design obtained from batch flotation results before going to continuous flotation scale-up application. Considering the high costs involved in final design of continuous flotation application then, the route of pilot scale-up will result in notable savings.

Chapter 7 Developing ModSim simulator for continuous flotation plant

7.1 Introduction

The ultimate goal of a flotation plant is to yield the best recovery at the highest achievable grade. Sutherland (1981) identified three key performance indicators or factors for a flotation circuit:

(a) The chemical conditions in the pulp (i.e. reagent concentrations, pH, aeration).
(b) The physical conditions in the cells (i.e. agitation, air supply plus distribution, pulp level).
(c) The arrangement of the circuit (i.e. the sizes of the cells in each bank, the interconnections between the banks).

All the above factors are equally important since, the absence or wrong application of one of them will lead to the final goal not being obtained as per plan or per design. Because of the interlinking of these factors, this has caused flotation to be widely researched in trying to understand one of these factors or a combination of two or more of them. Continuous flotation plants employ different skilled personnel that focus on getting these factors to be aligned with production targets on a shiftily, daily, monthly and yearly basis.

This chapter will look at using ModSim software to develop continuous flotation plant simulator. Such a simulator should be able to show a basic mass balance of the flotation circuit. Predictions of recoveries and grades for different streams are some of the deliverables that the simulator should produce with a certain level of accuracy.

7.2 Flotation modelling

King (1972) has identified two main uses of flotation modelling i.e. firstly to aid in improving the design of flotation plants in scale-up of batch data to full-scale continuous operation. Secondly, the model will lead to improved plant operation as a result of better control. The classes of models are deterministic, they ignore random variations while predicting the same outcome from a given starting point. These are followed by stochastic models, i.e., the class which is more statistical in predicting the distribution of possible outcomes (Bhondayi, 2014). In flotation modelling, the two zones are usually considered are the pulp zone and the froth zone. Yianatos *et al*. (2012) described these zones as: collection (pulp) zone is where the particle-bubble aggregate is formed and carried to the pulp–froth interface, and cleaning (froth) zone is the one located between the pulp–froth interface and the concentrate overflow, where entrained particles have the chance to drop back to the collection zone. Different researchers have worked on the concept of flotation modelling like: King (1972); Sutherland (1977); Klimpel (1980); Finch and Dobby (1990); Finch *et al*. (2008) Polat and Chander (2000); Lelinski *et al*. (2002); Conradie *et al*. (2003); Yianatos *et al*. (2012) and Bhondayi (2014) just to name a few.

Some of the output from flotation modelling can be seen in the three figures shown below. Depending on the aim of modelling work being carried out there various results or outcomes that flotation modelling may achieve or yield. Such outcomes will take many forms and will by no means be limited to these three Figures 7.1, 7.2 and 7.3 shown here.

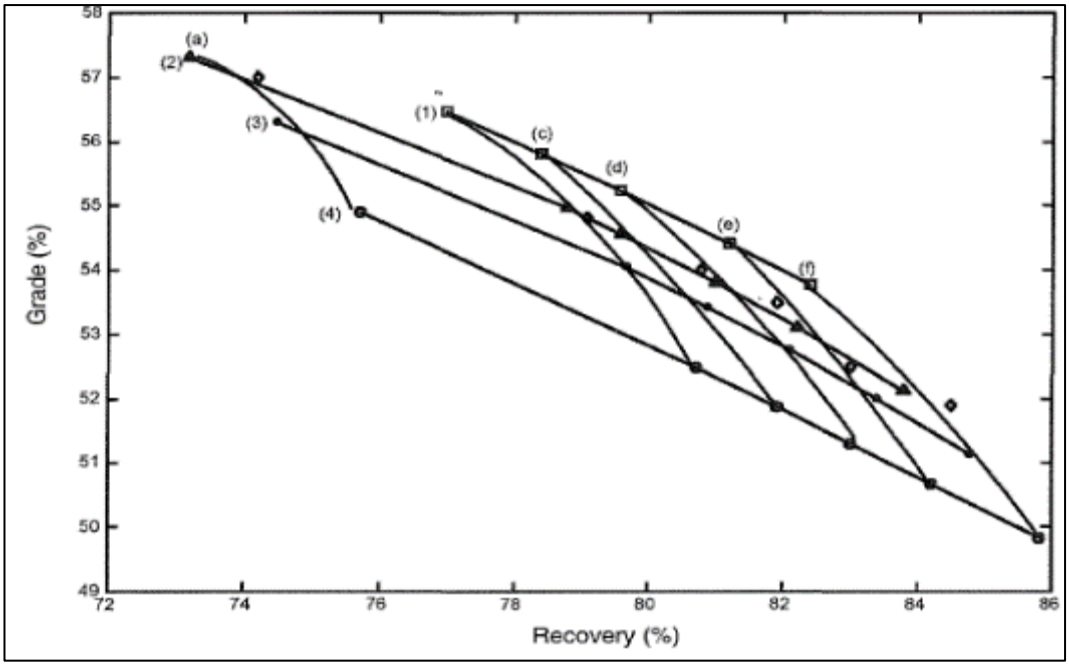

Figure 7.1: SMNE simulated grade recovery map (Conradie *et al*., 2003)

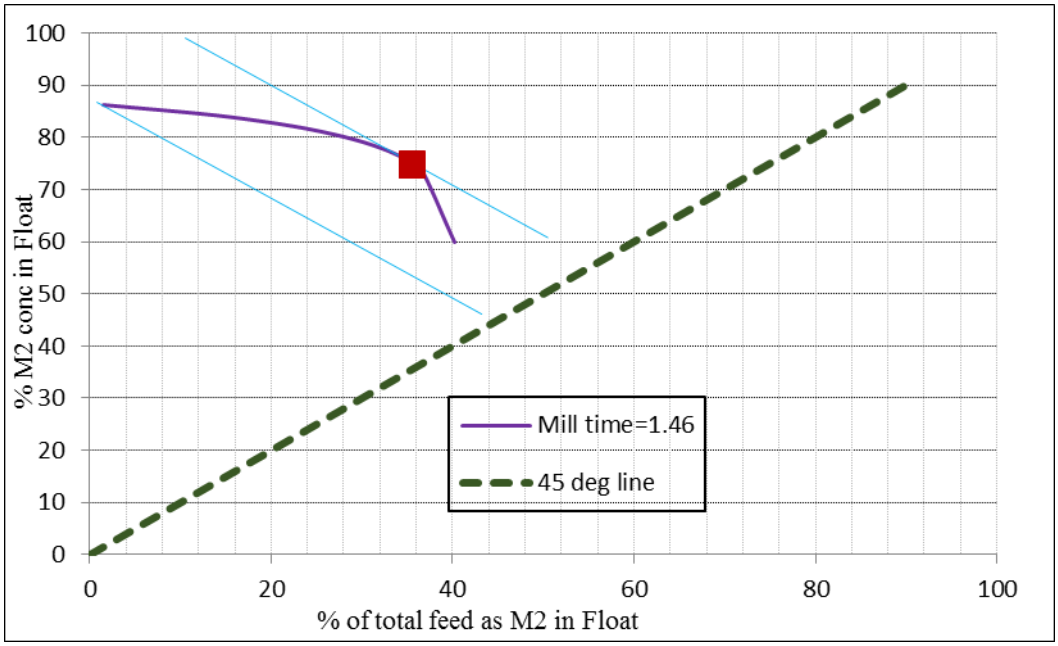

Figure 7.2: AR plot where the optimum operating condition is located for a particular linear objective function (Khumalo, 2015)

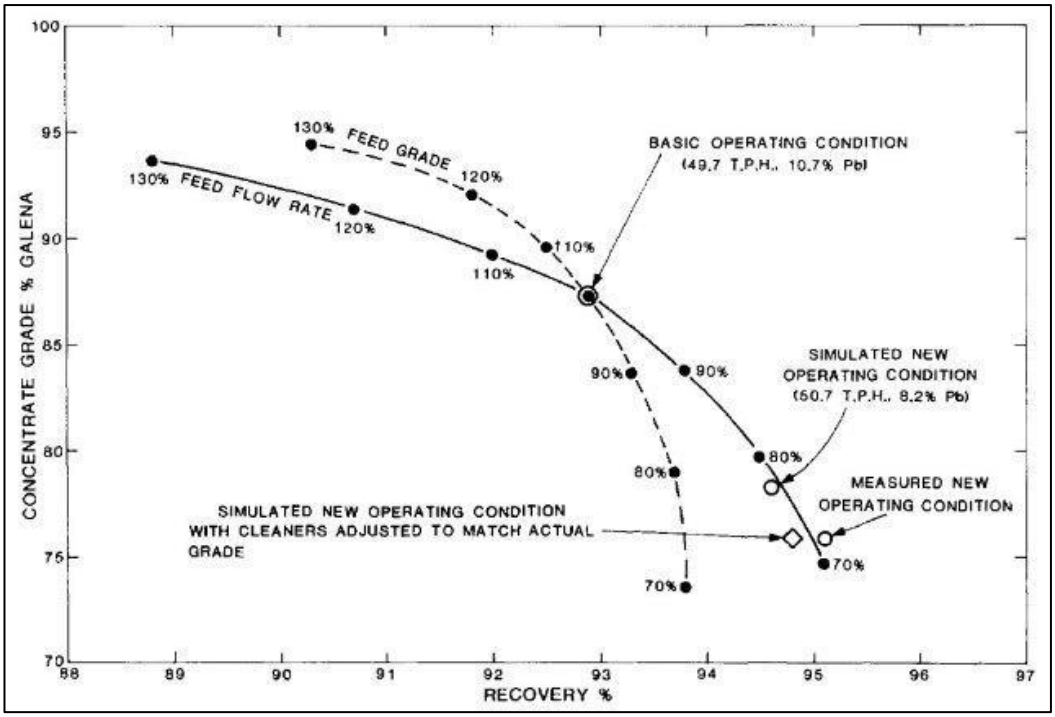

Figure 7.3: Steady-state response of plant to feed changes (Sutherland, 1977)

In the commercial market there are few softwares available to do flotation modelling and they include JK Simfloat mineral processing simulator (Schwarz and Alexander, 2006); MetSim simulator (Metsim, 2020), FloatStar mineral processing simulator (Mintek, 2020), ModSim modelling and simulation of mineral processing systems (King, 2012), LIMN flowsheet processor by David Wiseman (Theflowsheetguru, 2020; Wiseman, D., 2020), SUPASIM flotation model (Hay and Rule, 2003) and UsimPac mineral processing simulator (Caspeo, 2020). It must be noted that even though these softwares are available in the commercial market but their programming is closed for the use and they only give the user limited process modelling information (Yianatos *et al*., 2012). In this research work, ModSim has been used to do the flotation modelling.

7.3 The use of recovery-by-size in flotation modelling

The process of flotation is said to be able to take place in relatively fine particles because, if they are too large the adhesion between the particle and the bubble will be less than the particle weight and the bubble will therefore drop its load

(Finch and Dobby, 1990). It is clear that flotation theory has to do with size in order for successful recovery to take place. The process of flotation is complex and some models have been developed to try and better explain it. Drzymala *et al*. (2020) have consolidated the different types of flotation models in the simplified format shown in Figure 7.4. The three common variables as shown in Figure 7.4 can be one or two incentive parameters which cause a change in the system response such as a mass yield or a component recovery, and these can be investigated from either phenomenological, deterministic or empirical points of view including their combinations. The next section will look into recovery, size, combination of the two (recovery-by-size) and consider scale-up in relation to recovery-by-size.

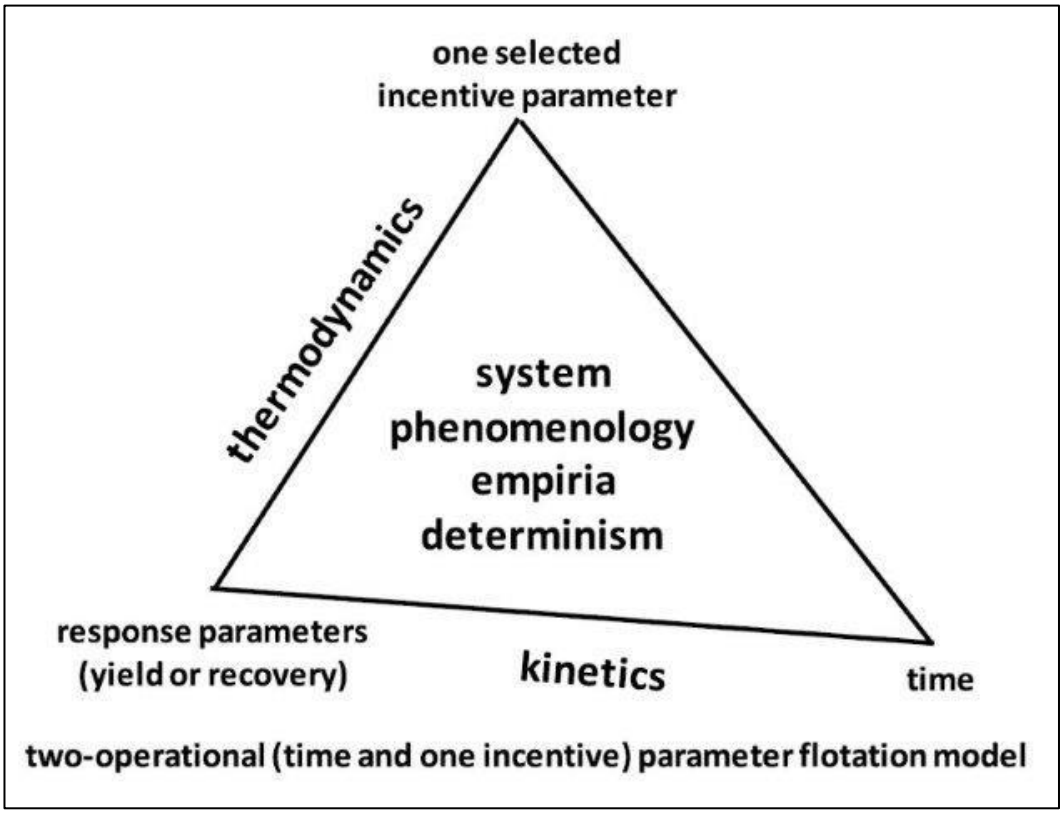

Figure 7.4: Flotation system with one incentive and time as variable parameters (Drzymala *et al*., 2020)

The recovery is one of the flotation performance measures that is key to track for any continuous flotation plant operation. In the batch flotation tests, the recovery is also used as part of the data analysis tools to assess the behaviour of the ore or chemicals being tested. Wills and Napier-Munn (2006) have derived recovery

equation with the use of a two-product formula and this is similar to Equation (3.2) used in this work. This two-product formula method is often used to provide information for plant control, although this will be retrospective, dependent on the time taken to receive and process the assay results. A slight drop or increase in recovery will have significant impact on the company's revenue; hence, it is important to monitor this flotation parameter.

7.4 Scale-up from recovery-by-size

Some researchers have looked at scale-up techniques with the use of batch testing where recovery-by-size was part of the exercise but others did not go the route of recovery-by-size. Dobby and Savassi (2005) presented the Flotation Economic Evaluation Tool (FLEET) modeling technique for scale-up from batch flotation using the MinnovEX Batch Flotation Testwork (MFT). In this approach, the flotation rate distribution (k-distribution) at the laboratory scale was characterized by a Weibull (Rosin–Rammler) distribution, which is commonly used for particle size distribution modelling. Each class in the k-distribution contains particles of different sizes and different mineral liberation. Savassi (2006) conducted a compartment model describing the mass transport in an industrial flotation cell. The model considered three zones (collection, quiescent and froth) and two transport mechanisms (true flotation and entrainment). The flotation rate distribution in the collection zone was represented by the same rate constant distribution obtained from the standard batch test of mill-float-test (MFT). Amelunxen and Amelunxen (2009) reported a methodology that considered a batch flotation sampling (global and per size classes) similar to MFT. The industrial cell model looked into two zones: collection and froth. In this approach, the batch flotation was conducted to obtain the maximum rate constant by fast removal of the froth zone.

In this work, the approach taken was to use batch flotation test and full continuous flotation plant sampling campaign. Recovery-by-size data obtained from batch flotation tests and parameters for the continuous flotation sampling campaign

have been applied to the ModSim software for the testing of recovery theories and developing a simulator for the continuous flotation plant.

7.5 Results from the use of ModSim

Information entered into ModSim software can be seen in Table 7.1 and this relates to the King Model which was successfully simulated. ModSim default parameters were used for Item no.3 – no.7 in Table 7.4 while, the volume of each cell was as per the design data. Item no.10 – no.12 were estimated from historical data and item no.8 – no.9 were based on the samples taken during sampling. Other flotation models explained earlier i.e. Klimpel and Sutherland were tested and found to be working, but Sutherland gave some negative numbers on other parameters which could not be clearly defined. A separate study may be required to further understand the cause of such behaviour.

7.5.1 Mass balancing in ModSim

Figure 7.5 and Table 7.2 were the direct screen shots from ModSim which were produced by running simulations with parameters in Table 7.1. ModSim had capabilities of populating results for each stream of the flotation circuit being modelled which in this case was feed, concentrate and tails (mainly for roughers, cleaners and re-cleaners).

Table 7.1: FLTK model flotation banks parameters used for simulation

#	Parameters description	Roughers	Cleaners	Re-cleaners	Comment
1	Number of cells in series for this bank	15	8	4	Design data
2	Cell volume (m^3)	8.5	8.5	8.5	Design data
3	Aeration rate in m^3 of air per m^3 of cell volume	1	1	1	ModSim default
4	Air free pulp (m^3)	7.083	7.083	7.083	ModSim default
5	Froth transmission coefficient	1	1	1	ModSim default
6	Bubble size (mm)	2	2	2	ModSim default
7	Bubble residence time (sec)	10	10	10	ModSim default
8	Percent solids in the feed	43.9	39.8	30	Plant survey

9	Percent solids in the concentrate	40	30	25	Plant survey
10	Particle size at maximum recovery (µm)	50	50	50	Plant survey
11	Largest floatable particle (µm)	1000	1000	1000	Plant survey
12	Specific flotation rate constants - one for each S-classs (sec^{-1})	4.86	4.86	4.86	By calculation

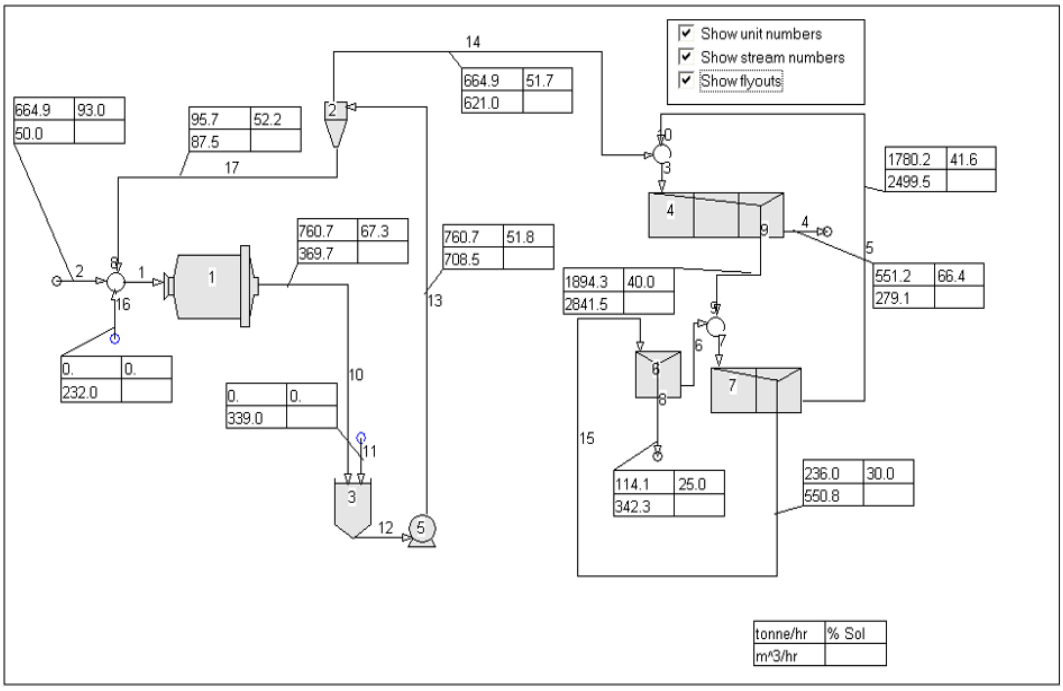

Figure 7.5: Mass balance flowsheet produced in ModSim

Table 7.2: Summary of mass balance from ModSim reporting

Stream	Solid flow tonne/hr	Water flow m^3/hr	% solids	Yield of Solids	Rec. of Copp	Grade of Copp
1	760.68	369.7	67.29	114.40	114.38	100.00
2	664.92	50.0	93.00	100.00	100.00	100.01
3	2445.48	3120.4	43.94	367.79	367.72	99.99
4	551.16	279.1	66.38	82.89	82.87	99.99
5	1780.20	2499.4	41.60	267.73	267.72	100.01
6	121.90	208.4	36.90	18.33	18.33	100.01
7	2016.00	3049.9	39.80	303.19	303.18	100.01
8	114.08	342.2	25.00	17.16	17.15	100.00
9	1894.32	2841.4	40.00	284.89	284.84	99.99
10	760.68	369.7	67.29	114.40	114.38	100.00
11	0.00	339.0	0.00			
12	760.68	708.4	51.78	114.40	114.38	100.00
13	760.68	708.4	51.78	114.40	114.38	100.00
14	664.92	621.0	51.71	100.00	100.00	100.01
15	235.98	550.8	29.99	35.49	35.49	100.00
16	0.00	231.9	0.00			
17	95.65	87.5	52.22	14.39	14.38	100.00

7.5.2 Particle size distribution in ModSim

The simulation from ModSim also produced the particle size distribution (PSD's) of the input and output material to flotation bank as shown in Figure 7.6 – 7.7. Cyclone overflow refers to the flotation feed in this testwork.

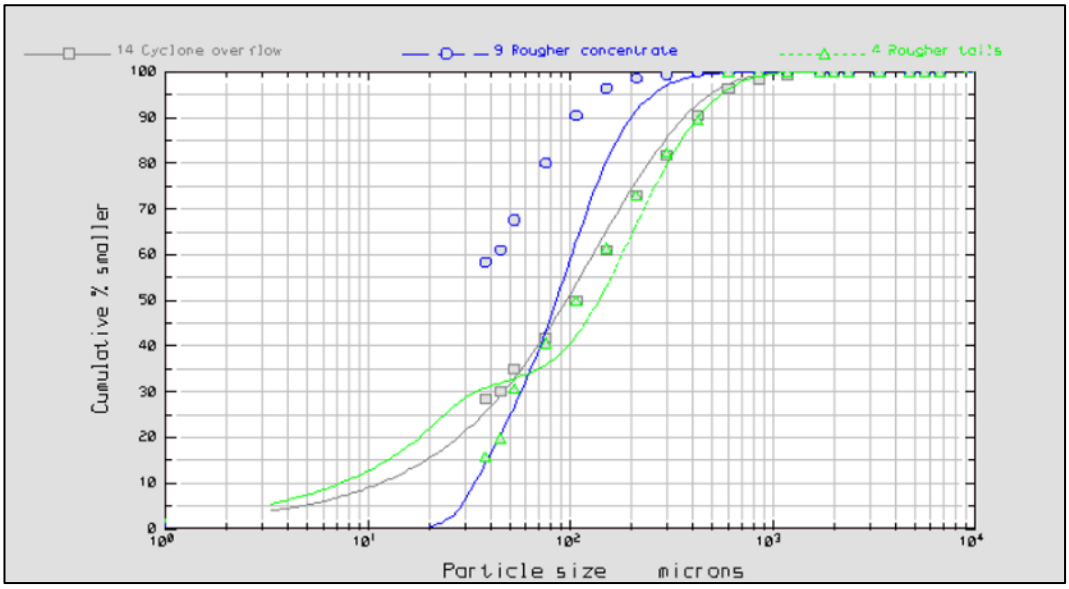

Figure 7.6: Linear-log X-axis of particle size distribution (PSD) (cleaners / re-cleaners)

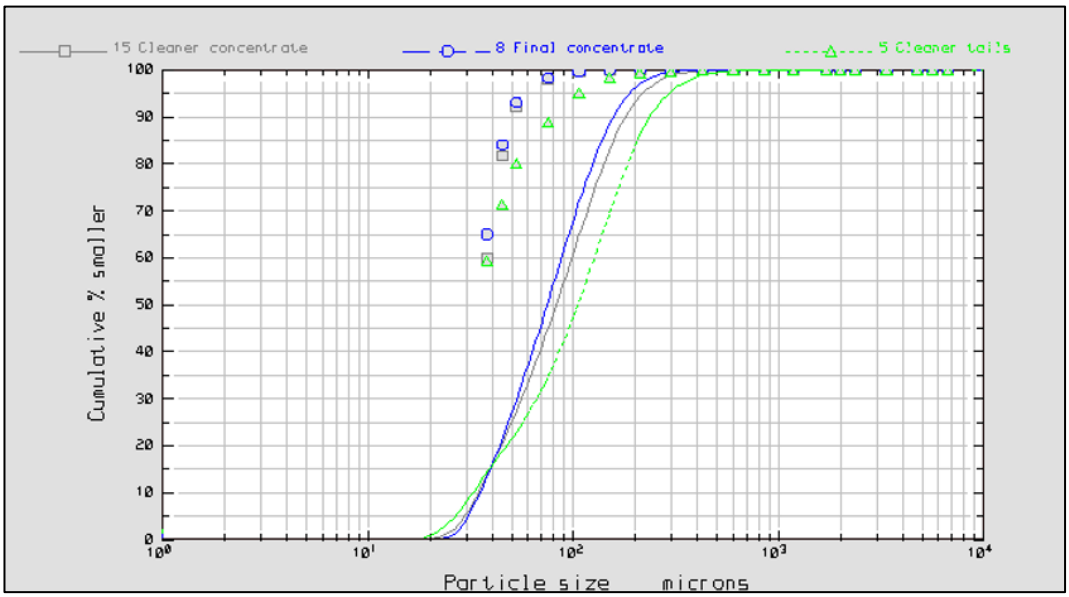

Figure 7.7: Linear-log X-axis of particle size distribution (PSD) (cleaners / re-cleaners)

7.5.3 Liberation analysis in ModSim

Composition used for the liberation analysis was the one based on mass. The masses were taken from the experimental PSD's conducted. Historical data was used for the specific gravities and ModSim populated the intervals as per composition classes. Calculated flotation rate constant was chosen for the distributed property in the setting up of S-classes. Figure 7.8 and 7.9 were the results generated from ModSim to reflect liberation of the material in the roughers and cleaners / re-cleaners.

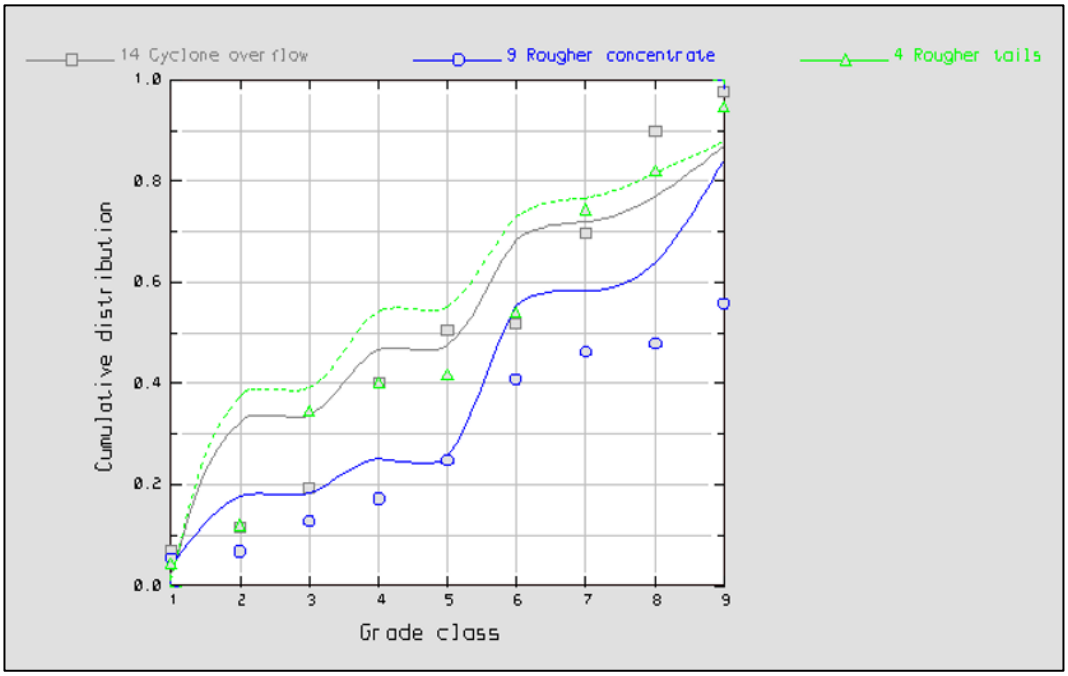

Figure 7.8: Liberation size class trends for feed, concentrate and tails (roughers)

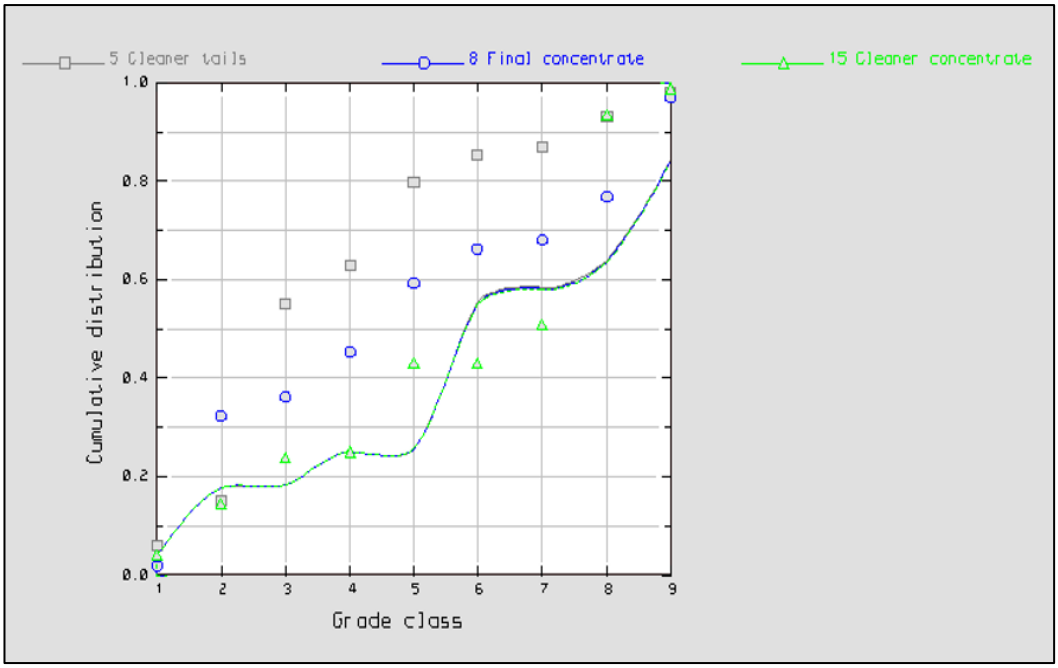

Figure 7.9: Liberation size class trends for feed, concentrate and tails (cleaners / re-cleaners)

7.6 Discussions from the use of ModSim

Based on the ratio of the final concentrate tonnage and flotation feed tonnage taken in Table 7.1, the mass pull for this circuit is at 17 %. Such mass pull is a bit too high as most flotation plants will run at around 10 % (Hay, 2010).This may be due to ModSim ignoring some other actual inefficiencies that do take place in a continuous flotation plant like spillages, reagents not dosed properly, unstable feed conditions, stop / start of equipment due to breakdowns, etc. Water distribution from feed to tails and to concentrate appeared to be acceptable. Additional water in the form of launder spray water or sumps water have not been included in the flowsheet presented, but this is not expected to change these results significantly. Overall, the mass balance from ModSim worked well as shown in Figure 7.5 and Table 7.2. Such mass balance was seen to conform with mass balance requirements (i.e. mass in = mass out) in every equipment of the continuous flotation plant. The developed mass balance can be confidently used

for simulation work in optimising the plant for whatever improvement or modification that may arise.

The experimental data for the particle size distribution (PSD) was not fitted very well in some other streams like rougher concentrate that deviated more on the fine sizes as in Figure 7.6. This may have been due to sampling or analysis errors which tend to accumulate and may result into larger deviations observed (Napier-Munn, 1995). Figure 7.7 combined cleaners and re-cleaners as one unit. Re-cleaner tails appeared to be difficult to sample as that is in the connection box of the re-cleaner last cell and cleaner first cell. It was then decided to combine these two banks and treated them as one bank for ease of doing particle size distribution. In terms of feed, concentrate and tails, cleaner concentrate was feed to re-cleaner while final concentrate was the concentrate of this bank leaving cleaner tails as tails of this combined bank. Model fit results moved away from experimental data over the full particle size ranges as shown in Figure 7.7. It was noticed that the Y-axis continued to the negatives making the model fit trends to extend vertically. There was not an option from ModSim to limit or restrict the axis to be within a certain preferred range. Poor fit may be overcome by re-sampling, re-analysing and applying different model parameters but, only if assuming the model is appropriate.

The roughers showed a consistent distribution of liberation in the grade classes as in Figure 7.8. The feed to the roughers, i.e., cyclone overflow liberation model did not fit the experimental data well especially at beginning and end of the size classes. Both the roughers concentrate and tails liberation model had predictions that were slightly higher than experimental results in all the size classes. It was noticed that the cleaner / re-cleaner liberation model results of all the three streams i.e. feed, concentrate and tails were predicted to be closely related to each other, as in Figure 7.9. Unfortunately, the liberation model for cleaner / re-cleaner only fitted the concentrate experimental data and deviated largely from the feed and tails data. Considering that particles reporting in the cleaners and re-cleaners should have been fully liberated then differences observed may have to

be further investigated. The built-in liberation model in ModSim, i.e., Ljubijana Model could not produce Andrews-Mika diagram as this needed more data which was not part of the scope of this work. Generation of Andrews-Mika diagrams can be looked at separately as part of follow-up research to the present study.

7.7 Conclusions

ModSim has shown that it has capabilities of modelling continuous flotation circuits. There is a need to interlink its use with laboratory data as some of parameters required in ModSim can be obtained in the laboratory environment e.g. particle size distribution (PSD's). The batch flotation testwork is the one to give parameters like flotation rate constant (k) and ultimate (maximum) recovery which also form part of the required inputs in the model. Flexibility of having three flotation models to use is helpful; as one has the opportunity to compare different results or sometimes the other model may not converge then, one can switch to the different type. With the use of King's flotation model, a simulator in the form of a complete ModSim mass balance flowsheet was developed for a continuous flotation plant. Key areas where such a simulator will find its use is in continuous improvement projects or plant modifications that may be implemented.

The results produced from ModSim were able to define the streams of feed, concentrate and tails. The poor fit or no fit to experimental data as observed can be improved by redefining the model parameters which will require new samples to be taken and other laboratory tests conducted. It must also be noted that ModSim can also be used by including milling circuit as well as dewatering or filtration circuits which are part and parcel of mineral processing circuits in production environment. Due to the scope of this research, focus had to be put only on the flotation circuit. The other shortcomings experienced in ModSim were seen as opening up other opportunities for further research especially in the flotation studies.

Chapter 8 Summary of the conclusions and recommendations

8.1 Recovery-by-size significance

The testwork done required proper and systematic approach since it involved batch flotation in the laboratory and continuous flotation operation. Most of the literature reviewed mainly focused on one part of this exercise and very few had conducted both simultaneously. Looking at the history and future of flotation, it showed that there is still a lot of research opportunities for both batch flotation and continuous flotation plant. The short-comings experienced during this testwork were noted and where possible solutions to mitigate those short-comings were applied. Equipping the continuous flotation plant with controls like SCADA proved very handy in collecting reliable operational data and making sure that stability was observed constantly during the sampling campaign. Tight measures applied during sample preparation and handling of laboratory results were key in making sure that reliable data was generated for analysis. Basic things like sample labelling, correct dates, adhering to SHEQ standards, etc. were part of the routines. Proper communication amongst personnel also played a major role as that ensured that all involved in laboratory or plant experimental work were having the same information of what needed to be done.

The batch flotation testwork has shown that size fraction does affect recovery of valuable material. The flotation time proved to increase the amount of recovery achieved at any size fraction. At fine sizes of around 19 µm the recoveries ranged from 83 % to 94 % for the batch flotation tests. The model results also fitted within the same ranges with the exception of 20 min flotation results that were slightly above 95 %. The peak where the recoveries were highest was seen to be around 50 µm and 250 µm for the batch flotation tests. This was in agreement with the work by other researchers like Gaudin *et al.* (1931); King (2012); Rule and Anyimadu (2007) and Wang (2016). The coarsest size fraction measured at 638 µm

average which for the batch flotation tests gave recoveries within the range of 78 % for the shorter flotation time to 90 % for the longer flotation time. These show that the coarse size fraction can also be recovered by mainly flotation process which agrees with Valery Jnr. and Jankovic (2002).

There was a gradual increase in recovery with respect to the time seen in the batch flotation test results of Recovery vs. Time curves. Modelling the batch flotation experimental results did work out as simulation followed the pattern of experimental results but predicted higher recoveries. The highest peak for the flotation rate constant (k) given by parameter $\Phi_j(d_{pi})$ was at a range of 0.6 – 1.0 min^{-1} and this was obtained at particle size fraction just below 50 µm. The Chi-square was chosen since the comparisons involved more than two sets of data. The combined experimental and model data did not show significant difference as its p-value was more than 0.05. The null hypothesis can be accepted in this situation.

The continuous flotation operation had three sets of data produced i.e. first set based on overall plant performance done by sampling feed, concentrate and tails. The second set was based on roughers row cell-by-cell while the third set of results came from cleaners / re-cleaners row cell-by-cell. The continuous plant flotation overall recovery figures at fine sizes were found to be at the range of 66 % to 77 % and they were highest with figures of 80 % to 90 % at 40 µm and at 100 µm recoveries were 72 % to 88 %. The highest peak of rougher recoveries was within particle size ranges of 45 µm to 100 µm and this was seen in all the banks found in the rows. Based on experimental results, highest recovery of roughers came to 66.3 % but this could go up to recovery of 88.6 % as predicted by the model in conditions of intermediate fractions. The re-cleaners (bank 1) showed lower recoveries in all its particle sizes as compared to the cleaners (bank 2 and 3). It must be noted that in this particular circuit bank 2 can also form part of recleaner or cleaner depending on the circumstances of recovery and grade requirements. In terms of best performance, re-cleaners had its highest recovery of 76.1 % while cleaners could go as high as 80.0 % on average. The last banks of both roughers

and cleaners appeared to be the ones with higher errors compared to the others as observed in error analysis trends. Practically in the continuous plant, the last banks tend to experience slow frothing shown by smaller bubbles (Lotter *et al.*, 2014). The last banks were also considered to be prone to sliming conditions and these noted problems of these banks were thought to have contributed to the higher errors seen in the data analysis. In terms of flotation rate constant for all three sets of continuous flotation results, it was noticed that the highest peak was at the 1.0 min^{-1} at particle size of below 50 µm. Statistics done for the continuous flotation plant, cell-by-cell of roughers and cleaners / re-cleaners followed the Chi-square method as seen in Tables 5.8 – 5.10. Different p-values were obtained i.e. continuous flotation plant p-value = 0.1207, cell-by-cell roughers p-value = 0.0003 and cell-by-cell cleaners / re-cleaners p-value = 0.1369. Based on the p-values obtained, it can be seen that the roughers were the ones that had significant difference since its p-value was lower than 0.05.

8.2 Scale-up application

In this work, four scale-up methods were looked at, i.e., gas dispersion, kinetics of flotation, dimensional similitude and carrying capacity. The gas dispersion scale-up method showed that specific froth residence time increased more than three times from batch flotation to continuous flotation but, the froth residence time under the same conditions was close to ten times increase from batch to continuous flotation. There was almost close to double of the constant from relation between τ_{fs} plus k when looking at batch flotation to continuous flotation. The use of flotation kinetics scale-up showed that the batch flotation recovery results differed by more than 25 % when compared to the plant recovery flotation results. The lower flotation rate constant (K_{max}) from the continuous flotation, i.e., 0.1 compared to 4.8 of batch flotation was seen as the contributing factor of the plant lower recoveries and this may be linked to the mineralogy of the ore. A scale-up factor of 1.25 was obtained from using dimensional similitude scale-up method done on Wemco cells. This factor of 1.25 is what the designer may then use in

sizing the flotation cells for the same ore type and cell type. The carrying capacity scale-up method brought notable differences in the final results of the carrying capacities when size (P_{80}) and froth recovery (R_f) were used. The comparison of published data with this research in the use of carrying capacity, the C_R values showed -ve 77.9 % difference while R_F differed by +ve 27.1 %. The different cell types, conditions of testing and ore types used may justify these differences observed.

In the kinetics scale-up validation using flotation rate constant (k) it was shown that the averages of the batch and continuous flotation data sets were very minimal as they were around 0.1 which translated to less than 20 % difference. When using concentrate grade for validation it was shown that batch flotation came to 9.14 %Cu while overall continuous flotation was at 38.02 % and cell-by-cell flotation was at 32.43 %Cu. On the other hand, the use of recovery for validation showed batch flotation to have recovery of 89.71 % and overall continuous flotation was at 68.70 % while with cell-by-cell flotation recovery came to 56.81 %. Another technique for validation applied in this work made use of upgrade ratios. It was found that by using only the first concentrate grade results from batch flotation, the average results came to 9.63 as explained in Section 6.6.5. The average upgrade ratio (c/f) for batch flotation averaged at 15.02 with overall continuous flotation giving 71.31 and cell by cell came to 18.35. The sizing technique of scale-up validation was further explored. Elemental (Cu) sizing distribution of batch flotation vs. continuous flotation gave a correlation of R^2 = 0.9921 which is considered a very strong correlation. The different scale-up validation techniques were seen to be key in identifying weaknesses and strengths of the whole scale-up work conducted. When comparing this work with what has been done by other researchers, there were similarities in results or trends that could be drawn but also differences existed in other areas.

The scale-up from batch flotation to continuous flotation was found to be possible with the approaches applied. The different methods used gave results that will require the design engineer to make that responsible choice based on the

information at his / her disposal. The beauty of applying different approaches was that one will not be confined to one solution even if, it does not look feasible for the application to be used in it. The use of published data is recommended in comparing results obtained. This must be done by taking into consideration the parameters like: cell types, ore types, experimental or plant conditions that such published data was generated or used in them.

8.3 Recovery-by-size and simulator development

The flotation process is still considered complex even though some models have been developed to try and explain it. Recovery and size can be investigated from either a phenomenological, deterministic or empirical point of view (Drzymala *et al*., 2020). In this work, the approach taken was to use batch flotation tests and full continuous flotation plant sampling campaign. Recovery-by-size data obtained from batch flotation tests and parameters for the continuous flotation sampling campaign have been applied to the ModSim software for the testing of recovery-by-size application in continuous flotation plant simulator development.

The results produced from ModSim were able to define the streams of feed, concentrate and tails. Based on the ratio of the final concentrate tonnage and flotation feed tonnage, the mass pull for this circuit was at 17 %. With the use of King's flotation model, a simulator in the form of a complete ModSim mass balance flowsheet was developed for a continuous flotation plant. Key areas where such a simulator will find its use is in continuous improvement projects or plant modifications that may be implemented. The roughers showed a consistent distribution of liberation in the grade classes while, it was noticed that the cleaner / re-cleaner had model fit results moving away from experimental data over the full particle size ranges in the linear-log X-axis plots. The poor fit or no fit to experimental data as observed could be improved by redefining the model parameters which will require new samples to be taken and other laboratory tests conducted. It must also be noted that ModSim can also be used by including milling circuit as well as dewatering or filtration circuit which are part and parcel

of mineral processing circuits in production environment. Due to the scope of this research, focus had to be put only in flotation circuit. The other shortcomings experienced in ModSim were seen as opening up other opportunities for further research especially in flotation studies. ModSim has shown that it has capabilities of modelling continuous flotation circuits. There is a need to interlink its use with laboratory data as some of parameters required in ModSim can be obtained in the laboratory environment, e.g. particle size distribution (PSD's). The batch flotation testwork is the one to give parameters like flotation rate constant (k) and ultimate (maximum) recovery which also form part of the required inputs in the model.

8.4 Overall conclusions

Flotation studies continue to be critical as part of the research to help the mining industry to improve their efficiencies. This has been shown by the amount of available literature that could be accessed from this research, but still a lot of it was not even reached. Recovery-by-size from batch flotation tests was shown to be affected by flotation residence time. An optimum particle size was found to be around 102 µm. Different scale-up methods (gas dispersion, kinetics, dimensional similitude and carrying capacity) were successfully used to scale from batch flotation to continuous operation. Scale-up validation techniques (kinetics, concentrate grade, recovery, statistics and overall) were used to confirm the reliability and trustworthiness of scale-up data used. The recovery-by-size theories were explained further by making use of ModSim which enabled mass balancing, particle size distribution and liberation analysis. The history, present and future of flotation in terms of batch and continuous were looked at intensely. The findings of this work suggest that more research on flotation still needs to be done in line with the demands of the 4IR future.

8.5 Recommendations for improvement opportunities

This research has managed to meet the requirements as per its scope of work even though there may have been some limitations on certain aspects. There are other ideas which came out that opened up opportunities for further research. Below are some of these improvement opportunities that may be pursued further to advance the scientific knowledge:

- Investigate the effect of ultra-fines as part of recovery-by-size data determined in batch testing. Make use of ultra-fines in estimating the performance of continuous flotation operations. This will be key in assisting mines that have their reserves depleted and are now turning into treating old tailings dumps that contains lots of ultra-fines.
- Conduct sampling survey and analyse recovery-by-size data to be used in ModSim built-in liberation model, i.e., Ljubijana Model for producing the Andrews-Mika diagram. This will assist with 3D-diagrams that will show how liberation is in the flotation feed, concentrate and tails.
- Study to be conducted to determine the readiness of the SA mining industry to embrace 4th Industrial Revolution (4IR). This will have to be benchmarked with the other mines outside South Africa. Failure for this industry to be ready for 4IR may affect its competitiveness on a global scale and even its ability to secure or create employment for this country.
- Investigate the use of cumulative concentrate grades method and applying lock-cycle flotation tests to validate concentrate grade factor. Such a factor makes use of the ratio between continuous flotation concentrate grade to batch flotation concentrate grade.
- Determine the effect of increasing the agitation rate for coarser particles which may increase off-the-bottom suspension and increased particle concentration suspended in the pulp. It is believed that this situation will create a more favourable condition for bubble-particle encounter and hence higher recoveries.

- Explore the use of regrinding circuit which caters for the coarse particles to see how that will affect the overall scale-up process. Similar scale-up validation techniques may be used to affirm results from data with regrinding circuit.

- Use similar approach done in this research but, investigate the use of hot floats (plant samples taken at flotation feed of either roughers or scavengers or cleaners or re-cleaners to conduct laboratory flotation test with them while they are hot or immediately after sampling them) versus batch flotation testing. Comparative analysis of the recovery-by-size of both hot floats and batch flotation tests can then be looked at with the inclusion of the necessary statistics. In the same testwork, apply scale-up approaches followed by their validation. The use of ModSim will be advantageous in this situation and will be strongly recommended.

- Conduct a separate study to look into the effect of conditioning time where, different durations of conditioning times will have to be compared with no conditioning. This will be key in the comparison of continuous flotation systems that runs at steady state with batch systems that can be set to run at certain conditioning time.

References

Agar, G.E., 2000. Calculation of locked cycle flotation test results. Minerals Engineering, vol. 13, no. 14 – 15, pp. 1533 – 1542

Alexander, D.J., Runge, K.C., Franzidis, J.P., Manlapig, E.V., 2000. The application of multicomponent floatability models to full scale flotation circuits. 7th Mill Operators Conference, Australian International Mining and Metallurgy (AIMM), Kalgoorlie, Australia (October), pp. 167 – 178

Allen, T. 1997. Particle size measurement. 5th Edition, vol. 1, Chapman and Hall, London

Amelunxen, R., Amelunxen, P., 2009. Methodology for executing, interpreting, and applying kinetic flotation tests in scale-up, Part 1. Gecamin Seminar, Santiago, Chile

Amelunxen, P., Sandoval, G., Barriga, D., Amelunxen, R., 2014. The implications of the froth recovery at the laboratory scale. Minerals Engineering, vol. 66 – 38, no. 22, pp. 54 – 61

Amelunxen, P., LaDouceur, R., Amelunxen, R., Young, C., 2018. A phenomenological model of entrainment and froth recovery for interpreting laboratory flotation kinetics tests. Minerals Engineering, vol. 125, no. 3, pp. 60 – 65

Banisi, S., Farzaneh, M., 2004. Effect of ball size change on the performance of grinding and flotation circuits. The European Journal of Mineral Processing and Environmental Protection, vol. 4, no. 3, pp. 194 – 202

Barbery, G., 1991. Mineral liberation: Measurement, simulation and practical use in mineral processing. LES Editions GB, Quebec, Canada

Behera, S.K., Mulaba-Bafubiandi, A.F., 2016. Microbes assisted mineral flotation a future prospective for mineral processing industries: A review. Mineral Processing and Extractive Metallurgy Review, vol. 38, no. 2, pp. 96 – 105

Bennie, D.I., 2013. An investigation of froth effects in scavenging flotation of platinum from UG-2 ore. MSc dissertation, University of KwaZulu-Natal, Durban

Bhondayi, C., 2014. A study of flotation froth phase behaviour. PhD Thesis, University of the Witwatersrand, Johannesburg

Boeree, C.R., 2014. Up-scaling of froth flotation equipment. MSc Thesis, Delft University of Technology, Netherlands

Bruijn, K., van't Riet, K., Smith, J.M., 1974. Power consumption with aerated Rushton turbine. Transactional Institute of Chemical Engineering, vol. 52, pp. 88 – 104

Bu, X., Xie, G., Peng, Y., Ge, L., Ni, C., 2017. Kinetics of flotation order of process, rate constant distribution and ultimate recovery. Physicochemical Problems of Mineral Processing, vol. 53, no. 1, pp. 342 – 365

Bunyak, D., 2000. To float or sink: A brief history of flotation milling. Mining History Journal, vol. 7, no. 23, pp. 35 – 44

Bushel, C., 2012. The PGM flotation predictor: Predicting PGM ore flotation performance using results from automated mineralogy systems. Minerals Engineering, vol. 36 – 38, no. 16, pp. 75 – 80

Carpenter, M., Bauer, T., Erdogan, B., 2012. Management Principles (v.1.0). Creative Commons, Chapter 1, pp. 10 – 45

Caspeo, 2020. USIM PAC: Process modeling and simulation software. https://www.caspeo.net/process-modeling-simulation-software-usim-pac/ [accessed on 04 November 2020]

Chimwani, N., 2014. An attainable region approach to optimizing product size distribution for flotation purposes. PhD Thesis, University of the Witwatersrand, Johannesburg

Conradie, A.v.E., Bascur, O., Aldrich, C., Nieuwoudt, I., 2003. Integrated comminution and flotation neurocontrol using evolutionary reinforcement

learning. Applications of Computers and Operations Research in the Minerals Industries (APCOM 31), Cape Town, South Africa, 14 – 16 May 2003, Southern African Institute of Mining and Metallurgy, pp. 209 – 216

De Araudjo, A.C., Peres, A.E.C., 1995. Froth Flotation: relevant facts and the Brazilian case. Serie Technologia Mineral, CETEM, vol. 70, Rio de Janeiro, Brazil

Ding, L., Gustafsson, T., 2000. Dynamic modelling of flotation circuits. IFAC Future Trends in Automation in Mineral and Metal Processing, Finland, pp. 197 – 202

Dobby, G., Savassi, O., 2005. An advanced modeling technique for scale-up of batch flotation results to plant metallurgical performance. Proceedings of the Centenary of Flotation Symposium, Brisbane, Australia (June), pp. 99 – 103

Dos Santos, N., Savassi, O., Peres, A., Martins, A., 2014. Modeling flotation with a flexible approach – Integrating different models to the compartment model. Minerals Engineering, vol. 66 – 68, no. 7, pp. 68 – 76

Dos Santos, N.A., 2018. Modelling flotation per size liberation class – Part 3 Modelling recoveries using particle surface area. Minerals Engineering, vol. 129, pp. 15 – 23

Dos Santos, N.A., Galery, R., 2018. Modelling flotation per size liberation class – Part 1: Minimizing the propagation of experimental errors in the estimate of flotation recovery. Minerals Engineering, vol. 128, pp. 254 – 265

Drzymala, J., Bednarek-Gąbka, P., Kowalczuk, P.B., 2020. Simplified empirical and phenomenological evaluation of relation between particle size and kinetics of flotation. Powder Technology, vol. 366, no. 41, pp. 112 – 118

Dworzanowski, M., 2014. Maximizing haematite recovery within a fine and wide particle-size distribution using wet high-intensity magnetic separation. Journal of the Southern African Institute of Mining and Metallurgy, vol. 114, no. 7, pp. 559 – 567

Egya-Mensah, D., 1998. Hydrodynamics and gas dispersion in industrial flotation cells. MSc Dissertation, University of Cape Town, Rondebosch

Espinoza-Gomez, R., Finch, J.A., Yianatos, J.B., Dobby, G.S., 1988. Flotation column carrying capacity: particle size and density effects. Minerals Engineering, vol. 1, no. 2, pp. 77 – 79

Evans, C.L., Wightman, E.M., Manlapig, E.V., Coulter, B.L., 2011. Application of process mineralogy as a tool in sustainable processing. Minerals Engineering, vol. 24, no. 12, pp. 1242 – 1248

Fallenius, K., 1979. A new set of equations for the scale-up of flotation cells. In Proceedings of the XIII International Mineral Processing Congress, pp. 232 – 258

Farrokhpay, S., 2011. The significance of froth stability in mineral flotation – A review. Advances in Colloid and Interface Science, vol. 166, no. 1 – 2, pp. 1 – 7

Ferreira, J.P., Loveday, B.K., 2000. An improved model for simulation of flotation circuits. Minerals Engineering, vol. 13, no. 14 – 15, pp. 1441 – 1453

Finch, J.A., Dobby, G.S., 1990. Column flotation. Pergamon Press, New York

Finch, J., Nesset, J., Acuna, C., 2008. Role of frother on bubble production and behaviour in flotation. Minerals Engineering, vol. 21, no. 12 – 14, pp. 949 – 957

Fogler, H.S., 1999. Elements of chemical reaction engineering, 3rd Edition. Prentice Hall, New York

Ford, M.A., 1979. Simulation of ore dressing plants. PhD Thesis, University of the Witwatersrand, Johannesburg

Fuerstenau, D.W., 1980. Fine particle flotation. In: Somasundaran, P. (Eds.), Fine Particles Processing, vol. 1, American Institute of Mining, Metallurgical, and Petroleum Engineers (AIME), pp. 669 – 706

Gao, Y., Ierapetritou, M.G., Muzzio, F.J., 2013. Determination of the confidence interval of the relative standard deviation using convolution. Journal of Pharmaceutical Innovation, vol. 8, pp. 72 – 82

Gaudin, A.M., Groh, J.O., Henderson, H.B., 1931. The effect of particle size on flotation. American Institute of Mining and Metallurgical Engineers (AIME), Technical Publication, no. 414, pp. 3 – 23

Gorain, B.K., Franzidis, J.P., Manlapig, E.V., 1995. Studies on impeller type, impeller speed and air flow rate in an industrial scale flotation cell. Part 2: Effect on gas holdup. Minerals Engineering, vol. 8, no. 12, pp. 1557 – 1570

Gorain, B.K., Franzidis, J.P., Manlapig, E.V., 1996. Studies on impeller type, impeller speed and air flow rate in an industrial scale flotation cell. Part 3: Effect on superficial gas velocity. Minerals Engineering, vol. 9, no. 6, pp. 639 – 654

Gorain, B.K., Franzidis, J.P., Manlapig, E.V., 1997. Studies on impeller type, impeller speed and air flow rate in an industrial scale flotation cell. Minerals Engineering, vol. 10, no. 4, pp. 367 – 379

Gorain, B.K., Harris, M.C., Franzidis, J.P., Manlapig, E.V., 1998. The effect of froth residence time on the kinetics of flotation cell – Part 4: Effect of bubble surface area flux on flotation kinetics. Minerals Engineering, vol. 11, no. 7, pp. 627 – 638

Gorain, B.K., Harris, M.C., Franzidis, J.P., Manlapig, E.V., 1999. The empirical prediction of bubble surface area flux in mechanical flotation cells from cell design and operating data. Minerals Engineering, vol. 12, no. 3, pp. 309 – 322

Gorain, B.K., Harris, M.C., Franzidis, J.P., Manlapig, E.V., 2000. Flotation cell design. https://www.911metallurgist.com/blog/wp-content/uploads/2015/06/Flotation-Cell-Design.pdf [accessed on 04 November 2020]

Hadler, K., Smith, C.D., Cillers, J.J., 2010. Recovery vs. mass pull: The link to air recovery. Minerals Engineering, vol. 23, no. 7, pp. 994 – 1602

Hahn, B., Valentine, B.T., 2007. Essential MATLAB for engineers and scientists, 3rd Edition. Butterworth – Heinemann, Oxford

Harris, C.C., Lepetic, V., 1966. Flotation cell design. Minerals Engineering, vol. 18, no. 1, pp. 67 – 72

Harris, C.C., Mensah-Biney, R.K., 1977. Aeration characteristics of laboratory flotation machine impellers. International Journal of Mineral Processing, vol. 4, no. 1, pp. 51 – 67

Harris, A., Venkatesan, L., Greyling, M., 2013. A practical approach to plant-scale flotation optimization. Journal of the Southern African Institute of Mining and Metallurgy, vol. 113, no. 3, pp. 263 – 272

Hay, M.P., 2005. Using the SUPASIM flotation model to diagnose and understand flotation behaviour from laboratory through to plant. Minerals Engineering, vol. 18, no. 8, pp. 762 – 771

Hay, M.P., 2010. A case study of optimising UG2 flotation performance. Part 2: Modelling improved PGM recovery and Cr2O3 rejection at Northam's UG2 concentrator. Minerals Engineering, vol. 23, no. 11 – 13, pp. 868 – 876

Hay, M.P., Rule, C.M., 2003. SUPASIM: A flotation plant design and analysis methodology. Minerals Engineering, vol. 16, no. 11, pp. 1103 – 1109

Heiskanen, K., 2013. Flotation research – does advancement require a paradigm shift?. Proceedings of the 6th International Flotation Conference, Cape Town, South Africa, pp. 1 – 18

Hernandez-Aguilar, J.R., Coleman, R.G, Gomez, C.O., Finch, J.A., 2004. A comparison between capillary and imaging techniques for sizing bubbles in flotation systems. Minerals Engineering, vol. 17, no. 1, pp. 53 – 61

Holmes, R., 2002. Sampling and measurement – The foundation of accurate metallurgical accounting. Process Value Tracking Symposium, Australian Institute of Mining and Metallurgy (AusIMM), Brisbane, Australia

Hu, W., 2014. Flotation circuit optimisation and design. PhD Thesis, Imperial College, London

Humphreys, D., 2019. Mining productivity and the fourth industrial revolution. Mineral Economics, vol. 10, no. 9, pp. 1 – 11

Hunt, B.R., Lipsman, R.L., Rosenberg, J.M., 2001. A guide to MATLAB for beginners and experienced users. Cambridge University Press, United Kingdom

Jameson, G.J., Allum, P., 1984. A survey of bubble sizes in industrial flotation cells. AMIRA International, Melbourne, pp. 18 – 25

Jordens, A., Marion, C., Grammatikoupoulos, T., Waters, K.E., 2016. Understanding the effect of mineralogy on muscovite flotation using QEMSCAN. International Journal of Mineral Processing, vol. 155, no. 3, pp. 6 – 12

Jowett, A., 1969. The development of studies in froth flotation kinetics. De Ingenieur (Niderl), vol. 81, no. 38, pp. 11 – 17

Khumalo, R.B., 2015. Optimisation of a combined milling and flotation circuit. MSc Dissertation, University of South Africa (UNISA), Johannesburg

King, R.P., 1972. Model for the design and control of flotation plants. Applications of Computers and Operations Research in the Minerals Industries (APCOM 10), Johannesburg, South Africa, 10 – 14 April 1972, South African Institute of Mining and Metallurgy, pp. 341 – 350

King, R.P., 1978. A pilot-plant investigation of a kinetic model for flotation. Journal of the Southern African Institute of Mining and Metallurgy, vol. 78, no. 12, pp. 325 – 338

King, R.P., Schneider, C.L., 1998. Mineral liberation and the batch comminution equation. Minerals Engineering, vol. 11, no. 12, pp. 1143 – 1160

King, R.P., 2012. Modelling and simulation of mineral processing systems, 2nd Edition. Schneider, C.L., King, E.A. (Eds.), Society for Mining, Metallurgy, and Exploration

Klimpel, R.R., 1980. Selection of chemical reagents for flotation. In: Mular, A., Bhappu, R. (Eds.), Mineral Processing Plant Design, 2nd Edition. American Institute of Metallurgical Engineers (AIME), New York, pp. 907 – 934

Kohmuench, J.N., Mankosa, M.J., Thanasekaran, H., Hobert, A., 2018. Improving coarse particle flotation using the HydroFloat™ (raising the trunk of the elephant curve). Minerals Engineering, vol. 121, pp. 137 – 145

Lelinski, D., Allen, J., Redden, L., Weber, A., 2002. Analysis of the residence time distribution in large flotation machines. Minerals Engineering, vol. 15, no. 7, pp. 499 – 505

Little, L., Becker, M., Wiese, J., Mainza, A.N., 2015. Auto-SEM particle shape characterisation: Investigating fine grinding of UG2 ore. Minerals Engineering, vol. 82, no. 21, pp. 92 – 100

Little, L., Mainza, A.N., Becker, M., Wiese, J.G., 2016. Using mineralogical and particle shape analysis to investigate enhanced mineral liberation through phase boundary fracture. Powder Technology, vol. 301, no. 52, pp. 794 – 804

Lotter, N.O., Whiteman, E., Bradshaw, D.J., 2014. Modern practice of laboratory flotation testing for flowsheet development – A review. Minerals Engineering vol. 66 – 68, no. 23, pp. 2 – 12

Lynch, A.J., Johnson, N.W., McKee, D.J., Thorne, G.C., 1973. The behaviour of minerals in sulphide flotation processes, with reference to simulation and control. Journal of the Southern African Institute of Mining and Metallurgy, vol. 74, no. 9, pp. 349 – 362

Ma, G., Xia, W., Xie, G., 2018. Effect of particle shape on the flotation kinetics of fine coking coal. Journal of Cleaner Production, vol. 195, no. 230, pp. 470 – 475

Macfarlane, A., 2001. The implementation of new technology in southern African mines: Pain or panacea. Journal of the Southern African Institute of Mining and Metallurgy, vol. 101, no. 3, pp. 115 – 126

Mackay, I., Videla, A.R., Brito-Parada, P.R., 2020. The link between particle size and froth stability – Implications for reprocessing of flotation tailings. Journal of Cleaner Production, vol. 242, no. 118436, pp. 1 – 8

Matis, K.A., Mavros, P., 1991. Foam/froth flotation. Part II. Removal of particulate matter. Separation and Purification Methods, vol. 20, no. 2, pp. 163 – 198

McIvor, R.E., Finch, J.A., 1990. A guide to interfacing of plant grinding and floatation operations. Minerals Engineering, vol. 4, no. 1, pp. 9 – 23

Mesa, D., Brito-Parada, P.R., 2019. Scale-up in froth flotation: A state-of-the-art review. Separation and Purification Technology, vol. 210, no. 76, pp. 950 – 962

Metsim, 2020. Metsim International. https://metsim.com/products/#modules [accessed on 04 November 2020]

Minerals Council SA, 2018. Minerals Council South Africa, downloads https://www.mineralscouncil.org.za/downloads/634-facts-and-figures-2017 [accessed on 10 July 2020]

Minnitt, R.C.A., 2014. Sampling in the South African minerals industry. Journal of the Southern African Institute of Mining and Metallurgy, vol. 114, no. 1, pp. 63 – 81

Mintek, 2020. Floatstar, http://www.mintek.co.za/wp-content/uploads/2011/09/FloatStar-Flotation-Stabilisation-and-Optimisation.pdf [accessed on 04 November 2020]

Moys, M.H., 1978. A study of a plug-flow model for flotation froth behaviour. International Journal of Mineral Processing, vol. 5, no. 1, pp. 21 – 38

Muller, D., de Villers, P.G.R., Humphries, G., 2010. A holistic approach to flotation mass pull and grade control. 13th Symposium on Automation in Mining, Mineral and Metal Processing (IFAC), 2 – 4 August, Cape Town, South Africa, pp. 133 – 136

Multani, R.S., Waters, K.E., 2019. Flotation recovery-by-size comparison of pyrrhotite superstructures with and without depressants. Minerals Engineering, vol. 130, pp. 92 – 100

Musingwini, C., 2016. Presidential Address: Optimization in underground mine planning– developments and opportunities. Journal of the Southern African Institute of Mining and Metallurgy, vol. 116, no. 9, pp. 809 – 820

Nagaraj, D.R., Farinato, R.S., 2016. Evolution of flotation chemistry and chemicals: A century of innovations and the lingering challenges. Minerals Engineering, vol. 96 – 97, no. 19, pp. 2 – 14

Napier-Munn, T.J., 1995. Detecting performance improvements in trials with time-varying mineral processes, Minerals Engineering, vol. 8, no. 8, pp. 843 – 858

Nazari, S., Shafaei, S.Z., Gharabaghi, M., Ahmadi, R., Shahbazi, B., 2018. Effect of frother type and operational parameters on nano bubble flotation of quartz coarse particles. Journal of Mining & Environment, vol. 9, no. 2, pp. 539 – 546

Nelson, M.G., Traczyk, F.P., Lelinski, D., 2002. Design of mechanical flotation machines (Chapter 8). In: Mular, A.L., Halbe, D.N., Barratt, D.J. (Eds.), Mineral Processing Plant Design, Practice and Control, SME, pp. 1179 – 1203

Newcombe, B., Bradshaw, D., Wightman, E., 2012. Development of a laboratory method to predict plant flash flotation performance. Minerals Engineering, vol. 39, no. 8, pp. 228 – 238

Newcombe, B., 2014. Predicting plant scale flash flotation performance – Validation of laboratory methodology and applications for use. Minerals Engineering, vol. 57, no.10, pp. 57 – 67

Newell, R., 2006. Hydrodynamics and scale-up in Rushton turbine flotation cells. PhD Thesis, Ian Walk Research Institute, University of South Australia

Nienow, A.W., Wisdom, D.J., 1974. Flow over disc turbine blades. Chemical Engineering Science, vol. 29, no. 9, pp. 1994 – 1997

Opperman, S.N., Nebbe, D., Power, D., March 2002. Flotation at Goedehoop Colliery. Journal of the Southern African Institute of Mining and Metallurgy, vol. 102, no. 7, pp. 405 – 410

Panopoulos, G., King, R.P., Juckes, A.H., 1986. The effect of particle-size distribution on the flotation of two South African coals. Journal of the Southern African Institute of Mining and Metallurgy, vol. 86, no. 5, pp. 141 – 152

Parry, J.M., 2006. Ultrafine grinding for improved mineral liberation in flotation concentrates. MSc Thesis, University of British Colombia, Canada

Patwardhan, A.W., Pandit, A.B., Joshi, J.B., 2003. The role of convection and turbulent dispersion in blending. Chemical Engineering Science, vol. 58, no. 13, pp. 2951 – 2962

Pease, J.D., Curry, D.C., Young, M.F., 2005. Designing flotation circuits for high fines recovery. Minerals Engineering, vol. 19, no. 10, pp. 831 – 840

Peleka, E.N., Matis, K.A., 2016. Hydrodynamic aspects of flotation separation. Open Chemistry, vol. 14, no. 10, pp. 132 – 139

Perez-Garibay, R., Estrada-Ruiz, R.H., Gallegos-Acevedo, P.M., 2010. Relationship between the bubble surface flux that overflows and the mass flowrate of solids in the concentrate of flotation processes. Minerals Engineering, vol. 23, no. 7, pp. 541 – 548

Perry, R.H., Green, D.W., Maloney, J.O., 1997. Perry's Chemical Engineers' Handbook, 7th Edition. The McGraw-Hill Companies, New York

Pirard, E., 1989. Applications of shape analysis in ore beneficiation. In: Process Mineralogy IX: Applications to Mineral Beneficiation, Metallurgy, Gold, Diamonds (TMS), pp. 205 – 218

Pogorely, A.D., 1962. Limits of the use of the kinetic equation proposed by K.F. Beloglazov. Izv. Vuz. Tsvetllaya Metallurgia, no. 1, pp. 33 – 40

Polat, J., Chander, S., 2000. First order flotation kinetics models and methods for estimation of the true distribution of flotation rate constants. International Journal of Minerals Processing vol. 58, no. 1 – 4, pp. 145 – 166

Radmehr, V., Shafaei, S.Z., Noaparast, M., Abdollahi, H., 2018. Optimizing flotation circuit recovery by effective stage arrangements: a case study. Minerals, vol. 8, #417, pp. 1 – 14

Rahman, R.M., Ata, S., Jameson, G.J., 2015. Study of froth behaviour in a controlled plant environment – Part 1: Effect of air flow rate and froth depth. Minerals Engineering, vol. 81, no. 3, pp. 152 – 160

Ramlall, N.V., Loveday, B.K., 2015. A comparison of models for the recovery of minerals in a UG2 platinum ore by batch flotation. Journal of the Southern Institute of Mining and Metallurgy, vol. 115, pp. 221 – 228

Reis, A.S., Reis Filho, A.M., Demuner, L.R., Barrozo, M.A.S., 2020. Effect of bubble size on the performance flotation of fine particles of a low-grade Brazilian apatite ore. Powder Technology, vol. 356, no. 29, pp. 884 – 891

Reuter, M.A., Van Deventer, J.S.J., 1990. The use of linear programming in the optimal design of flotation circuits incorporating regrind mills. International Journal of Mineral Processing, vol. 28, no. 1 – 2, pp. 15 – 43

Reyes Bahena, J.L., Lopez Valdiveso, A., Manlaping, E.V., Franzidis, J.P., 2006. Optimization of flotation circuits by modelling and simulations. Proceedings of China-Mexico Workshop on Minerals Particle Technology, San Luis Potosi, Mexico, pp. 155 – 165

Rodrigues, W.J., Leal Filho, L.S., Masani, E.A., 2001. Hydrodynamic dimensionless parameters and their influence on flotation performance of coarse particles. Minerals Engineering, vol. 14, no. 9, pp. 1047 – 1054

Rule, C.M., Anyimadu, A.K., 2007. Flotation cell technology and circuit design – An Anglo Platinum perspective. Journal of the Southern Institute of Mining and Metallurgy, vol. 107, no. 10, pp. 615 – 622

Runge, K., 2010. Laboratory flotation testing – An essential tool for ore characterisation. Flotation Plant Optimisation – Spectrum Series, vol. 16, pp. 155 – 173

Savassi, O.N., Alexandar, D.J., Franzidis, J.P., Manlapig, E.V., 1998. An empirical model for entrainment in industrial flotation plants. Minerals Engineering, vol. 11, no. 3, pp. 243 – 215

Savassi, O., 2006. Estimating the recovery of size-liberation classes in industrial flotation cells: a simple technique for minimizing the propagation of the experimental error. International Journal of Mineral Processing, vol. 78, no. 2, pp. 85 – 92

Schubert, H., Bischofberger, C., Koch, P., 1982. Influence of hydrodynamics in flotation processes. XIV lnternational Mining Process Congress, Toronto, Paper IV, vol. 15, no. 17, pp. 1 – 15

Schwarz, S., Alexander, D. 2006. JKSimFloat V6.1 Plus: Improving flotation circuit performance by simulation. In: Proceedings International Conference of Mineral Process Modelling, Simulation and Control Conference, 6 – 7 June, Ontario, Canada, pp. 1 – 13

Seaman, D.R., Franzidis, J.P., Manlapig, E.V., 2004. Bubble load measurement in the pulp zone of industrial flotation machines – A new device for determining the froth recovery of attached particles. International Journal of Mineral Processing, vol. 74, no. 1, pp. 1 – 13

Singh, A., Louw, J.J., Hulbert, D.G., 2003. Flotation stabilization and optimization. Journal of the South African Institute of Mining and Metallurgy, vol. 103, no. 9, pp. 581 – 588

Sishi, M.N., Telukarie, A., 2018. Implementation of Industry 4.0 technologies in the mining industry: A case study. 2017 IEEE International Conference on Industrial Engineering and Engineering Management (IEEM), 10 – 13 December 2017, Singapore, pp. 201 – 205

Smar, V.D., Klimpel, R.R., Aplan, F.F., 1994. Evaluation of chemical and operational variables for the flotation of a copper ore – Part I: Collector concentration, frother

concentration, and air flow rate. International Journal of Mineral Processing, vol. 42, Issues No. 3 – 4, pp. 225 – 240

Smith, P.G., Warren, L.J., 1989. Entrainment of particles into flotation froths. International Journal of Mineral Processing Extractive Metallurgy, vol. 5, no. 1 – 4, pp. 123 – 145

Sousa, R., Futuro, A., Pires, C.S., Leite, M.M., 2017. Froth flotation of Aljustrel sulphide complex ore. Physicochemical Problems of Mineral Processing, vol. 53, no. 2, pp. 758 – 769

Souza Pinto, T.C., Braga, A.S., Leal Filho, L.S., Deglon, D.A., 2018. Analysis of key mixing parameters in industrial Wemco mechanical flotation cells. Minerals Engineering, vol. 123, no. 46, pp. 167 – 172

Steyn, J.J., 2012. Developing a framework for the design of the milling and rougher circuits for a platinum-bearing UG2 ore. PhD Thesis, University of Cape Town, Rondebosch

Sutherland, D.N., 1977. An appreciation of galena concentration using a steady-state flotation model. International Journal of Mineral Processing, vol. 4, no. 2, pp. 149 – 162

Sutherland, D.N., 1981. A study of the optimization of the arrangement of flotation circuits. International Journal of Mineral Processing, vol. 7, no. 4, pp. 319 – 346

Sutherland, D.N., 1989. Batch flotation behaviour of composite particles. Minerals Engineering, vol. 2, no. 3, pp. 351 – 367

Taggart, A.F., 1921. A manual of flotation process. John Wiley & Sons Inc., London – Chapman & Hall Limited

Theflowsheetguru, 2020. http://theflowsheetguru.com.au/limn.html, [accessed on 25 March 2020]

Trahar, W.J., Warren, L.J., 1976. The flotability of very fine particles – a review. International Journal of Mineral Processing, vol. 3, no. 2, pp. 103 – 131

Trahar, W.J., 1981. A rational interpretation of the role of particle size in flotation. International Journal of Mineral Processing, vol. 8, no. 4, pp. 289 – 327

Truter, M., 2010. Scale-up of mechanically agitated flotation processes based on the principles of dimensional similitude. MSc Thesis, University of Stellenbosch, Matieland

Tsatouhas, G., Grano, S.R., Vera, M., 2005. Case studies on the performance and characterization of the froth phase in industrial flotation circuits. Minerals Engineering, vol. 19, no. 6 – 8, pp. 774 – 783

Turk, T., Gocer, S., Guner, M.K., Ersoy, B., Kalyoncu, E., Bulut, G., 2019. Developments in flotation technology. International Mineral Processing Conference (IMPC), 31 October – 2 November 2019, Antalya, Turkey, pp. 310 – 321

Valery Jnr., W., Jankovic, A., 2002. The future of comminution. Proceedings of 34th IOC on Mining and Metallurgy Conference, Bor Lake, Yugoslavia, 30 September – 3 October, pp. 287 – 298

Van't Riet, K., Smith, J.M., 1974. The behaviour of gas-liquid mixtures near Rushton turbine blades. Chemical Engineering Science, vol. 28, no. 4, pp. 1031 – 1037

Varadi, R., Runge, K., Franzidis, J.P., 2010. The rate variable batch test (rvbt) – A research method of characterising ore floatability. XXV International Mineral Processing Congress (IMPC) Proceedings, Brisbane, Queensland, Australia, 6 – 10 September, pp. 2471 – 2480

Vianna, S.M., 2004. The effect of particle size, collector coverage and liberation on the floatability of galena particles in an ore. PhD Thesis, University of Queensland, Australia

Wang, L., 2016. Entrainment of fine particles in froth flotation. PhD Thesis, University of Queensland, Australia

Wasmund, E.B., 2014. Flotation technology for coarse and fine particle recovery. I Congreso Internacional De Flotacion De Minerales Lima, Peru, August 2014, pp. 1 – 6

White, M.E., 1974. Drainage models for mineral components in flotation froths, BSc Thesis, University of Queensland, Australia

Wills, B.A., Napier-Munn, T.J., 2006. Mineral processing technology: An introduction to the practical aspects of ore treatment and mineral recovery. 7th Edition. Elsevier Science and Technology Books

Wiseman, D., 2020. Limn The Flowsheet Processor. www.davidwiseman.com.au, [accessed on 25 March 2020]

Woods, R., 1994. Chemisorption of thiols and its role in flotation. Proceedings of IV Meeting of the Southern Hemisphere on Mineral Technology and III Latin American Congress on Froth Flotation. Concepcion, Chile, pp. 1 – 14

Xia, J., Rinne, A., Gronstrand, S., 2009. Effect of turbulence models on prediction of fluid flow in an Outotec flotation cell. Minerals Engineering vol. 22, no. 11, pp. 880 – 885

Xian-ping, L., Xue-kun, T., Li-ping, H., Li-ying, L., 2011. Effects of size distribution on flotation kinetics of chalcopyrite. International Conference on Environment Science and Engineering, IPCBEE, Singapore, vol. 8, pp. 81 – 85

Yianatos, J.B., 2003. Design, modelling and control of flotation equipment. In XXII International Mineral Processing Congress, Lorenzen, L. (Eds.), Cape Town, South Africa, 29 September – 3 October, Southern African Institute of Mining and Metallurgy, Johannesburg, pp. 59 – 68

Yianatos, J., Larenas, J., Moys, M., Diaz, F., 2008. Short time mixing response in a big flotation cell. International Journal of Mineral Processing, vol. 89, no. 1 – 4, pp. 1 – 8

Yianatos, J.B., Finch, J.A., Laplante, A.R., 1986. Apparent hindered settling in a gas-liquid-solid countercurrent column. International Journal of Mineral Processing, vol. 18, no. 3 – 4, pp. 155 – 165

Yianatos, J.B., Bergh, L.G., Aguilera, J., 2003. Flotation scale-up: use of separability curves. Minerals Engineering, vol. 16, no. 4, pp. 347 – 352

Yianatos, J.B., Contreras, F.A., 2010. On the carrying capacity limitation in large flotation cells. Canadian Metallurgical Quarterly, vol. 49, no. 4, pp. 345 – 352

Yianatos, J.B., Contreras, F.A., Morales, P., Coddou, F., Elgueta, H., Ortiz, J., 2010. A novel scale-up approach for mechanical flotation cells. Minerals Engineering, vol. 23, no. 11 – 13, pp. 877 – 884

Yianatos, J., Carrasco, C., Bergh, L., Vinnett, L., Torres, C., 2012. Modelling and simulation of rougher flotation circuits. International Journal of Mineral Processing, vol. 112 – 113, no. 5, pp. 63 – 70

Yianatos, J.B., Henriquez, F.D., Oroz, A.G., 2005. Characterization of large size flotation cells. Minerals Engineering, vol. 19, no. 6 – 8, pp. 531 – 538

Yianatos, J.B., Henriquez, F.D., 2006. Short-cut method for flotation rates modelling of industrial flotation banks. Minerals Engineering, vol. 19, no. 13, pp. 1336 – 1340

Zaidenberg, I.S., Lisovikilt, D.I., Burovo, I.A., 1964. One approach to the construction of a mathematical model for the flotation process. Soviet Journal of Non-ferrous Metals, vol. 5, no. 7, pp. 26 – 32

Zheng, X., Franzidis, J.P., Johnson, N.W., Manlapig, E.V., 2005. Modelling of entrainment in industrial flotation cells: the effect of solids suspension. Minerals Engineering, vol. 18, no. 2, pp. 51 – 58

Zheng, X., Johnson, N.W., Franzidis, J.P., 2006. Modelling of entrainment in industrial flotation cells: water recovery and degree of entrainment. Minerals Engineering, vol. 19, no. 11, pp. 1191 – 1203

Zuniga, H.G., 1935. Flotation recovery is an exponential function of its rate. Boletin de la Sociedad Nacional de Minero, Santiago, Chile, vol. 47, pp. 83 – 86

Appendices

Appendix A: Flotation results from alternative recovery method (Equation 3.1)

In this Appendix the results from Equation 3.1 were being analysed as some comparison to Equation 3.2 to see any major differences in these recovery methods. The same procedure followed with Equation 3.2 explained in Chapter 3 was also followed for this other recovery method. It must be noted that Equation 3.1 does not include concentrate grade in its calculation. Results from Table A1 – A4 and Figures A1 – A8 appeared to be in agreement with recovery method using Equation 3.2. It must be noted that these two recovery methods can be used independently to one another but, Equation 3.1 is only a crude approximation and its results may not necessarily come out the same as that of Equation 3.2.

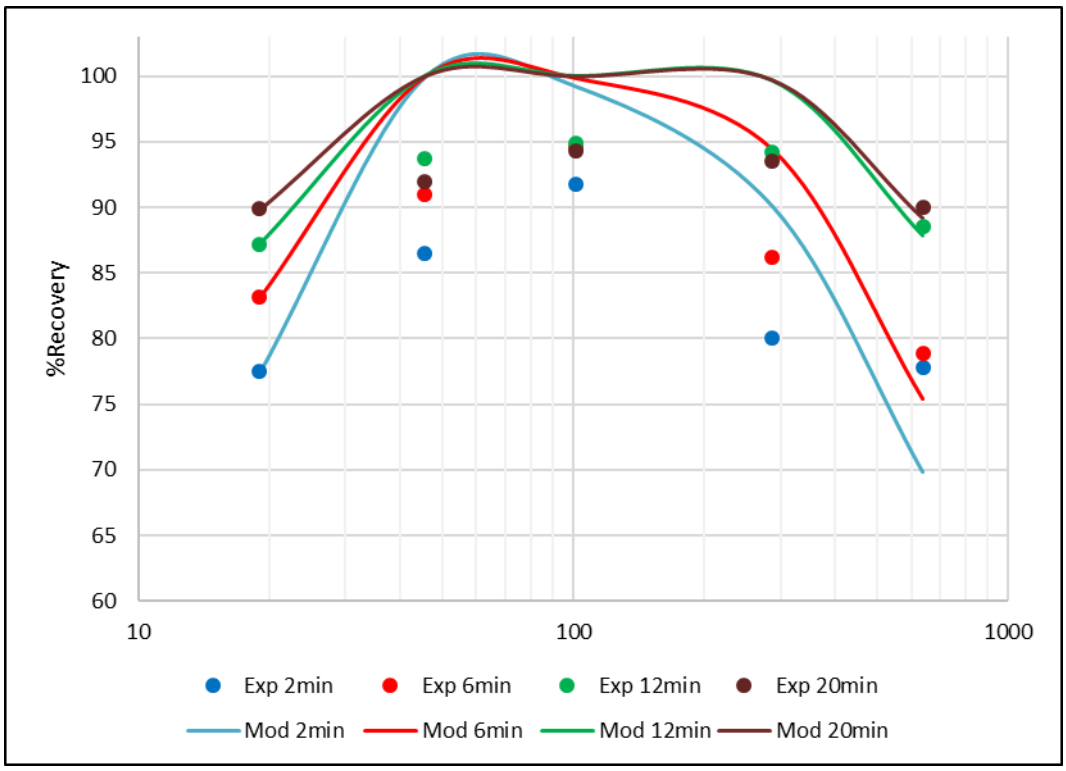

Figure A1: Recovery-by-size from batch flotation tests data

Table A1: Summary of batch flotation results using alternative method

Size	Experimental recoveries				Model recoveries			
	Exp 2 min	Exp 6 min	Exp 12 min	Exp 20 min	Mod 2 min	Mod 6 min	Mod 12 min	Mod 20 min
638	77,76	78,90	88,52	89,98	69,83	75,41	87,86	89,16
288	80,00	86,17	94,23	93,49	90,07	94,44	99,64	99,72
102	91,73	94,57	94,90	94,32	99,18	99,87	100,00	100,00
46	86,53	91,00	93,67	91,94	99,87	99,99	100,00	100,00
19	77,47	83,14	87,15	89,93	77,36	83,11	87,22	89,81
AVG	**82,70**	**86,75**	**91,69**	**91,93**	**87,26**	**90,56**	**94,94**	**95,74**

Table A2: Summary of continuous plant flotation results using alternative method

Size (µm)	Experimental recoveries				Model recoveries			
	1st trial	2nd trial	3rd trial	AVG - trial	Mod 1st trial	Mod 2nd trial	Mod 3rd trial	Mod-AVG
638	52.20	35.16	40.22	42.53	47.40	29.01	34.61	37.01
288	73.78	49.97	63.68	62.48	75.61	50.36	60.71	62.23
102	88.35	72.86	84.01	81.74	97.46	78.29	91.43	89.06
46	89.64	82.74	79.79	84.06	99.63	89.48	98.01	95.71
19	76.17	65.42	73.28	71.62	75.92	65.12	72.45	71.17
AVG	**76.03**	**61.23**	**68.19**	**68.48**	**79.20**	**62.45**	**71.44**	**71.03**

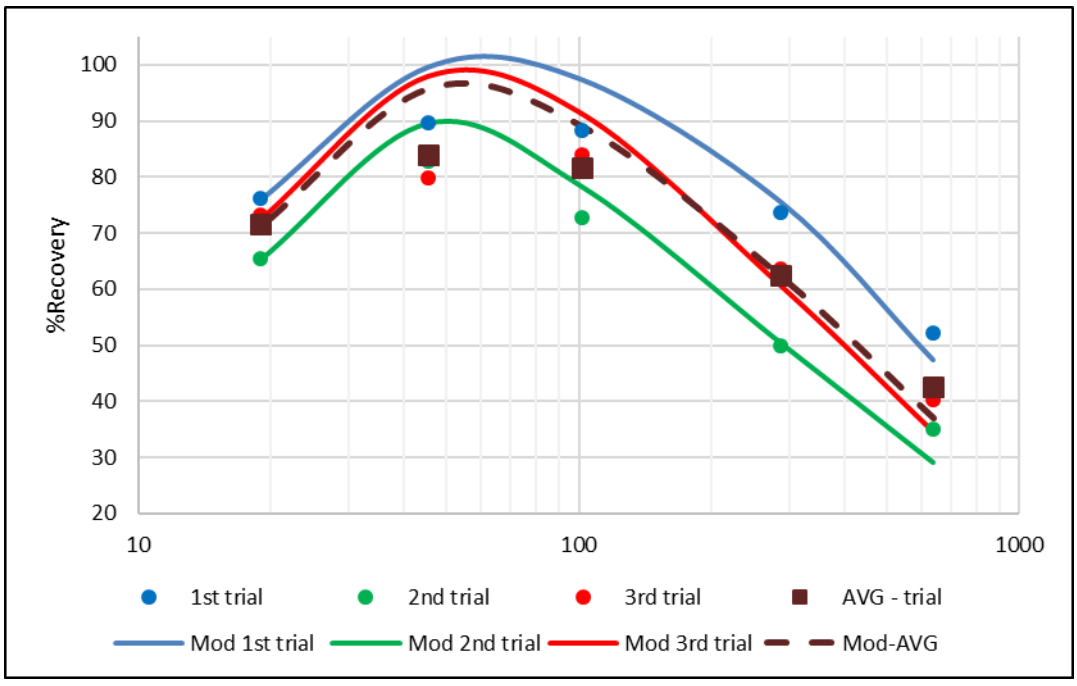

Figure A2: Recovery-by-size from continuous plant flotation tests data

Table A3: Summary of cell-by-cell flotation plant results using alternative method (roughers)

Size (µm)	Experimental recoveries				Model recoveries			
	Bank1	Bank2	Bank3	Bank4	Mod Bank1	Mod Bank2	Mod Bank3	Mod Bank4
638	35.20	35.50	32.81	39.52	13.17	15.48	16.88	20.80
288	46.31	49.93	45.88	51.79	26.70	30.90	33.30	39.90
102	54.60	58.73	62.48	65.89	55.76	61.99	64.92	73.14
46	49.44	54.04	58.22	62.01	72.28	77.82	79.70	87.54
19	37.47	40.19	39.84	54.33	32.17	35.20	35.91	51.16
AVG	**44.61**	**47.68**	**47.85**	**54.71**	**40.02**	**44.28**	**46.14**	**54.51**

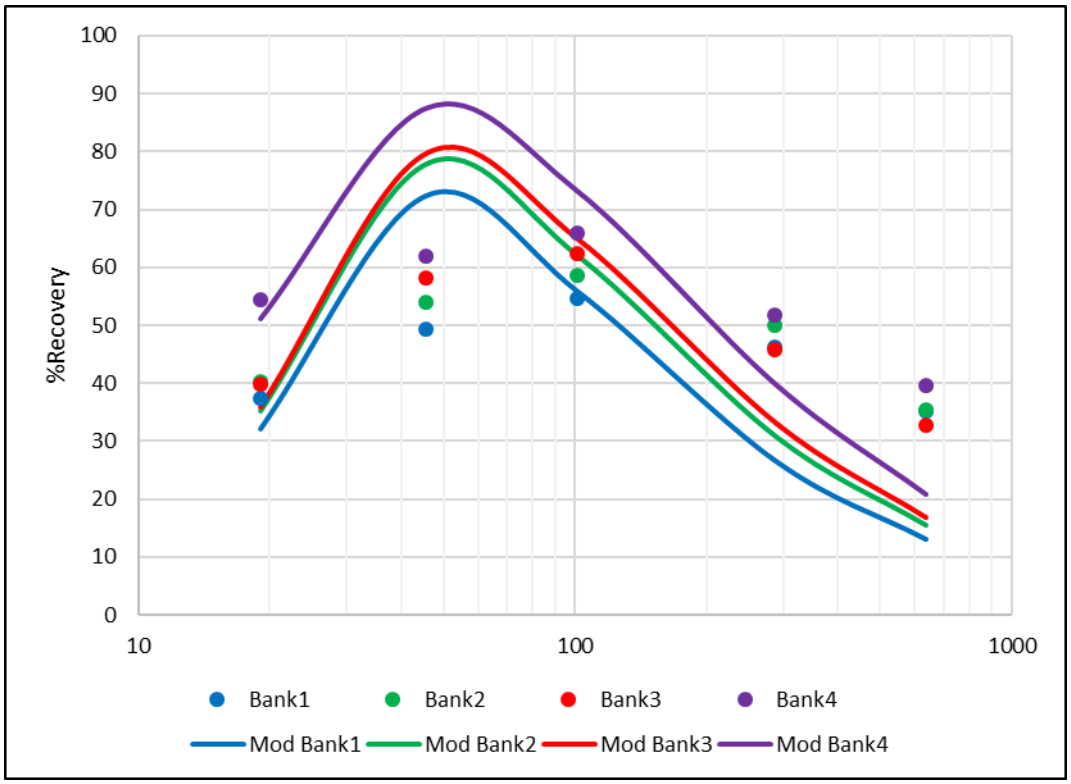

Figure A3: Recovery-by-size from cell-by-cell flotation plant tests data (roughers)

Table A4: Summary of cell-by-cell flotation plant results using alternative method (cleaners / re-cleaners)

Size (µm)	Experimental recoveries			Model recoveries		
	Bank1	Bank2	Bank3	Mod Bank1	Mod Bank2	Mod Bank3
638	44.68	49.48	56.30	28.07	36.76	47.88
288	64.18	69.87	74.90	51.45	63.40	75.99
102	72.91	72.74	80.18	84.34	92.47	97.30
46	59.59	65.93	71.61	92.87	97.59	99.21
19	39.93	50.58	43.91	35.78	48.82	43.16
AVG	**56.26**	**61.72**	**65.38**	**58.50**	**67.81**	**72.71**

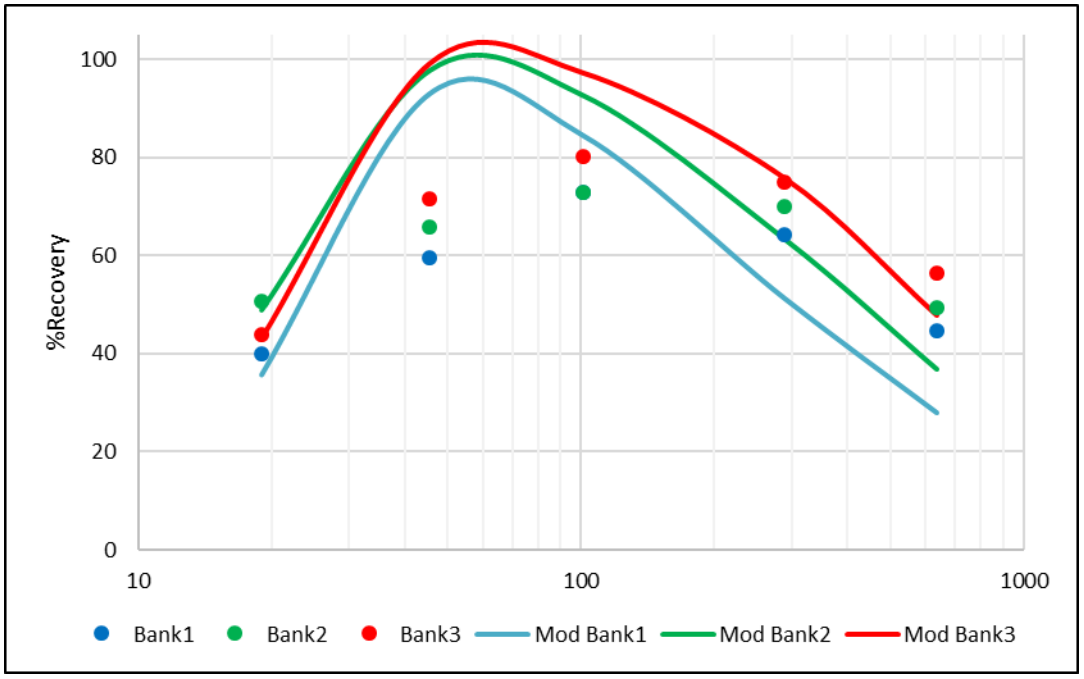

Figure A4: Recovery-by-size from cell-by-cell flotation plant tests data (cleaners / re-cleaners)

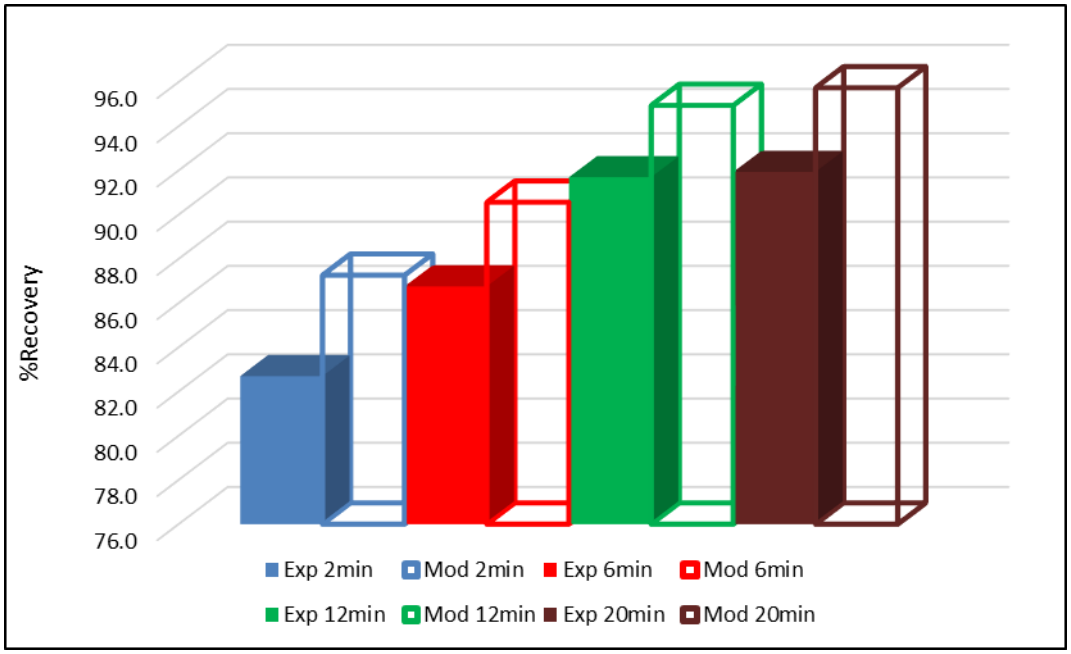

Figure A5: Recovery vs. Time - minutes 3-D trends from batch flotation tests data

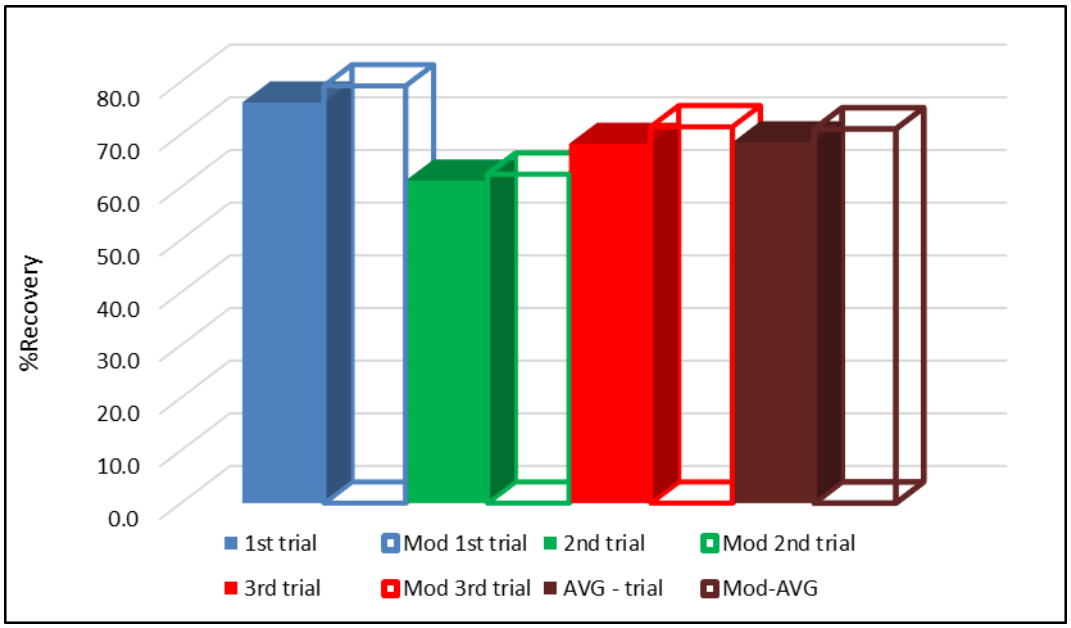

Figure A6: Recovery vs. Time – minutes 3-D trends from continuous plant flotation tests data

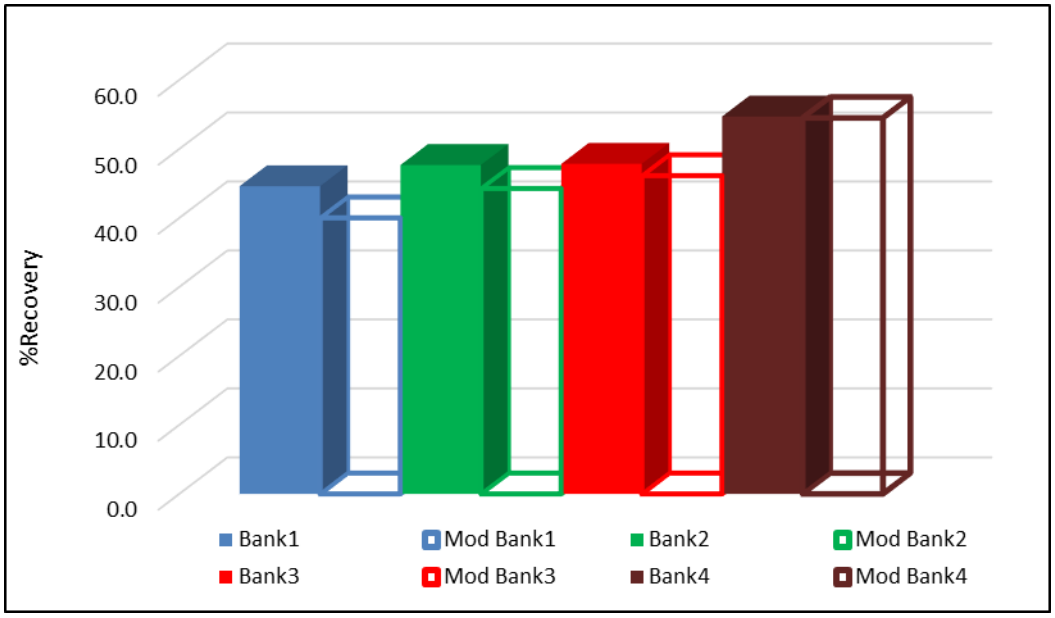

Figure A7: Recovery vs. Time – minutes 3-D trends from cell-by-cell flotation plant tests data (roughers)

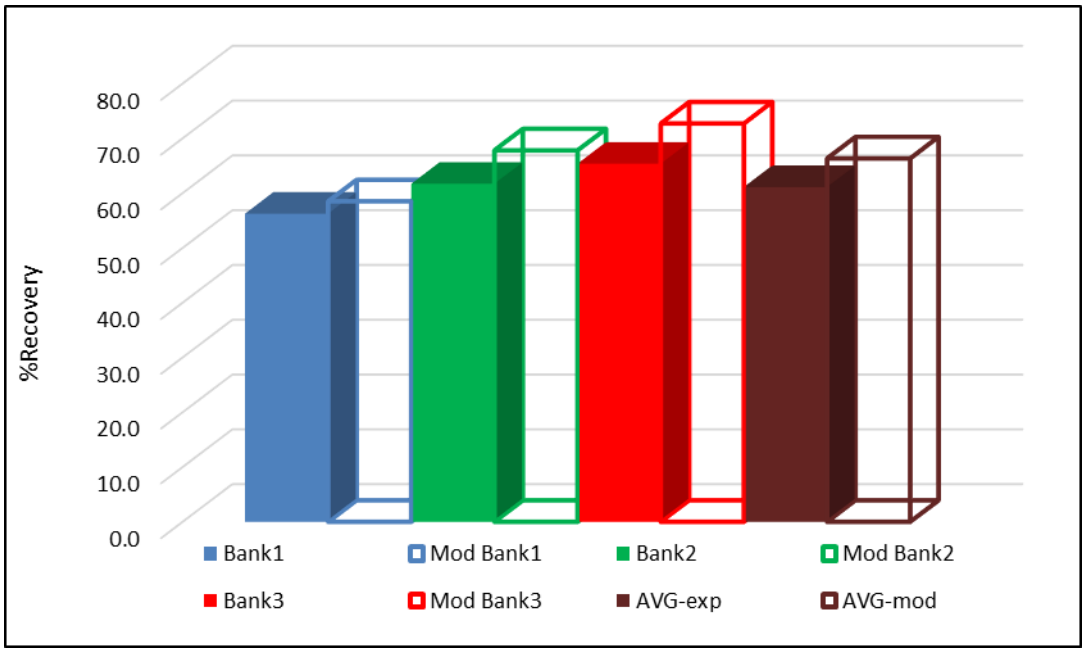

Figure A8: Recovery vs. Time – minutes 3-D trends from cell-by-cell flotation plant tests data (cleaners / re-cleaners)

Appendix B: Conducting batch flotation tests

In this Appendix B, the experimental work of conducting batch flotation tests is shown in pictorial format. The type of flotation machine and rod mill used and method of preparing samples to be ready to send for grade analysis at Chemical Laboratory have been shown.

Figure B1: Batch flotation testing in the laboratory

Figure B2: Conc and tails samples before screening into different size fractions

Figure B3: Different screened size fractions ready for laboratory analysis

Figure B4: Coarse size fractions (+850 µm-425 µm) averaging 638 µm

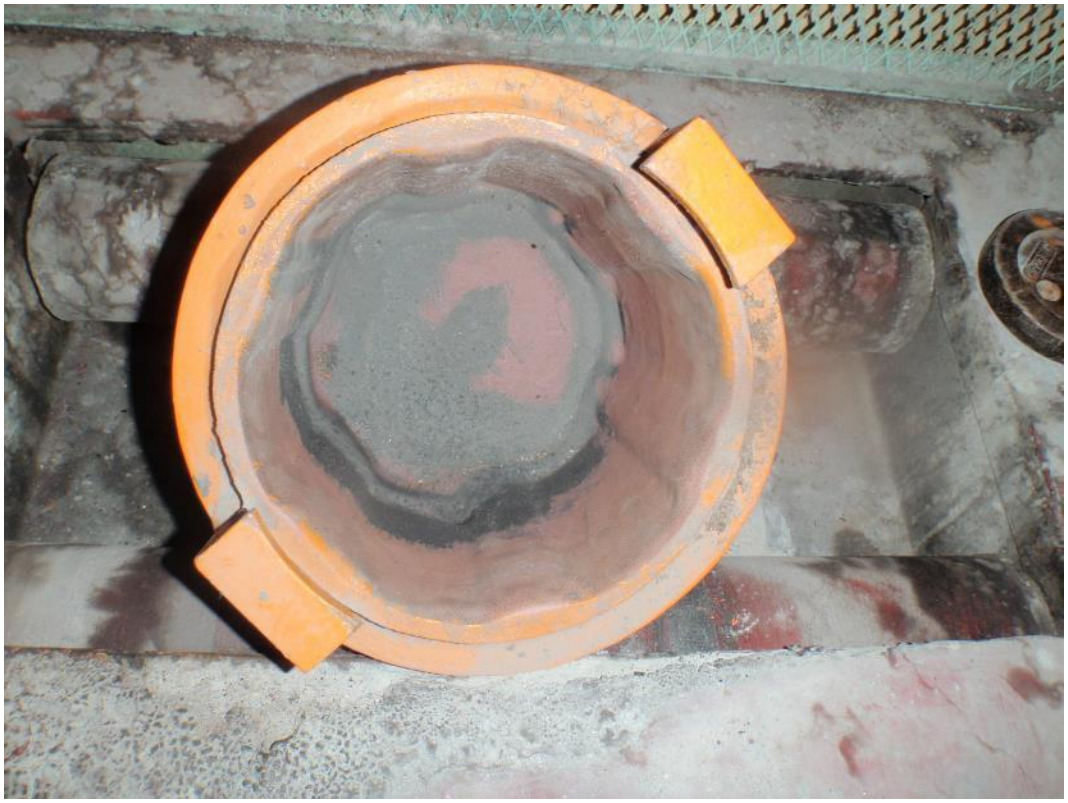

Figure B5: Type of laboratory rod mill used

Figure B6: Laboratory rod mill with rods used during milling

Appendix C: Conducting continuous flotation tests

The Appendix below show the way continuous flotation test was done mainly the sampling campaign. Photos show different points of feed, concentrate and tails including sampling equipment used.

Figure C1: Sampling of feed samples

Figure C2: Sampling of concentrate samples

Figure C3: Sampler for tails samples

Figure C4: Plant samples collected

Appendix D: Dimensional similitude scale-up method detail analysis

The table shown below gives some more details of how the dimensional analysis calculations were carried up. This looks at both batch and continuous flotation calculations with some comments where necessary.

Table D1: Additional results of dimensional similitude scale-up method

Symbol	Description	Batch	Calculated	Continuous	Comments
k_{app}	Apparent flotation rate constant		0.0023		$k_{app} = k_{ac}*\alpha*\beta*\gamma$
k_b	Batch flotation rate constant	0.37			
k_{ac}	Continuous flotation rate constant			0.46	
ξ	Rate of K_{ac} to K_b		1.25		$\xi = k_{ac}/k_b$
α_{fe}	Froth effect	0.53		0.66	
β	Cell mixing effect		0.015		$\beta = \left(\frac{\varphi(N=1)}{\varphi(N \neq 1)} I_\eta\right)$
γ	Particle segregation effect	0.63		0.50	$\gamma = \tau_S/\tau_L$
K_c	Collection zone rate constant	0.62		0.77	
φ	Ratio of mixing condition		2.88		$\varphi = \tau_{plant}/t_{batch} * (k_{max})_{plant}/(k_{max})_{batch}$
N	Number of cells in series			15	Used 13, 11, 9, 7, 5, 3 &1 as domain range
η	Dimensionless recovery(ratio of rec to max. rec)	0.961	0.962	0.963	$\eta = R/R_\infty$
τ_S	Effective solids residence time	5		10	
τ_L	Effective liquid residence time	8		20	
k_{app}/k_b	Ratio between apparent flotation rate constant and batch flotation rate constant as a function of dimensionless parameters		0.006		$k_{app}/k_b = \xi*\alpha*\beta*\gamma$
A	Cell cross sectional area (m^2)		8.20		For the calculation of bubble surface area flux: $S_b = 6*J_g/d_b$
Q	Air flowrate (m^3/s)		3.15		
J_g	Superficial gas velocity (m/s)		0.38		
d_b	Mean bubble diameter (m)		0.06		
S_b	Bubble surface area flux (1/s)		38.42		

Appendix E: ModSim stream results

In this Appendix, results generated from ModSim are being shown. These results show unit equipment data sheet mainly for rougher bank / cells, cleaner bank / cells and recleaner bank / cellsas shown in Figures E1 – E7.

Table E1: ModSim rougher bank / cells results - a

```
UNIT EQUIPMENT DATA SHEET - BANK OF FLOTATION CELLS
**************************************************

    Unit number   4           MODSIM model name FLTK
      Job name: Mill-float 1

There are 15 cells in this bank and  3 banks in parallel
Volume of cells in this bank     8.500 m**3
Aeration rate   1.0000 m**3/min per m**3 of cell volume.
Air-free pulp volume     7.083 m**3
Froth transmission coefficient   1.000
Bubble size   2.000 mms
Bubble residence time     10.00 secs
Percent solids in feed   69.2
Percent solids in concentrate   40.0
Maximum flotation recovery at    50.0 microns
Largest floatable particle      1000. microns
Flotation rate constants are distributed over   1 values:
 4.86

          Unit number   4  Cell number   1
 Bubble loading= 100.00%
Pulp residence time=   114.56 secs
 Difference between pulp vol and res time * flowrate =  11.4
 Iterations needed=   10
          Unit number   4  Cell number   2
 Bubble loading=  21.79%
Pulp residence time=     0.11 secs
 Difference between pulp vol and res time * flowrate =  7.10
 Iterations needed=   10
          Unit number   4  Cell number   3
 Bubble loading=   0.02%
```

Table E2: ModSim rougher bank / cells results - b

```
          Unit number   4  Cell number   3
 Bubble loading=   0.02%
Pulp residence time=     0.00 secs
 Difference between pulp vol and res time * flowrate =  7.08
 Iterations needed=   10
          Unit number   4  Cell number   4
 Bubble loading=   0.00%
Pulp residence time=     0.00 secs
 Difference between pulp vol and res time * flowrate =  7.08
 Iterations needed=   10
          Unit number   4  Cell number   5
 Bubble loading=   0.00%
Pulp residence time=     0.00 secs
 Difference between pulp vol and res time * flowrate =  7.08
 Iterations needed=   10
          Unit number   4  Cell number   6
 Bubble loading=   0.00%
Pulp residence time=     0.00 secs
 Difference between pulp vol and res time * flowrate =  7.08
 Iterations needed=   10
          Unit number   4  Cell number   7
 Bubble loading=   0.00%
Pulp residence time=     0.00 secs
 Difference between pulp vol and res time * flowrate =  7.08
 Iterations needed=   10
          Unit number   4  Cell number   8
 Bubble loading=   0.00%
Pulp residence time=     0.00 secs
 Difference between pulp vol and res time * flowrate =  7.08
 Iterations needed=   10
```

Table E3: ModSim rougher bank / cells results - c

```
          Unit number   4  Cell number   9
 Bubble loading=   0.00%
Pulp residence time=     0.00 secs
 Difference between pulp vol and res time * flowrate =  7.08
 Iterations needed=   10
          Unit number   4  Cell number  10
 Bubble loading=   0.00%
Pulp residence time=     0.00 secs
 Difference between pulp vol and res time * flowrate =  7.08
 Iterations needed=   10
          Unit number   4  Cell number  11
 Bubble loading=   0.00%
Pulp residence time=     0.00 secs
 Difference between pulp vol and res time * flowrate =  7.08
 Iterations needed=   10
          Unit number   4  Cell number  12
 Bubble loading=   0.00%
Pulp residence time=     0.00 secs
 Difference between pulp vol and res time * flowrate =  7.08
 Iterations needed=   10
          Unit number   4  Cell number  13
 Bubble loading=   0.00%
Pulp residence time=     0.00 secs
 Difference between pulp vol and res time * flowrate =  7.08
 Iterations needed=   10
          Unit number   4  Cell number  14
 Bubble loading=   0.00%
Pulp residence time=     0.00 secs
 Difference between pulp vol and res time * flowrate =  7.08
 Iterations needed=   10
          Unit number   4  Cell number  15
 Bubble loading=   0.00%
```

Table E4: ModSim cleaner bank / cells results - a

```
 UNIT EQUIPMENT DATA SHEET - BANK OF FLOTATION CELLS
 ***************************************************

     Unit number   7           MODSIM model name FLTK
       Job name: Mill-float 1

 There are  8 cells in this bank and  1 banks in parallel
 Volume of cells in this bank     8.500 m**3
 Aeration rate   1.0000 m**3/min per m**3 of cell volume.
 Air-free pulp volume     7.083 m**3
 Froth transmission coefficient   1.000
 Bubble size   2.000 mms
 Bubble residence time     10.00 secs
 Percent solids in feed   46.6
 Percent solids in concentrate   30.0
 Maximum flotation recovery at    50.0 microns
 Largest floatable particle      1000. microns
 Flotation rate constants are distributed over   1 values:
  4.86

          Unit number   7  Cell number   1
 Bubble loading= 100.00%
Pulp residence time=    52.89 secs
 Difference between pulp vol and res time * flowrate = -.261E-01
 Iterations needed=   10
          Unit number   7  Cell number   2
 Bubble loading=  99.42%
Pulp residence time=     0.05 secs
 Difference between pulp vol and res time * flowrate =  7.08
 Iterations needed=   10
```

Table E5: ModSim cleaner bank / cells results - b

```
          Unit number   7  Cell number   3
 Bubble loading=   6.79%
Pulp residence time=     0.00 secs
 Difference between pulp vol and res time * flowrate =  7.08
 Iterations needed=   10
          Unit number   7  Cell number   4
 Bubble loading=   0.03%
Pulp residence time=     0.00 secs
 Difference between pulp vol and res time * flowrate =  7.08
 Iterations needed=   10
          Unit number   7  Cell number   5
 Bubble loading=   0.00%
Pulp residence time=     0.00 secs
 Difference between pulp vol and res time * flowrate =  7.08
 Iterations needed=   10
          Unit number   7  Cell number   6
 Bubble loading=   0.00%
Pulp residence time=     0.00 secs
 Difference between pulp vol and res time * flowrate =  7.08
 Iterations needed=   10
          Unit number   7  Cell number   7
 Bubble loading=   0.00%
Pulp residence time=     0.00 secs
 Difference between pulp vol and res time * flowrate =  7.08
 Iterations needed=   10
          Unit number   7  Cell number   8
 Bubble loading=   0.28%
Pulp residence time=     0.00 secs
 Difference between pulp vol and res time * flowrate =  7.08
 Iterations needed=   10
```

Table E6: ModSim recleaner bank / cells results - a

```
UNIT EQUIPMENT DATA SHEET - BANK OF FLOTATION CELLS
**************************************************

    Unit number   6           MODSIM model name FLTK
      Job name: Mill-float 1

There are  4 cells in this bank and  1 banks in parallel
Volume of cells in this bank     8.500 m**3
Aeration rate   1.0000 m**3/min per m**3 of cell volume.
Air-free pulp volume     7.083 m**3
Froth transmission coefficient   1.000
Bubble size   2.000 mms
Bubble residence time     10.00 secs
Percent solids in feed   30.0
Percent solids in concentrate   25.0
Maximum flotation recovery at    50.0 microns
Largest floatable particle      1000. microns
Flotation rate constants are distributed over   1 values:
 4.86

          Unit number   6  Cell number   1
 Bubble loading= 100.00%
Pulp residence time=    50.97 secs
 Difference between pulp vol and res time * flowrate = -.350E-01
 Iterations needed=   10
```

Table E7: ModSim recleaner bank / cells results - b

```
          Unit number   6  Cell number   2
 Bubble loading=  94.38%
Pulp residence time=     0.05 secs
 Difference between pulp vol and res time * flowrate =  7.09
 Iterations needed=   10
          Unit number   6  Cell number   3
 Bubble loading=   0.73%
Pulp residence time=     0.00 secs
 Difference between pulp vol and res time * flowrate =  7.08
 Iterations needed=   10
          Unit number   6  Cell number   4
 Bubble loading=   0.00%
Pulp residence time=     0.00 secs
 Difference between pulp vol and res time * flowrate =  7.08
 Iterations needed=   10
```

Appendix F: ModSim liberation results

As ModSim was used to do analysis on liberation then Tables F1 – F7 shown below reflects on the results that came out from this exercise. Liberation analysis was also conducted in all the streams involved in the circuit but the focus of the report has been on roughers, cleaners and re-cleaners.

Table F1: ModSim liberation results summary - a

LIBERATION SPECTRA
****

Stream number 1

G-class	Fractional distribution	Cumulative recovery of mineral 1	Cumulative grade of mineral 1	Cumulative recovery of mineral 2	Cumulative grade of mineral 2
1	0.0200	4.34	100.00	0.00	0.00
2	0.3050	66.35	94.09	4.65	5.91
3	0.0120	68.46	93.63	5.19	6.37
4	0.1300	87.84	86.69	15.04	13.31
5	0.0090	88.94	86.12	15.99	13.88
6	0.2070	108.56	73.26	44.19	26.74
7	0.0360	111.01	71.16	50.17	28.84
8	0.0500	113.05	67.76	59.99	32.24
9	0.1000	114.39	60.67	82.69	39.33
10	0.1310	114.39	52.73	114.38	47.27

Table F2: ModSim liberation results summary - b

Stream number 2

G-class	Fractional distribution	Cumulative recovery of mineral 1	Cumulative grade of mineral 1	Cumulative recovery of mineral 2	Cumulative grade of mineral 2
1	0.0200	3.79	100.00	0.00	0.00
2	0.3050	58.00	94.09	4.06	5.91
3	0.0120	59.85	93.63	4.54	6.37
4	0.1300	76.79	86.69	13.15	13.31
5	0.0090	77.75	86.12	13.98	13.88
6	0.2070	94.90	73.26	38.63	26.74
7	0.0360	97.04	71.16	43.86	28.84
8	0.0500	98.82	67.76	52.45	32.24
9	0.1000	100.00	60.67	72.29	39.33
10	0.1310	100.00	52.72	100.00	47.28

Stream number 3

G-class	Fractional distribution	Cumulative recovery of mineral 1	Cumulative grade of mineral 1	Cumulative recovery of mineral 2	Cumulative grade of mineral 2
1	0.0227	4.93	100.00	0.00	0.00
2	0.2834	62.65	94.17	4.33	5.83
3	0.0113	64.65	93.71	4.84	6.29
4	0.1217	82.82	86.78	14.07	13.22
5	0.0086	83.87	86.19	14.99	13.81
6	0.2214	104.91	72.13	45.21	27.87
7	0.0351	107.29	70.09	51.06	29.91
8	0.0508	109.37	66.64	61.05	33.36
9	0.1121	110.88	58.83	86.54	41.17
10	0.1331	110.88	51.00	118.80	49.00

Table F3: ModSim liberation results summary - c

Stream number 4

G-class	Fractional distribution	Cumulative recovery of mineral 1	Cumulative grade of mineral 1	Cumulative recovery of mineral 2	Cumulative grade of mineral 2
1	0.0128	1.81	100.00	0.00	0.00
2	0.3634	49.78	93.91	3.60	6.09
3	0.0139	51.36	93.47	4.00	6.53
4	0.1519	66.06	86.53	11.47	13.47
5	0.0100	66.86	85.98	12.16	14.02
6	0.1767	77.74	75.73	27.79	24.27
7	0.0380	79.41	73.52	31.90	26.48
8	0.0481	80.69	70.29	38.03	29.71
9	0.0640	81.25	65.62	47.47	34.38
10	0.1211	81.25	57.67	66.50	42.33

Stream number 5

G-class	Fractional distribution	Cumulative recovery of mineral 1	Cumulative grade of mineral 1	Cumulative recovery of mineral 2	Cumulative grade of mineral 2
1	0.0410	1.14	100.00	0.00	0.00
2	0.1351	4.65	95.17	0.26	4.83
3	0.0067	4.80	94.66	0.30	5.34
4	0.0645	6.03	87.89	0.93	12.11
5	0.0060	6.12	87.13	1.01	12.87
6	0.3199	10.00	62.90	6.58	37.10
7	0.0289	10.25	61.38	7.19	38.62
8	0.0562	10.55	57.75	8.61	42.25
9	0.1945	10.88	45.99	14.25	54.01
10	0.1471	10.88	39.22	18.80	60.78

Table F4: ModSim liberation results summary - d

Stream number 6

G-class	Fractional distribution	Cumulative recovery of mineral 1	Cumulative grade of mineral 1	Cumulative recovery of mineral 2	Cumulative grade of mineral 2
1	0.0406	0.41	100.00	0.00	0.00
2	0.1375	1.70	95.14	0.10	4.86
3	0.0065	1.76	94.65	0.11	5.35
4	0.0691	2.23	87.58	0.35	12.42
5	0.0062	2.27	86.83	0.38	13.17
6	0.2671	3.44	64.97	2.07	35.03
7	0.0316	3.54	63.06	2.31	36.94
8	0.0549	3.64	59.10	2.81	40.90
9	0.2137	3.78	45.44	5.06	54.56
10	0.1727	3.78	37.59	6.99	62.41

Stream number 7

G-class	Fractional distribution	Cumulative recovery of mineral 1	Cumulative grade of mineral 1	Cumulative recovery of mineral 2	Cumulative grade of mineral 2
1	0.0408	3.53	100.00	0.00	0.00
2	0.1361	14.57	95.15	0.83	4.85
3	0.0067	15.04	94.65	0.95	5.35
4	0.0663	18.98	87.76	2.95	12.24
5	0.0061	19.28	87.01	3.21	12.99
6	0.2994	30.61	63.66	19.49	36.34
7	0.0299	31.42	62.01	21.47	37.99
8	0.0556	32.33	58.26	25.83	41.74
9	0.2020	33.41	45.78	44.13	54.22
10	0.1571	33.41	38.59	59.30	61.41

Table F5: ModSim liberation results summary - e

Stream number 8

G-class	Fractional distribution	Cumulative recovery of mineral 1	Cumulative grade of mineral 1	Cumulative recovery of mineral 2	Cumulative grade of mineral 2
1	0.0407	1.94	100.00	0.00	0.00
2	0.1364	8.05	95.15	0.46	4.85
3	0.0066	8.31	94.65	0.52	5.35
4	0.0669	10.51	87.72	1.64	12.28
5	0.0061	10.67	86.97	1.78	13.03
6	0.2935	16.81	63.89	10.59	36.11
7	0.0302	17.26	62.20	11.70	37.80
8	0.0554	17.75	58.41	14.10	41.59
9	0.2042	18.36	45.72	24.30	54.28
10	0.1600	18.36	38.41	32.83	61.59

Stream number 9

G-class	Fractional distribution	Cumulative recovery of mineral 1	Cumulative grade of mineral 1	Cumulative recovery of mineral 2	Cumulative grade of mineral 2
1	0.0408	3.12	100.00	0.00	0.00
2	0.1359	12.87	95.15	0.73	4.85
3	0.0067	13.28	94.65	0.84	5.35
4	0.0660	16.75	87.78	2.60	12.22
5	0.0061	17.02	87.03	2.83	12.97
6	0.3036	27.17	63.50	17.42	36.50
7	0.0297	27.88	61.87	19.16	38.13
8	0.0557	28.68	58.15	23.02	41.85
9	0.2005	29.63	45.83	39.07	54.17
10	0.1551	29.63	38.72	52.31	61.28

Table F6: ModSim liberation results summary - f

Stream number 10

G-class	Fractional distribution	Cumulative recovery of mineral 1	Cumulative grade of mineral 1	Cumulative recovery of mineral 2	Cumulative grade of mineral 2
1	0.0200	4.34	100.00	0.00	0.00
2	0.3050	66.35	94.09	4.65	5.91
3	0.0120	68.46	93.63	5.19	6.37
4	0.1300	87.84	86.69	15.04	13.31
5	0.0090	88.94	86.12	15.99	13.88
6	0.2070	108.56	73.26	44.19	26.74
7	0.0360	111.01	71.16	50.17	28.84
8	0.0500	113.05	67.76	59.99	32.24
9	0.1000	114.39	60.68	82.69	39.32
10	0.1310	114.39	52.73	114.38	47.27

Stream number 12

G-class	Fractional distribution	Cumulative recovery of mineral 1	Cumulative grade of mineral 1	Cumulative recovery of mineral 2	Cumulative grade of mineral 2
1	0.0200	4.34	100.00	0.00	0.00
2	0.3050	66.35	94.09	4.65	5.91
3	0.0120	68.46	93.63	5.19	6.37
4	0.1300	87.84	86.69	15.04	13.31
5	0.0090	88.94	86.12	15.99	13.88
6	0.2070	108.56	73.26	44.19	26.74
7	0.0360	111.01	71.16	50.17	28.84
8	0.0500	113.05	67.76	59.99	32.24
9	0.1000	114.39	60.68	82.69	39.32
10	0.1310	114.39	52.73	114.38	47.27

Table F7: ModSim liberation results summary - g

Stream number 13

G-class	Fractional distribution	Cumulative recovery of mineral 1	Cumulative grade of mineral 1	Cumulative recovery of mineral 2	Cumulative grade of mineral 2
1	0.0200	4.34	100.00	0.00	0.00
2	0.3050	66.35	94.09	4.65	5.91
3	0.0120	68.46	93.63	5.19	6.37
4	0.1300	87.84	86.69	15.04	13.31
5	0.0090	88.94	86.12	15.99	13.88
6	0.2070	108.56	73.26	44.19	26.74
7	0.0360	111.01	71.16	50.17	28.84
8	0.0500	113.05	67.76	59.99	32.24
9	0.1000	114.39	60.68	82.69	39.32
10	0.1310	114.39	52.73	114.38	47.27

Stream number 14

G-class	Fractional distribution	Cumulative recovery of mineral 1	Cumulative grade of mineral 1	Cumulative recovery of mineral 2	Cumulative grade of mineral 2
1	0.0200	3.79	100.00	0.00	0.00
2	0.3050	58.00	94.09	4.06	5.91
3	0.0120	59.85	93.63	4.54	6.37
4	0.1300	76.79	86.69	13.15	13.31
5	0.0090	77.75	86.12	13.98	13.88
6	0.2070	94.90	73.26	38.63	26.74
7	0.0360	97.04	71.16	43.86	28.84
8	0.0500	98.82	67.76	52.45	32.24
9	0.1000	100.00	60.67	72.29	39.33
10	0.1310	100.00	52.72	100.00	47.28

Table F8: ModSim liberation results summary - h

Stream number 15

G-class	Fractional distribution	Cumulative recovery of mineral 1	Cumulative grade of mineral 1	Cumulative recovery of mineral 2	Cumulative grade of mineral 2
1	0.0407	2.35	100.00	0.00	0.00
2	0.1366	9.76	95.15	0.56	4.85
3	0.0066	10.07	94.65	0.63	5.35
4	0.0673	12.74	87.70	1.99	12.30
5	0.0061	12.94	86.95	2.17	13.05
6	0.2889	20.24	64.07	12.66	35.93
7	0.0304	20.80	62.34	14.01	37.66
8	0.0553	21.40	58.53	16.91	41.47
9	0.2058	22.14	45.68	29.36	54.32
10	0.1622	22.14	38.27	39.83	61.73

Stream number 16

G-class	Fractional distribution	Cumulative recovery of mineral 1	Cumulative grade of mineral 1	Cumulative recovery of mineral 2	Cumulative grade of mineral 2
1	0.0200	0.55	100.00	0.00	0.00
2	0.3053	8.35	94.09	0.59	5.91
3	0.0120	8.62	93.63	0.65	6.37
4	0.1301	11.05	86.69	1.89	13.31
5	0.0090	11.19	86.12	2.01	13.88
6	0.2070	13.66	73.27	5.56	26.73
7	0.0360	13.97	71.17	6.31	28.83
8	0.0500	14.22	67.77	7.54	32.23
9	0.0999	14.39	60.69	10.40	39.31
10	0.1309	14.39	52.75	14.38	47.25

Appendix G: ModSim particle size distribution (PSD's) and sampling feed rate used in ModSim mass balance

As ModSim was used to the PSD's for the circuit used in sampling. The main reason for such PSD's was to allow mass balance to be done in the continuous flotation involved. Selected streams were taken as ModSim could only show 10 streams at a time as shown in Figure G1 – G3. Mainly some of the recycle streams were then left out. The feed rate of 665 t/h shown in mass balance done on ModSim was obtained from the average taken during the sampling exercise. Figure G4 shows the variation of feed during the sampling campaign.

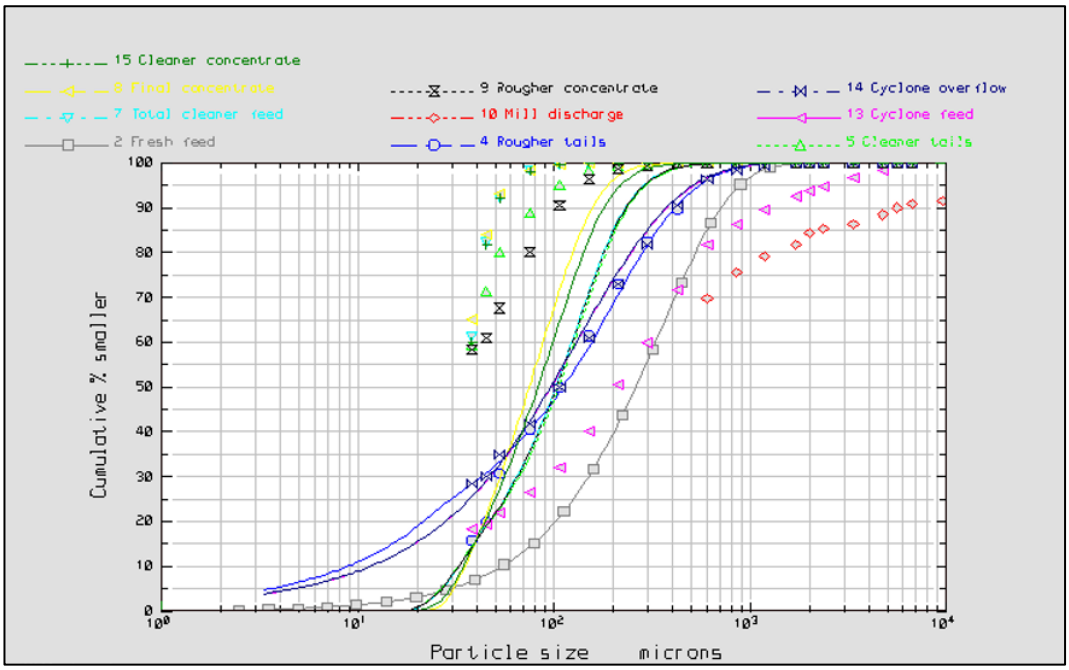

Figure G1: ModSim continuous flotation plant PSD's (Log-Log X-axis)

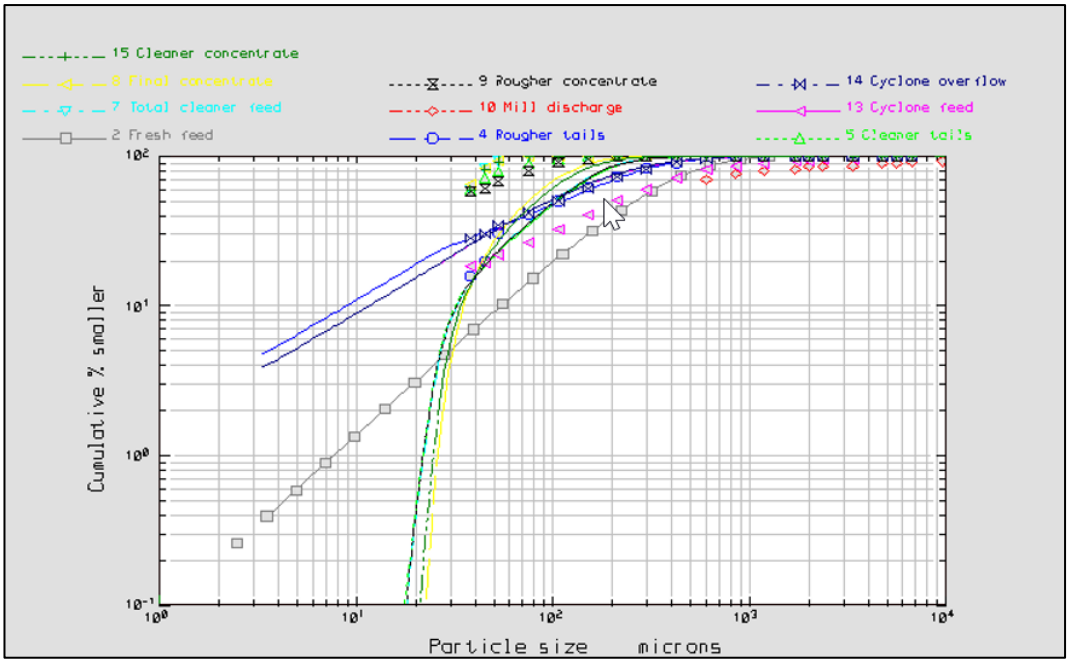

Figure G2: ModSim continuous flotation plant PSD's (Linear-Log X-axis)

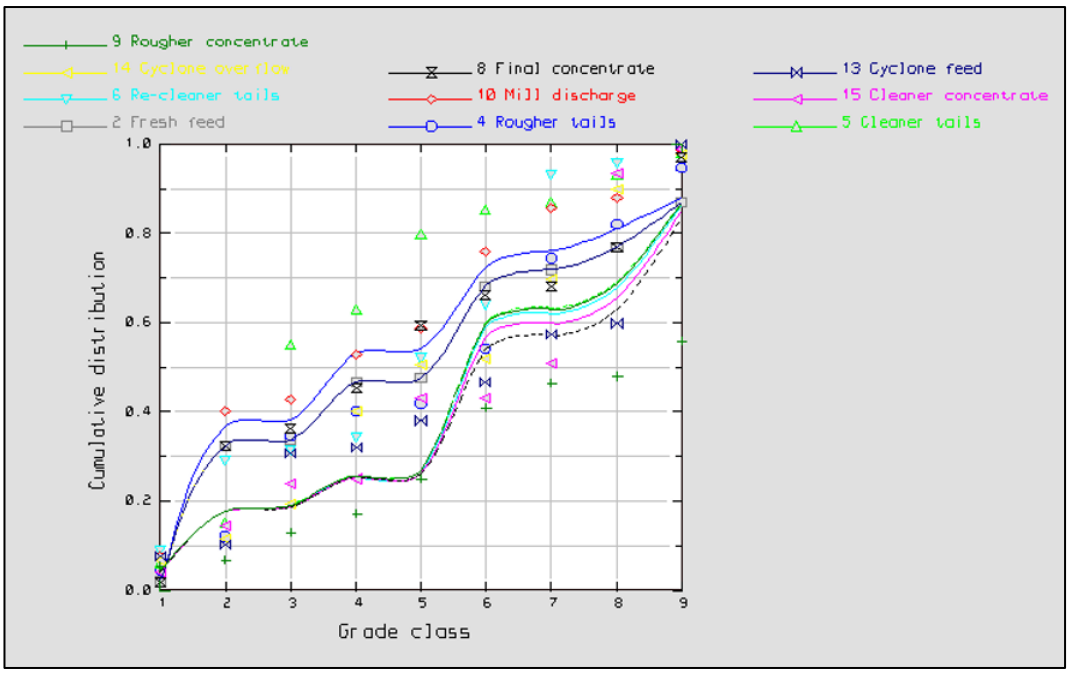

Figure G3: ModSim continuous flotation plant combined liberation plots

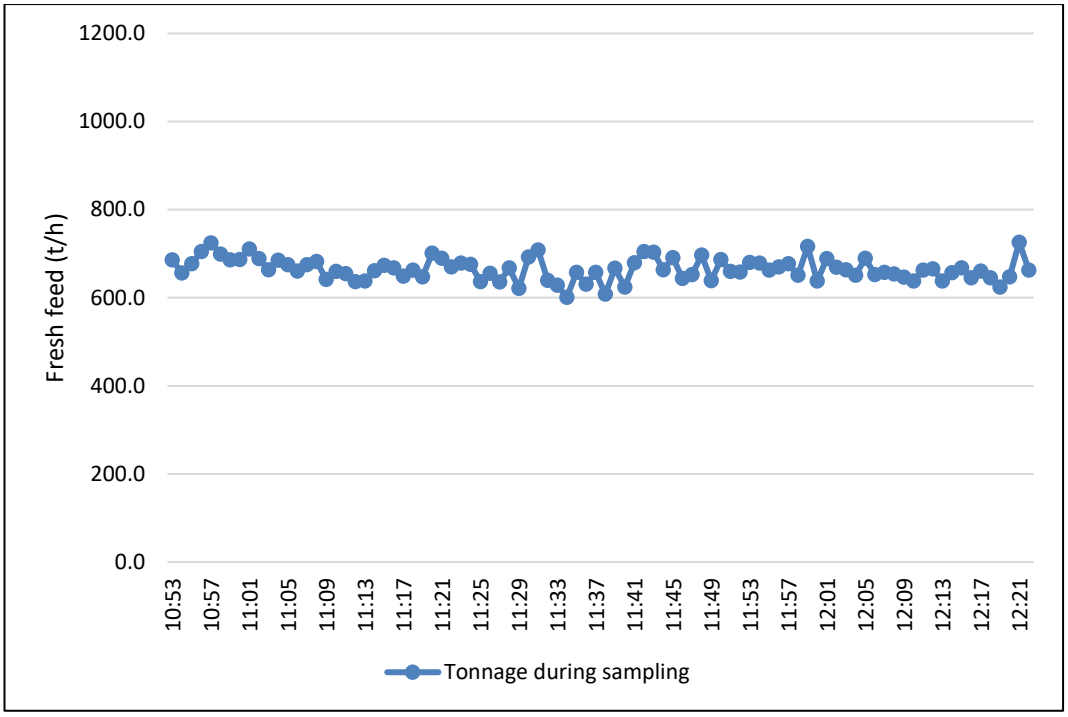

Figure G4: Feed rate (t/h) variation during sampling campaign

Appendix H: ModSim Echo-File background information

In running the simulations using ModSim some other calculations happen in the background before results get displayed in the flowsheet. Information taking place in the background does get stored in the Echo File folder under Run Tab. Below is some of the information obtained in the Echo File. Stream 2 i.e. fresh feed stream is the one which had more detailed results and that can be seen in the Tables reflected below.

Table H1: ModSim Echo-file data - a

```
                    MINERAL NAMES
                    *************
   Copp     Copp     Copp     Copp     Copp     Copp     Copp


                    MINERAL SPECIFIC GRAVITIES
                    **************************
   2.700        2.600        2.710        2.950        3.170        3.400
   3.650


                    PARTICLE SIZES
                    ******************
 0.2000E-02  0.1414E-02  0.1000E-02  0.7071E-03  0.5000E-03  0.3536E-03
 0.2500E-03  0.1768E-03  0.1250E-03  0.8839E-04  0.6250E-04  0.4419E-04
 0.3125E-04  0.2210E-04  0.1563E-04  0.1105E-04  0.7813E-05  0.5524E-05
 0.3906E-05  0.2762E-05


                    MASS FRACTIONS IN G-CLASSES
                    ***************************

G-CLASS 1      1.000  0.000  0.000  0.000  0.000  0.000  0.000
G-CLASS 2      0.937  0.063  0.000  0.000  0.000  0.000  0.000
G-CLASS 3      0.813  0.187  0.000  0.000  0.000  0.000  0.000
G-CLASS 4      0.687  0.313  0.000  0.000  0.000  0.000  0.000
G-CLASS 5      0.563  0.437  0.000  0.000  0.000  0.000  0.000
G-CLASS 6      0.437  0.563  0.000  0.000  0.000  0.000  0.000
G-CLASS 7      0.313  0.687  0.000  0.000  0.000  0.000  0.000
G-CLASS 8      0.188  0.812  0.000  0.000  0.000  0.000  0.000
G-CLASS 9      0.062  0.938  0.000  0.000  0.000  0.000  0.000
G-CLASS10      0.000  1.000  0.000  0.000  0.000  0.000  0.000
```

Table H2: ModSim Echo-file data - b

```
                  VOLUME FRACTIONS IN G-CLASSES
                  *****************************

G-CLASS 1     1.000  0.000  0.000  0.000  0.000  0.000  0.000
G-CLASS 2     0.935  0.065  0.000  0.000  0.000  0.000  0.000
G-CLASS 3     0.807  0.193  0.000  0.000  0.000  0.000  0.000
G-CLASS 4     0.679  0.321  0.000  0.000  0.000  0.000  0.000
G-CLASS 5     0.554  0.446  0.000  0.000  0.000  0.000  0.000
G-CLASS 6     0.428  0.572  0.000  0.000  0.000  0.000  0.000
G-CLASS 7     0.305  0.695  0.000  0.000  0.000  0.000  0.000
G-CLASS 8     0.182  0.818  0.000  0.000  0.000  0.000  0.000
G-CLASS 9     0.060  0.940  0.000  0.000  0.000  0.000  0.000
G-CLASS10     0.000  1.000  0.000  0.000  0.000  0.000  0.000


                  PHYSICAL PROPERTIES
                  *******************


PHYS PROP 1
-----------
   2.700       2.694       2.681       2.668       2.655       2.643
   2.631       2.618       2.606       2.600

PHYS PROP 2
-----------
   2.643       2.631       0.000       1.000      0.5000       1.000
   1.000       1.000

PHYS PROP 5
-----------
   2.618       2.606       2.600       2.700       2.694       2.681
   2.668       2.655       2.643       2.631
```

Table H3: ModSim Echo-file data - c

```
                  STREAM NUMBER  2
                  ****************
        TOTAL MASS SOLIDS= 184.7
        PERCENTAGE SOLIDS= 93.00

 MASS IN EACH CATEGORY:
                                  D-CLASSES
                1       2       3       4       5       6       7       8
                9      10      11      12      13      14      15      16
               17      18      19      20
SCL 1 GCL 1   0.00    0.01    0.03    0.06    0.09    0.10    0.09    0.08
              0.06    0.04    0.03    0.02    0.01    0.01    0.01    0.00
              0.00    0.00    0.00    0.00
SCL 1 GCL 2   0.00    0.04    0.14    0.30    0.43    0.47    0.44    0.36
              0.28    0.20    0.14    0.10    0.07    0.05    0.03    0.02
              0.01    0.01    0.01    0.01
SCL 1 GCL 3   0.00    0.00    0.01    0.02    0.02    0.03    0.02    0.02
              0.02    0.01    0.01    0.01    0.00    0.00    0.00    0.00
              0.00    0.00    0.00    0.00
SCL 1 GCL 4   0.00    0.02    0.06    0.13    0.18    0.20    0.19    0.15
              0.12    0.09    0.06    0.04    0.03    0.02    0.01    0.01
              0.01    0.00    0.00    0.00
SCL 1 GCL 5   0.00    0.00    0.01    0.01    0.02    0.02    0.02    0.01
              0.01    0.01    0.01    0.00    0.00    0.00    0.00    0.00
              0.00    0.00    0.00    0.00
SCL 1 GCL 6   0.02    0.14    0.52    1.10    1.57    1.74    1.62    1.34
              1.03    0.75    0.53    0.36    0.25    0.17    0.11    0.07
              0.05    0.03    0.02    0.04
SCL 1 GCL 7   0.00    0.00    0.01    0.03    0.04    0.04    0.04    0.03
              0.02    0.02    0.01    0.01    0.01    0.00    0.00    0.00
              0.00    0.00    0.00    0.00
```

Table H4: ModSim Echo-file data - d

SCL 1 GCL 8	0.00	0.01	0.04	0.08	0.11	0.13	0.12	0.10
	0.07	0.05	0.04	0.03	0.02	0.01	0.01	0.01
	0.00	0.00	0.00	0.00				
SCL 1 GCL 9	0.00	0.03	0.12	0.25	0.36	0.40	0.37	0.31
	0.24	0.17	0.12	0.08	0.06	0.04	0.03	0.02
	0.01	0.01	0.00	0.01				
SCL 1 GCL10	0.00	0.01	0.05	0.10	0.15	0.16	0.15	0.12
	0.10	0.07	0.05	0.03	0.02	0.02	0.01	0.01
	0.00	0.00	0.00	0.00				
SCL 2 GCL 1	0.00	0.01	0.05	0.11	0.15	0.17	0.16	0.13
	0.10	0.07	0.05	0.04	0.02	0.02	0.01	0.01
	0.00	0.00	0.00	0.00				
SCL 2 GCL 2	0.00	0.01	0.03	0.06	0.09	0.10	0.10	0.08
	0.06	0.04	0.03	0.02	0.01	0.01	0.01	0.00
	0.00	0.00	0.00	0.00				
SCL 2 GCL 3	0.00	0.00	0.00	0.01	0.01	0.01	0.01	0.01
	0.00	0.00	0.00	0.00	0.00	0.00	0.00	0.00
	0.00	0.00	0.00	0.00				
SCL 2 GCL 4	0.00	0.00	0.00	0.00	0.00	0.00	0.00	0.00
	0.00	0.00	0.00	0.00	0.00	0.00	0.00	0.00
	0.00	0.00	0.00	0.00				
SCL 2 GCL 5	0.00	0.00	0.00	0.01	0.01	0.01	0.01	0.01
	0.01	0.00	0.00	0.00	0.00	0.00	0.00	0.00
	0.00	0.00	0.00	0.00				
SCL 2 GCL 6	0.00	0.04	0.14	0.29	0.41	0.46	0.43	0.35
	0.27	0.20	0.14	0.10	0.07	0.04	0.03	0.02
	0.01	0.01	0.01	0.01				
SCL 2 GCL 7	0.00	0.01	0.03	0.07	0.09	0.10	0.10	0.08
	0.06	0.04	0.03	0.02	0.01	0.01	0.01	0.00
	0.00	0.00	0.00	0.00				

Table H5: ModSim Echo-file data - e

SCL 2 GCL 8	0.00	0.02	0.08	0.18	0.26	0.28	0.26	0.22
	0.17	0.12	0.09	0.06	0.04	0.03	0.02	0.01
	0.01	0.01	0.00	0.01				
SCL 2 GCL 9	0.00	0.03	0.11	0.23	0.33	0.36	0.34	0.28
	0.22	0.16	0.11	0.08	0.05	0.03	0.02	0.02
	0.01	0.01	0.00	0.01				
SCL 2 GCL10	0.00	0.02	0.08	0.18	0.26	0.28	0.26	0.22
	0.17	0.12	0.09	0.06	0.04	0.03	0.02	0.01
	0.01	0.01	0.00	0.01				
SCL 3 GCL 1	0.00	0.00	0.02	0.03	0.05	0.05	0.05	0.04
	0.03	0.02	0.02	0.01	0.01	0.01	0.00	0.00
	0.00	0.00	0.00	0.00				
SCL 3 GCL 2	0.01	0.04	0.15	0.32	0.46	0.51	0.48	0.40
	0.30	0.22	0.16	0.11	0.07	0.05	0.03	0.02
	0.01	0.01	0.01	0.01				
SCL 3 GCL 3	0.00	0.00	0.01	0.01	0.02	0.02	0.02	0.01
	0.01	0.01	0.01	0.00	0.00	0.00	0.00	0.00
	0.00	0.00	0.00	0.00				
SCL 3 GCL 4	0.00	0.03	0.10	0.21	0.30	0.33	0.31	0.25
	0.19	0.14	0.10	0.07	0.05	0.03	0.02	0.01
	0.01	0.01	0.00	0.01				
SCL 3 GCL 5	0.00	0.00	0.01	0.01	0.02	0.02	0.02	0.02
	0.01	0.01	0.01	0.00	0.00	0.00	0.00	0.00
	0.00	0.00	0.00	0.00				
SCL 3 GCL 6	0.00	0.01	0.04	0.09	0.13	0.15	0.14	0.11
	0.09	0.06	0.04	0.03	0.02	0.01	0.01	0.01
	0.00	0.00	0.00	0.00				
SCL 3 GCL 7	0.00	0.01	0.03	0.06	0.09	0.10	0.09	0.07
	0.06	0.04	0.03	0.02	0.01	0.01	0.01	0.00
	0.00	0.00	0.00	0.00				

Table H6: ModSim Echo-file data - f

SCL 3 GCL 8	0.00	0.00	0.01	0.02	0.03	0.03	0.03	0.02
	0.02	0.01	0.01	0.01	0.00	0.00	0.00	0.00
	0.00	0.00	0.00	0.00				
SCL 3 GCL 9	0.01	0.07	0.26	0.54	0.78	0.86	0.80	0.66
	0.51	0.37	0.26	0.18	0.12	0.08	0.05	0.04
	0.02	0.02	0.01	0.02				
SCL 3 GCL10	0.01	0.07	0.25	0.52	0.75	0.83	0.77	0.64
	0.49	0.36	0.25	0.17	0.12	0.08	0.05	0.04
	0.02	0.02	0.01	0.02				
SCL 4 GCL 1	0.00	0.00	0.02	0.04	0.05	0.06	0.05	0.04
	0.03	0.02	0.02	0.01	0.01	0.01	0.00	0.00
	0.00	0.00	0.00	0.00				
SCL 4 GCL 2	0.00	0.03	0.11	0.24	0.34	0.38	0.35	0.29
	0.22	0.16	0.11	0.08	0.05	0.04	0.02	0.02
	0.01	0.01	0.00	0.01				
SCL 4 GCL 3	0.00	0.01	0.02	0.04	0.06	0.07	0.07	0.05
	0.04	0.03	0.02	0.01	0.01	0.01	0.00	0.00
	0.00	0.00	0.00	0.00				
SCL 4 GCL 4	0.01	0.06	0.22	0.46	0.66	0.73	0.68	0.56
	0.43	0.31	0.22	0.15	0.10	0.07	0.05	0.03
	0.02	0.01	0.01	0.02				
SCL 4 GCL 5	0.00	0.00	0.02	0.03	0.05	0.05	0.05	0.04
	0.03	0.02	0.02	0.01	0.01	0.01	0.00	0.00
	0.00	0.00	0.00	0.00				
SCL 4 GCL 6	0.00	0.03	0.09	0.20	0.28	0.31	0.29	0.24
	0.19	0.13	0.10	0.07	0.04	0.03	0.02	0.01
	0.01	0.01	0.00	0.01				
SCL 4 GCL 7	0.00	0.00	0.00	0.01	0.01	0.01	0.01	0.01
	0.01	0.01	0.00	0.00	0.00	0.00	0.00	0.00
	0.00	0.00	0.00	0.00				

Table H7: ModSim Echo-file data - g

SCL 4 GCL 8	0.00	0.00	0.01	0.02	0.03	0.04	0.04	0.03
	0.02	0.02	0.01	0.01	0.01	0.00	0.00	0.00
	0.00	0.00	0.00	0.00				
SCL 4 GCL 9	0.00	0.00	0.02	0.04	0.05	0.06	0.05	0.04
	0.03	0.02	0.02	0.01	0.01	0.01	0.00	0.00
	0.00	0.00	0.00	0.00				
SCL 4 GCL10	0.00	0.02	0.06	0.14	0.20	0.22	0.20	0.17
	0.13	0.09	0.07	0.05	0.03	0.02	0.01	0.01
	0.01	0.00	0.00	0.01				
SCL 5 GCL 1	0.00	0.00	0.01	0.02	0.02	0.03	0.02	0.02
	0.01	0.01	0.01	0.01	0.00	0.00	0.00	0.00
	0.00	0.00	0.00	0.00				
SCL 5 GCL 2	0.01	0.05	0.20	0.42	0.60	0.67	0.62	0.51
	0.39	0.29	0.20	0.14	0.09	0.06	0.04	0.03
	0.02	0.01	0.01	0.02				
SCL 5 GCL 3	0.00	0.00	0.01	0.01	0.02	0.02	0.02	0.02
	0.01	0.01	0.01	0.00	0.00	0.00	0.00	0.00
	0.00	0.00	0.00	0.00				
SCL 5 GCL 4	0.00	0.02	0.06	0.14	0.19	0.22	0.20	0.17
	0.13	0.09	0.07	0.04	0.03	0.02	0.01	0.01
	0.01	0.00	0.00	0.01				
SCL 5 GCL 5	0.00	0.00	0.01	0.02	0.02	0.03	0.02	0.02
	0.02	0.01	0.01	0.01	0.00	0.00	0.00	0.00
	0.00	0.00	0.00	0.00				
SCL 5 GCL 6	0.00	0.01	0.02	0.05	0.07	0.08	0.07	0.06
	0.04	0.03	0.02	0.02	0.01	0.01	0.00	0.00
	0.00	0.00	0.00	0.00				
SCL 5 GCL 7	0.00	0.01	0.05	0.11	0.16	0.18	0.17	0.14
	0.11	0.08	0.06	0.04	0.03	0.02	0.01	0.01
	0.01	0.00	0.00	0.00				

Table H8: ModSim Echo-file data - h

SCL 5 GCL 8	0.00	0.02	0.07	0.15	0.22	0.24	0.22	0.19
	0.14	0.10	0.07	0.05	0.03	0.02	0.02	0.01
	0.01	0.00	0.00	0.01				
SCL 5 GCL 9	0.00	0.01	0.02	0.05	0.07	0.07	0.07	0.06
	0.04	0.03	0.02	0.02	0.01	0.01	0.00	0.00
	0.00	0.00	0.00	0.00				
SCL 5 GCL10	0.00	0.00	0.01	0.03	0.04	0.05	0.04	0.04
	0.03	0.02	0.01	0.01	0.01	0.00	0.00	0.00
	0.00	0.00	0.00	0.00				
SCL 6 GCL 1	0.00	0.00	0.00	0.00	0.01	0.01	0.01	0.01
	0.00	0.00	0.00	0.00	0.00	0.00	0.00	0.00
	0.00	0.00	0.00	0.00				
SCL 6 GCL 2	0.01	0.11	0.41	0.86	1.24	1.37	1.27	1.05
	0.81	0.59	0.42	0.29	0.19	0.13	0.09	0.06
	0.04	0.03	0.02	0.03				
SCL 6 GCL 3	0.00	0.01	0.04	0.08	0.12	0.14	0.13	0.10
	0.08	0.06	0.04	0.03	0.02	0.01	0.01	0.01
	0.00	0.00	0.00	0.00				
SCL 6 GCL 4	0.01	0.05	0.19	0.39	0.56	0.62	0.58	0.48
	0.37	0.27	0.19	0.13	0.09	0.06	0.04	0.03
	0.02	0.01	0.01	0.01				
SCL 6 GCL 5	0.00	0.00	0.00	0.00	0.00	0.00	0.00	0.00
	0.00	0.00	0.00	0.00	0.00	0.00	0.00	0.00
	0.00	0.00	0.00	0.00				
SCL 6 GCL 6	0.00	0.02	0.09	0.18	0.26	0.29	0.27	0.22
	0.17	0.12	0.09	0.06	0.04	0.03	0.02	0.01
	0.01	0.01	0.00	0.01				
SCL 6 GCL 7	0.00	0.00	0.00	0.00	0.00	0.00	0.00	0.00
	0.00	0.00	0.00	0.00	0.00	0.00	0.00	0.00
	0.00	0.00	0.00	0.00				

Table H9: ModSim Echo-file data - i

SCL 6 GCL 8	0.00	0.01	0.05	0.11	0.15	0.17	0.16	0.13
	0.10	0.07	0.05	0.04	0.02	0.02	0.01	0.01
	0.00	0.00	0.00	0.00				
SCL 6 GCL 9	0.00	0.01	0.02	0.05	0.07	0.08	0.07	0.06
	0.04	0.03	0.02	0.02	0.01	0.01	0.00	0.00
	0.00	0.00	0.00	0.00				
SCL 6 GCL10	0.00	0.04	0.14	0.29	0.42	0.46	0.43	0.35
	0.27	0.20	0.14	0.10	0.07	0.04	0.03	0.02
	0.01	0.01	0.01	0.01				
SCL 7 GCL 1	0.00	0.00	0.01	0.02	0.03	0.03	0.03	0.03
	0.02	0.01	0.01	0.01	0.00	0.00	0.00	0.00
	0.00	0.00	0.00	0.00				
SCL 7 GCL 2	0.00	0.04	0.14	0.30	0.43	0.48	0.45	0.37
	0.28	0.21	0.15	0.10	0.07	0.05	0.03	0.02
	0.01	0.01	0.01	0.01				
SCL 7 GCL 3	0.00	0.00	0.01	0.02	0.02	0.03	0.02	0.02
	0.02	0.01	0.01	0.01	0.00	0.00	0.00	0.00
	0.00	0.00	0.00	0.00				
SCL 7 GCL 4	0.00	0.02	0.06	0.13	0.18	0.20	0.19	0.15
	0.12	0.09	0.06	0.04	0.03	0.02	0.01	0.01
	0.01	0.00	0.00	0.00				
SCL 7 GCL 5	0.00	0.00	0.01	0.03	0.04	0.05	0.04	0.03
	0.03	0.02	0.01	0.01	0.01	0.00	0.00	0.00
	0.00	0.00	0.00	0.00				
SCL 7 GCL 6	0.01	0.04	0.15	0.33	0.47	0.52	0.48	0.40
	0.31	0.22	0.16	0.11	0.07	0.05	0.03	0.02
	0.01	0.01	0.01	0.01				
SCL 7 GCL 7	0.00	0.01	0.02	0.05	0.07	0.08	0.07	0.06
	0.05	0.03	0.02	0.02	0.01	0.01	0.00	0.00
	0.00	0.00	0.00	0.00				

Table H10: ModSim Echo-file data - j

SCL 7 GCL 8	0.00	0.03	0.12	0.26	0.37	0.41	0.38	0.31
	0.24	0.18	0.12	0.09	0.06	0.04	0.03	0.02
	0.01	0.01	0.00	0.01				
SCL 7 GCL 9	0.00	0.02	0.09	0.19	0.28	0.31	0.29	0.24
	0.18	0.13	0.09	0.06	0.04	0.03	0.02	0.01
	0.01	0.01	0.00	0.01				
SCL 7 GCL10	0.01	0.06	0.22	0.47	0.67	0.74	0.69	0.57
	0.44	0.32	0.22	0.15	0.10	0.07	0.05	0.03
	0.02	0.01	0.01	0.02				
SCL 8 GCL 1	0.00	0.00	0.02	0.04	0.05	0.06	0.05	0.04
	0.03	0.02	0.02	0.01	0.01	0.01	0.00	0.00
	0.00	0.00	0.00	0.00				
SCL 8 GCL 2	0.00	0.01	0.03	0.07	0.10	0.11	0.10	0.09
	0.07	0.05	0.03	0.02	0.02	0.01	0.01	0.00
	0.00	0.00	0.00	0.00				
SCL 8 GCL 3	0.00	0.00	0.00	0.01	0.01	0.01	0.01	0.01
	0.00	0.00	0.00	0.00	0.00	0.00	0.00	0.00
	0.00	0.00	0.00	0.00				
SCL 8 GCL 4	0.00	0.00	0.01	0.03	0.04	0.04	0.04	0.03
	0.03	0.02	0.01	0.01	0.01	0.00	0.00	0.00
	0.00	0.00	0.00	0.00				
SCL 8 GCL 5	0.00	0.00	0.02	0.03	0.05	0.05	0.05	0.04
	0.03	0.02	0.02	0.01	0.01	0.00	0.00	0.00
	0.00	0.00	0.00	0.00				
SCL 8 GCL 6	0.01	0.05	0.17	0.35	0.51	0.56	0.52	0.43
	0.33	0.24	0.17	0.12	0.08	0.05	0.04	0.02
	0.02	0.01	0.01	0.01				
SCL 8 GCL 7	0.00	0.03	0.13	0.27	0.39	0.43	0.40	0.33
	0.25	0.18	0.13	0.09	0.06	0.04	0.03	0.02
	0.01	0.01	0.01	0.01				

Table H11: ModSim Echo-file data - k

SCL 8 GCL 8	0.00	0.00	0.01	0.02	0.04	0.04	0.04	0.03
	0.02	0.02	0.01	0.01	0.01	0.00	0.00	0.00
	0.00	0.00	0.00	0.00				
SCL 8 GCL 9	0.00	0.00	0.01	0.03	0.04	0.05	0.04	0.04
	0.03	0.02	0.01	0.01	0.01	0.00	0.00	0.00
	0.00	0.00	0.00	0.00				
SCL 8 GCL10	0.00	0.02	0.08	0.18	0.26	0.28	0.26	0.22
	0.17	0.12	0.09	0.06	0.04	0.03	0.02	0.01
	0.01	0.01	0.00	0.01				
SCL 9 GCL 1	0.00	0.00	0.01	0.03	0.04	0.04	0.04	0.03
	0.03	0.02	0.01	0.01	0.01	0.00	0.00	0.00
	0.00	0.00	0.00	0.00				
SCL 9 GCL 2	0.01	0.06	0.20	0.43	0.62	0.68	0.64	0.53
	0.40	0.29	0.21	0.14	0.10	0.07	0.04	0.03
	0.02	0.01	0.01	0.02				
SCL 9 GCL 3	0.00	0.00	0.01	0.01	0.02	0.02	0.02	0.01
	0.01	0.01	0.01	0.00	0.00	0.00	0.00	0.00
	0.00	0.00	0.00	0.00				
SCL 9 GCL 4	0.01	0.09	0.33	0.70	1.01	1.12	1.04	0.86
	0.66	0.48	0.34	0.23	0.16	0.11	0.07	0.05
	0.03	0.02	0.01	0.03				
SCL 9 GCL 5	0.00	0.00	0.01	0.01	0.02	0.02	0.02	0.02
	0.01	0.01	0.01	0.00	0.00	0.00	0.00	0.00
	0.00	0.00	0.00	0.00				
SCL 9 GCL 6	0.01	0.05	0.18	0.38	0.54	0.60	0.56	0.46
	0.35	0.26	0.18	0.13	0.08	0.06	0.04	0.03
	0.02	0.01	0.01	0.01				
SCL 9 GCL 7	0.00	0.00	0.02	0.03	0.05	0.06	0.05	0.04
	0.03	0.02	0.02	0.01	0.01	0.01	0.00	0.00
	0.00	0.00	0.00	0.00				

Table H12: ModSim Echo-file data - l

SCL 9 GCL 8	0.00	0.00	0.01	0.02	0.03	0.03	0.03	0.02
	0.02	0.01	0.01	0.01	0.00	0.00	0.00	0.00
	0.00	0.00	0.00	0.00				
SCL 9 GCL 9	0.01	0.05	0.17	0.36	0.51	0.56	0.52	0.43
	0.33	0.24	0.17	0.12	0.08	0.05	0.04	0.02
	0.02	0.01	0.01	0.01				
SCL 9 GCL10	0.00	0.04	0.14	0.29	0.42	0.46	0.43	0.35
	0.27	0.20	0.14	0.10	0.07	0.04	0.03	0.02
	0.01	0.01	0.01	0.01				
SCL10 GCL 1	0.00	0.00	0.00	0.01	0.01	0.01	0.01	0.01
	0.01	0.01	0.00	0.00	0.00	0.00	0.00	0.00
	0.00	0.00	0.00	0.00				
SCL10 GCL 2	0.04	0.30	1.13	2.38	3.42	3.78	3.52	2.91
	2.24	1.63	1.15	0.79	0.54	0.36	0.24	0.16
	0.11	0.07	0.05	0.09				
SCL10 GCL 3	0.00	0.00	0.00	0.00	0.00	0.00	0.00	0.00
	0.00	0.00	0.00	0.00	0.00	0.00	0.00	0.00
	0.00	0.00	0.00	0.00				
SCL10 GCL 4	0.00	0.02	0.06	0.12	0.17	0.19	0.18	0.15
	0.11	0.08	0.06	0.04	0.03	0.02	0.01	0.01
	0.01	0.00	0.00	0.00				
SCL10 GCL 5	0.00	0.00	0.00	0.00	0.01	0.01	0.01	0.00
	0.00	0.00	0.00	0.00	0.00	0.00	0.00	0.00
	0.00	0.00	0.00	0.00				
SCL10 GCL 6	0.01	0.09	0.33	0.69	1.00	1.10	1.03	0.85
	0.65	0.47	0.34	0.23	0.16	0.11	0.07	0.05
	0.03	0.02	0.01	0.03				
SCL10 GCL 7	0.00	0.00	0.00	0.01	0.01	0.01	0.01	0.01
	0.01	0.01	0.00	0.00	0.00	0.00	0.00	0.00
	0.00	0.00	0.00	0.00				
SCL10 GCL 8	0.00	0.00	0.01	0.02	0.04	0.04	0.04	0.03
	0.02	0.02	0.01	0.01	0.01	0.00	0.00	0.00
	0.00	0.00	0.00	0.00				
SCL10 GCL 9	0.00	0.00	0.02	0.04	0.05	0.06	0.05	0.04
	0.03	0.02	0.02	0.01	0.01	0.01	0.00	0.00
	0.00	0.00	0.00	0.00				
SCL10 GCL10	0.00	0.02	0.06	0.12	0.18	0.20	0.18	0.15
	0.12	0.09	0.06	0.04	0.03	0.02	0.01	0.01
	0.01	0.00	0.00	0.00				

Appendix I: Flotation testwork setup

The batch flotation tests had for different flotation times chosen that is 2 min, 6 min, 12 min and 20 min. The figure below shows all the conditions for each flotation time that was applied.

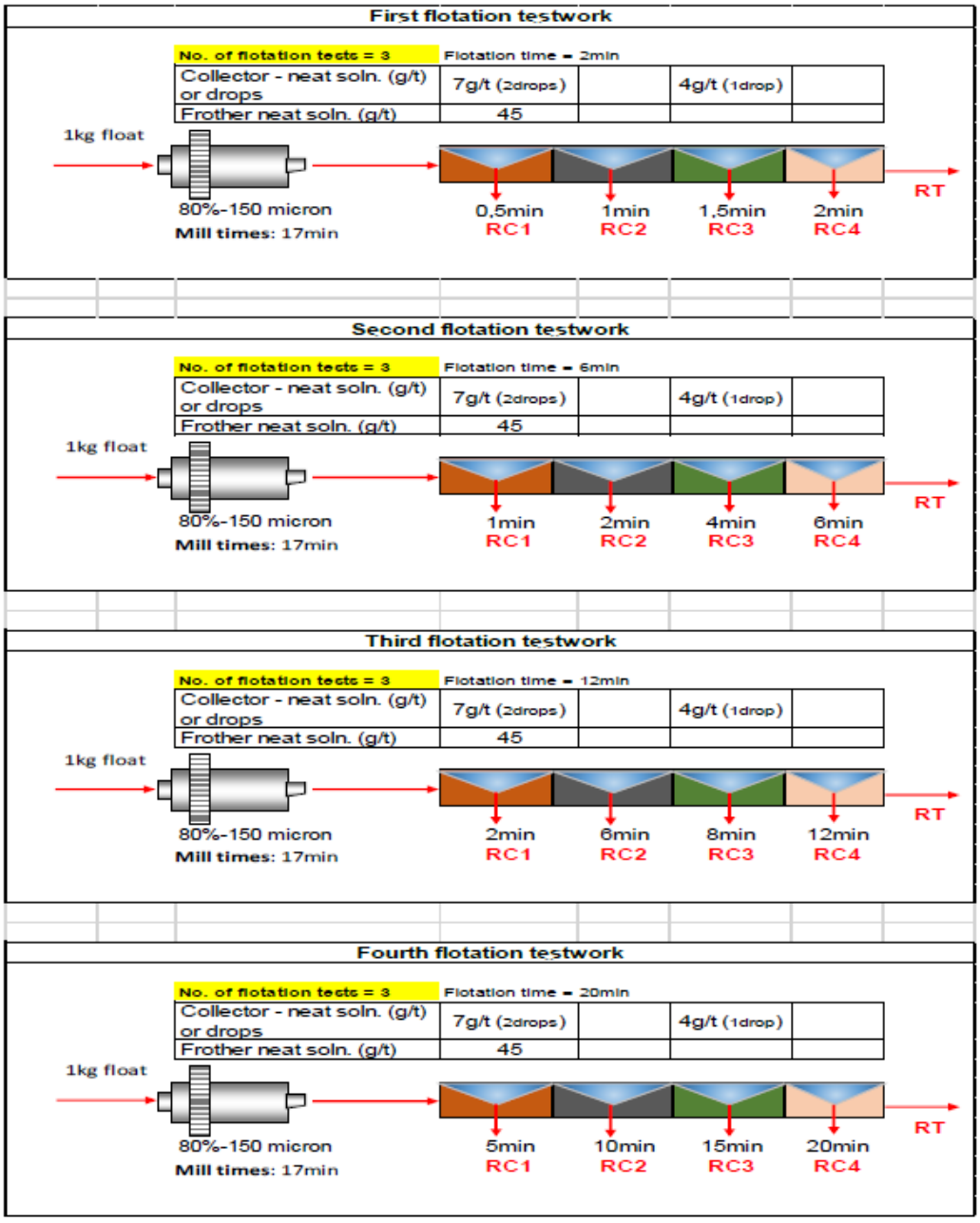

Figure I1: Different flotation times of experimental flotation batch design